Chaos in Daisyworld does apply:

New results lead to "biological homeostasis of the global environment" redefinition from Chaos theory perspective

Camilo Hincapié Gutiérrez

Advisor:
Boris Anghelo RODRÍGUEZ REY, Ph.D.

Co-advisor:
John Alejandro MARTÍNEZ, Ph.D.
Gloria MACHADO RODRÍGUEZ, Ph.D.

Investigation Group:
Fundamentos y Enseñanza de la Física y los Sistemas Dinámicos

In fulfillment of the requirements for the degree of:
MASTER OF SCIENCE IN PHYSICS

Universidad de Antioquia
FACULTAD DE CIENCIAS EXACTAS Y NATURALES
INSTITUTO DE FÍSICA

UNIVERSIDAD
DE ANTIOQUIA
1 8 0 3

December 8, 2019

Dedicated to:

My beautiful and wonderful wife, Leidy Johanna, who is my company when I have needed the most, and with her love has helped me to overcome barriers and to strive to do my best. May God allow me to always be by your side.

My mother, Licinia Isabel, who strove to give me everything and to teach me to be better every day. You always wanted the best for me, and I honor you by telling you that I love you.

Thanks

Contents

List of Figures

List of Tables

Preface

This thesis is the product of several years of investigation on **climate system modelling**, which was begun by my advisor **John Alejandro Martinez** under advise of our group leader **Boris Anghelo Rodríguez Rey**. As physicists, they were immediately captured by **Daisyworld** model: the model was as simple as powerful to describe mathematically a hypothetical mechanism of planetary homeostasis.

Boris, detected several research paths and he invited me to join the group to continue the investigation. Under his advise, I have found the freedom to choose the path I wanted to follow in my academical development. Indeed, this thesis is the product of my multiple scattered readings: it was 2016 when, out of the clear blue sky, I found a relatively new paper (Weaver, 2012 [1]), where the authors assured that *studies on chaotic behaviour in **Daisyworld** has been shown to be fundamentally flawed*. I got dismayed by this assertion, and after exposing the subject in the group, we decided to begin a deeper investigation about that.

As **Daisyworld** is based on the theory of **Energy Balance Models**, which are the simplest climate models, we decided to write down in **chapter 1** a brief discussion about climate modelling and the power hidden in **"simple toy models"** such as the **Energy Balance Models**. Then, in **chapter 2**, we present the theoretical foundations in which **Daisyworld** was born as the mathematical basis for **Gaia theory**, and we describe widely the concepts involved in its construction –from **Energy Balance Models** to mathematical formulation of Daisyworld–, and the results it generates. In addition, we present the conceptual discussion which leads to Weaver's assertion and which originated this work. Finally, in **chapter 3**, we present our corrections on the study on chaotic behaviour in **Daisyworld**, we summarize all the results obtained and the evidence that leads us to firmly asses that **chaos in Daisyworld does apply** and that this leads to redefine what should be understood by **biological homeostasis of the global environment**. In the development of my thoughts, it was necessary to count with the wisdom of my last adviser, the profesor **Gloria Machado Rodríguez**, and all of her biology students. I dare to say that the interdisciplinary environment created by our group was fundamental to this investigation.

Abstract

Daisyworld is a **"simple toy model"** for understanding the coupling of a **simplified climate system** with **biota**. This **simplified climate system** lacks an atmosphere and ocean, and only focus on the balance of energy incoming and outgoing the planet, then it is perfectly described by an **Energy Balance Model**. On the other hand, **biota** is described by **population dynamics models**, specifically by an **epidemic model** based on **ordinary differential equations (ODEs)** which generates a dynamical behaviour governed only by fixed points (see **subsection 2.3.2**, **subsection 2.3.3** and **subsection 2.3.4**). But if other **population dynamics models**, such as **iterated maps of logistic type**, were used, then richer behaviour such as chaotic dynamics would be expected (see **section 2.4**). Recently, Ian S. Weaver has said that **"studies on chaotic behaviour in Daisyworld has been shown to be <u>fundamentally flawed</u>"** [1], referring to Zeng's work on **"Chaos on Daisyworld"** [2].

However, when one studies the fundamentals of **population dynamics theory** and the consequent evidence at Earth of populations that can be described by **iterated maps**, one finally crashes with the question: how can we dare to affirm that chaotic dynamics –originated by discrete population dynamics– is fundamentally flawed? Do we comprehend enough this evidence as to say that the possibility of this chaotic dynamics on other planets doesn't need to be considered?

In this thesis, we study the origins of this misconception by Weaver –started from both Zeng's work [2,3] and Jascourt's criticism to him [4]–, and we rewrite the population dynamics equations when **biota** is modeled using **iterated maps** from its correct biological foundations (see **chapter 3**), so that we restate a model of **Daisyworld** with **discrete population dynamics**. Afterwards, we proceed to **characterize Daisyworld's dynamics** for this new model. This model exhibit complex dynamics characterized by chaos and multifractality with clear biological meanings, and the existence of striking behaviour such as overpopulation and catastrophes like massive extinctions. One fundamental question is raised from this study: **Should the concept of homeostasis, as understood by Gaia theory, be redefined?**. We then propose a redefinition of homeostasis using all the information gathered by the characterization that we performed.

Keywords — Daisyworld, Homeostasis, Population Dynamics, Climate, Chaos, Multifractality, Extinction, Overpopulation, Habitability

Chapter 1

Introduction

In this chapter we first define what climate is (**section 1.1**), in order to define the basic types of climate models (**section 1.2**). Then we remark the importance of **"simple toy models"** in getting insight of patterns emergence in complex systems (**section 1.3**). Finally, having defined this context, we dedicate the last section to put on the table our scientific question and the objectives we seek with this thesis (**??**).

1.1   What is climate?

In order to define what **climate** is, we first must make sure what climate is not. In most cases, people often confuse the terms **climate** with **weather**, but they are different. Indeed, **climate** is a hierarchically higher concept which involves **weather**, as Gettelman and Rood define it [5]:

> ***Climate*** *is the* <u>*distribution*</u> *of possible **weather states** (either for the globe or for a specific geographical location).*

The key word here is **distribution**:

> *A **distribution of weather states** is a* <u>*set*</u> *of **weather events** which are recorded over an agreed* <u>*time interval*</u> *(seasons, decades or longer) so that one can compile the probabilities of occurrence of any event (see **Figure 1.1**).*

According to this, **weather events** are the **microstates** that together make up the **climate**, and there will be some events whose frecuency is higher than other events. **Climate**, as being a distribution, is better described when all its **higher-order statistics** –such as variance (variability)– are known than just when the mean (average) is given, since **taking only averages destroys information**. If we seek to know the **climate distribution**, then our task, in addition to describing its **higher-order statistics**, is to find out the <u>patterns</u> and <u>regularities</u> in **weather states**. Now

> *A **weather state** is the set of values of all the* <u>*variables*</u> *describing the **climate system**.*
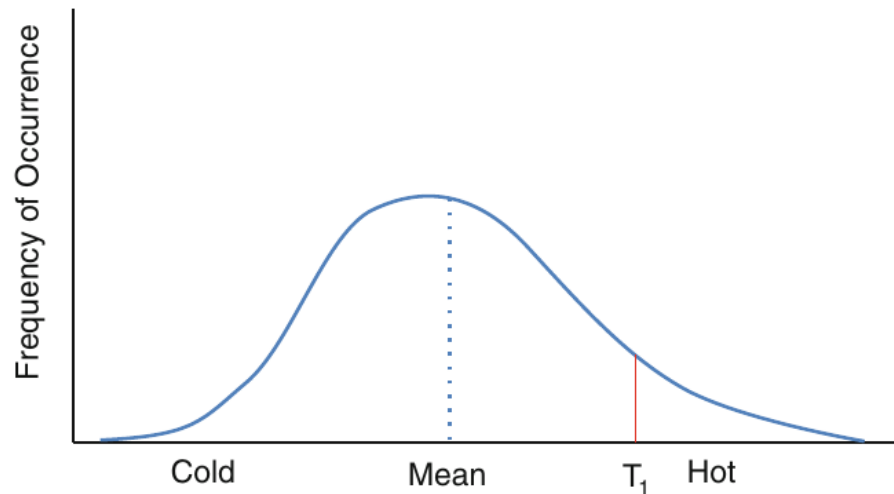
Figure 1.1: Example of a **distribution function** in which **temperature** is taken as main variable to characterize the **weather state**. The vertical axis represents the **frequency of occurrence** and T_1 one specific **weather event**. **Image taken from [5]**.

¿What are these **variables**? If we were talking about planet Earth, the **climate system** would be defined as:

> *The totality of the atmosphere, hydrosphere, biosphere and geosphere and their interactions.*
>
> — United Nations' Framework Convention on Climate Change - FCCC (1992).

In general the variables needed to characterize **climate system** are those that describe the **termo-hydrodynamic state** of the system: temperature T, density ρ, pressure p and the particles velocity vector $\vec{v}$ (which gives us a set of three more vairables $\vec{v} = [v_x, v_y, v_z]$). Each of these variables take different values at different geographical locations, and their values are calculated from **basic governing equations** which should describe next features:

- **Conservation of energy:** also known as the *first law of thermodynamics*. It describes how an input of energy is related with increase of internal energy of the system or the work done.

- **Conservation of momentum:** also know as *Newton's second law of motion*. It describes how "forces" are related with changes in velocity vector of the system.

- **Conservation of mass:** also know as *continuity equation*. It describes how density in a specific volume changes according to mass flows inside and ouside that volume. This must be applied to air, ocean and any moisture of them and other chemical components we want to characterize.

- **Equation of state:** it describes state of matter under a given set of physical conditions. It is a thermodynamic equation relating state variables, such as pressure, volume, temperature, or internal energy.

The set of equations used to describe last characteristics constitute the **model** of the **climate system**. The variables computed directly from this model, or in other words, the variables which are the outcome of this model, are known as **prognostic variables**. On the other hand, those variables which are calculated as **function of prognostic variables** are known as **diagnostic variables**, and we can think of them as derived from the former ones.

As another remark, when we say that the values of these variables are calculated from equations, we are assuming that **climatic system** is a deterministic system –i.e. later states are determined from current ones by means of some sort of "simple rules"–. This is a powerful assumption since it is what allows us to predict system behaviour.

1.2   Climate models

According to McGuffie and Henderson-Sellers [6], there are four basic types of climate models (ranging from simplest to the most complex):

(1) **Energy balance models (EBMs):** are zero- or one-dimensional models predicting the surface (strictly the sea-level) temperature as a function of the energy balance of the Earth.

(2) **One-dimensional models:** such as **radiative–convective (RC) models** and **single column models (SCMs)** focus on processes in the vertical. RC models compute the (usually global average) temperature profile by explicit modelling of radiative processes and a "convective adjustment" which re-establishes a predetermined lapse rate. SCMs are single columns "extracted" from a three-dimensional model and include all the processes that would be modelled in the three-dimensional version but without any of the horizontal energy transfers.

(3) **Dimensionally constrained models:** The oldest are the **statistical dynamical (SD) models**, which deal explicitly with surface processes and dynamics in a zonally averaged framework and have a vertically resolved atmosphere. These models have been the starting point for the incorporation of reaction chemistry in global models and are still used in some **Earth Models of Intermediate Complexity (EMICs)**.

(4) **Global circulation models (GCMs):** The three-dimensional nature of the atmosphere and ocean is incorporated. These models can exist as fully coupled ocean–atmosphere models or "coupled climate system models" or, for testing and evaluation, as independent ocean or atmospheric circulation models. These models attempt to simulate as many processes as possible and produce a three-dimensional picture of the time evolution of the state of the ocean and atmosphere. Vertical resolution is typically much finer than horizontal resolution but, even so, the number of layers is usually much less than the number of columns.

We can also add another basic type of climate model:

(5) **Regional climate models (RCMs):** Also named as **limited-area models**, are those which have boundaries: *They do not represent the entire surface of the Earth.* The

limited area enables them to be run with finer resolution than a global model. Finer horizontal resolution is good for representing the effects of surface features like mountains (topography). In this sense, it is useful to correctly represent the effects of the mountains, which then can be used to understand the climate of a region near or within mountain ranges. These models may also include more processes because they represent smaller regions. The difficulty is that they boundaries which must be specified in order to solve the system. Nevertheless, the climate calculated by the GCM is used as input at the edges of the RCM [7].

1.3   When less is better

The list of types of models presented in last section increases in complexity and need of computational power. Now, in describing **Earth's climate system** we seek to understand how are related the whole of the atmosphere (and all the gases which compounds it), the oceans (including the cryosphere), the land and all living organisms among them (including human beings); and furthermore we seek to predict its behaviour. So one would be tempted to think that the best choice to model Earth's climate is *to construct the model with the greatest possible fidelity and to include the most comprehensive range of physical, chemical, and biological processes that can be handled on today's most powerful computing systems.* Last assumption would lead us to think that the only measure of success of a climate model is the resolution achieved and that it is constrained by the speed of computation performed. Lorenzo M. Polvani reminds us that this measure of success is biased:

> *Although this modeling approach is important for making accurate projections, it imposes substantial limitations when it comes to obtaining a fundamental understanding of the Earth system. The large number of simulated processes and the high resolution at which the simulations are typically performed require that these complex simulations be run on very expensive supercomputers. This requirement greatly limits our ability to explore the models' sensitivities to different system components and climate forcings. As a consequence, our ability to deeply understand the behavior of these models is limited. (...). In a nutshell, complex models may be good for simulating the climate system but may not be as valuable for understanding it.*

> — Polvani [8].

But one can also allude that, apart from the problem of computer power, there exists a parsimony principle which states that the most simple explanation should be the most accurate. Then it is straightforward to remember that *the purpose of the climate models is to gain insight into the climate system and its interactions* [9] and that *a model must be a simplification of the real world.* Then, as McGuffie and Hennderson-Sellers states:

> *Simple models may be sufficient to answer particular, well-specified problems and provide insight that might otherwise be hidden by the complexity of a larger model.*

> — McGuffie and Henderson-Sellers [9].

In addition, Nevison et al. say:

> *Qualitative understanding obtained through analyzing simple models provides guidance for interpreting results of much more complex models such as general circulation models (GCMs) (Gal-Chen and Schneider, 1976 [10]), and for identifying observational needs and new research directions.*

> — Nevison et al. [11].

The power hidden in simple models can be understood by next analogy:

> *Consider, by analogy, another field that must deal with exceedingly complex systems—molecular biology. How is it that biologists have made such dramatic and steady progress in sorting out the human genome and the interactions of the thousands of proteins of which we are constructed? Without doubt, one key has been that nature has provided us with a hierarchy of biological systems of increasing complexity that are amenable to experimental manipulation, ranging from bacteria to fruit fly to mouse to man. Furthermore, the nature of evolution assures us that much of what we learn from simpler organisms is directly relevant to deciphering the workings of their more complex relatives. What good fortune for biologists to be presented with precisely the kind of hierarchy needed to understand a complex system! Imagine how much progress would have been made if they were limited to studying man alone.*

> — Held [12].

Chapter 2

Theoretical basis of the Daisyworld model

We dedicate this chapter to make a journey across the theoretical basis of **Daisyworld model**, begining from **Energy Balance Models (EBMs)** principles (**section 2.1**), then reviewing briefly the basics of **Gaia theory** (**section 2.2**), to arrive to the mathematical basics of **Daisyworld model** (**section 2.3**). There, we present the concept of **"biological homeostasis of the global environment"** as it was understood first by James Lovelock. Then we turn to review the possibility of chaotic dynamics in Daisyworld (**section 2.4**) and finally we present some of the criticisms it endured (**section 2.5**).

2.1   Energy Balance Models (EBMs)

We have stated before, in **section 1.3**, that our climate system is enormously complex, so there is an inherent need to develop tools which allows us to understanding it. At this point, the simplicity of **energy balance models**, combined with the ease of interpreting the results, make them ideal instructional tools that help scientists to get insight on the behavior of the **climate system**. EBMs have helped in the development of new parametrizations and methods of evaluating sensitivity for more complex and realistic models. Currently, we are not only intereseted in Earth's climate understanding, but also in figure up the climate at other planets, and then this type of models can also be extrapolated and applied to scenarios beyond Earth's climate.

EBMs are based on the concept that **the energy fluxes into and out of the climate system as a whole (or parts of it) must balance unless there is a change in the internal energy of the system**, and then seek to predict the behaviour of planet's temperature T. Zero-dimensional EBMs are the most basic models and they aim to calculate the rate of change of temperature dT/dt which is proportional to the net energy available to raise temperature:

$$\frac{\mathrm{d}T}{\mathrm{d}t} \quad \propto \quad \text{Net energy available to raise temperature}$$

EBMs can take two very simple forms (see **Figure 2.1**):

- **Zero-dimensional models:** in which the planet is considered as a single point in space having a global mean effective temperature T.

- **One-dimensional EBMs:** which considers the temperature as being latitudinally re-solved, so the temperature is a function of latitude ϕ: $T = T(\phi)$. Since temperature is allowed to vary from latitude to latitude, one also has to introduce a horizontal energy transfer term between adjacent latitudes.
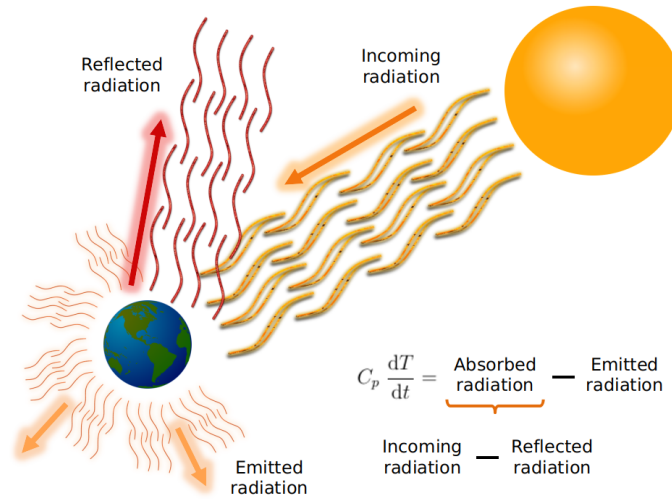
(a) **Zero-dimensional EBMs scheme**. The planet is considered as a single point in space having a global mean effective temperature T.
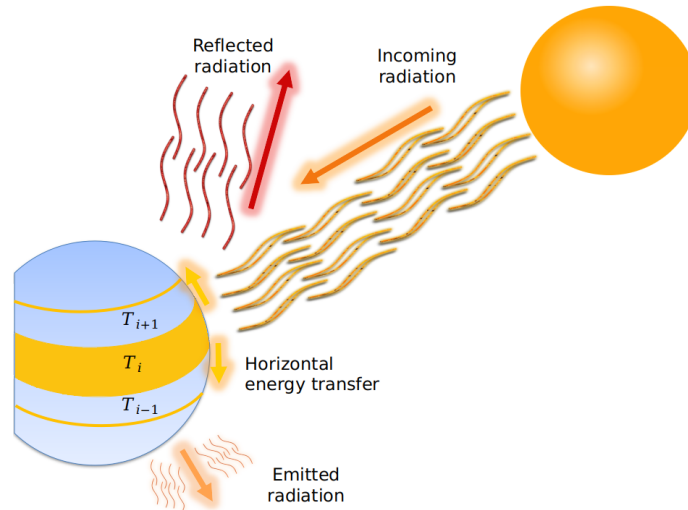
(b) **One-dimensional EBMs scheme**. A horizontal energy transfer term is introduced in order to allow temperature variations from latitude to latitude. **Image based on** [13].

Figure 2.1: Conceptual differences between this **Zero-dimensional EBMs** and **One-dimensional EBMs**.

In EBMs, the temperature T plays a fundamental rol as being the only prognostic climatic variable. In this thesis, we are interested on the former type of EBMs. Next we expand their definition.

2.1.1 Zero-dimensional EBMs

As we saw above, **Zero-dimensional EBMs** correspond to models in which the planet is seen as a point. This allows us to neglect effects such as changes in temperature due to the planet's rotation. The change in the planet's temperature T is calculated from balance –i.e. the difference– between the **absorbed energy R_i** in form of radiation –where subscript i denotes **radiation input**–, and the **emitted energy R_o** in form of radiation –where subscript o denotes **outgoing radiation**–. This planetary radiative energy balance is mathematically expressed as:

$$C_p \frac{\mathrm{d}T}{\mathrm{d}t} = R_i - R_o \tag{2.1}$$

where C_p is the heat capacity of the system and can be thought of as the system's "thermal inertia". From a physical point of view, if absorbed and emitted radiation are in exact balance – situation referred as **perfect energy balance**–, then there cannot be net change in temperature $(\mathrm{d}T/\mathrm{d}t = 0)$ and it is said that equilibrium has been reached. **Equation 2.1** can be used to ascertain this equilibrium climatic state [14]:

$$\frac{\mathrm{d}T}{\mathrm{d}t} = 0 \quad \therefore \quad R_i = R_o \tag{2.2}$$

and so the temperature T turns from a **prognostic variable** into a **diagnostic variable**. The last equation can be interpreted as if we were considering a system in which $\mathrm{d}T/\mathrm{d}t$ is too small compared to absorbed and outgoing energy, then one can consider $\mathrm{d}T/\mathrm{d}t \sim 0$ in these systems. On the other hand, if thermal inertia of the system C_p is small, then the right hand term in **Equation 2.1** can be considered small too $(C_p\mathrm{d}T/\mathrm{d}t \sim 0)$, and again the system must have been reached the temperature of equilibrium. From timescales perspective, the last situation corresponds to the one in which, in absence of thermal inertia,the system is capable to reach equilibrium by "instantaneously" equating outgoing radiation to that absorbed.

Finally, Nevison et al. [11] highlight that "Earth is well known to be in imperfect balance, both spatially and temporally, between incoming solar and outgoing longwave radiation (Peixoto and Oort, 1992)" so **Equation 2.1** should be used if the objective is to resemble Earth realistically.

2.1.2 Where does the energy come from?

The following discussion is mostly about planet Earth, but the general physics also applies to other planets.

According to Jose P. Peixoto [15], our **Sun** is the primary source of energy in our planet and then our climate system is driven by solar radiation. Another source of energy is upward conduction of heat from the Earth's interior (due to radioactive decay), but it is negligible. On the other hand, in the case of giant planets, such as Jupiter and Neptune, there exists an energy contribution from their interior that cannot be neglected since it is probably as important as sunlight in driving, for example, atmospheric motions [16]. In these planets, the upward energy is originated in the pressure of the gases which compound them, and that is fundamentally due to gravity. This pressure in giant planets is related to gases reactions and production of

electromagnetic radiation which can heat the planet from its interior. Although gravity plays a key role in the hydrological cycle of our planet, where it leads to conversion of potential energy to kinetic energy, it cannot be treated as an energy source like it is in the case of giant planets. Then, for the following discussion to apply to planets like our planet, we are going to assume that the only source of energy is the star around which the planet is orbiting.

As Peixoto remarks, the energy supplied by our Sun in form of radiation is partly absorbed, partly scattered, and partly reflected by the various gases of the atmosphere, aerosols, and clouds. The remainder that reaches the Earth's surface is largely absorbed by its components (oceans, lithosphere, cryosphere and biosphere), and only a small part is reflected. This absorbed energy can be transformed into heat (internal energy) or it can be used to do work against the environment.

To measure energy input from our star, we calculate **solar spectral irradiance**, which is the measure of the radiant energy from the Sun as a function of wavelength [17]. It is known that all mass radiates energy depending on temperature and that the hotter a body, the more energy it radiates. Now, in general any star can be treated as a **black body**, which is, by definition, not only a perfect absorber –since it absorbs all incident electromagnetic radiation, regardless of frequency or angle of incidence–, but also an ideal emitter –since it also emits the maximum possible amount of energy at a given temperature–. **Planck's law** states that the amount and quality of the energy emitted by a black body are uniquely determined by its temperature and not by the body's shape or composition, and this energy emitted is isotropic, i.e, its intensity is independent of the direction [15].

In addition, **Stefan–Boltzmann law** –which can be derived from **Planck's law**–, states that the total energy radiated per unit surface area of a black body across all wavelengths per unit time $\bar{j}$ is proportional to the fourth power of the thermodynamic temperature T, and the constant of proportionality is the Stefan-Boltzmann constant σ. Stefan-Boltzmann constant is named after Slovenian physicist Josef Stefan formulated it in 1879 and after it was later derived in 1884 by Austrian physicist Ludwig Boltzmann, demonstrating that this constant can be calculated from other more fundamental constants related to molecular, atomic and subatomic levels, using the theory of quantum mechanics and statistical mechanics [18]. Thus, Stefan–Boltzmann constant links the amount of heat that is emitted by a black body with its temperature, and this relationship is expressed by:

$$\bar{j} = \sigma T^4 \tag{2.3}$$

Using **Equation 2.3** we can conclude that the Sun's surface temperature is $6,000$[K] (see **Figure 2.2**). Finally, **Wien displacement law** –which can be derived from **Planck's law** too–, states that for black body radiation the wavelength of maximum emission is inversely proportional to the absolute temperature. This law explains why stars are of different colors: cooler stars are red, since they emit the most radiation in the red wavelengths, whilst hotter stars –like our Sun– emit the most radiation in the yellow/green part of the spectrum.
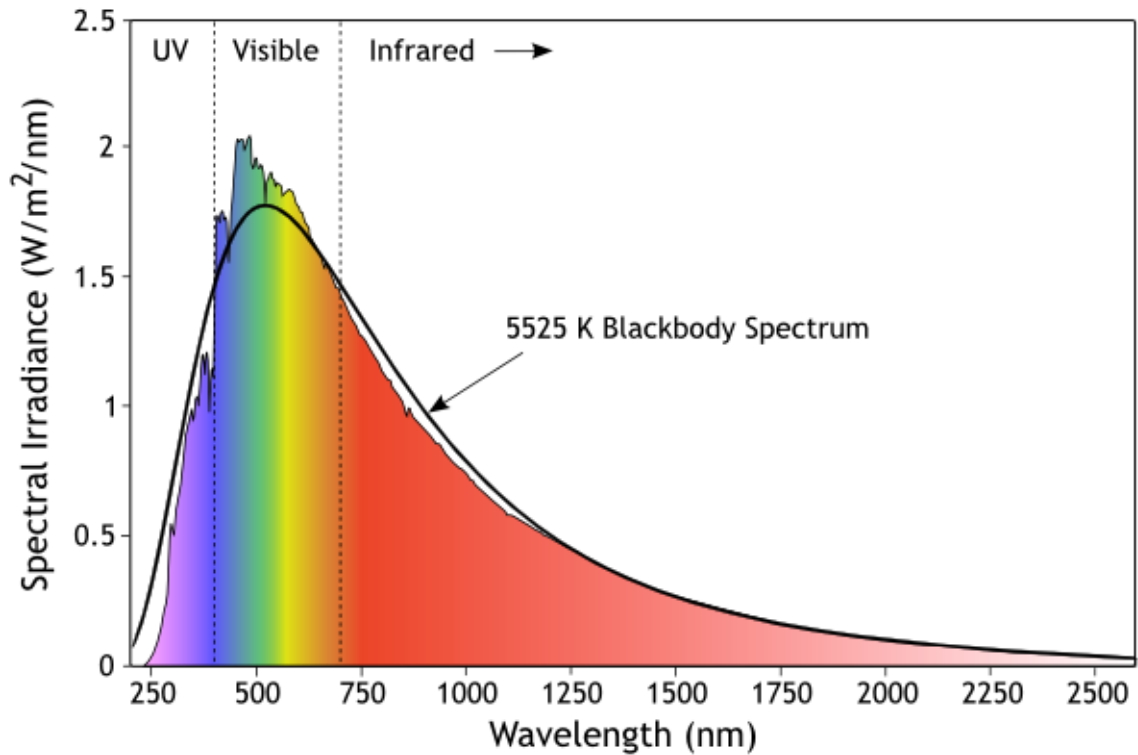
(a) Solar spectral irradiance with distinction of ultraviolet, visible and infrared zone. We can see that the peak radiation of the Sun (surface temperature = 6,000 [K]) is centered among light of wavelenghts we call visible. This is the reason why our eyes evolved to be able to "see" in the visible where the maximum solar emission is. **Image depicted by** Samuel J. Fogarty **and taken from** Quora: Which wavelength (or color) of sunlight contains the most heat?.
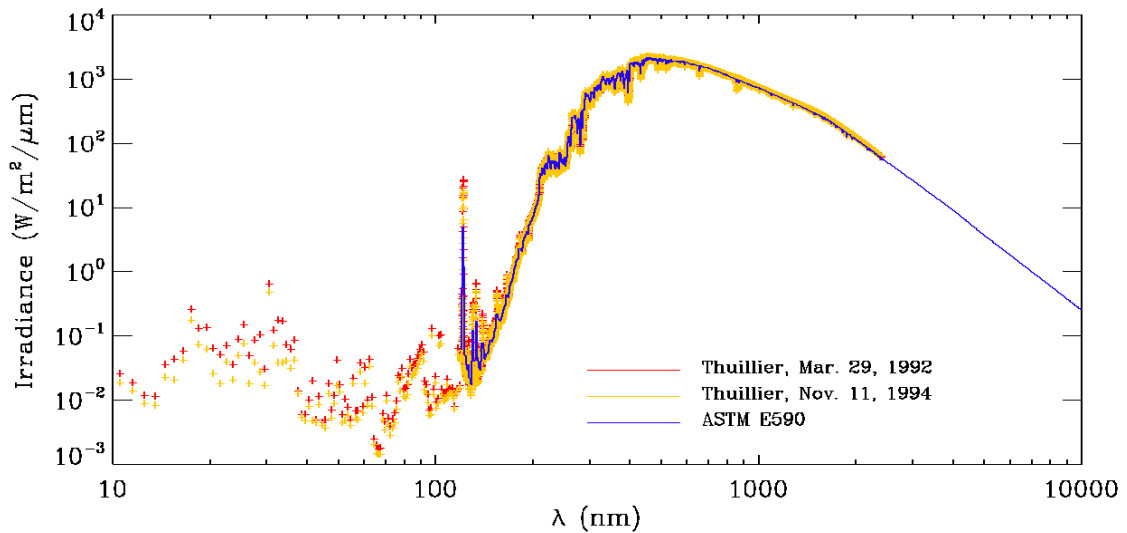
(b) Three models of solar spectral irradiance. **Image taken from** Solar Irradiance - NASA's articles.

Figure 2.2: **Solar spectral irradiance**.

As we said before, knowing the curve of solar emission and the amount of energy radiated by Sun that reaches our planet is important because when this energy comes in the atmosphere, it is absorbed by the **Earth's climate system**. As we said before, **this energy is not completely absorbed:** some part is reflected out to the space and the rest is absorbed. The

amount of reflected incoming energy depends essentially on the composition of the body in which the radiation falls (including atmosphere itself). The ratio of **reflected radiation** over **incoming radiation** is called **albedo A**. Surfaces with **high albedo** are those which reflect high percentage of **incoming radiation**, and we see them as **bright surfaces** (such as snow, ice, bright sand, white clouds). In contrast, surfaces with **low albedo** are those which reflect low percentage of **incoming radiation**, and we see them as **dark surfaces** (such as dark green trees, the ocean, asphalt). As you should have already noticed, the difference between having **high** or **low albedo** lies in the amount of energy absorbed: bodies with **high albedo** absorb less energy than bodies with **low albedo**, and then bodies with **high albedo** are colder than bodies with **low albedo**, which get warmer since they absorb more energy that will be available to raise their temperature (see **Figure 2.3**). Furthermore, after absorbed energy warms the body (clouds, atmosphere, surface of the earth/ice/ocean), this body "re-emits" it, but now at longer wavelengths and lower energy since the temperature of the body is much lower than the Sun.
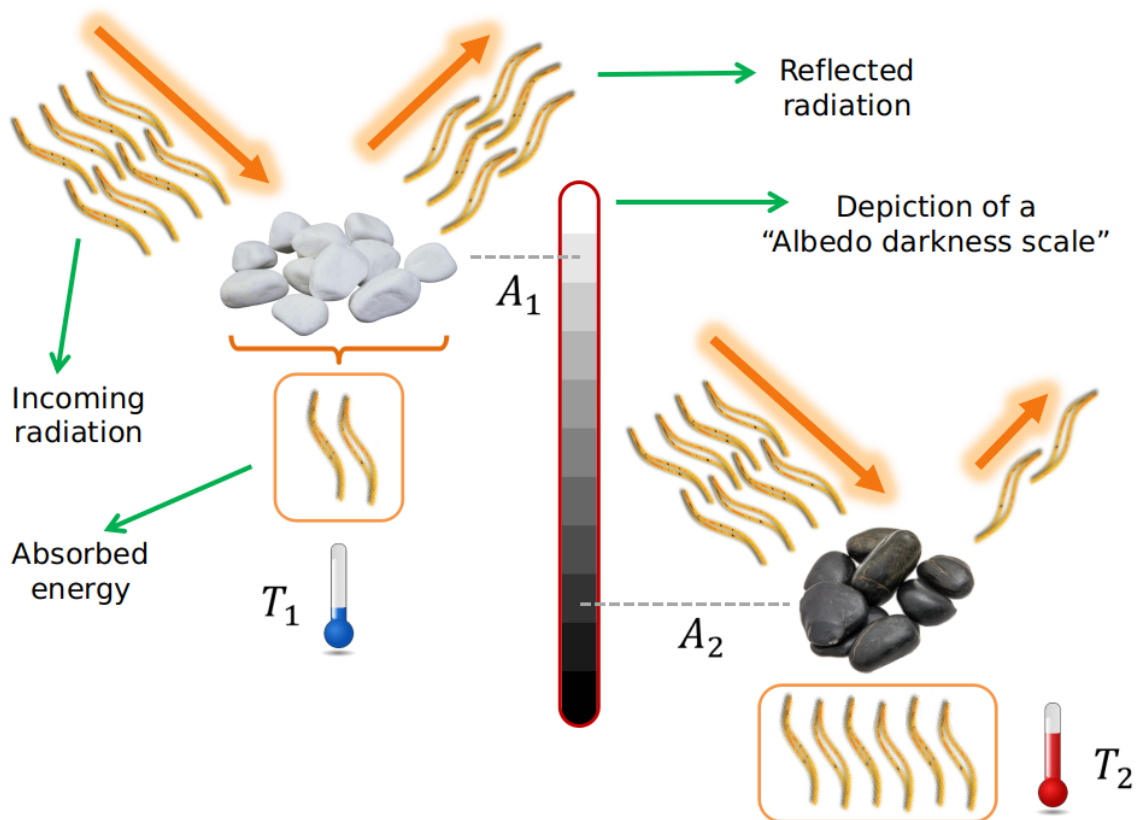
Figure 2.3: **Albedo explanation scheme**. The difference between having **high** or **low albedo** lies in the amount of energy absorbed: bodies with **high albedo** absorbs less than bodies with **low albedo**, and then bodies with **high albedo** are colder than bodies with **low albedo** which get warmer since they absorb more energy that will be available to raise their temperature.

On the other hand, the amount of energy absorbed by any planet also depends on how much energy is incoming from its star. The **irradiation** of a body depends primarily on the strength of its **star's luminosity** –luminosity $L_\odot$ is the total amount of electromagnetic energy emitted per unit of time by a star–, which can be intrinsically variable due to the stellar activity or,

in the long-term scale, the star evolution. The **irradiation** of a body also depends on the **planet's orbital properties** (distance, eccentricity, and spin–orbit tilt) that lead to seasonal and long-term changes, the **planet's rotation rate** (spin) around its axis and, as we said previously, on the planet's albedo.
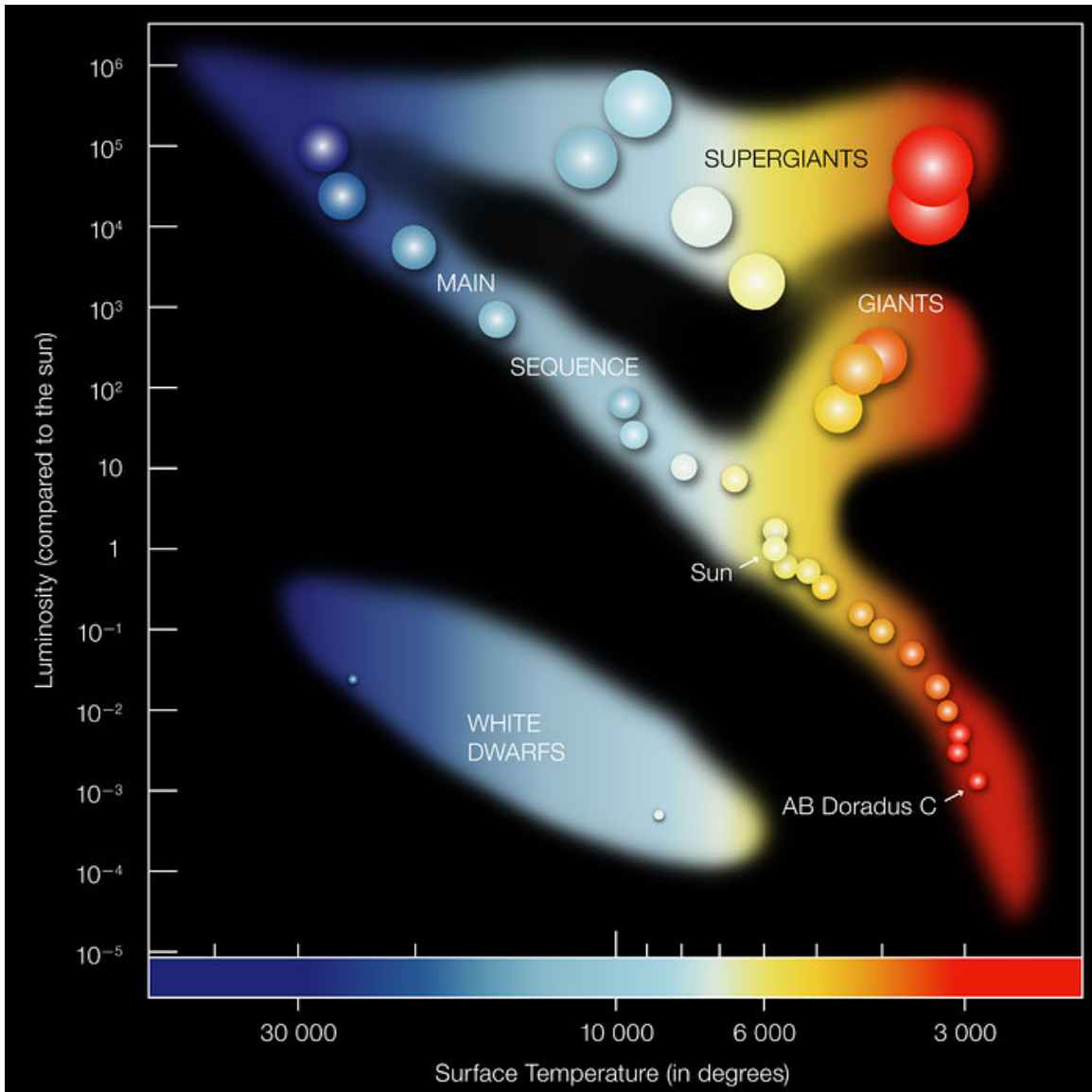
Figure 2.4: **Hertzsprung-Russell diagram**. In the Hertzprung-Russell diagram the temperatures of stars are plotted against their luminosities. The position of a star in the diagram provides information about its present stage and its mass. Stars that burn hydrogen into helium lie on the diagonal branch, the so-called main sequence. Red dwarfs like AB Doradus C lie in the cool and faint corner. AB Doradus C has itself a temperature of about 3,000 degrees and a luminosity which is 0.2% that of the Sun. When a star exhausts all the hydrogen, it leaves the main sequence and becomes a red giant or a supergiant, depending on its mass (AB Doradus C will never leave the main sequence since it burns so little hydrogen). Stars with the mass of the Sun which have burnt all their fuel evolve finally into a white dwarf (left low corner). **Image taken from Hertzsprung-Russell Diagram - European Southern Observatory**.

The classification and evolution of the stars using their physical properties can be done by means

of the "Hertzsprung-Russell diagram", which the relation between luminosity and effective temperature of the star (see **Figure 2.4**). In general, most stars pass a large part of their lifetime in a stable stage called the **main sequence**, converting hydrogen to helium through thermonuclear fusion reactions [19]. The details of the stellar evolution phases before, during, and after the main sequence depend basically on the star mass, and they beyond the scope of this thesis, however it is enough to know that during the main sequence the lifetime also depends on its mass, and in the case of our Sun, it is expected to live for $\sim 10,000 \times 10^6$ years (it has already passed $4,600 \times 10^6$ years on the main sequence). In addition, the long-term luminosity variation of the Sun during its main sequence phase can be represented by the formula:

$$L_\odot(t) \simeq L_\odot(t_0) \left[1 + 0.3 \left(1 - \frac{t}{t_0} \right) \right]^{-1}$$

where $t_0 = 4,500 \times 10^6$ years, is the approximate current age of the Sun and $L_\odot(t_0) = 3.85 \times 10^{26}$ W. On much shorter timescales (from days to years), current changes in the solar luminosity related to its magnetic activity (e.g., sunspots and its 11 year cycle) affect the short wavelength radiation and energetic particle emissions. Variations in the UV irradiance can induce changes in the stratospheric chemistry. This variability can be coupled with intrinsic changes in the magnetic environment of the planet (its own magnetic field) and modulate the cosmic ray flux reaching a planetary atmosphere.

On the other hand, star insolation reaching a planet also depends on the **orbital eccentricity**, and on the **obliquity** (also known as **axial tilt**) [19]. This gives rise, on a short timescale (yearly), to the seasonal radiation and temperature variations. However, the mutual gravitational interaction between the planets leads to a long-term periodic or quasi-periodic variability of their orbital parameters. The geological evidence on Earth and Mars shows the long-term signature (timescales of 10^4–10^6 years) of cyclical temperature changes due to the variability in the incoming solar radiation produced by "orbital cycles". The theory on the cyclical variability of the insolation due to orbital variability is known as **Milankovitch cycles** and it was introduced in the 1920s by Milutin Milankovic, a Serbian astrophysicist who began investigating the cause of Earth's ancient ice ages. The quasi-periodic changes resulting from the gravitational perturbations on the Earth by the planets and the Moon affect the following orbital parameters on a long-term scale: eccentricity, obliquity of the spin axis (see **Figure 2.5**). These kind of orbital variations are also likely to be a generic feature of other planets, with strong implications for the fate of planetary atmospheres (for example, understanding the potential for habitability on other systems).

Nevertheless, Milankovitch cycles are insufficient to explain the full range of ancient climate change, which also requires greenhouse gas and albedo variations, but they are a primary forcing that must be accounted for:

Additional examples of climatic oscillations include the recently discovered millenial-scale oscillation in northern hemisphere temperature (of amplitude 2˚C) (Keigwin, 1996; Bond et al., 1997) and Earth's ice age or glaciation cycles, with a dominant periodicity of 100,000 years and amplitude of 10˚C. Earth's glaciation cycles are commonly attributed to externally forced Milankovitch variations, i.e., small changes in Earth's orbital parameters. However, climate models driven by Milankovitch forcings have had difficulty accurately reproducing the observed cycles, particularly the dominant 100 000 year peak (Ghil and Le Treut, 1981; Pollard, 1982).

— Nevison et al. [11].
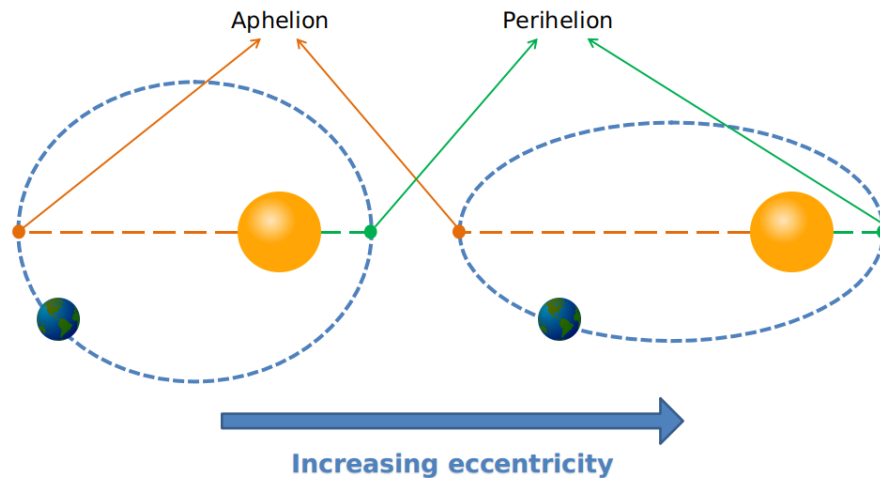
(a) **Eccentricity scheme.** Eccentricity of the Earth's orbit causes the Earth to be slightly closer or farther from the sun during the year. The **aphelion** is the point in the orbit of an object where it is farthest from the Sun. The point in orbit where an object is nearest to the Sun is called the **perihelion**. **Image based on** [20].
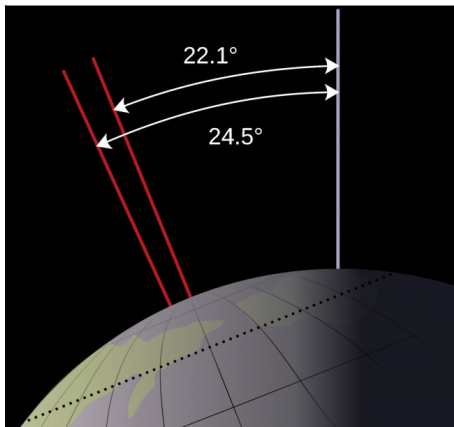
(b) **Axial tilt scheme.** Slight changes in Earth's axial tilt changes the amount of solar radiation falling on certain locations of Earth. **Image taken from** [21].
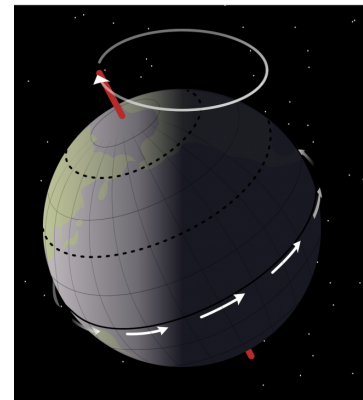
(c) **Precession scheme.** As Earth spins on its axis it wobbles slightly, similar to when a spinning top slows down. This wobble is called precession, and has an affect on seasonal extremes. **Image taken from** [21].

Figure 2.5: **Milankovitch cycles scheme.** The Milankovitch cycles describe how relatively slight changes in Earth's movement affect the amount of solar heat that is incident on the Earth's surface and subsequently influence climatic patterns.

2.2   Gaia theory foundations

In his review article **Gaia and natural selection** [22] of 1998, Timothy M. Lenton sketched what would be considered as *the most faithful summary of foundations of Gaia Theory.*

He highlighted the importance that had *the search for life on other planets* to give birth to the main concepts in this theory. In fact, Lovelock was initially trying to state which kind of physical evidences can be appealed in order to establish the presence of life on a planet, when he realized that **most organisms shift their physical environment away from equilibrium** [23]. Specially, **the presence of abundant life on a planet may be detectable by atmospheric analysis**, because the atmosphere is used by organisms to supply resources and as a repository for wasting products, that in general consist of reactive gases at levels that are different by many orders of magnitude from the photochemical steady states that would be expected in atmospheres forced only by solar ultraviolet radiation [24, 25]. According to Lenton,

> *This perturbed state is remarkable in that the atmospheric composition is fairly stable over periods of time that are much longer than the residence times of the constituent gases, indicating that life may regulate the composition of the Earth's atmosphere. This concept became the foundation of Gaia theory [26].*

> — Timothy M. Lenton [22].

Another key concept, as Lenton remarks, is that the Sun is thought to have warmed by about 25% [27] since the origin of life on Earth, over 3.8 billions years ago [28]. In response of this solar forcing, Earth's surface temperature would have been increased by about 18 °C, however, the surface temperature has remained within life tolerable values, which leads us to think that life would have been involved in regulating the climate, although Walker et al. [29] propose a purely geochemical mechanism to explain this fact. Nevertheless, one cannot simply ignore the fact that environmental conditions, and in particular surface temperature, has remained under favorable values for life in front of forcing and the question for ascertain the role of life in our climate system remains unanswered in a definite way.

Therefore, in a fruitful year (1974), Lovelock and Margulis [30–32] proposed **the Gaia Hypothesys**, which can be sumarized as:

> *Living organisms contribute automatically and unconsciously to self-regulating feedback mechanisms that have kept the Earth's surface environment stable and habitable for life [33, 34].*

And then, **Gaia theory seeks to explain these mechanisms and how they arise**. Gaia theory highlights the fact that environment impose physico-chemical constrains which determines what type of life and how much of it can settle down to available space. On the other hand, life itself alters environment on different scales, including the global scale. So:

One can think the biota and their environment as two elements of a closely coupled system: perturbations of one will affect the other and this may in turn feed back in the original change. The feedback may tend either to enhance or to diminish initial perturbation, depending on whether its sign is positive or negative (see Figure 2.6).

— James E. Lovelock [35].
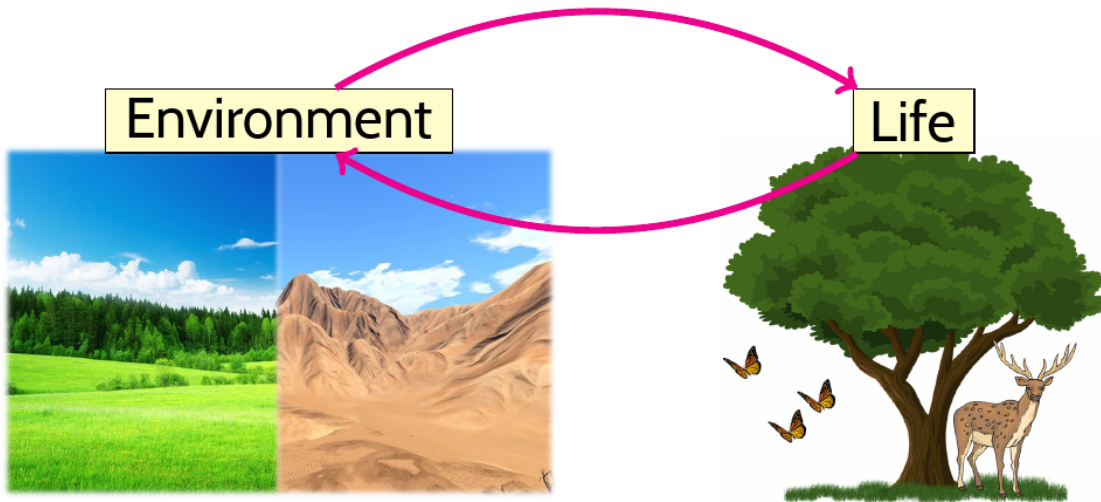
Figure 2.6: **Gaia - Coupled system scheme**. Life and its environment are two elements of a closely coupled system. Changes in one of them affects the other, so we cannot separate them and we must develop insight of them as a whole.

2.3   Daisyworld model

2.3.1   Daisyworld's relevance for Gaia theory

Due to the great complexity involved in studying the coupling of the environment and the complete biota as a whole, and because there are no aspects of their interaction that can be modeled faithfully through any mathematical equation, Lovelock chose to study an artificial world with a biosphere enormously simplified and specifically designed to "display the characteristic in which we are interested –namely, close-coupling of the biota and the global environment" [35]. Before studying the initial model of Lovelock, it is important to highlight, as Lovelock did, that:

This artificial world does not attempt to model the Earth, however, it is an imaginary world that seeks to exhibit a property that is believed important on Earth.

— James E. Lovelock [35]

Then Daisyworld becomes into a mathematical model/device to study biota-climate interactions which contributes to **Gaia theory** foundations.

$$C_p \frac{dT}{d\tau} = \underbrace{SL(1-A)}_{} - \underbrace{\sigma T^4}_{}$$

Absorbed radiation   Emitted radiation

Perfect energy balance:

$$\frac{dT}{d\tau} = 0 \quad \therefore \quad \sigma T^4 = SL(1-A)$$
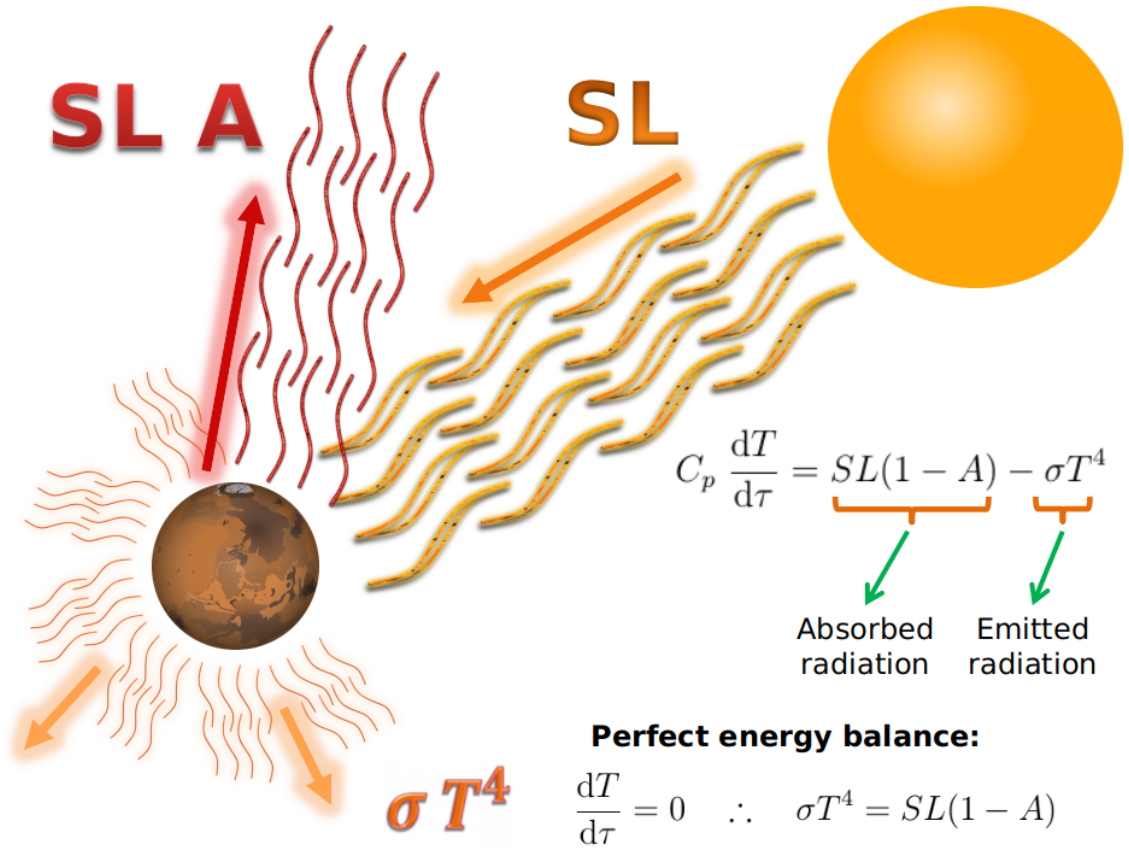
Figure 2.7: **Daisyworld EBM scheme**. **DWL** is perfect energy balanced, then absorbed radiation equals emitted radiation.

2.3.2   Original Daisyworld formulation (DWL)

Lovelock's Daisyworld (DWL) [35], is a mathematical model belonging to **Zero-dimensional EBMs**, and then prognostic climatic variable in Daisyworld is **effective temperature T** of the planet. **DWL** was first formulated as a planet that lacks atmosphere, and therefore of greenhouse effect. Later works –such as *"Role of a simplified hydrological cycle and clouds in regulating the climate-biota system of Daisyworld"* by Salazar, J. F., & Poveda, G. [36] –, included hydrological cycles and other features, but in this discussion we are going to stay faithful with the original model proposed by Lovelock.

The **incoming radiation $R_\star$** from the star can be parameterized as:

$$R_\star = SL$$

where S is the solar constant –i.e. the radiation from Sun incident over planet Earth– and L is a dimensionless parameter that represents the percentage of luminosity of the Daisyworld star $R_\star$ relative to that of our sun S. If we assume that A is the **total albedo** of the planet, then the **reflected radiation $R_{\text{reflected}}$** can be parametrized as:

$$R_{\text{reflected}} = SLA$$

Then, **absorbed radiation** R_i is:

$$R_i = R_\star - R_{\text{reflected}} = SL - SLA = SL(1 - A) \tag{2.4}$$

On the other side, as Daisyworld lacks atmosphere, then **emitted radiation** R_o can be calculated using **Stefan-Boltzmann law** (**Equation 2.3**):

$$R_o = \sigma T^4 \tag{2.5}$$

Then **Equation 2.1** becomes in:

$$C_p \frac{\mathrm{d}T}{\mathrm{d}\tau} = SL(1 - A) - \sigma T^4 \tag{2.6}$$

We have chosen to used time variable τ to describe evolution of T in order to distinguish it from other temporal scales that are important in Daisyworld model –we are going to use the time variable t to describe population dynamics–. Nevertheless, in **DWL** it is assumed that there is **perfect energy balance** (**Equation 2.2**) and last equation for T becomes (see **Figure 2.7**):

$$\frac{\mathrm{d}T}{\mathrm{d}\tau} = 0 \quad \therefore \quad \sigma T^4 = SL(1 - A) \tag{2.7}$$

This planet is inhabited by two types of flowers which are differentiated only by their colors: **black** or **white**. To be exact, what is called *"color"* of the flowers is nothing more than their **albedoes** (refer to **subsection 2.1.2** and **Figure 2.3**). In this sense, Lovelock calls the flowers with a **high albedo** as **"white" flowers** (flowers that reflect much of the incident radiation and their reflectivity is greater than that of their environment), and those with **low albedo** as **"black" flowers** (flowers that absorb most of the radiation that reaches them and their reflectivity is less than that of their surroundings). Due to their albedo, each species modify local temperatures because of their different reflectivities of incident solar radiation, thus **white flowers** have local temperatures colder than their surroundings, whilst **black flowers** have local temperatures warmer than their surroundings. We are going to treat the **white flowers** with the **subscript "1"** and **black** ones with the **subscript "2"**, thus A_1 and T_1 are albedo and local temperature for **white flowers**, while A_2 and T_2 are albedo and local temperature for **black** ones. In addition, bare ground has its own albedo and local temperature too. In **DWL** [35], the whole bare ground is fertile –**fertile ground** is susceptible to be populated by flowers whilst **not fertile** is not–, but in later works like that by Nevison et al. [11], we can find that bare ground can have a part fertile and another not fertile. In this aspect, we are going to follow Nevison's idea, and we will treat the **fertile ground** with the **subscript "F"** and **not fertile ground** with the **subscript "NF"** (see **Figure 2.8**), but in order to remain faithful to **DWL**, we will later assume that the whole bare ground is fertile, as Lovelock did (see **Table 2.3**).

Both types of flowers compete for the available space and their growth rates depend on the local temperatures. We are going to denote as a_1 the fractional area covered by **white flowers** and a_2 the fractional area covered by **black** ones. x will denote the fractional area of **fertile ground** not covered by either species and p the total fractional area of the planet that is fertile ground.
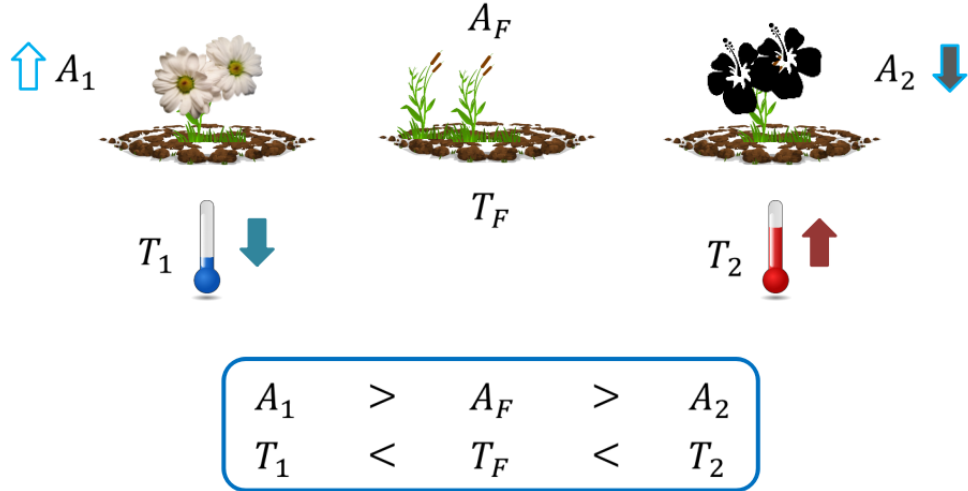
Figure 2.8: **Daisyworld flowers scheme**. **DWL** is inhabited by **white flowers (subscript "1")** and **black flowers (subscript "2")**. Since **black flowers** abosorb more energy than **white flowers**, because black flowers albedo is less than that of white flowers ($A_2 < A_1$), then local temperature of **black flowers** are warmer than that of **white flowers** ($T_2 > T_1$). On the other side, **fertile ground** has an intermediate albedo A_F, and then its local temperature T_F is intermediate too.

Then the fractional area of fertile ground which is uncolonized by flowers is:

$$x = p - (a_1 + a_2) \tag{2.8}$$

and the fractional area of the planet that is **not fertile** is $(1 - p)$ (see **Figure 2.9a**). Now, consider **Equation 2.8**: it poses an important constraint over the system since as we are talking about **areas**, then all p, a_1, a_2 and x must be positive, and so we must demand:

$$(a_1 + a_2) \leq p \tag{2.9}$$

See **Figure 2.9b** for a graphical example in the state space (a_1, a_2). We are going to refer to this space as **population phase space**.

For modelling population dynamics for each species of flowers, and thus changes in a_1 and a_2, Lovelock decided to use an **epidemic model** based on **ordinary differential equations (ODEs)**, which was a model of the invasion process, used first by Carter and Prince [37], in order to explain biogeographical distribution of plants spread, so describing population dynamics through modelling the area covered by population. This model consisted in next set of differential equations:

$$\frac{\mathrm{d}a_i}{\mathrm{d}t} = a_i(x\beta_i - \gamma) \qquad \text{for } i = 1, 2 \tag{2.10}$$
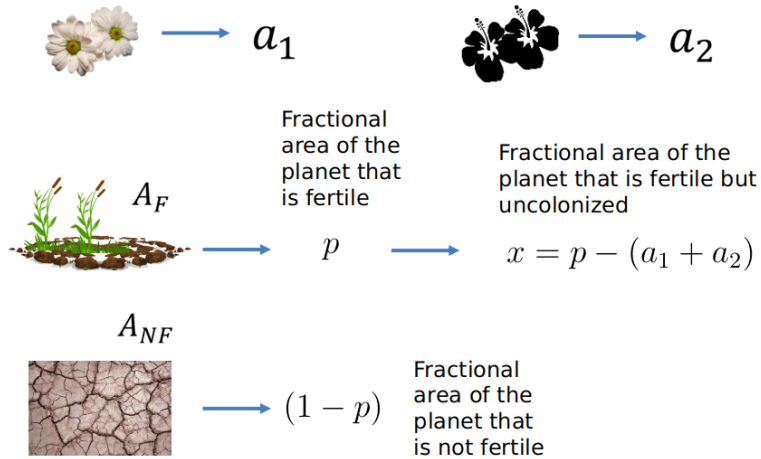
(a) **Daisyworld basic areas scheme**. It shows basic depictions for conceptual definitions of areas in **DWL**.
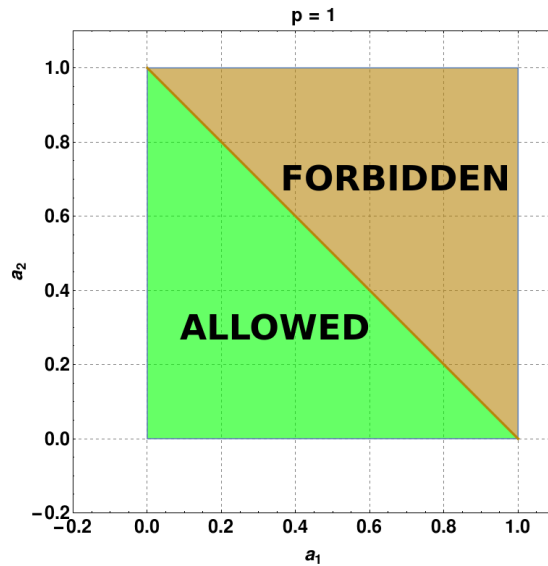
(b) **Daisyworld forbidden areas scheme**. It shows the abstract space (a_1, a_2) and the forbidden and allowed subspaces as determined by **Equation 2.9** for $p = 1$. Forbidden area corresponds to solutions with no biological sense.

Figure 2.9: **Daisyworld areas scheme**. Conceptual depiction for areas in **DWL**.

Equation 2.10 contains two new variables: β_i which is the **growth rate** for species i and γ which can be considered as the **death rate** and it is the same for both species. Although last assumption is not trivial since in fact it is more probable to have different death rates for different species –depending on, for example, their adaptation to environment or resources availability–, we must remark that in order to simplify the complexity of the system, it is sensible to assume that both death rates are equal.

At this point, it is important to discuss a fundamental characteristic of the functional form that Lovelock proposes for the growth rates of the flowers (see **Figure 2.10**). Lovelock expresses that "a sharp curve of the rate of growth as a function of temperature is a fundamental property of living things". According to this, the function for the growth rate must have a maximum that must correspond to the **optimum temperature** T_{opt} for flowers growing. The pointy function proposed by Lovelock is a parabola dependent on the local temperature T_i and centered on $T_{opt} = 295.5$ K, which becomes zero for T_i values outside the interval $(278.15\text{ K}, 313.15\text{ K})$:

$$\beta_i = \max\left[0,\ 1 - \left(\frac{T_{opt} - T_i}{17.5\text{ K}}\right)^2\right] \tag{2.11}$$

In this way, Lovelock intends to model that deviations of T_i with respect to T_{opt} would lead the flowers to have either lower growth rates or no growth rates at all. Although this approach to β_i is unrealistic because it neglects the possibility of adaptation of species to variable environmental conditions, i.e. it assumes T_{opt} fixed and don't take into account the possibility that "T_{opt} evolves", this discussion would cause us to depart from the purpose of this thesis. A good reference for starting the discussion on this topic is the article **"Daisyworld is Darwinian: constraints on adaptation are important for planetary self-regulation"** [38].
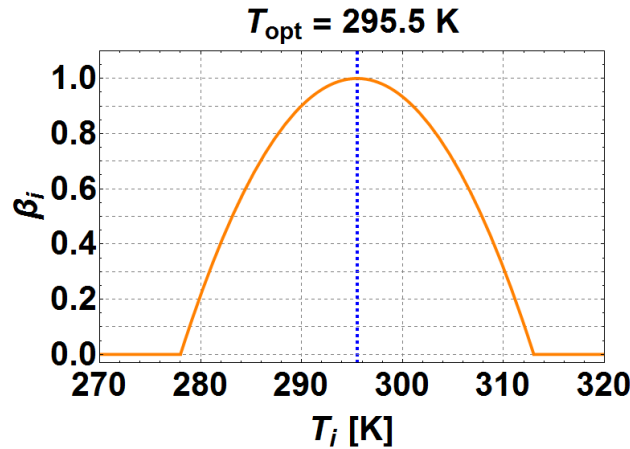
Figure 2.10: **Daisyworld growth rate scheme**. The pointy function proposed by Lovelock is a parabola dependent on the local temperature T_i and centered on $T_{opt} = 295.5$ K, which becomes zero for T_i values outside the interval $(278.15\text{ K}, 313.15\text{ K})$.

Having seen how to determine changes in a_1 and a_2, the next step in the model is to establish a relationship between population changes and climate. This coupling is achieved by means of **total albedo**, which is calculated as a sumatory of system's albedos, weighted with its corresponding areas (see **Figure 2.11**):

$$A = (1 - p)A_{NF} + xA_F + \sum_i a_i A_i \tag{2.12}$$

Finally, as we have stated before, we have $A_1 > A_F > A_2$, hence, according to the amount of energy absorbed by the corresponding areas with these albedos, we must have:

$$T_1 < T_F < T_2 \tag{2.13}$$

Daisyworld
most populated
with black flowers

Daisyworld
sparsely
populated

Daisyworld
most populated
with white flowers

$A \approx A_2$

$A \approx A_F$

$A \approx A_1$
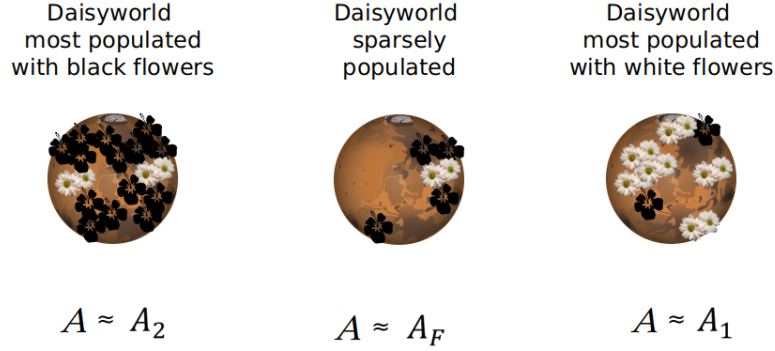
Figure 2.11: **Daisyworld population example**. It shows how **total albedo** fits according to how Daisyworld is populated.

Until now, we lack of an equation for calculating theses temperatures. Lovelock realized that any equation that is proposed to calculate the value of the temperatures T_i must fulfill last condition and must also preserve the balance of the energy emitted by the planet, that is, it must be fulfilled that the radiation flux F that is emitted by the planet is equal to σT^4. Additionally, F must be equal to the sum of the fluxes emitted by each area of the planet, that is:

$$F = \sum_j F_j = \sum_j \sigma T_j^4 \qquad \text{for } j = NF, F, 1, 2 \tag{2.14}$$

Lovelock proposes that T_j should be calculated as:

$$T_j^4 = Q(A - A_j) + T^4 \qquad \text{for } j = NF, F, 1, 2 \tag{2.15}$$

With last equation, **Equation 2.13** is fulfilled, and in addition we have for **Equation 2.14**:

$$F = \sum_j \sigma T_j^4 = \sigma Q A \sum_j a_j - \sigma Q \sum_j (a_j A_j) + \sigma T^4 \sum_j a_j = \sigma T^4$$

Where we have taken into account that in this notation:

$$\sum_j a_j = \underbrace{a_{NF}}_{(1-p)} + \underbrace{a_F}_{x=p-(a_1+a_2)} + a_1 + a_2 = (1-p) + (p - (a_1 + a_2)) + a_1 + a_2 = 1$$

And in the same manner (but briefly):

$$\sum_j (a_j A_j) = A$$

We are going to discuss the role of Q in **Equation 2.15**. From **Equation 2.7** we have:

$$A = 1 - \frac{\sigma}{SL} T^4$$

Substitution of A in **Equation 2.15** leads to:

$$T_j^4 = Q(1 - A_j) + \left(1 - Q\frac{\sigma}{SL}\right) T^4$$

34

Then if $Q = 0$:

$$T_j^4 = T^4$$

which corresponds to a situation of *perfect conduction of energy from regions with high temperature to regions with low temperature*, since all temperatures are equal to T. On the other hand, if we have $Q = SL/\sigma$:

$$T_j^4 = \frac{SL}{\sigma}(1 - A_j)$$

which corresponds to a situation of *perfect insulation between regions with different temperature*, since temperature of each region is determined by means of a perfect energy balance between locally absorbed energy and emitted energy in form of radiation. Situations in which $Q > SL/\sigma$ imply that enegy conduction is performed from regions of low temperature to regions of high temperature, and this corresponds to situations that are not physically plausible. Thus, the interval of allowed values for Q are:

$$0 \quad \leq \quad Q \quad \leq \quad \frac{SL}{\sigma}$$

where to greater Q corresponds greater thermal insulation between regions with different temperature. Now, in **DWL**, Lovelock preferred to use a lineal aproximation to **Equation 2.15**:

$$T_j = q(A - A_j) + T \qquad \text{for } j = NF, F, 1, 2 \tag{2.16}$$

where:

$$q = \frac{Q}{4T_{opt}^3}$$

According to Lovelock, this aproximation introduces an error of 2 K for the range of temperatures of interest. The interval of allowed values for q are (taking $T_{opt} = 295.5$ K as Lovelock did):

$$0 \quad \leq \quad q \quad \leq \quad \frac{SL}{4\sigma T_{opt}^3}$$

The complete set of equations for DWL, the definition of its variables as well as of its parameters and their values are summarized in **Table 2.1**, **Table 2.2** and **Table 2.3**.

A final remark which deserves our attention must be done for **Equation 2.7**:

> **Remark 1**
>
> As we explain in **subsection 2.1.1**, **perfect energy balance** described by **Equation 2.1** –and then by **Equation 2.7**– stands for a situation where the equilibrium solution of the equation **Equation 2.1** –and hence **Equation 2.6**– has been achieved, i.e. **the change in temperature has ceased because enough time has elapsed so that outgoing radiation has equated to that absorbed**.

Now it should be clear why we decided to used time variable τ to describe evolution of T and to distinguish it from time variable t in which population dynamics occurs. The sentence in bold above means that the time variable τ changes faster than t, so in the temporal scale t of the flowers population, the equilibrium solution is achieved almost instantaneously. Thus, when a_1 or a_2 changes, $T(\tau)$ changes too, and we can describe T as function of t: $T(t)$.

Original Daisyworld (DWL) equations	
$\sigma T^4 = SL(1 - A)$	Perfect energy balance for climate system
$x = p - (a_1 + a_2)$	
$\dfrac{\mathrm{d}a_i}{\mathrm{d}t} = a_i(x\beta_i - \gamma)$ for $i = 1, 2$	Population dynamics $a_i(t)$ using ODEs
$A = (1 - p)A_{NF} + xA_F + \sum_i a_i A_i$	Coupling between population dynamics $a_i(t)$ and total albedo A
$\beta_i = \max\left[0,\ 1 - \left(\dfrac{T_{opt} - T_i}{17.5\ \mathrm{K}}\right)^2\right]$	Flowers growth rate which is coupled to local temperatures T_i
$T_j = q(A - A_j) + T$ for $j = NF, F, 1, 2$	Coupling between effective temperature T of the planet and local temperatures T_j for regions with different albedos

Table 2.1: **Original Daisyworld (DWL) equations**. Set of equations used by Lovelock in [35].

Original Daisyworld (DWL) variables	
$T(t)$	Prognostic variable for climate system temperature
$A(t)$	Total albedo (mean albedo) of the planet
$a_1(t)$	Fraction of fertile ground area populated by flowers of species 1
$a_2(t)$	Fraction of fertile ground area populated by flowers of species 2
$x(t)$	Fraction of fertile ground area which is not populated by either species of flowers
$\beta_i(t)$	Flowers growth rate which is coupled to local temperatures T_i
$T_j(t)$	Local temperature for regions with of the type $j = NF, F, 1, 2$

Table 2.2: **Original Daisyworld (DWL) variables**. Set of variables of the system of equations summarized in **Table 2.1**.

Original Daisyworld (DWL) parameters			
Parameter	**Value**	**Units**	**Meaning**
σ	1789.44	erg cm^{-2} yr^{-1} K^{-4}	Stefan-Boltzmann law constant
S	2.89×10^{13}	erg cm^{-2} yr^{-1}	Solar constant
γ	0.3	yr^{-1}	Flowers death rate
p	1	Dimensionless	Total area of fertile ground
q	20	K	Conduction energy coefficient
A_{NF}	0.5	Dimensionless	Not fertile ground albedo
A_F	0.5	Dimensionless	Fertile ground albedo
A_1	0.75	Dimensionless	White flowers albedo
A_2	0.25	Dimensionless	Black flowers albedo
T_{opt}	295.5	K	Flowers growth optimum temperature
L		Dimensionless	Percentage of luminosity of the Daisyworld star $R_\star$ relative to that of our Sun S

Table 2.3: **Original Daisyworld (DWL) parameters**. Set of parameters of the system of equations summarized in **Table 2.1** and their corresponding values as used by Lovelock [35]. Note that Lovelock assumed the whole bare ground to be fertile, then $p = 1$. Parameter L appears without a designated value because it is used by Lovelock as a parameter to perform sensitivity test.

2.3.3   Original Daisyworld results

In his seminal paper [35], Lovelock solved the set of equations summarized in **Table 2.1** and, based on the solutions obtained, he presented several ideas which served as conceptual basis for studies on feedback mechanisms for regulating climate; but one result became fundamental for stating the potential **biological homeostasis of the global environment**: *Lovelock showed that, provided a luminosity L, this system of equations exhibit a steady state with an effective temperature T, shifted from that of a dead planet, and near to T_{opt}, so promoting the maximum population of any type of flowers allowed under those conditions. He also showed that there exists remarkable steady states where both species of flowers coexist and the effective temperature T will actually **decrease** in response to an **increase** of star luminosity, i.e. an increase of L. He assumed that the process of increasing L is slow, so that the system has time to reach steady state at each value of L.* So:

The exact value for $\mathrm{d}T/\mathrm{d}L$, in this steady states where both flowers coexist, is:

$$\frac{\mathrm{d}T^*}{\mathrm{d}L} = -\frac{q\sigma T^*}{4SL^2\left(1 - \frac{q\sigma}{SL}\right)}$$

where the asterisks denotes the steady state for coexistence. Last equation must be negative provided that $q < SL/\sigma$. **Figure 2.12** shows this result. Even more, Lovelock even proved that for this steady state where both species of flowers coexist, their local temperatures are constant regardless of the initial conditions of both populations:

$$\mathbf{T_i^*} \rightarrow \begin{cases} T_1^* &=& T_{opt} - \frac{1}{2}q\left(A_1 - A_2\right), \\ \\ T_2^* &=& T_{opt} + \frac{1}{2}q\left(A_1 - A_2\right). \end{cases}$$
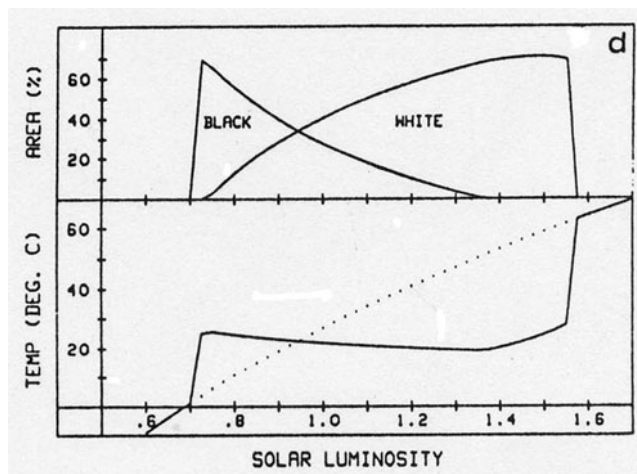
Figure 2.12: **Daisyworld original result**. It shows the behaviour of the complete model and exhibits the expected stable region where the two species of flowers coexist and verifies Lovelock's prediction of a decrease in effective temperature T with increasing luminosity L, i.e. $\mathrm{d}T/\mathrm{d}L < 0$ when both species coexist. Dotted line represent the temperature of a dead planet. **Image taken from [35]**.

So, one can venture to say that Lovelock understood biological homeostasis as:

> ### Concept 1: Biological homeostasis of the global environment
>
> **Biological homeostasis of the global environment** is the conjecture that there exists mechanisms in the interaction biota-climate which allow to emerge a **steady state** with environmental conditions away from those expected in a dead planet, and that are near life suitable values, even under forcings which would cause environmental conditions non suitable for life.

2.3.4 Unraveling DWL

(a) **DWL steady values of T as function of L.**

(b) **DWL steady values of T as function of L and coexistence region**.

(c) **DWL steady values of a_i as function of L.**

(d) **DWL steady values of a_i as function of L and coexistence region**.
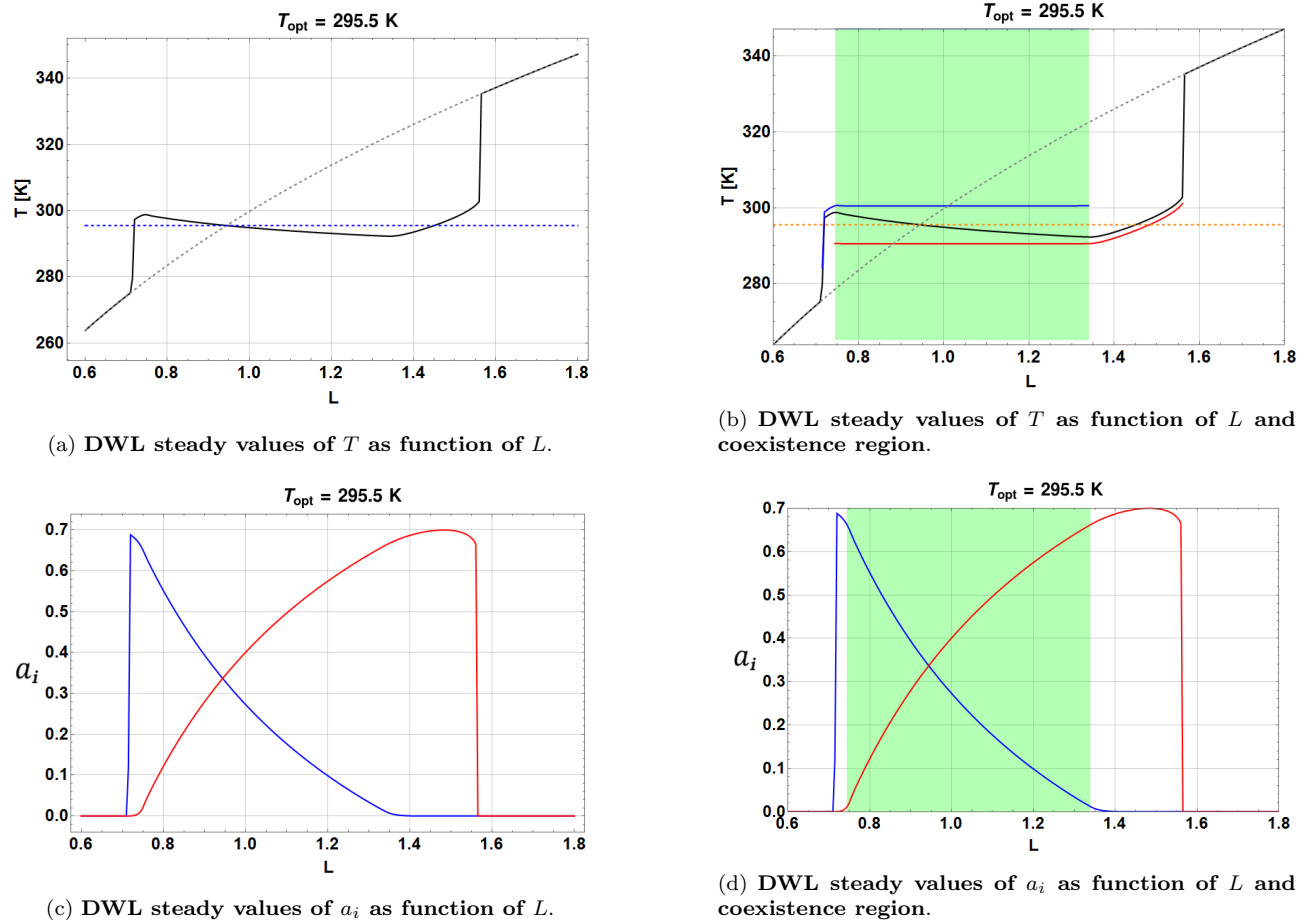
Figure 2.13: **DWL steady values of T and a_i as function of L**. **(a) DWL steady values of T as function of L**: **Black** line corresponds to effective temperature T for DWL model. Dotted gray line corresponds to effective temperature T for a planet without any flower (a **dead planet**). Dotted blue line corresponds to the value of $T_{opt} = 295.5$ K. **(c) DWL steady values of a_i as function of L**: Red line corresponds to the value of white flowers area a_1 whilst Blue line corresponds to the value of black flowers area a_2. **(b) DWL steady values of T as function of L and coexistence region**: The same as **(a)** but Dotted orange line corresponds to the value of $T_{opt} = 295.5$ K. Red line corresponds to the value of white flowers local temperature T_1 whilst Blue line corresponds to the value of black flowers local temperature T_2, and it can be seen that their difference is constant. In **(b)** and **(d)**, we have highlighted with a green shadow the region where both species of flowers coexist. From **(b)** it can be seen graphically that $\mathrm{d}T/\mathrm{d}L < 0$ when both species coexist.

Figure 2.13 shows solutions for **DWL**. The process to produce them, as described by Lovelock [35], is a kind of **sensitivity test**:

Concept 2: Sensitivity test in DWL

In a **sensitivity test**, modellers examine the behaviour of their modelled climate system by altering one component and studying the effect of this change on the model's steady state.

In **DWL**, the **sensitivity test** is intended to trace the path followed by the temperature of the steady state and is performed using next procedure: *for a fixed value of L, the initial conditions of a_1 y a_2 are taken equal to steady values of the previous value of L, but if previous values are zero, then the initial value is taken to be equal to* 0.01. *Then system of equations of DWL (**Table 2.1**) are integrated until the new steady state is reached. Afterwards, L is increased and the process is repeated again.*

Other initial conditions can be used, but as there exists some L for which the system has multistability, then it exhibits hysteresis and the initial condition determines which steady state it will end up.

In this way, Lovelock modelled the process in which star luminosity $R_\star$ increases slowly in such a way that flowers have enough time to reach steady states for each value of L.

As we are dealing with steady states, it is more illuminating to draw up a **bifurcation diagram** and some **phase portraits** where we sketch vectorial flux of the system in the **population phase space**. Remember that a the qualitative structure of this vectorial flux can change whenever parameters values are changed, i.e. fixed points can appear or disappear, or its stability can change. The latter is also true for other more complex structures such as limit cycles or chaotic attractors. In our case, it is of interest to know **how stability of fixed points changes as function of** L, because we will see that system of equations of DWL (**Table 2.1**) only allows dynamics of fixed points.
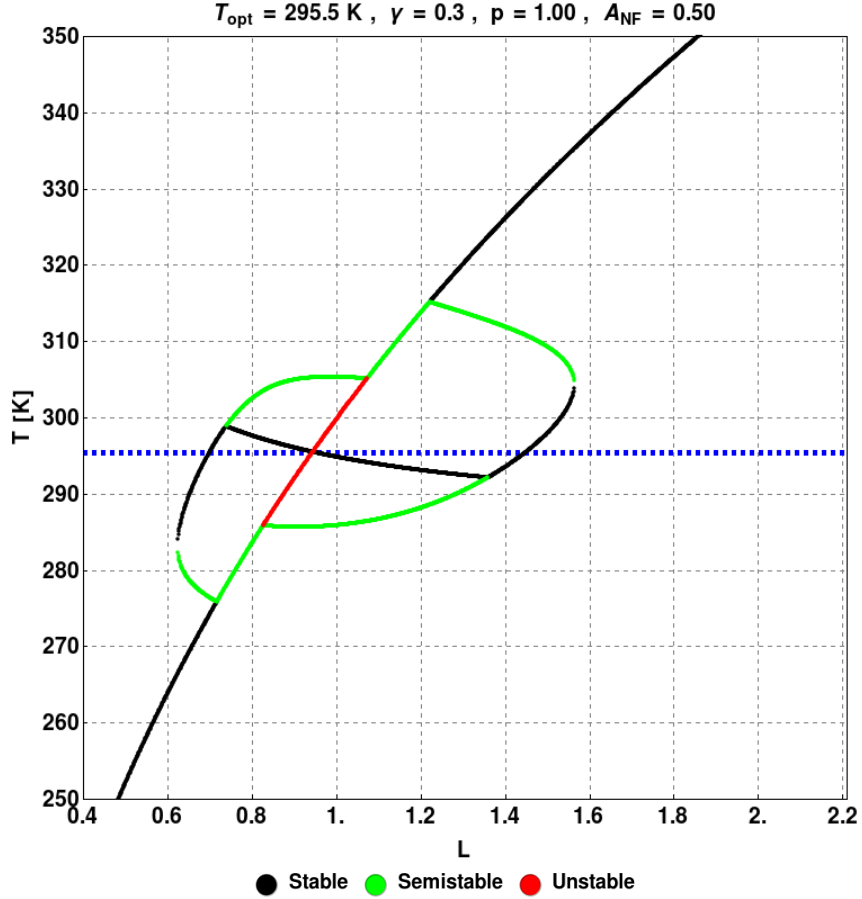
Figure 2.14: **DWL bifurcation diagram**. It shows the behaviour of effective temperatures T of all possible fixed points of the system of equations of DWL (see **Table 2.1**). Dotted blue line corresponds to the value of $T_{opt} = 295.5$ K. Values of L where curve separates or coalesces are known as **bifurcation points**. We have separated by means of colors the temperatures corresponding to fixed points of different stability.

From **Figure 2.14** it is clear that **homeostasis** in DWL is achieved thanks to the existence of a **global stable node**. We refer to the **stable node** where both species coexist, which is the one which appears inside allowed regions for L in the interval $(0.740, 1.359)$. We can see the route in **phase portrait** followed by this point in next figures: **Figure 2.16b**, **Figure 2.16c**, **Figure 2.16d**, **Figure 2.17a**, **Figure 2.17b**, **Figure 2.17c**, **Figure 2.17d** and **Figure 2.18a**. From **Figure 2.14**, **Figure 2.15**, **Figure 2.16**, **Figure 2.17** and **Figure 2.18**, we can conclude that:

- DWL dynamics is characterized by multistability (see **Figure 2.15c** or **Figure 2.17d**), and thus te system can exhibit hysteresis [39].

- Semistable points, also named as saddles, only exist over axis a_1 or a_2, and then they correspond to solutions where only one species survive.

- The special luminosity $L = 0.944$ is the critical one where effective temperature of fixed point of coexistence and effective temperature of the death planet are the same and equal to $T_{opt} = 295.5$ K.
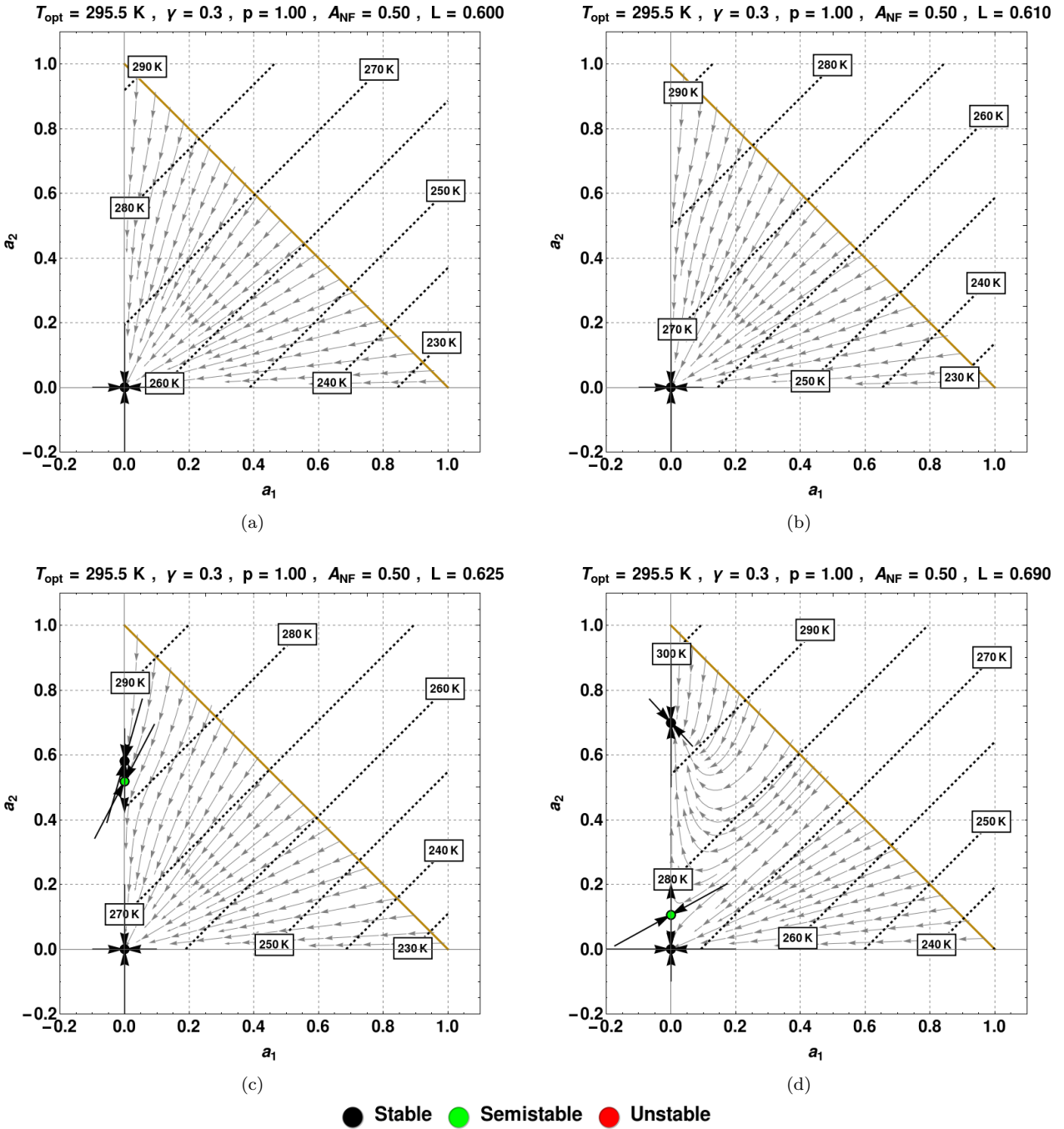
Figure 2.15: **DWL phase portraits**. It shows phase portraits for different values of L. It also shows effective temperature T contour lines in steps of $\Delta T = 10$ K. It can be seen how bifurcations reported in **Figure 2.14** occurs.
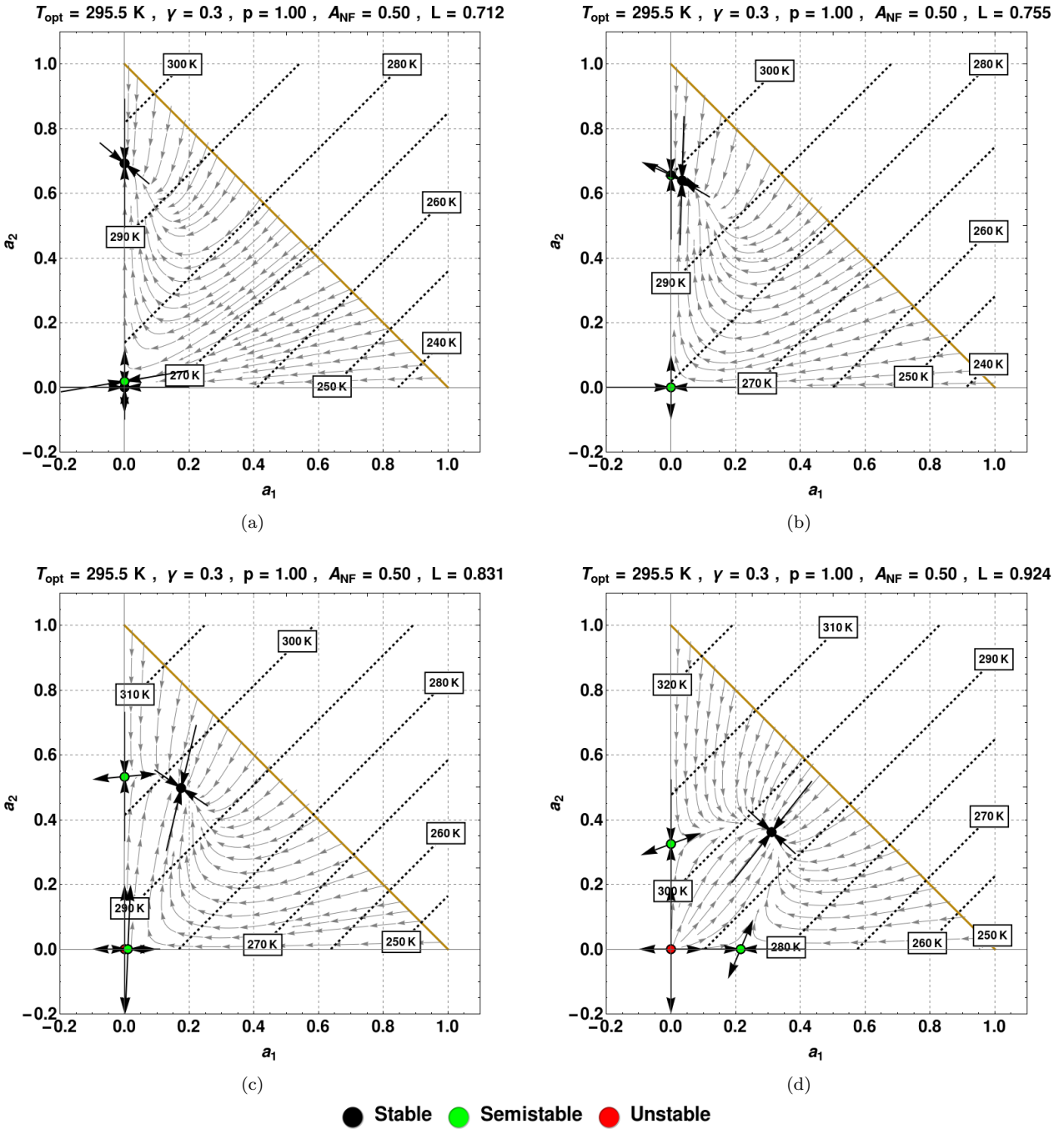
Figure 2.16: **DWL phase portraits**. It shows phase portraits for different values of L. It also shows effective temperature T contour lines in steps of $\Delta T = 10$ K. It can be seen how bifurcations reported in **Figure 2.14** occurs.
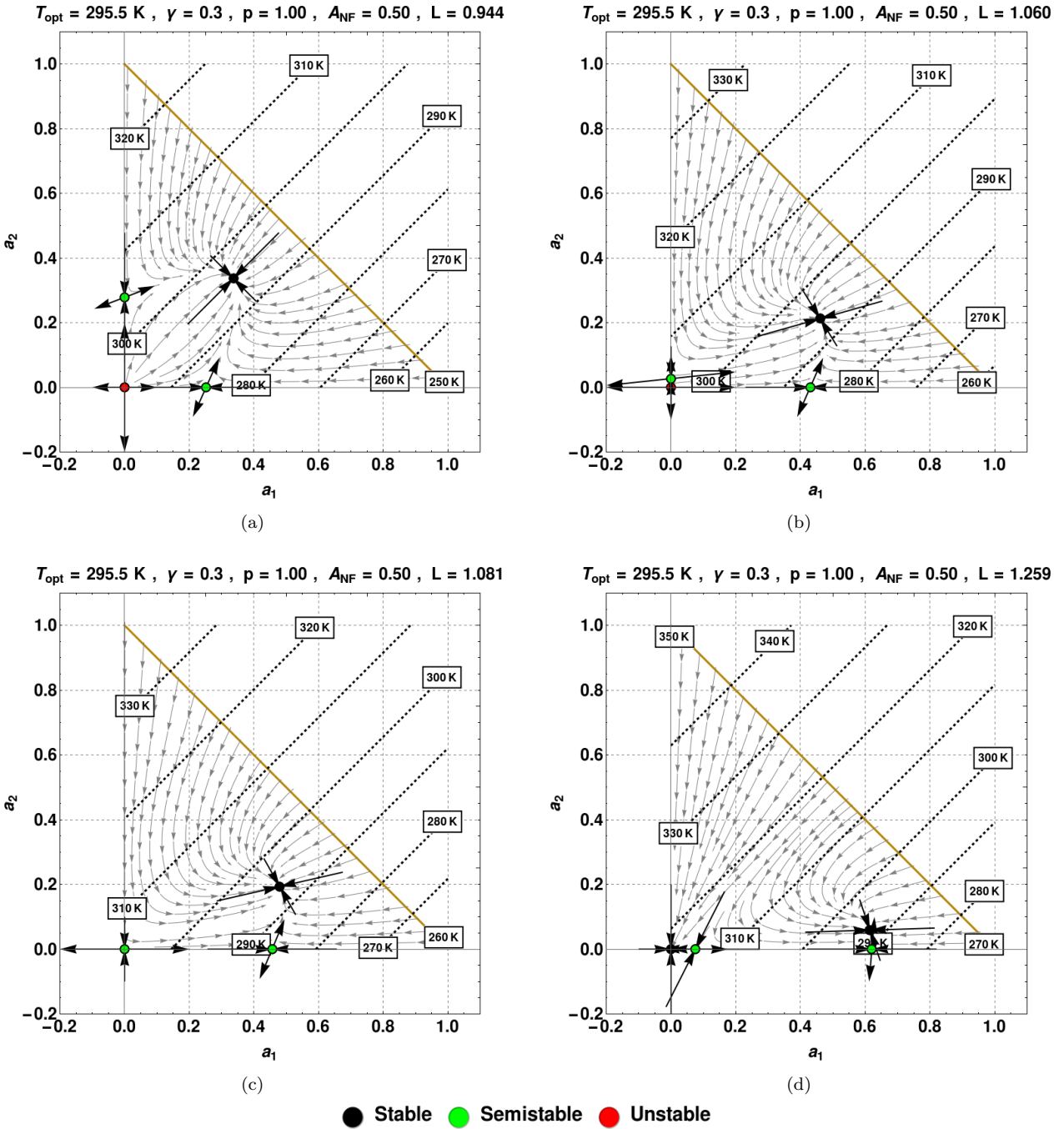
Figure 2.17: **DWL phase portraits**. It shows phase portraits for different values of L. It also shows effective temperature T contour lines in steps of $\Delta T = 10$ K. It can be seen how bifurcations reported in **Figure 2.14** occurs.
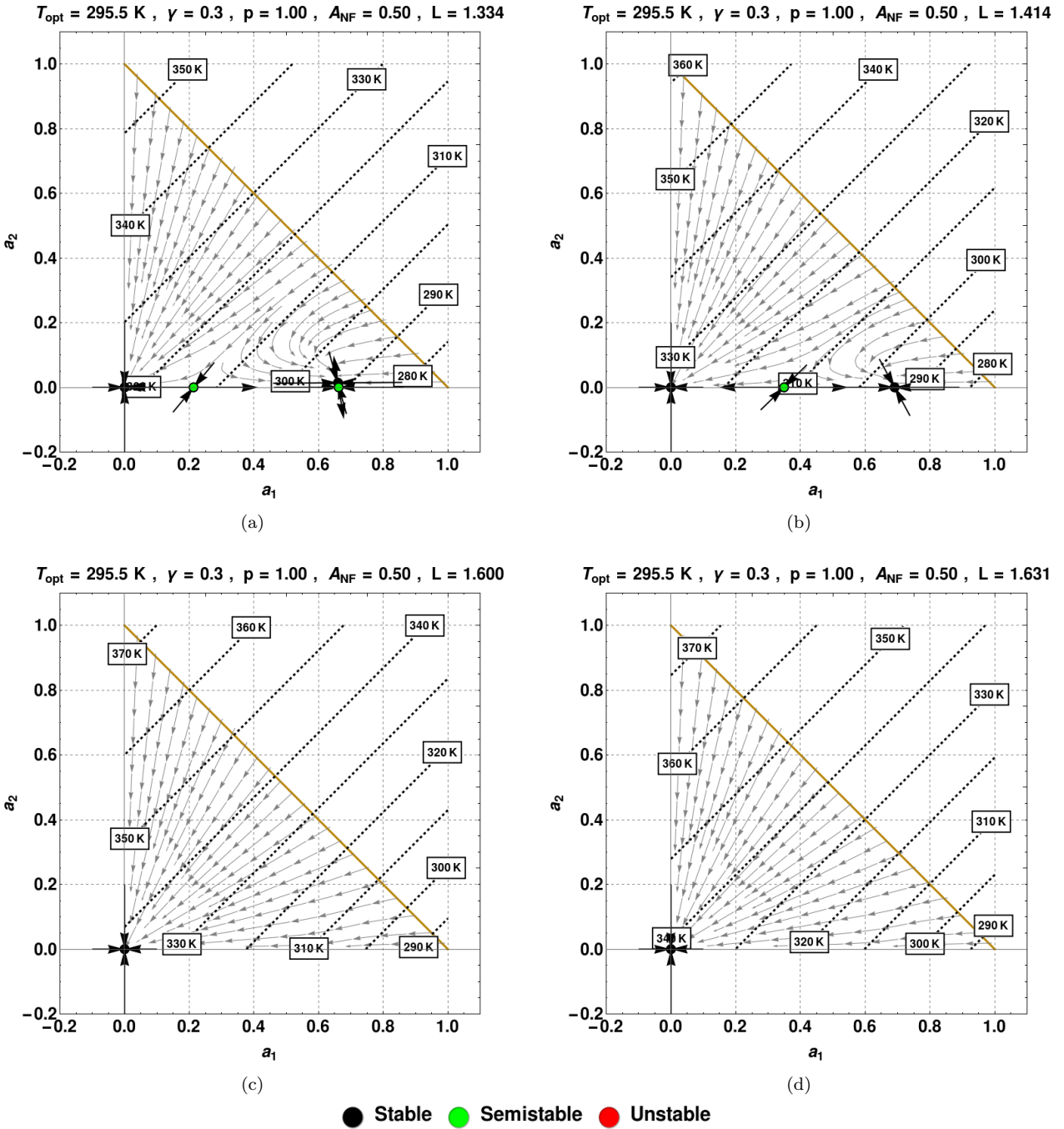
Figure 2.18: **DWL phase portraits**. It shows phase portraits for different values of L. It also shows effective temperature T contour lines in steps of $\Delta T = 10$ K. It can be seen how bifurcations reported in **Figure 2.14** occurs.

2.4   Possibility of Chaos in Daisyworld

As we saw in **subsection 2.3.4**, DWL model is governed by dynamics of fixed points and multistability. The most striking behaviour we can expect is the presence of hysteresis. Nevertheless, it is due to this dynamics of fixed points and the presence of a **global stable node** in the **population phase space** for a wide range of luminosities L, and its location near T_{opt} contour line, that the system exhibits what Lovelock called the **biological homeostasis of global environment**, i.e. the fact that population dynamics promotes that environmental conditions remain near life suitable values and away from those expected in a dead planet, even under forcing which would cause environmental conditions non suitable for life.

In 1990, Xubin Zeng and R. A. Pielke, from *Department of Atmospheric Science, Colorado State University*, in addition to R. Eykholt, from *Department of Physics, Colorado State University*, started from DWL model [35] to study the interaction between biota and their environment in more detail. They used a forward-difference scheme to assert that DWL model [35] must be discretized. By doing this, they found that periodic states, and even **chaotic states**, emerge when a new parameter controlling the feedback between biota and environmental temperature is included in the model. These results showed that stable climatic conditions are not always maintained in Daisyworld, despite the presence of daisies which supply the required feedback that should stabilize climatic conditions, as Lovelock proposed. Then they said:

> *While Daisyworld is a simple model, the mathematical analysis of this model raises questions about the validity of the **Gaia hypothesis**.*
>
> — Zeng et al. [2].

mathematical analysis raised questions about the validity of **Gaia hypothesis** [2].

2.4.1   What is "Chaos"?

Strogatz defines it as [40]:

> *Chaos is aperiodic long-term behaviour in a deterministic system that exhibits sensitive dependence on initial conditions.*
>
> — Strogatz [40]

The three primary characteristics of this definition are:

Cond-1 **To be a <u>deterministic system</u>**, that is a system in which the later states of the system are determined from the earlier ones, and so, the equations of motion (i.e. mathematical rules for evolution of the system) are completely determined. In contrasts, a **stochastic** or **random system** is one in which mathematical rules relating future states from previous ones involves some sort of uncertainty.

Cond-2 **To have <u>aperiodic long-term behaviour</u>**, which means that there are solutions of the system that, in long-term, don't behave periodically or quasiperiodically, neither settle down to a fixed point. The best technique to test this requirement is to perform an analysis of **power spectra** of time series produced by the system. The **chaotic** behaviour is characterized by the presence of a **broadband noise**. Indeed, the only problem with this test is that it cannot discriminate between **noise (stochastic deviations in variables)** and **chaos**.

Cond-3 **To exhibit <u>sensitive dependence on initial conditions</u>**, that is to say that trajectories starting very close together will rapidly diverge from each other, and thereafter have totally different futures. The practical implication is that long-term prediction becomes impossible in a system like this –despite being deterministic–, where small uncertainties are amplified enormously fast, thus, in a very real sense, chaotic systems are unpredictable in long-term. The best technique to test this requirement is corroborate if the system has a **positive Lyapunov exponent**.

The **Lyapunov exponent λ** is statistical measure of the divergence (or convergence) of nearby trajectories in phase space, so it is referred as a predictability loss measure. According to the value of the Lyapunov exponent we can have the next situations:

- **$\lambda > 0$**: it corresponds to a system which exhibit divergence of nearby trajectories. The greater the value of λ, the dramatically divergent are the trajectories, and so the faster the predictability in the system is lost.

- **$\lambda = 0$**: it corresponds to a system in which trajectories don't diverge and neither converge, so their distance in phase space remains constant.

- **$\lambda < 0$**: it corresponds to a system in which exhibit convergence of nearby trajectories. It is the opposite case of $\lambda < 0$

A system with n dimensions –n is the **euclidean dimension** of the system– has n **Lyapunov exponents**. So, if the system is described by 2 diagnostic variables (euclidean dimension = 2), then it has 2 Lyapunov exponents. The values of the **Lyapunov exponents** are in general different, but to confirm the existence of **chaos** in the system, one only needs to test if at least one of them is **positive**, so if one organizes the **Lyapunov exponents** in descending order:

$$\lambda_{n \equiv \max} > \lambda_{n-1} > \cdots > \lambda_{1 \equiv \min}$$

and $\lambda_{\mathbf{max}}$ then the system exhibit dependence on initial conditions. The algorithm to calculate $\lambda_{\mathbf{max}}$ can be found in [41].

A final remark on **chaotic systems** is that it often show the existence of an **strange attractor** in phase space. An **attractor** is a closed set Γ with the following properties [40]:

Prop-1 Γ is invariant, in the sense that any trajectory which start in Γ starts in Γ for all time.

Prop-2 Γ attracts an open set of initial conditions, that is to say that there exists an open set Ω which tends to Γ as $t \to \infty$, i.e. that Ω is attracted to Γ. The largest such Ω is called the **basin of attraction** of the attractor Γ.

Prop-3 Γ is minimal, in the sense that there is no proper subset of Γ that satisfies item **Prop-1** and item **Prop-2**.

The last definition holds for fixed points, limit cycles, quasiperiodic sets or chaotic attractor sets. Now, a **strange attractor** is the one that exhibits sensitive dependence on initial conditions, i.e. a chaotic attractor set. **Strange attractors** were originally called strange because they are often **fractal sets**:

> *Roughly speaking, fractals are complex geometric shapes with fine structure at arbitrarily small scales. Usually they have some degree of self-similarity. In other words, if we magnify a tiny part of a fractal, we will see features reminiscent of the whole. Sometimes the similarity is exact; more often it is only approximate or statistical.*

— Strogatz [42]

Now, we can measure the complexity of the fractal by means of its **fractal dimension**. This dimension can be seen as the measure of the tendency of the fractal to fill the space. The **euclidean dimension** ζ is the number of independent variables of the system –not to be confused with parameters–, while **fractal dimension** ν is the minimum number of coordinates needed to describe every point in the fractal set. For instance, a smooth curve is one-dimensional because every point on it is determined by one number (the arc length from some fixed reference point on the curve). And we have that:

$$\nu \leq \zeta$$

In general, when **fractal dimension** of some set is fractional, then one can affirm that this set is fractal. Being strict, a **chaotic set** needs not to be fractal, but this property is a confirmation that its dynamical behaviour is highly complex. Please refer to the textbook **"Chaos and Time-Series Analysis" - J. C Sproot** [43] to review different methods used to calculate **fractal dimension**.

Finally, the standard calculation of fractal dimension ignores the fact that most real fractal objects are not precisely self-similar and thus may have different dimensions on different size scales and on different parts of the object, i.e. standard calculation of fractal dimension neglects the non uniformity of the set [44]. Thus, one can speak of **monofractal**, when such non uniformity doesn't exists and the fractal is homogeneous, or **multifractal**, when non uniformity does exists and the fractal is inhomogeneous.

2.4.2 Zeng's Daisyworld formulation (DWZ)

Zeng et al. (1990), hereafter **Z90**, included two main changes. First one is about including a parameter C controlling the feedback between biota and environmental temperature, i.e. to change growth rate β_i (**Equation 2.11**) functional form:

$$\beta_i = \max\left[0, \ C\left(1 - \left(\frac{T_{opt} - T_i}{17.5 \text{ K}}\right)^2\right)\right] \tag{2.17}$$

and they considered $1 \leq C \leq 4$, thus allowing a greater growth rate.

Second change is about population dynamics. **Z90**, proposed that **Equation 2.10** needs to be discretized in order be solved numerically, and using a forward-difference scheme, they aproximated it to:

$$a_{i;\, n+1} = a_{i;\, n} + \Delta t \left(\frac{\mathrm{d}a_i}{\mathrm{d}t}\right)_n \qquad \Rightarrow \qquad a_{i;\, n+1} = a_{i;\, n} + \Delta t\left[a_{i;\, n}\left(x_n\beta_{i;\, n} - \gamma\right)\right] \tag{2.18}$$

where n stands for n-th time step (and it would be interpreted in popluation dynamics terms as n-th generation, but some biological clarifications must be made before such interpretation can be stated), whilst Δt stands for the time step and implies that there is a time delay between flowers population, represented by a_i, and their local temperatures T_i. Though last change borns from a numerical approach, they argued that in order to accurately approximate **Equation 2.10**, Δt must be small, however this allows the flowers to adjust to temperature variations instantaneously, which they said, is unphysical. Then, they asserted that a more realistic model is to let Δt be the generation time since this is the characteristic response time of the flowers population and they believed that **Equation 2.18** was *"a more realistic description of the interaction between daisies and their environment than is **Equation 2.10**, which implies an instantaneous feedback"*. Thus, taking the generation time as the unit of time and $\Delta t = 1$, they got:

$$a_{i;\, n+1} = a_{i,n}\left(1 + x_n\beta_{i;\, n} - \gamma\right) \tag{2.19}$$

Now, if a situation of *perfect insulation between regions with different temperature*, i.e. $Q = SL/\sigma$ in **Equation 2.15**, then:

$$T_j^4 = \frac{SL}{\sigma}(1 - A_j)$$

and so β_i is constant. For one species: $\beta_n \equiv \beta$. Furthermore:

$$
\begin{aligned}
a_{n+1} &= a_n\left(1 + x_n\beta - \gamma\right) \\
&= a_n\left(1 + (p - a_n)\beta - \gamma\right) \\
&= a_n\left(\underbrace{(1 + p\beta - \gamma)}_{r} - a_n\beta\right) \\
&= a_n\left(r - a_n\beta\right)
\end{aligned}
$$

Lastly, making the change of variable:

$$x_n = \frac{\beta}{r}a_n \qquad \therefore \qquad a_n = \frac{r}{\beta}x_n$$

then, it is obtained:

$$\frac{r}{\beta}x_{n+1} = \frac{r}{\beta}x_n\left(r - \frac{r}{\beta}x_n\beta\right)$$

$$x_{n+1} = rx_n\left(1 - x_n\right) \tag{2.20}$$

And Robert May proved last equation has both periodic and **chaotic** behaviour [45]. Of course, **Equation 2.19** cannot be reduced to **Equation 2.20**, however, it allows us to think about the possibility of existence of periodic and **chaotic** behaviour in DWZ. Thus, parameter C somehow controls the appearance of these behaviours in the same way r does in **Equation 2.20**.

2.4.3 DWZ main results

Although **Equation 2.20** was obtained for the especial case of $Q = SL/\sigma$ and considering only one species, Zeng showed that chaos, and even periodic oscillations, also hold for a situation of two species and $Q \leq SL/\sigma$ (see **Figure 2.19**).
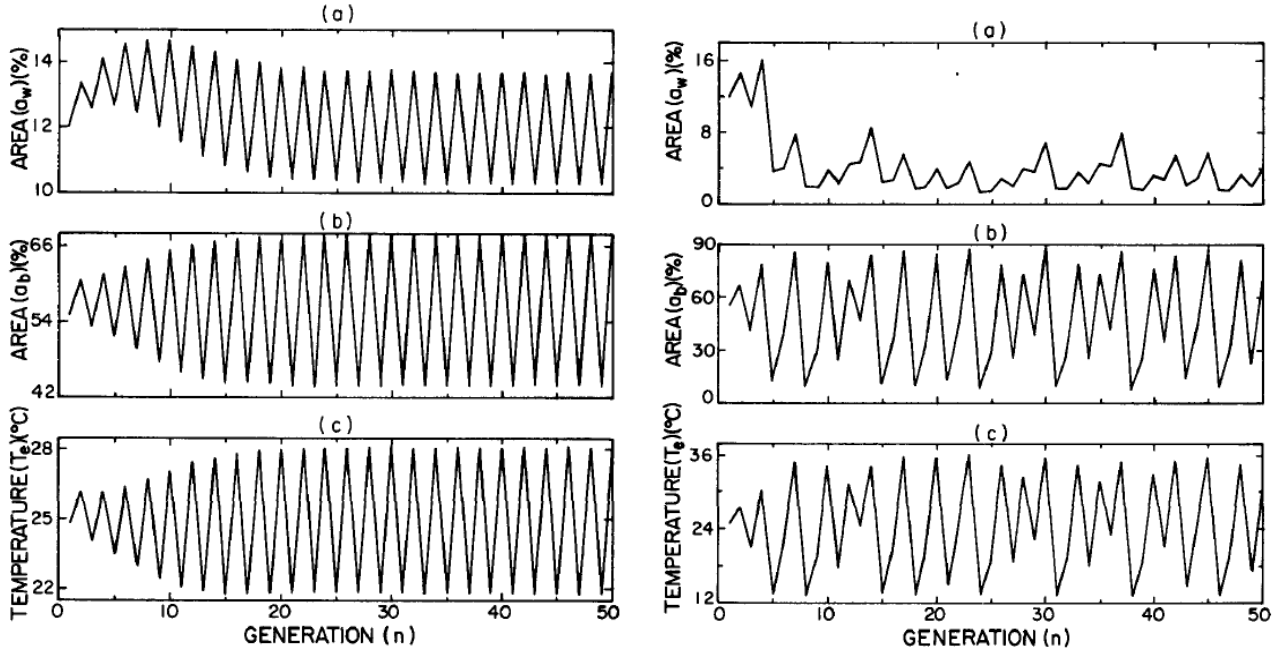
(a) **DWZ periodic time series**. Periodic behaviour of Daisyworld with two species at $L = 0.80$, $C = 3.0$, and $\gamma = 0.8$. **(a)** a_w (in our notation a_1), **(b)** a_b (in our notation a_2) and **(c)** T_e (in our notation T).

(b) **DWZ chaotic time series**. Chaotic behaviour of Daisyworld with two species at $L = 0.80$, $C = 4.0$, and $\gamma = 1.0$. **(a)** a_w (in our notation a_1), **(b)** a_b (in our notation a_2) and **(c)** T_e (in our notation T).

Figure 2.19: **DWZ time series**. **Images taken from** [2].

In order to verify the existence of chaos in **Figure 2.19b**, Zeng calculated next indicators of chaos:

- **Power spectra:** the results indicate that it corresponds to aperiodic behaviour (see **Figure 2.20** and refer to item **Cond-2**).

- **Fractal dimension:** Zeng measured it using the **correlation dimension** algorithm, and the result for time series of **Figure 2.19b** was $\nu = 1.9$. This fractional value is characteristic of chaos (refer to **subsection 2.4.1**).

- **Lyapunov exponents** Zeng found that one of the exponents for times series of **Figure 2.19b** was $\lambda = 0.47$ indicating chaos (refer to item **Cond-3**).
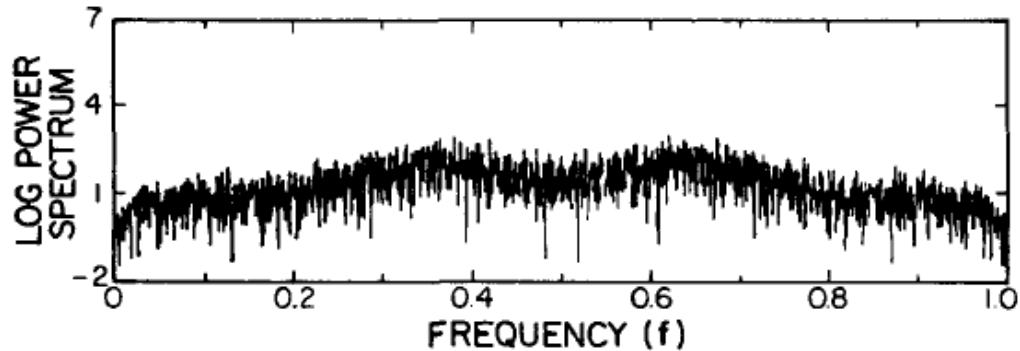
Figure 2.20: **DWZ power spectrum**. It shows power spectrum calculated for time series of **Figure 2.19b**. This power spectrum is like a broadband noise profile, then indicating that the time series is aperiodic. **Image taken from [2]**.

Since Zeng incremented the value of parameter C from 1.0 to 4.0, finding chaos for the last one, he argued that **the above results has shown that the coupling strength C is the most important parameter in determining the qualitative behaviour of Daisyworld**. Then, Zeng concluded:

> *These results show that Daisyworld is not always in steady state as predicted by the **Gaia hypothesis**; instead, the state of Daisyworld can show extreme sensitivity to minor fluctuations in the effective temperature or the areas covered by daisies when in its chaotic regime. Therefore, **the presence of daisies on the imaginary planet does not always stabilize the climate conditions of the environment**. (...) More complete coupled modelling of the interaction of climate with the biosphere and the litosphere on the Earth, including the existence of chaotic states, needs to be developed.*

> — **Z90**, [2].

2.5 Criticism to DWZ

Recently, in 2012, Ian S. Weaver and James G. Dyke, from *School of Electronics and Computer Science, University of Southampton (United Kingdom)*, made a beautiful and illustrative work title **"The importance of timescales for the emergence of environmental self-regulation"** [1], where they analyzed how homeostasis in Daisyworld depends on timescales of different components of the system. However, they asserted that:

> *Oscillations and chaotic behaviour in Daisyworld were reported by **Z90** (1990), a study that has since been shown to be fundamentally flawed (Jascourt and Raymond, 1992).*
>
> — Weaver & Dyke, [1].

Indeed, before Weaver, other authors like Nevison et al. [11], were convinced, by the work done by Jascourt and Raymond (1992), that Zeng's comment, about the validity of the Gaia hypothesis from the perspective of chatic states in **DWZ**, made not sense:

> *Jascourt and Raymond (1992), who rebutted the claim by Zeng et al. (1990) that the occurrence of chaos in a discrete version of daisyworld contradicts homeostasis. Among the other reasons stated in their rebuttal, Jascourt and Raymond showed that the long-term means of the chaotic temperature states predicted by Zeng et al. still exhibit homeostasis.*
>
> — Nevison et al. [11].

We looked at Jascourt's work [4] and found:

> ***Z90**, are unclear about the connection between the differential and discrete systems, misattribute their chaos to the coupling between biota and temperature, and fail to mention the unphysical their model produces for some initial conditions. Further, we have discovered that long-term means of the chaotic states obtained by **Z90**, are close to the equilibrium of the Lovelock's differential system and have small variance, stabilizing Daisyworld against external forcing. (...) Differential and discrete Daisyworld systems are mathematically and physically distinct systems and should not be confused with each other.*
>
> — Jascourt & Raymond, [4].

The major weak points that Jascourt alludes to Zeng are:

P-1 **"Z90, are unclear about the connection between the differential and discrete systems, misattribute their chaos to the coupling between biota and temperature, and fail to mention the unphysical their model produces for some initial conditions"**. Jascourt remarks that *"the physical relationship between the discrete and the differential systems is the **lag of the forcing function**, which we shall call the **feedback"**. In this manner, Jascourt argued that in DWL both feedback factors, that from population and that from temperature, operate instantaneously; while in DWZ both the population and temperature dependencies are assumed to be delayed by one generation. Then he uses delayed equations, such as $\beta = \beta(t - t_{\text{lag}})$, to solve the system, and to examine the effect of delaying the temperature feedback or population feedback, to conclude that chaos in DWZ is originated from population feedback and not from the lag of temperature feedback, and thus, the environmental temperature feedback is of only secondary importance in destabilizing the system. Furthermore, Jascourt reported that 52% of initial conditions were in the basin of the chaotic attractor of DWZ and that the other 48% of the initial conditions lead to unphysical results with negative populations –but he didn't show any diagram of these percentage or the solutions–.

P-2 "**We have discovered that long-term means of the chaotic states obtained by Z90, are close to the equilibrium of the Lovelock's differential system and have small variance, stabilizing Daisyworld against external forcing**". Jascourt takes averages over 30 generations to state last idea. Thus, he says that *discrete Daisyworld doesn't contradict Gaia hypothesis* and he presents **Figure 2.21**, where he reports Δt was adjusted to the minimum value needed for chaos for each value of luminosity.

P-3 "**Differential and discrete daisyworld systems are mathematically and physically distinct systems**". Indeed, we agree with this judgment. We disagree in the way Zeng presented the derivation of **Equation 2.19**, which corresponds to a discrete system, from **Equation 2.18** which is a numerical approximation to **Equation 2.10**. Although the motivation argued by Zeng that *"Δt in **Equation 2.18** must be small in order to accurately approximate **Equation 2.10**, but this allows the flowers to adjust to temperature variations instantaneously, which is really unphysical"* is plausible, and then it seems sensible to take $\Delta t = 1$ and link it with generation time, **it is a misconception to take this approach in order to posit a discrete population model**.

Finally, we found valuable the reply made by Zeng to Jascourt & Raymong [3], where he says that *much of their criticism is based on simple misunderstandings, since they considered both (DWL and DWZ) as two different models of the same physical system in which daisies interact strongly with their environment. Then DWZ was proposed as an alternative model of Daisyworld, not as a mathematical approximation to the differential model of DWL. And he adds that he and his team regret that this point was not as clear as they had intended.* Nevertheless, **he doesn't present any new derivation of the model from primer principles**, and we are surprised that all this misconceptions have thrived enough to make Weaver et al. to say that possibility of chaos in Daisyworld has been shown to be fundamentally flawed.
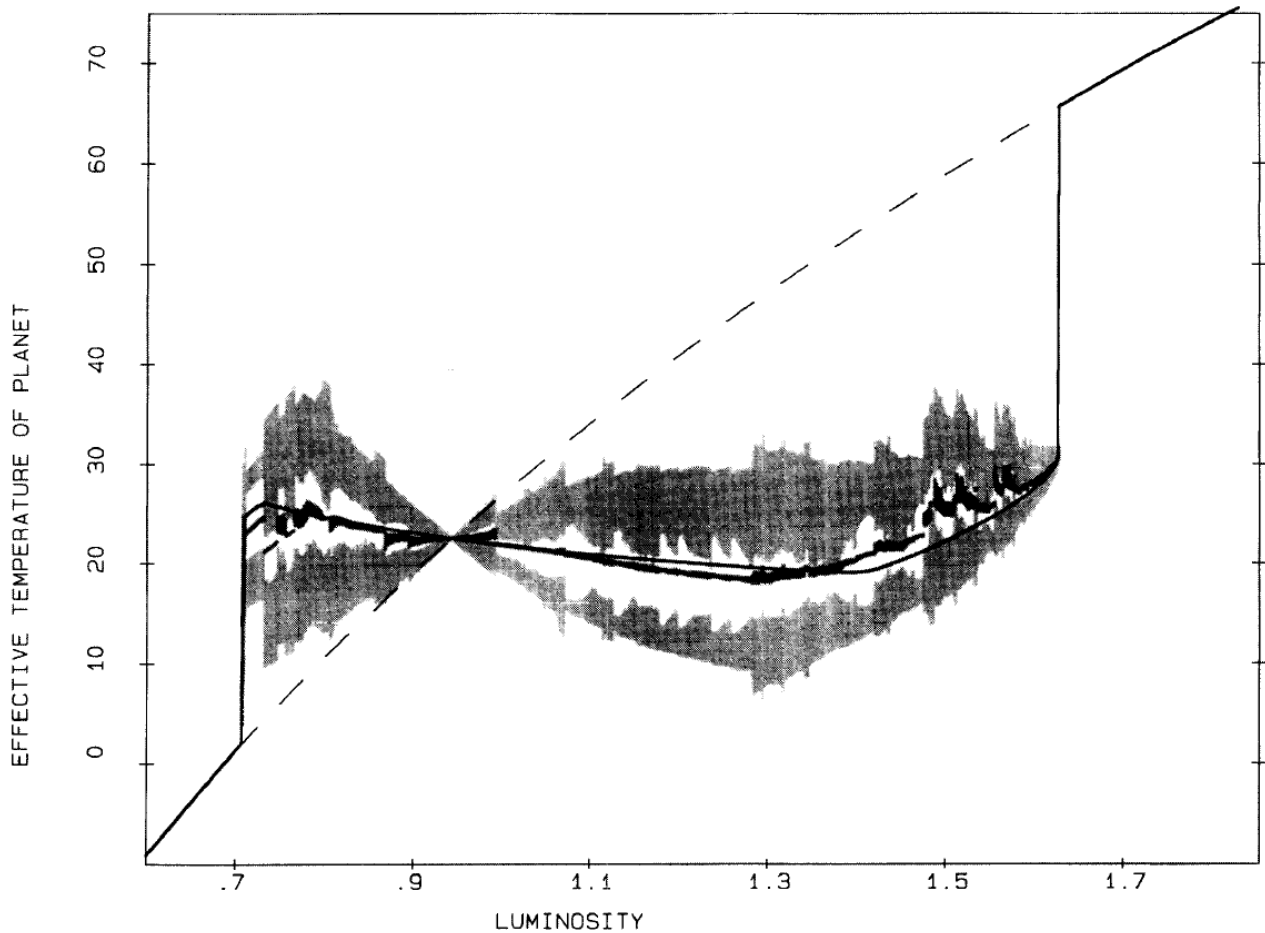
Figure 2.21: **DWZ - Jauscourt result**. As reported by Jascourt: solid line is solution to differential Daisyworld, showing homeostasis as luminosity is increased. Dark shading covers temperatures within one standard deviation of the 30-generation means of chaotic solutions to discrete Daisyworld, showing that de 30-generation climate for chaotic states also exhibits homeostasis. Light shading covers temperatures of individual generations within one standard deviation of the means for temperatures above and below the median, roughly indicating the distribution of temperatures for the chaotic states. Most values are much closer to the stable climatic conditions than to the temperature the planet would have without any daisies (dashed line). Parameter values were: $C = 4.0$, $p = 1.0$, $A_1 = 0.75$, $A_2 = 0.25$, $q = 20$, $\gamma = 1.0$, Δt adjusted to near the minimum needed for chaos for each value of luminosity. **Image taken from** [4].

2.5.1 Misconceptions in "Biological homeostasis of the global environment" concept

Although in **Concept 1** we made a claim about what we believe that Lovelock was referring as **"biological homeostasis of the global environment"**, now we are prepared to see how other authors understand it. First, Jascourt and Raymond claimed:

> *The presence of **daisies stabilizes the climate** against external forcing even with chaotic states in the discrete model of Daisyworld. The **average climate over 30 generations is extremely close to the equilibrium climate** of differential Daisyworld. Thus, discrete Daisyworld does not contradict the Gaia hypothesis, but rather supports the conclusions that Watson and Lovelock made based on differential Daisyworld.*
>
> — Jascourt & Raymond, [4].

This statement reveals that Jascourt and Raymond were thinking about **equilibrium states and homeostasis** in the same spirit that Lovelock and Watson were. Indeed, Jascourt and Raymond used averages to show that the type of chaos they found resembled the equilibrium states of **DWL**. As we saw in **section 2.5**, Nevison got convinced by this claim of Jascourt and Raymond, saying that the **"long-term means of the chaotic temperature states predicted by Zeng et al. still exhibit homeostasis"**. Thus the **equilibrium state**, embody by the existence of an **stable node** in population phase space where any of the daisies survive, becomes in the unique regulatory agent of the system, or in other words, the system exhibits homeostasis because it can be approximated to this equilibrium point. But:

- Is adequate that interpretation?

- What if long-term means of chaos would had been far away from **equilibrium states**?

First, since **chaos** exhibit **aperiodic long-term behaviour** (item **Cond-2**) and **sensitive dependence on initial conditions** (item **Cond-3**), we should know that the system travels through the space of states, inside the strange attractor, in an irregular way; and second, **chaos** cannot be approximated to **equilibrium states**, its dynamical properties are too different. Thus, if chaos in Daisyworld were not fundamentally flawed, then this interpretation seems as a misconception. So:

> Should homeostasis concept be redefined in order to prevent this misconception of averaging chaotic temperature states to resemble equilibrium states?

Chapter 3

Chaos in Daisyworld does apply

As we said in **subsection 2.4.2**, although subscripts n in **Equation 2.18** would be interpreted in population dynamics terms as n-th generation, **some biological clarifications must be made before such interpretation can be stated**, and it is supported in the fact that Δt appears in that equation, so Δt can be adjusted to any value, but this would cause numeric problems to arise, and the dynamics would be subject to numerical errors. Discretization must be made carefully. Even though, populations have complex dynamics and the model must be chosen to be biologically adjusted to this dynamics. Then, in order to derive **Equation 2.19** in an alternative way, we appeal to fundamentals of population dynamics established by Robert May [45] and derived from biological foundations that we explore in the next section.

3.1 Biological foundations for differential and discrete models in population dynamics

Robert May noticed that:

> *In some biological populations, **growth is a continuous process and generations overlap**; the appropriate mathematical description involves **nonlinear differential equations**. In other biological situations, **population growth takes place at discrete intervals of time and generations are completely non-overlapping**; the appropriate mathematical description is in terms of **nonlinear difference equations**.*

> — May [45].

In addition, James D. Murray writes down:

> Differential equation models, whether ordinary, delay, partial or stochastic, imply a continuous overlap of generations. Many species have no overlap whatsoever between successive generations and so population growth is in discrete steps. For primitive organisms these can be quite short in which case a continuous (in time) model may be a reasonable approximation. However, depending on the species the step lengths can vary widely. A year is common. With **fruit fly** emergence from pupae it is a day, for cells it can be a number of hours while for bacteria and viruses it can be considerably less.

In the models we discuss in this chapter (...) we have scaled the time-step to be 1. Models must thus relate the population at time $t + 1$, denoted by N_{t+1}, in terms of the population N_t at time t. This leads us to study **difference equations**, or discrete models, of the form:

$$N_{t+1} = f(N_t)$$

where $f(N_t)$ is in general a nonlinear function of N_t. (...) From a practical point of view, if we know the form of $f(N_t)$ it is a straightforward matter to evaluate N_{t+1} and subsequent generations by simply using last equation recursively.

The skill in modelling a specific population's growth dynamics lies in determining the appropriate form of $f(N_t)$ to reflect known observations or facts about the species in question (...). It should be noted here that **there is no simple connection** between **difference equation models** and what might appear to be the **continuous differential equation** analogue, even though a finite difference approximation results in a discrete equation.

— Murray [52].

Then, it should be clear that both models refer to populations with different underlying phenomena and so, are dynamically different, and neither can approximate each other. Now, **Figure 3.1** is a pictorial scheme for describing **individual's aging process** –including individual's birth and individual's death–, then according to May's statement, one must understand that **Daisyworld planet** as described by **subsection 2.3.2** would be inhabited by two kind of flowers:

- **Flowers with overlapping generations:** For this kind of flowers, in the limit of uncountable individuals, one cannot trace individuals births neither individuals deaths, since these events can occur probably at any time. In this situation, one must appeal to models for **populations with overlapping generations** as described by **Figure 3.2a** and then **DWL** is the right mathematical model.

- **Flowers with non-overlapping generations:** For this kind of flowers, in the limit of fixed generation time and synchronized generations, i.e. for which growth and births are synchronized, one must appeal to models for **populations with non-overlapping generations** as described by **Figure 3.2b** and then **DWZ** could be the adequate mathematical model –though it should be reformulated from its foundations–.
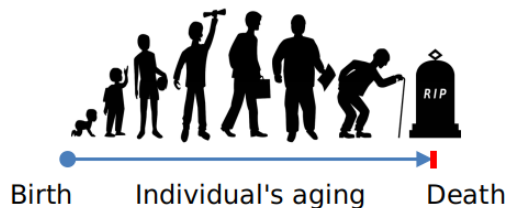
Figure 3.1: **Individual's aging scheme.** This image is a representation of the **individual's aging process**, in which individual's birth is represented by a **blue dot**, individual's aging is represented by the temporal **blue line** and individual's death is represented by a **red dot**.

$$\frac{dN}{dt} = f(N; \{\rho\})$$

Set of
individuals
with
overlapping
generations

Limit of
uncountable
individuals

$\{\rho\} \equiv$ set of
environmental
variables

Number of
individuals

6
5
4
3
2
1

t
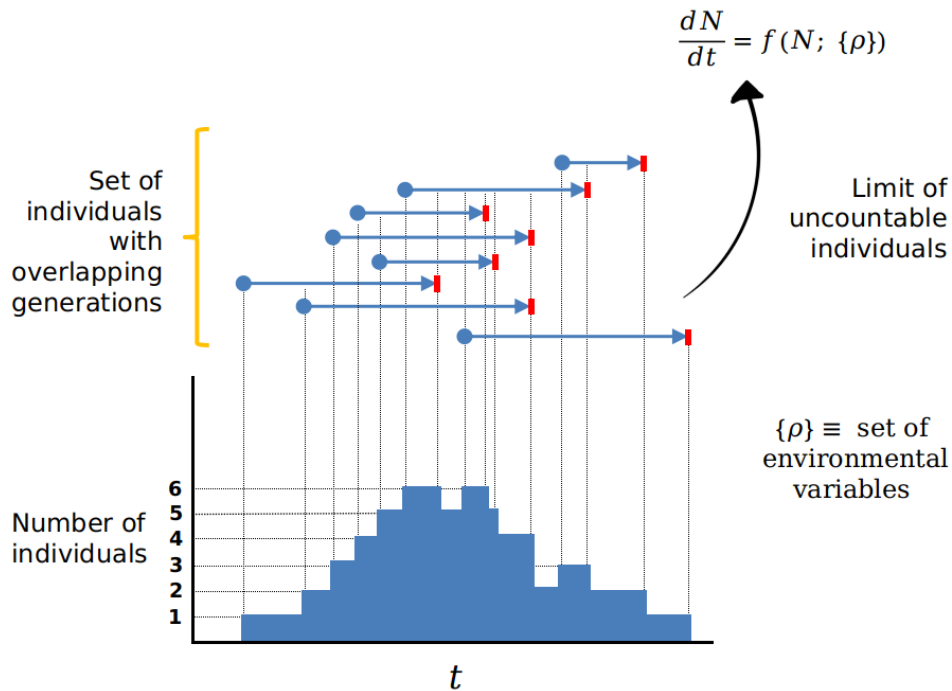
(a) **Populations with overlapping generations scheme.** These are populations for which **growth is a continuos process** and **generations overlap**. For this kind of populations, in the limit of uncountable individuals where the tracing of births and deaths becomes a problem to deal with, the most adequate mathematical models for describing populations dynamics are **nonlinear differential equations**.

$$N_{n+1} = f(N_n; \{\rho\})$$

Set of
individuals
with
non-overlapping
generations

Assuming
a fixed
generation
time and that
next number of
individuals
depends on
current one

Number of
individuals

6
5
4
3
2
1

$\{\rho\} \equiv$ set of
environmental
variables

Δt

t

0 1 2 3 4 5 6

n
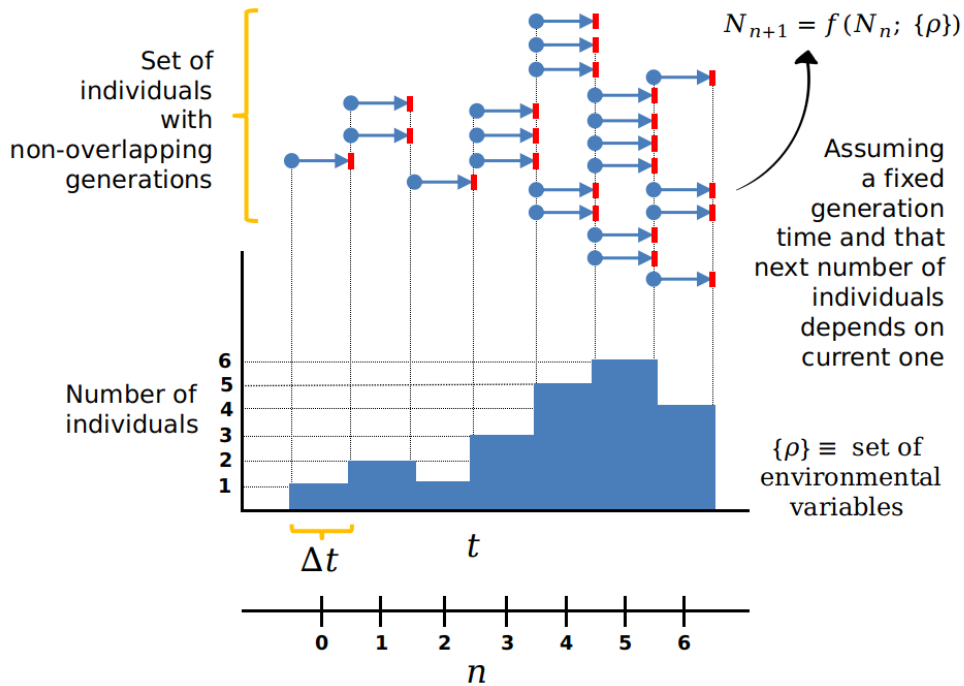
(b) **Populations with non-overlapping generations scheme.** These are populations for which **growth takes place at discrete intervals of time** and whose coupling with the environment is inherently delayed one (or more) generations. For this kind of populations, assuming a fixed generation time Δt, one can use the **generation number n** as the time variable instead of t, and assuming that the next number of individuals N_{n+1} depends on the current one N_n, then the most adequate mathematical models for describing populations dynamics are **nonlinear difference equations**, also known as **iterated maps**.

Figure 3.2: **Population dynamics scheme.** Differences between using **nonlinear differential equations** or **nonlinear difference equations** for modeling the population dynamics and the fundamental biological properties describe in each case.

3.1.1   Biological discussion: how do populations behave?

The famous Leonardo de Pisa, after known as Fibonacci, posed a modelling exercise involving an hypothetical growing rabbit population. It consists of starting at the beginning of the breeding season with a pair of immature rabbits, male and female, which after one reproductive season produce two pairs of male and female immature rabbits after which the parents then stop reproducing. Their offspring pairs then do exactly the same and so on. So if one wants to determine the number of pairs of rabbits at each reproductive period, one can prove that if the number of pairs of rabbits N_t –male and female– at time t, depends on the number in N_{t-1} and the number before that one N_{t-2}:

$$N_t = N_{t-1} + N_{t-2} \tag{3.1}$$

giving raise to the famous *Fibonacci sequence*. In this model, the reproductive period has been normalized to 1. We venture to say that this and the *logistic model* could be the most famous discrete models used in population dynamics. Before we continue, we must say that this models exhibit the possibility of a dramatic drop in the population to low values close, bringing up the question of extinction of a species. If the population drops to a negative value, then the species is clearly extinct. In fact extinction is almost inevitable if N_t drops to low values.

Now, the major reason for modelling the dynamics of a population is, as it is in climate modelling, to understand the principle controlling features and to be able to predict its consequent behaviour under a change of parameters including those of the environment. Now, chaotic dynamics, and its seemingly random behaviour, poses serious problems from a modelling point of view:

> *Are the data obtained which exhibit this kind of behaviour generated by a deterministic model or by a stochastic situation? It is (...) a problem to decide which is appropriate and it may not actually be one we can resolve in a specific situation. What modelling can do, however, is to point to how sensitive the population dynamics can be to changes in environmental parameters, the estimation of which is often difficult and usually important.*

> — Murray [52].

In the following, we seek to show examples of how discrete dynamics emerge in nature. First, we must note that **populations which resemble the situation showed in Figure 3.2b, are those whose parents die immediately before –or after– a new generation is born.** In 1954, Lamont C. Cole [53] aim that one can classify populations by means of two kind of reproductive strategies:

- **Semelparity:** it refers to the mechanism of reproducing only once in a lifetime, i.e. the condition of multiplying only once in a life time, whether such multiplication involves fission, sporulation, or the production of eggs, seeds, or live young; and so reproductive efforts are spent only once in a lifetime, when individuals are mature to reproduce.

- **Iteroparity:** it refers to the mechanism of reproducing repeatedly, i.e. more than once in a lifetime; and so reproductive efforts are spent periodically, or even continuously along the mature phase of lifetime.

Cole noticed that reproduction in semelparous forms may occur at the age of only 20 minutes in certain bacteria, of a few hours in many protozoa, or of a few weeks or months in many insects. He also remarked that many semelparous plants and animals are annuals; in other semelparous organisms reproduction may occur only after a number of years of maturation, for example, two or more years in **dobson flies** and **Pacific salmon**, and many years in **"century plants" (Agave)** and the periodic cicada or **"17-year locust" (Magicicada septe zdecim)**. The number of potential off spring produced by semelparous individuals varies from two in the case of **binary fission** to the literally trillions (2×10^{13}) of spores produced by a large **puffball (Calvatia gigantea)**. In summary, he said that nearly all annual plants and animals, as well as many protozoa, bacteria, insects, and some perennial forms such as century plants and the Pacific salmon, are semelparous species. Another case of semelparity is that of the deep-sea octopus Graneledone boreopacifica [54], whose female protects the clutch of fertilized eggs until they hatch after a period of 53 months, and then it dies. According to Walton W. Dickhoff [55], the rapid aging and death of the Pacific salmon after a long migration and subsequent spawning in its natal stream is an intriguing end to a dramatic life cycle that is shared with other fishes: the best known examples of semelparous species include –besides **Pacific salmon**– the **teleosts**, the **eels**, and an agnathan, the **lamprey**, although semelparity has been observed in other species, for example, some **gobiid fishes**. Then:

> *It could be concluded that the occurrence of semelparity as a reproductive strategy of fishes is not uncommon. There may be several reasons for the existence of semelparity in fishes.*

> — Dickhoff [55].

On the other hand, Cole noticed that in the reproduction in iteroparous forms occurs after a period of maturation that may vary from as little as a few days in small **crustaceans** to over a century in the **giant sequoia**, and practically any intermediate value may be encountered. He remarked that after the first reproduction has occurred in iteroparous organisms it may be repeated at various intervals –for example, daily (as in some **tapeworms**), semiannually, annually, biennially, or irregularly (as in **man**)–. In addition, he stressed that in semelparous organisms, the litter size of iteroparous forms may also vary greatly; here it may vary from one –as is usual, for example, in **man**, **whales**, **bovines**, and **horses**– to many thousands –as in various **fishes**, **tapeworms**, or **trees**–. The litter size may be constant in a species, vary about some average, or change systematically with the age of the parent, in which case it may increase to some maximum –as in **tapeworms**– or climb to a maximum and then decline as in some **cladocerans**. Furthermore, he added, individuals may live on after their reproduction has ceased completely, and this post-reproductive period may amount to more than one-half of the normal life span.

Then, Cole punctuated:

> *One feels intuitively that natural selection should favor the perennial reproductive habit because an individual producing seeds or young annually over a period of several years obviously has the potential ability to produce many more offspring then is the case when reproduction occurs but once.*

It is, therefore, a matter of some interest to examine the effect of iteroparity on the intrinsic rate of natural increase in order to see if we can find an explanation for the fact that repeated reproduction is not more general.

— Cole [53].

Last comment is remarkable in the sense he claims that the direction of evolution and selective pressures that lead to either of this two reproductive strategies were not clear by the epoch and then they were an investigation problem –we believe that it stills being a topic in discussion as it challenges evolutionary biology–, and even less, if one could had said that populations tend to behave according to one of them and, although this question is beyond the scope of this thesis, what we can do according to the evidence at Earth is to ask: **how can one affirm that chaotic dynamics –originated by discrete population dynamics– is fundamentally flawed? Do we comprehend enough this evidence as to say that the possibility of this chaotic dynamics on other planets doesn't need to be considered?**

Turning back to semelparity, it is reported that the complete population die off, and this behaviour is also seen in plants. Indeed, it is said that semelparous plants are those in which plant resources are utilized entirely for one episode of reproduction, followed by degeneration and death of the entire plant. Semelparity occurs in all annual and biennial plants [56]. In addition, Cole affirmed that *"once semelparity had been established, there would be little selective pressure or advantage for some population to change from semelparous to iteroparous reproduction"* [53]. Furthermore, we can find works like that by Truman P. Young and Carol K. Augspurger [57] where they call semelparity as *"One of the more dramatic life histories in the natural world (...) characterized by a single, massive, fatal reproductive episode"* and they add:

Semelparity is a distinct life history in which a massive reproductive output is directly associated with preprogrammed whole organism death. In plants, the syndrome of death after first reproduction can occur on several levels:

- Death of the reproductive meristem or ramet.

- Death of the physiological individual, not including disconnected ramets.

- Death of the entire genetic individual.

— Young and Augspurger [57].

Sometimes, **semelparity** can be mixed with other mechanisms that make its behaviour even more complex. This is the case when **dormancy** is evidenced. **Dormancy** is a widely recognized behavioral and physiological state of both animals and plants that generally involves inactivity associated with metabolic depression and arrested development that promotes the survival of individuals during periods of harsh environmental conditions [58, 59]. This unfavorable environmental conditions can include high and low temperatures or moisture conditions and reduced food quality or availability. **Dormancy** can be a short-term event (< 24 h),

can occur for a few consecutive days, or may last an entire season or even many years. **Dormancy** can also involve a developmental arrest. This is the case of **diapause**, which is an ecological strategy for the avoidance of harsh conditions involving the cessation of development of a subadult life stage [58]. **Diapause** is not directly induced, but is triggered by genetically programmed responses to environmental cues that occur in advance of adverse conditions. Anticipatory induction allows time for substantial physiological changes prior to the arrival of adverse conditions [59]. **Diapause** is especially common in insects but is also observed in a wide variety of other invertebrate animals (e.g., **brine shrimp embryos**) and vertebrate animals (e.g., **annual killifish embryos**), as well as many plants (e.g., **buds**, **bulbs**, **rhizomes**, and **seeds**). Some plant seeds require drying out before they can develop, ensuring that adverse dry seasons pass before the embryo starts to develop. **Diapause** is also a reproductive strategy in a variety of mammals for the delayed implantation and development of embryos (e.g., **macropod marsupials**, **mustelids**, and **deer**). **Quiescence** is a period of inactivity [58], similar to **diapause**, but is a facultative response to an immediate change in environmental conditions that is terminated simply by the resumption of more favorable environmental conditions, rather than a programmed and obligate response. It may be a response to harsh environmental conditions such as low or high temperature, or drought. Many invertebrates and plants (particularly their seeds) become **quiescent**.

A remarkable example of **semelparity** mixed with **diapause** is the case of the **chameleon Furcifer labordi**, which was reported in 2008 by Kristopher B. Karsten [60]. He found that this tetrapod from the arid southwest of Madagascar has a post hatching life span of just 4-5 months. At the start of the active season (November), an age cohort of hatchlings emerges; larger juveniles or adults are not present. These hatchlings grow rapidly, reach sexual maturity in less than 2 months, and reproduce in January-February. After reproduction, senescence appears, and the active season concludes with population-wide adult death. Consequently, during the dry season, the entire population is represented by developing eggs that incubate for 8-9 months before synchronously hatching at the onset of the following rainy season.

On the other hand, there is **Cryptobiosis**, which is a more extreme state than **dormancy**, with almost no detectable activity or metabolism:

> *It is most prevalent in lower vertebrates, and is often a seasonal survival strategy to cold or desiccation. This last mechanism, referred as "hidden life" or "suspended animation" has been observed for a variety of invertebrate animals and plants during extreme environmental conditions. It was first described for invertebrate animals that survived an absence of water by becoming inactive and allowing their tissues to become desiccated (**anhydrobiosis**, e.g., **rotifers**). Two other forms of **cryptobiosis** also involve an altered state of cellular water, freezing temperatures (**cryobiosis**, e.g., a frozen insect), and high osmotic concentration (**osmobiosis**, e.g., brine shrimp eggs in a salt lake). Another form of **cryptobiosis** is survival of a lack of oxygen (**anoxybiosis**, e.g., killifish eggs sealed inside their egg capsule).*

*The best-known example of cryptobiotic animals is probably the eggs of **brine shrimp (Artemia)**, which can survive extended periods of complete desiccation, high salt concentration, or anoxia; their desiccated eggs are also remarkably resistant to extremes of temperature. Various "resurrection" plants are well-known examples of **cryptobiotic plants**, being able to recover from desiccation for extended periods. Seeds of some plants are also spectacularly resistant to desiccation, sometimes for very long periods of time (e.g., seeds more than 1000 years old of the **Indian lotus** from an ancient lake bed in China). All of these forms of **cryptobiosis** involve complete inactivity. Ecological advantages of **cryobiosis** include survival of harsh environmental conditions, and dispersal of highly resistant life stages. However, the physiological adaptations required by these animals and plants to survive extreme conditions at no detectable metabolic rate are generally complex and specialized.*

— Withers [58].

All the examples cited above gives us the biological basis to say that **discrete population dynamics** is real and evident at Earth, and to claim that it could also arise in exoplanets, and then to ask: **why not in Daisyworld?**.

Finally, we want to add a remark made by Zeng that:

The discrete model with a finite generation time is a first step toward including seasonal variation, since it synchronizes the birth at the beginning of each new generation, which corresponds to the beginning of the growing season rather than allowing continuous birth throughout the year.

— Zeng [3].

Although is seems that Zeng was thinking on population surviving under seasonal environmental forcings, as we saw in the discussion above, it is not the only way for developing population dynamics described by **Figure 3.2b**, and we just have to say that, as we will see in the next section, Zeng –and then Jascourt–, didn't take into account the biological differences between both kind of models.

3.2 Criticism to Zeng and Jascourt from a biological perspective

Although simple, the concepts treated in the last section (**section 3.1**) makes huge difference in the discussion addressed in **section 2.5**. To get started, we must remember that both mathematical descriptions lead to different dynamics. As Jascourt noted in **P-3**: *"Differential and discrete Daisyworld are mathematically and physically distinct systems"*, and then both approaches, that belonging to Zeng and that to Jascourt, have weak points.

First, Zeng invokes that populations cannot adjust to temperature variations instantaneously, saying that it is unphysical. This is a misconception born in a misconstruction of a numerical scheme. Remember that in **subsection 2.1.1**, specifically in the discussion about **perfect energy balance** and **Equation 2.2**, we stated what must be understood as an instantaneous change in temperature and as we have discussed in and after **Remark 1**, there are two temporal scales in play: τ (for temperature) and t (for population dynamics); and assuming **perfect energy balance** means that *"the time variable τ changes faster than t, so in the temporal scale t of the flowers population, the equilibrium solution for temperature is achieved almost instantaneously"*, i.e. when t changes significantly, τ has changed enough so that T has reached its equilibrium value because **absorbed energy R_i** and **emitted energy R_o** has equated. Then, the *"instantaneous temperature variations"* achieved in the system are a direct consequence of assuming **perfect energy balance**, and thus Zeng didn't take into account that this is a problem of different time scales in play.

On the other hand, remember that Zeng begins from **Equation 2.2** to derive **Equation 2.18**, and finally arrive at **Equation 2.19**. However, the first equation refers to a population dynamics in which one cannot assign a specific time to a specific generation, inasmuch as in a specific time t there exists a continuous of generations contributing to the population, i.e. in any time there exist births, individual aging and deaths, all happening at the same time and at different rates; and one must take dt as the differential time in which population dynamics is changing by the rate da_i/dt. But the third equation refers to a population in which all individuals of one generation are synchronized, and then it corresponds to the limit where individuals from one generation do not overlap with individuals of another generation (see **figure 3.1**). Thus, the path followed by Zeng for deriving **Equation 2.19** is self contradictory, but this fact does not mean that this equation is wrong, it just means that we have to derive it from other arguments.

On the other hand, even if population generations overlap, and one must use differential equations to describe population dynamics, and if there were any delay in population feedback, i.e. that both population and temperature were delayed in any time scale, then population must continue to be described by nonlinear differential equations. The discretized equation derived by Zeng is just a mathematical tool used for integration of differential equations and must be integrated with dt –i.e. small integration time–, no with Δt –i.e. with a time comparable to other quantities in the system–.

Second, turning to Jascourt, we have said that we are in agreement with his claim in item **P-3**, but this point itself makes weak his dissertation. When he uses delayed equations to solve the problem and then asserts that chaotic dynamics is due primarily to the lag in population feedback (see item **P-1**), his assertion is correct, but only for the delayed model he used to try to get insight of the relationship between discrete and differential systems. The trick of using delayed equations makes artificial the solution and so, it is not a clean way to deal with both systems. We dare to say that the solution obtained in this way doesn't resemble the real solution, and thus, the conclusions he made about chaos are particular to his model and can be criticized for not being natural. This way of introducing the effects of continuous systems into discrete systems is artificial, and for being so artificial, the original discussion of Daisyworld,

i.e. the biological interpretation, gets lost.

If the objective is to find the bridge between differential and discrete systems, as Jascourt tried, one must begin from the start with a complete formulation of the processes involved in terms of stochastic differential equations in which one can include the desired delays of the variables. So, again, Jascourt's conclusions are relevant only for his model and cannot be extrapolated to the fundamental biological interpretation of Daisyworld, in other words, they are not true from the fundamental point of view of seeking if generations are overlapping or not, and the implications for the coupling with climate. Maybe this misconception by Jascourt would lead him to adjust Δt when increasing L (see **Figure 2.21**), thus losing information about the system is affected by variations in L. Moreover, his handling of chaotic behaviour by means of taking time averages to posit that Zeng was wrong (see item **P-2**), is born in another misconception which ignores all properties conferred to the system by chaos. Although the result in **Figure 2.21** is interesting, we disagree with Jascourt in his procedure of taking time averages and even adjusting Δt for each value of L, since it is a tricky contraption used to claim that Zeng was wrong.

In **Figure 3.3** we made a graphical scheme which is intended to show the weak points of both Zeng and Jascourt. In the next chapter we are going to derive **Equation 2.19** in an alternative way. We will call this model: **Chaotic Daisyworld (DWC)**.
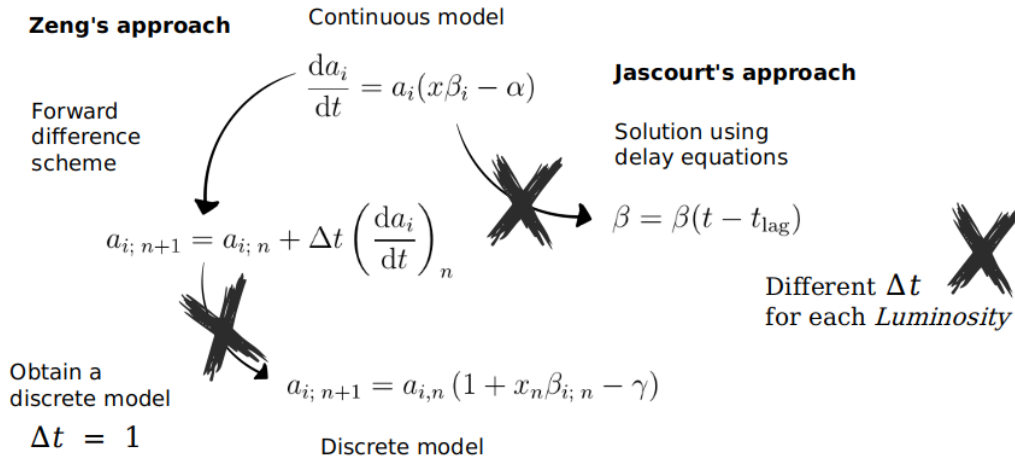
Figure 3.3: **Zeng's and Jascourt's weak points scheme.** Graphical scheme which is intended to show the weak points of both Zeng and Jascourt.

3.3 Alternative derivation for discrete Daisyworld (DWC)

We will keep all derivations and definitions made in **subsection 2.3.2** unchanged, but for population dynamics, we are going to suppose that we are dealing with **non-overlapping generations**. We will assume that the number of **white flowers** is N_1 and N_2 is that of **black flowers**. Both N_1 and N_2 are integers, and taking the generation time as the unit of

time, we have that in generation n the number of flowers of species i is $N_{i;\,n}$.

The planet itself cannot be inhabited to be populated by an infinite number of flowers, so there would be a N_{max} number of flowers which is supported by the planet. Then, we can define the **unitary cell (fraction of area of the planet occupied by one flower)** as:

$$f = \frac{p}{N_{max}} \tag{3.2}$$

for ease, we suppose this is the same for both species. Then the fraction of the planet occupied by species i in generation n is:

$$a_{i;\,n} = f \; N_{i;\,n} \tag{3.3}$$

Then, the fraction of fertile ground area which is uncolonized by flowers is:

$$x_n = p - (a_{1;n} + a_{2;n}) \tag{3.4}$$

From population dynamics theory, the difference ΔN_i between the number of flowers of species i in generation $n + 1$, i.e. $N_{i;\,n+1}$, and that in generation n, i.e. $N_{i;\,n}$, should depend on $N_{i;\,n}$ and the environment:

$$\Delta N_{i;\,n} \equiv N_{i;\,n+1} - N_{i;\,n} = \boldsymbol{F}(N_{i;\,n}, \text{ environmental variables })$$

So:

$$N_{i;\,n+1} = N_{i;\,n} + \underbrace{\boldsymbol{F}(N_{i;\,n}, \text{ environmental variables })}_{\Delta N_{i;\,n}}$$

Next, we follow the same spirit of Carter & Prince [37]:

$$
\begin{aligned}
\Delta N_{i;\,n} &= \text{Population size} * (\text{Space susceptible to be colonized} * \text{Growth factor} - \text{Death factor}) \\
&= N_{i;\,n}\,(x_n \beta_{i;\,n} - \gamma)
\end{aligned}
$$

Then:

$$N_{i;\,n+1} = N_{i;\,n} + N_{i;\,n}\,(x_n \beta_{i;\,n} - \gamma) \tag{3.5}$$

Finally, multiplying by f:

$$
\begin{aligned}
f \; N_{i;\,n+1} &= f \; N_{i;\,n} + f \; N_{i;\,n}\,(x_n \beta_{i;\,n} - \gamma) \\
&\Downarrow \\
a_{i;\,n+1} &= a_{i;\,n} + a_{i;\,n}\,(x_n \beta_{i;\,n} - \gamma)
\end{aligned} \tag{3.6}
$$

Where last equation corresponds to iterated equation for area covered by flower of species i in generation n, or simply **area covered map**. Thus, **Table 2.1** can be replaced now by its discrete form summarized in **Table 3.1**, where in addition to original **DWL** parameters (see **Table 2.3**), it appears the new paremeter C which controls the feedback between biota and

Discrete Daisyworld (DWC) equations	
$\sigma T_n^4 = SL(1 - A_n)$	Perfect energy balance for climate system in generation n
$x_n = p - (a_{1;n} + a_{2;n})$	
$a_{i;\,n+1} = a_{i;\,n} + a_{i;\,n}\left(x_n \beta_{i;\,n} - \gamma\right)$ for $i = 1, 2$	Area covered $a_{i;n}$ map
$A_n = (1 - p)A_{NF} + xA_F + \sum_i a_{i;\,n} A_i$	Coupling between area covered $a_{i;\,n}$ and total albedo A_n in generation n
$\beta_{i;\,n} = \max\left[0,\ C\left(1 - \left(\frac{T_{opt} - T_{i;\,n}}{17.5\ \text{K}}\right)^2\right)\right]$	Flowers growth factor which is coupled to local temperatures $T_{i;\,n}$ in generation n
$T_{j;\,n} = q(A_n - A_j) + T_n$ for $j = NF, F, 1, 2$	Coupling between effective temperature T_n of the planet and local temperatures $T_{j;\,n}$ for regions with different albedos in generation n

Table 3.1: **Discrete Daisyworld (DWC) equations**. Set of equations for **Discrete Daisyworld model (DWC)**.

local temperatures.

A final remark that must be done, is that $\beta_{i;\,n}$ in **Equation 3.5** –and in **Equation 3.6**–, doesn't have the same conceptual meaning than β_i in **Equation 2.10**. In the latter, it means a growth rate, whilst $\beta_{i;\,n}$ is a population growth factor since, as Δt in **Figure 3.2b** is fixed, then temporal dependence on this fixed time generation is neglected, and thus $\beta_{i;\,n}$ doesn't have any rate units $[t^{-1}]$. The same holds for γ in **DWL** and **DWC**.

However, without loss of generality, in the following we compare $\beta_{i;\,n}$ and β_i indistinctly, without making this conceptual clarification.

3.4 Discrete Daisyworld (DWC) comparison with Original Daisyworld (DWL)

As we saw in **subsection 2.3.4**, to draw a **bifurcation diagram** (see **Figure 2.14**), along with of some **phase portraits** (see **Figure 2.15**, **Figure 2.16**, **Figure 2.17** and **Figure 2.18**), were more illumating to understand the behaviour of **DWL** model (see **Figure 2.12**) and why

homeostasis as Lovelock defines it emerges. Indeed, it allowed us to see that the fixed point responsible of homeostasis in **DWL** is in fact a globally stable point for most of the values of L where it exists (remember that in **DWL** there exists multistability that leads to hysteresis). Let's analyze how these results change for **DWC** model.

First, **fixed points** a_i^* for both **DWL** and **DWC** are the same when the set of parameters of **Table 2.3** plus C remains unchanged:

$$\left.\frac{\mathrm{d}a_i}{\mathrm{d}t}\right|_{a_i^*} = \underbrace{a_i\left(x\beta_i - \gamma\right)|_{a_i^*}}_{=0}$$

$$\Downarrow$$

$$\Delta a_{i;\,n}|_{a_i^*} = \underbrace{a_{i;\,n}\left(x_n\beta_{i;\,n} - \gamma\right)|_{a_i^*}}_{=0}$$

$$(\textbf{3.7})$$

and as equations for T_n and A_n still being the same as for $T(t)$ and $A(t)$, so one expects the same temperature T contour lines, then one can expect the same shape for **bifurcation diagram**.

Second, **the calculation of the stability of the fixed points a_i^* for ODEs is different compared to iterated maps** [46, 47]. Thus **bifurcation diagram** changes not in shape but in description of stability. From **Figure 3.4** it is clear that the **global stable point** for L in the interval $(0.740, 1.359)$ and where both species coexisted for **DWL**, does not exist anymore in **Figure 3.4b**, and is replaced by a **semistable point**. Indeed, **Figure 3.4b**, shows more instabilities in this interval than **Figure 3.4a**, and since stable points have became unstable and there are not stable point for a wide range of values of L, we can suspect we are in front of a **period doubling route to chaos** [48].
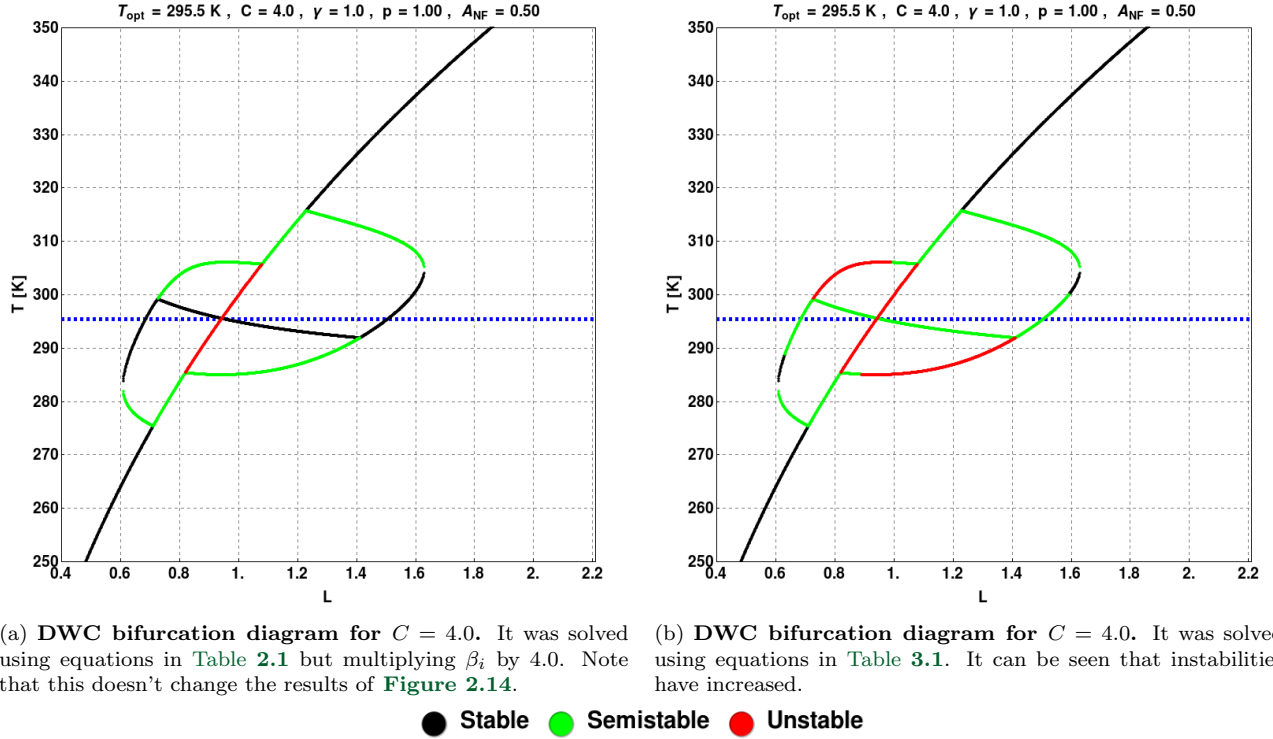
(a) **DWC bifurcation diagram for** $C = 4.0$**.** It was solved using equations in Table **2.1** but multiplying β_i by 4.0. Note that this doesn't change the results of **Figure 2.14**.

(b) **DWC bifurcation diagram for** $C = 4.0$**.** It was solved using equations in Table **3.1**. It can be seen that instabilities have increased.

● **Stable**   ● **Semistable**   ● **Unstable**

Figure 3.4: **DWC bifurcation diagram (panel a) compared with that of DWL (panel b).** Where $C = 4.0$, $\gamma = 1.0$ and the rest of parameters values are the same as in **Table 2.3**. Dotted blue line corresponds to the value of $T_{opt} = 295.5$ K. Bifurcation diagram in for **DWC** shows more instabilities.

3.4.1   Chaos enters the scene

We tested the existence of **chaos** in **DWC** dynamics using the same parameters values used by Zeng [2]. In order to do it, we produced a time series solving the system of equations in **Table 3.1** and iterating the system from the initial conditions $a_{1;\,0} = 0.1$ and $a_{2;\,0} = 0.4$, for a transient time of 1×10^6 generations and then for an asymptotic time of 1×10^6 generations. Part of the time series produced can be seen in **Figure 3.5**.

In our algorithm of evolution, we were careful to implement that those solutions that go to values near zero an then surpasses it going to negative values, correspond to solutions where population got extinct, so their real values are not negative but zero [3]. Using the algorithm of **the largest Lyapunov exponent $\lambda_{\mathbf{max}}$** [41], we found that $\lambda_{\max} = 0.4536$ which is a firm sign of **chaos**. In addition we plotted the **power spectrum** for both time series –that of a_1 and that of a_2–. The result can be seen in **Figure 3.6**, and it is clear that it correspond to a chaotic-like spectrum. Now, we can firmly assess that the time series produced is **chaotic** and so, **chaos** belongs to **DWC** dynamics.

In addition, we wanted to verify the existence of a **strange attractor** in **population phase space** when the system is **chaotic** [40], so we ploted asymptotic solution without transient (**Figure 3.7**) and then we used **box counting** method [42] to compute an estimate of its

70

fractal dimension ν. We found that $\nu = 1.840$ (**Figure 3.8**), which corresponds to the dimension of a **fractal set**, so confirming the existence of a **strange attractor**.

The both values we find for $\lambda_{\max}$ and ν are consistent with those of Zeng [2].
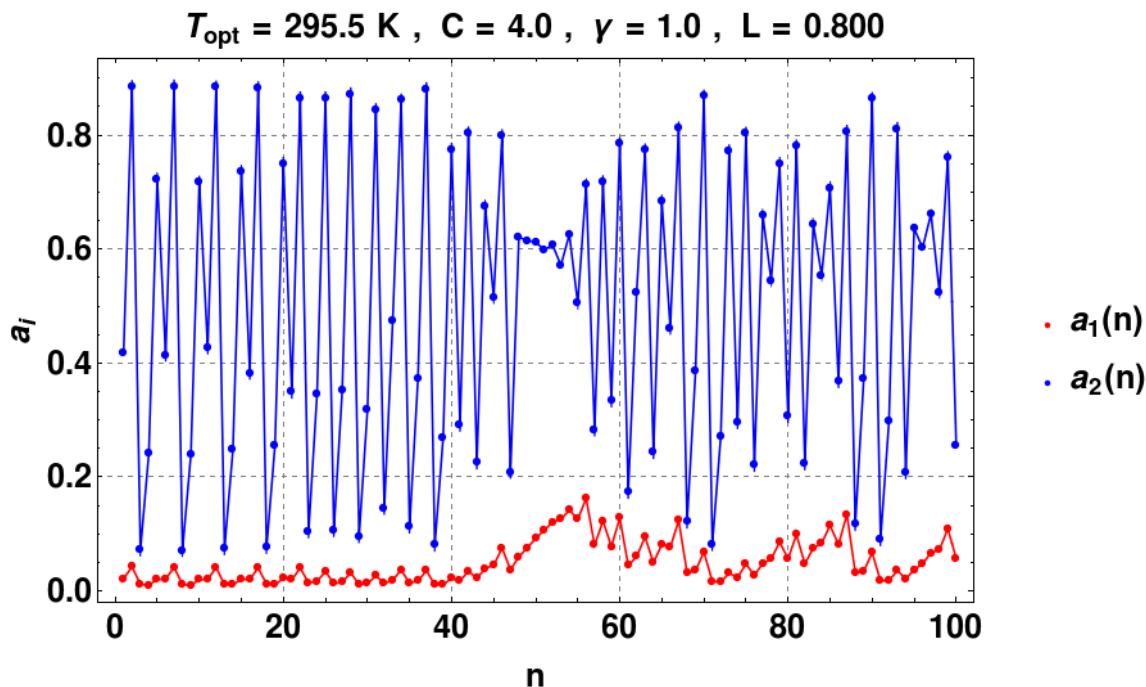
Figure 3.5: DWC time series for $C = 4.0$, $\gamma = 1.0$ and $L = 0.800$ after a transient time of 1×10^6 generations has passed. The initial conditions were $a_{1;\,0} = 0.1$ and $a_{2;\,0} = 0.4$.
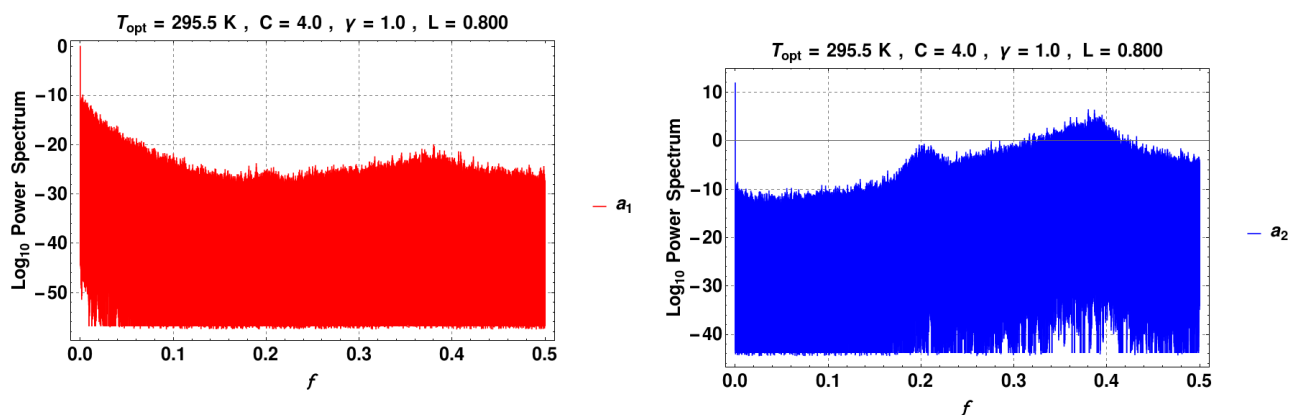
(a) DWC asymptotic state for $C = 4.0$, $\gamma = 1.0$ and $L = 0.800$, besides to temperature T contour lines.

(b) DWC power spectrum of a_2 time series.

Figure 3.6: DWC power spectrum for time series of **Figure 3.5**.
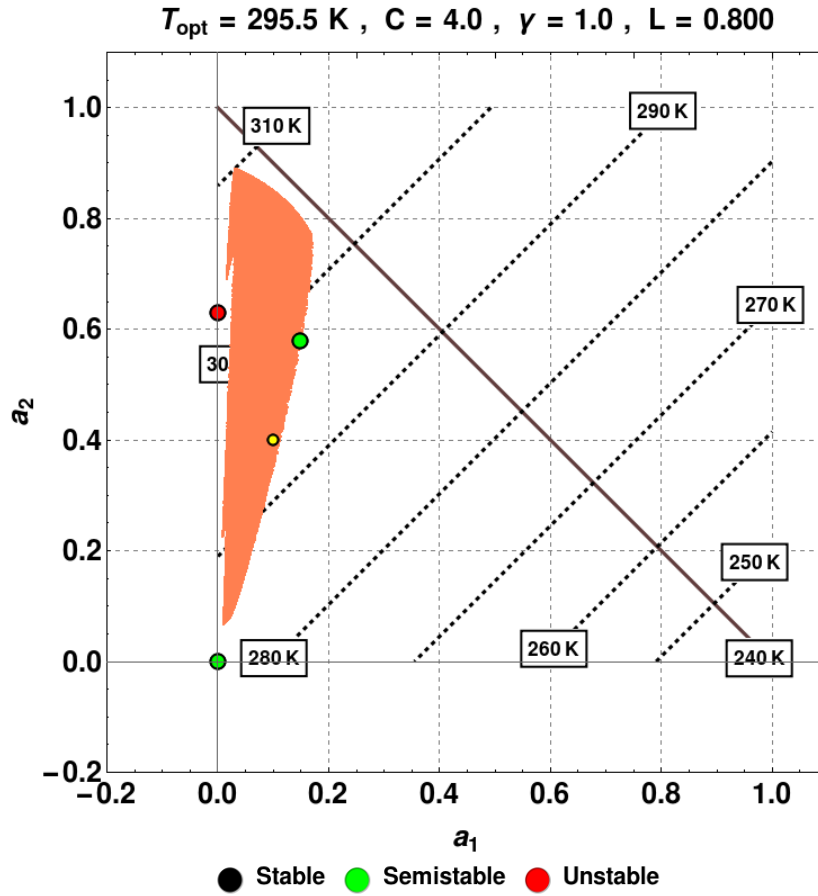
Figure 3.7: DWC asymtotic state in population phase space for $C = 4.0$, $\gamma = 1.0$ and $L = 0.800$. The initial conditions were $a_{1;\,0} = 0.1$ and $a_{2;\,0} = 0.4$ (this initial condition is marked with a **yellow dot**). The structure which appears in this figure may be a **strange attractor**, assumption that must be confirmed by calculating its **fractal dimension** ν.
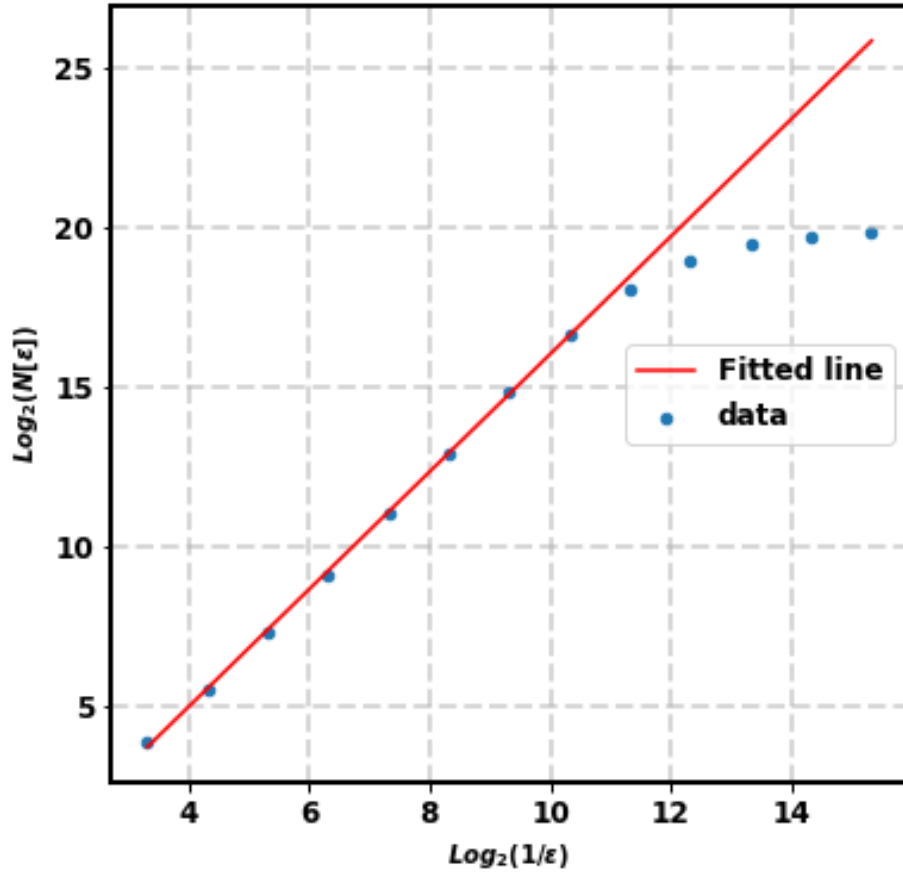
Figure 3.8: DWC box counting method for $C = 4.0$, $\gamma = 1.0$ and $L = 0.800$, and $a_{1;\,0} = 0.1$ and $a_{2;\,0} = 0.4$. In order to find the **fitted line**, we discarded last 5 points of the data, since they correspond to the region where saturation point due to numerical precision is found. The **fitted line** was computed using **least-square** method from **numpy** [49]. The slope of the **fitted line**, which would correspond to the **fractal dimension ν** of the structure found in **Figure 3.7** –which presumably is a **chaotic attractor**–, is $\nu = 1.840$, which corresponds to the dimension of a **fractal set**, so confirming that this structure corresponds to a **strange attractor**.

3.5 Discrete Daisyworld (DWC) - New results

Last subsection leads us to firmly state that **chaos** belongs to **DWC** dynamics. Nevertheless, we are aware that we need a better characterization of chaos in order to get insigth about how chaos emerges and what additional behaviour can be found in **DWC**. We know this insight would lead us to find better conclusions and avoid to make careless conclusions as saying that *"the possibility of chaos in daisyworld is fundamentally flawed"* without taking into account that it was a modelling misconception, not a proven theorem. By charanterizing chaos, we have found that there exist different type of dynamical regimes which shape structure in population phase space, and it was our work to identify them along with their corresponding **basins of attraction**. We have identified some sets of points belonging to different **dynamical regimes**:

- **Null:** it corresponds to the set of points which evolve to the point $(0,0)$; i.e. which evolve to a condition of **extinction**, or in other words, a **dead planet**.

- **FP not null:** it corresponds to the set of points which evolve to any fixed point except the point $(0,0)$; i.e. which evolve to a biological condition where either or both species survive without changes unless environmental conditions, determined by L, change.

- **Periodic:** it corresponds to the set of points which evolve to any periodic orbit.

- **Quasiperiodic:** it corresponds to the set of points which evolve in without "never" repeating any point again (at least in a sensible time window). Furthermore, as chaos is defined as having aperiodical behaviour and sensitivity to initial conditions, then we have opted to distinguish them using **largest Lyapunov exponent** in such a way that if no positive largest Lyaponunov exponent is measured for the time series generated from this points, then they must correspond to quasiperiodic behaviour. This keeps leaving the door open so that trajectories which are determined as belonging to this set, can really belong to **Periodic** set, but we take enough long time series to avoid this problem.

- **Chaotic:** using definition given in **subsection 3.4.1**, we decided to use only a **positive largest Lyapunov exponent** as an evidence os chaotic regime. Furthermore, we found there exist tree types of chaos:

  · **Chaotic (a_1, a_2):** which corresponds to the set of points which evolve to the chaos described in **subsection 3.4.1**, and where both species survive in a chaotic state.
  · **Chaotic $(a_1, 0)$:** this set of points share all of the properties described in **subsection 3.4.1**, but they they differ in that species a_2 eventually goes extinct, and only a_1 survives in a chaotically state forever.
  · **Chaotic $(0, a_2)$:** like former one, but now species a_1 eventually goes extinct, and only a_2 survives in a chaotically state forever.

The procedure followed for sketching up **basins of attraction** was to divide **population phase space** in a set of grid points separated by steps of $\Delta a = 0.01$. For each point we evolved the system of equations in **Table 3.1** for a transient time of 1000 generations and then for an asymptotic time of 2000 generations, then our algorithm checked next conditions in specified order:

(1) If last point is equal to $(0,0)$, then it belongs to **Null** regime.

(2) If last and penultimate points are equal, then it belongs to **FP not null** regime.

(3) If the time series produced has **positive largest lyapunov exponent**, then it belongs to **chaotic regime**. So, depending on whether any condition $a_1 = 0$ or $a_2 = 0$ is fulfilled, then the point in question belongs to the regime **Chaotic (a_1, a_2)**, **Chaotic $(a_1, 0)$** or **Chaotic $(0, a_2)$**.

(4) If the value of the last point of the time series matches with the value of another point of the time series, then it belongs to **Periodic** regime. But, if the all the intermediate points, between last point and the point which matches, are inside a hyperbox of side $\epsilon = 0.001$, then the system should be treated as belonging **FP not null** regime.

(5) Finally, if the last point never matches another point, then the system should be treated as belonging to **Quasiperiodic** regime, since it doesn't have **positive largest Lyapunov exponent**.

And then, we plotted all points generated from each initial condition, thus getting desired **basins of attraction**. In **Figure 3.9** we compare **DWL phase portrait (Figure 3.9a)** with **DWC basins of attraction (Figure 3.9b)** for $C = 4.0$, $\gamma = 1.0$ and $L = 0.800$, and the other parameters values summarized in **Table 2.3**. Furthermore, we decided to sketch up **asymptotic states** for $C = 4.0$, $\gamma = 1.0$, so we got a random initial condition from the set of points determined for each **chaotic regime** and we evolved the system of equations in **Table 3.1** for a transient time of 1×10^6 generations and then for an asymptotic time of 1×10^6 generations (**Figure 3.9c**), in addition with temperature T contour lines and the whole **basin of attraction** for **Null** regime. These graphics let us see –at least for the parameter values considered here– that:

Fact 1

The geometrical shape for frontiers between basins of attraction corresponding to different regime seems to follow a simple mathematical function.

Note that it is characterized by rectangles and triangles, and not by a complex basin of attraction.

Fact 2

Two **chaotic regimes** –**Chaotic $(0, a_2)$** and **Chaotic (a_1, a_2)**– coexist.

Note that in **Figure 3.9c**, there exists two chaotic attractors, the blue one and the orange one.

In order to corroborate **Fact 1**, we investigated contour lines of other system variables (see **Figure 3.10**), and we found that it seems that **Null** regime appears where both β_1 and β_2 cancel, **Chaotic $(0, a_2)$** appears where only β_1 cancels and **Chaotic (a_1, a_2)** appears where

both β_1 and β_2 are different to zero. This leads us to conclude that:

> **Conclusion 1**
>
> There exists a strong relationship between the shape of the basins of attraction and the β variable.

In order to extend the analysis made, we repeated all graphics for other values of L starting from $L = 0.400$ and finishing with $L = 2.200$ in steps of $\Delta L = 0.001$. From **Figure 3.11c** we see that:

> **Fact 3**
>
> Three **chaotic regimes** –**Chaotic $(a_1, 0)$**, **Chaotic $(0, a_2)$** and **Chaotic (a_1, a_2)**– coexist.

Then, from **Fact 2** and **Fact 3**, we can conclude that:

> **Conclusion 2**
>
> There exists **multifractality** in **DWC**. Furthermore, we can see that this multifractility is special since its different fractal sets are connected in a manifest manner with which species survive, so providing an inmediate biological interpretation about this multifractality (see **subsection 2.4.1**).

We also found evidence of complex **intermittency** in **DWC**, where **chaos** is interspersed with **periodic** oscillations (see **Figure 3.13**, **Figure 3.14** and **Figure 3.15**). In particular we note:

> **Fact 4**
>
> - From **Figure 3.13b** it is evident that **Null**, **Periodic**, **Quasiperiodic** and **Chaotic $(0, a_2)$** regimes coexist in population phase space for $L = 0.821$.
>
> - From **Figure 3.15b** it is evident that **Null**, **FP not null**, **Periodic** and two types of chaos –**Chaotic $(0, a_2)$** and **Chaotic (a_1, a_2)**– coexist in population phase space for $L = 0.831$.

Then we conclude that:

Conclusion 3

<u>DWC experiments exhibit highly complex hysteresis:</u> it has different types of **dynamical regimes** and there exist different values of L for which they coexist with each other.

The existence of **multiple stable long term behaviours** in **DWC** –which we have called **dynamical regimes**–, implies that any initial condition of the system in **population phase space** will evolve to the corresponding **dynamical regime** of the **basin of attraction** to which it belongs.

This fact makes **sensitivity tests**, as described in **Concept 2**, difficult to perform, since the path followed by the system when incrementing L depends on <u>how basins of attraction in **population phase space** changes</u> and <u>the location of the system in **population phase space** when L effectively changes</u>. Indeed, the existence of multiple stable long term behaviours, makes the system to exhibit **highly complex hysteresis**, so making the system too delicate, because combining increments of L and changes in basins of attraction would, for example, lead the system to extinct if it accidentally falls in the basin of attraction of extinction when L effectively changes.

In order to get a global picture of system dynamics, we sketched up **orbits diagrams** and the corresponding temperature T mean for $C = 4.0$ and $\gamma = 1.0$. From **Figure 3.16b**, it is evident how **period doubling** occurs and we can conclude that:

Conclusion 4

Period doubling is the **main route to chaos** in **DWC**.

Furthermore, in **Figure 3.16c** we plot temperature T mean, taking average along all asymptotic time series (1×10^6 generations). We see that the curve followed by T mean is too similar to **Figure 2.12**, nervertheless, it is quite different from **Figure 2.21**, by Jascourt. It would be because of the wrong procedure followed by Jascourt of adjusting Δt in **Equation 2.18** for the minimum value that exhibits chaos when changing L. One can think that Jascourt generated different models for each L value, but he didn't analyzed how changes in L modifies dynamical structure in **population phase space**. Next we expand the discussion about other important characteristics of these plots (**Figure 3.16b** and **Figure 3.16c**).
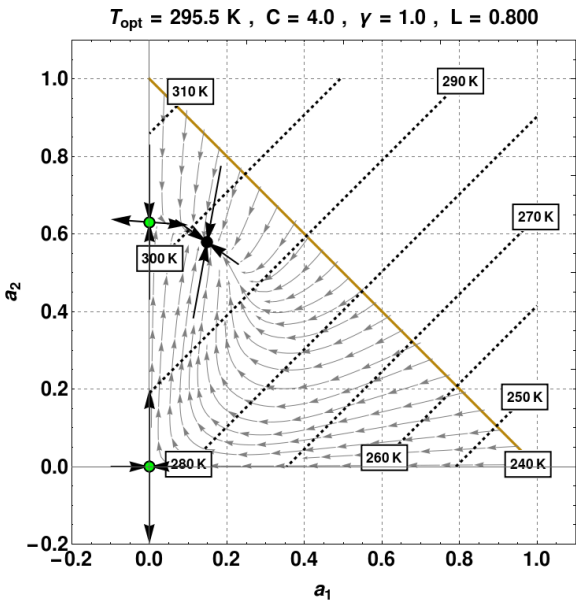
(a) DWL phase portrait $L = 0.800$.
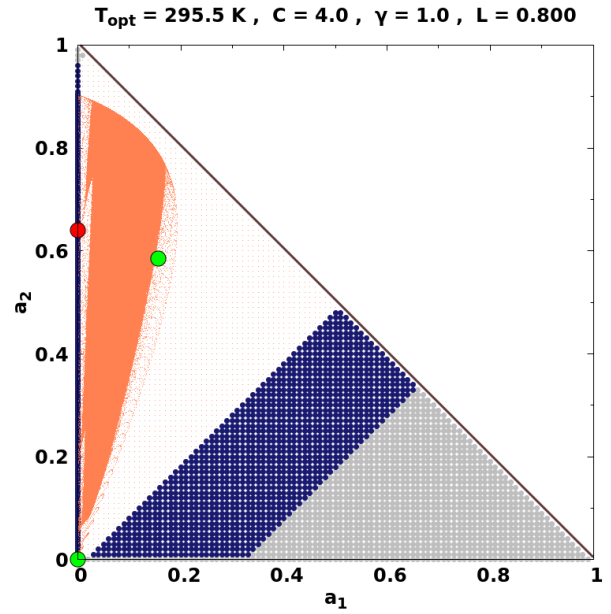
(b) DWC basins of attraction for $C = 4.0$, $\gamma = 1.0$ and $L = 0.800$.
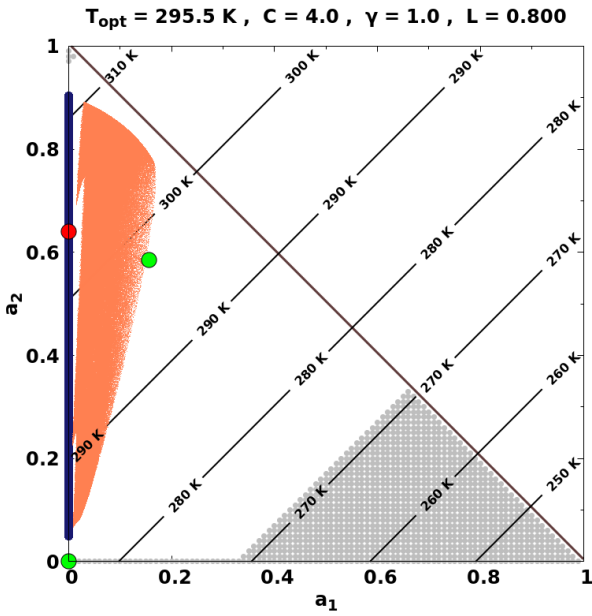
(c) DWC asymptotic state for $C = 4.0$, $\gamma = 1.0$ and $L = 0.800$, besides to temperature T contour lines.

Figure 3.9: Comparison between **DWL** phase portrait and **DWC** basins of attraction for $C = 4.0$, $\gamma = 1.0$ and $L = 0.800$.
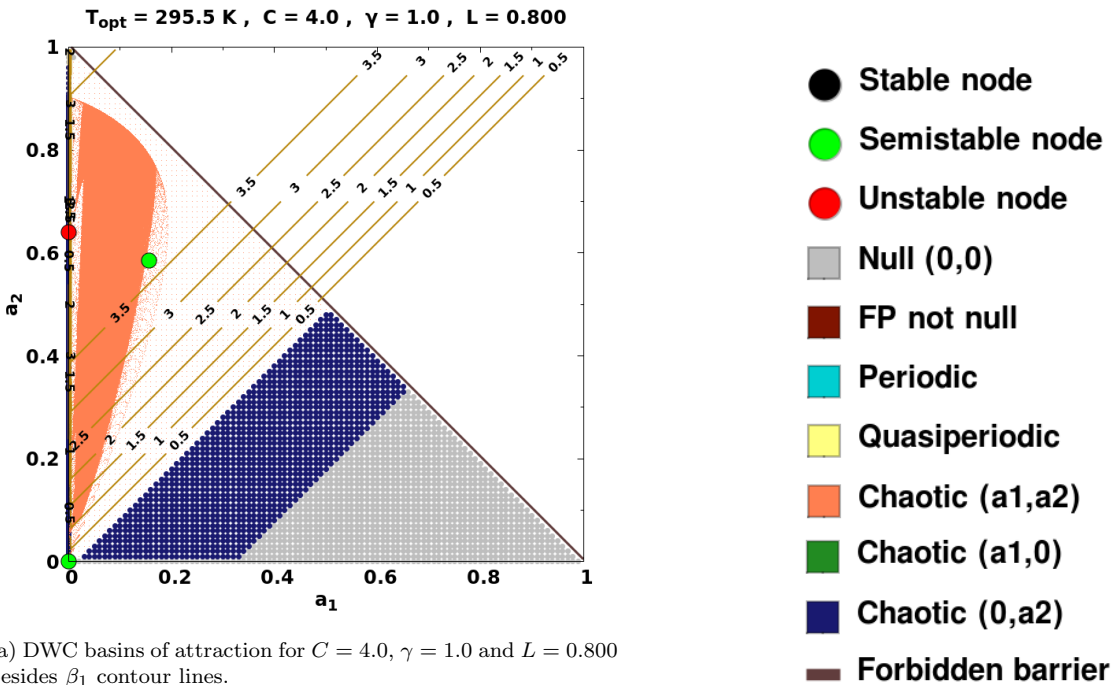
(a) DWC basins of attraction for $C = 4.0$, $\gamma = 1.0$ and $L = 0.800$ besides β_1 contour lines.
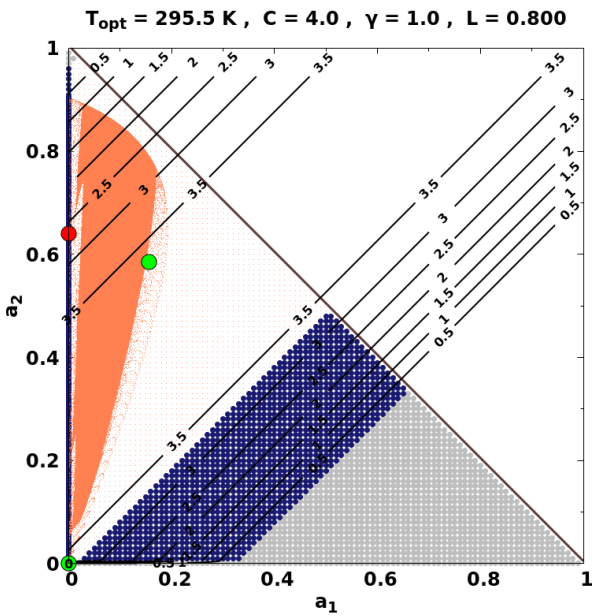
(b) DWC basins of attraction for $C = 4.0$, $\gamma = 1.0$ and $L = 0.800$ besides β_2 contour lines.

Figure 3.10: **DWC** basins of attraction and β_i contour lines for $C = 4.0$, $\gamma = 1.0$ and $L = 0.800$.
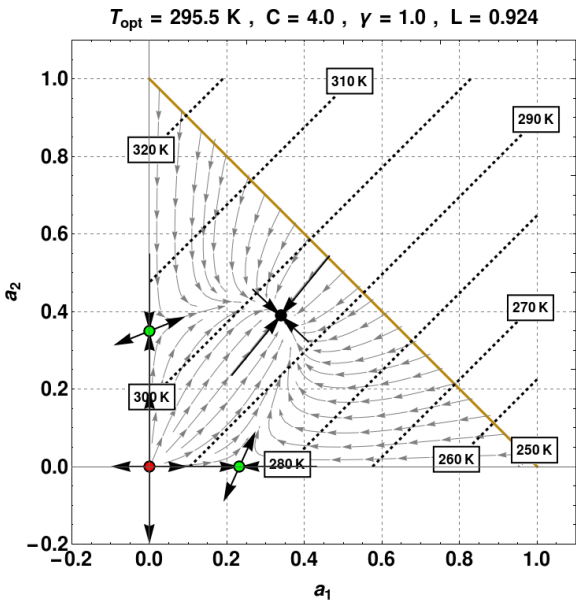
(a) DWL phase portrait $L = 0.924$.
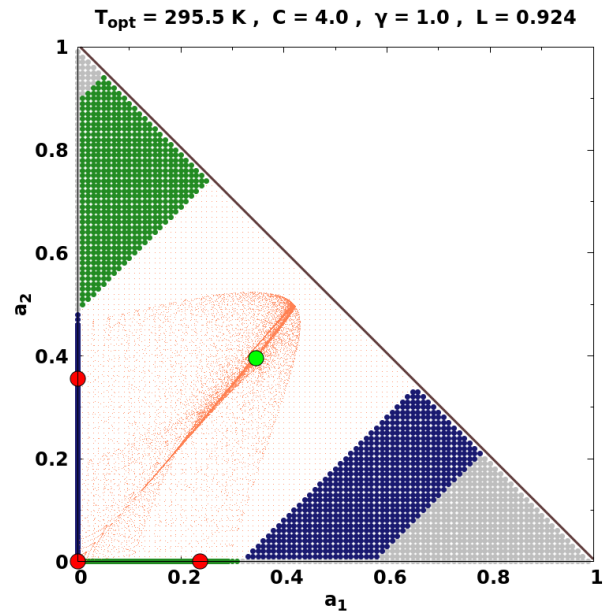
(b) DWC basins of attraction for $C = 4.0$, $\gamma = 1.0$ and $L = 0.924$.
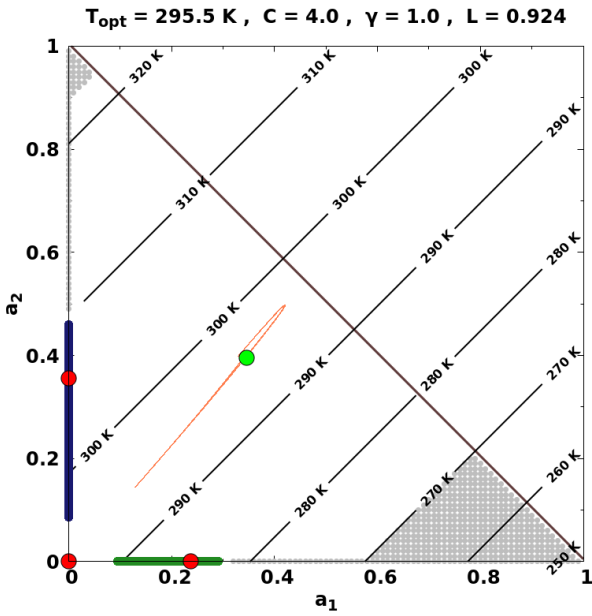
(c) DWC asymptotic state for $C = 4.0$, $\gamma = 1.0$ and $L = 0.924$, besides to temperature T contour lines.

Figure 3.11: Comparison between **DWL** phase portrait and **DWC** basins of attraction for $C = 4.0$, $\gamma = 1.0$ and $L = 0.924$.

T_{opt} = 295.5 K , C = 4.0 , γ = 1.0 , L = 0.924

(a) DWC basins of attraction for $C = 4.0$, $\gamma = 1.0$ and $L = 0.924$ besides β_1 contour lines.

T_{opt} = 295.5 K , C = 4.0 , γ = 1.0 , L = 0.924
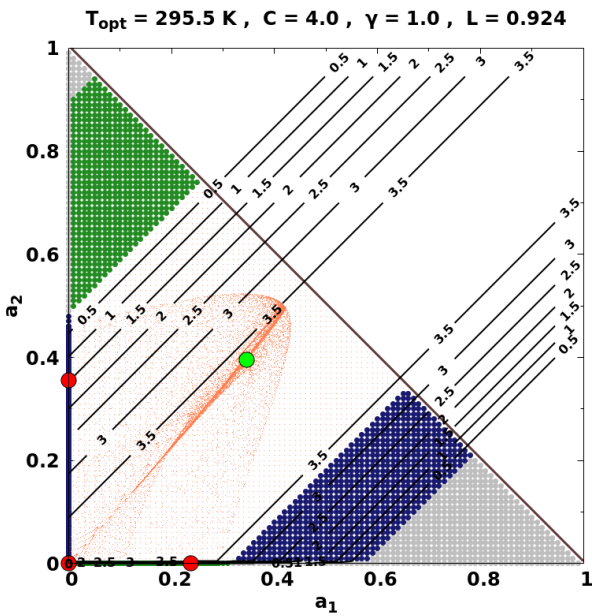
(b) DWC basins of attraction for $C = 4.0$, $\gamma = 1.0$ and $L = 0.924$ besides β_2 contour lines.

Figure 3.12: **DWC** basins of attraction and β_i contour lines for $C = 4.0$, $\gamma = 1.0$ and $L = 0.924$.

Legend:
- ● Stable node
- ● Semistable node
- ● Unstable node
- Null (0,0)
- FP not null
- Periodic
- Quasiperiodic
- Chaotic (a1,a2)
- Chaotic (a1,0)
- Chaotic (0,a2)
- Forbidden barrier

T_opt = 295.5 K , C = 4.0 , γ = 1.0 , L = 0.820

(a) DWC basins of attraction for $C = 4.0$, $\gamma = 1.0$ and $L = 0.820$.

T_opt = 295.5 K , C = 4.0 , γ = 1.0 , L = 0.821
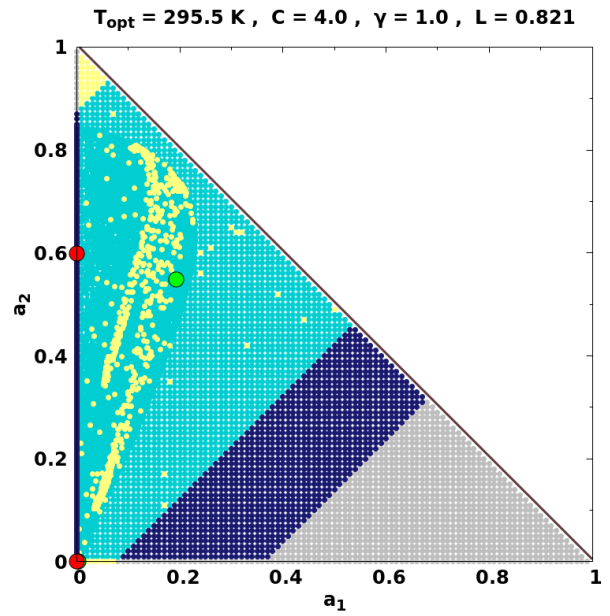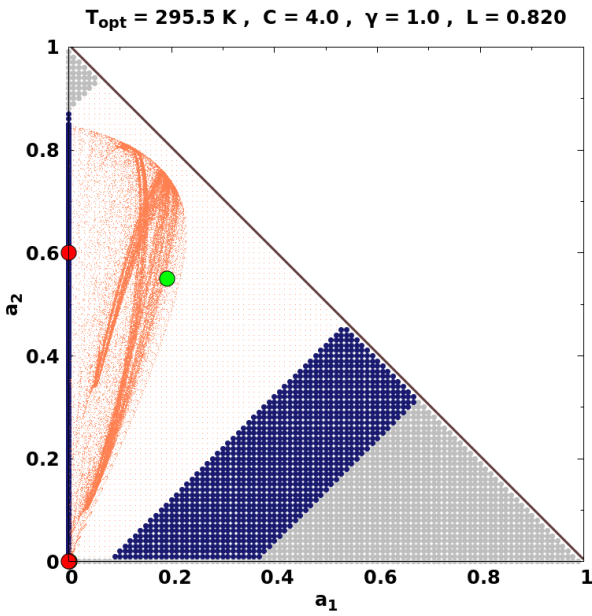
(b) DWC basins of attraction for $C = 4.0$, $\gamma = 1.0$ and $L = 0.821$.

T_opt = 295.5 K , C = 4.0 , γ = 1.0 , L = 0.822
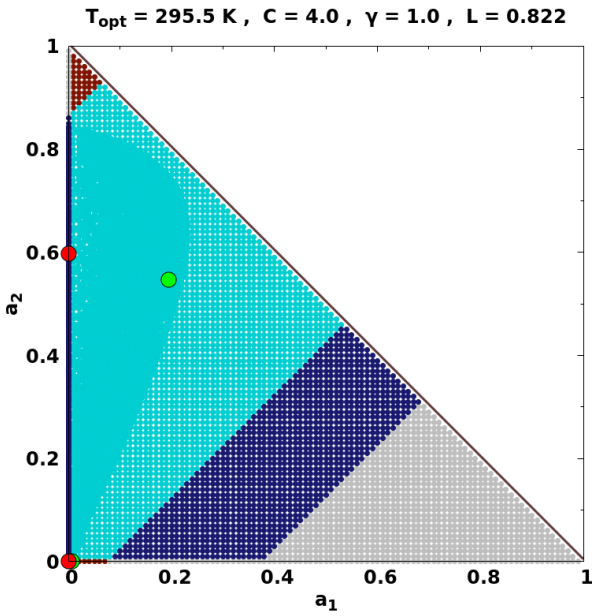
(c) DWC basins of attraction for $C = 4.0$, $\gamma = 1.0$ and $L = 0.822$.

- Stable node
- Semistable node
- Unstable node
- Null (0,0)
- FP not null
- Periodic
- Quasiperiodic
- Chaotic (a1,a2)
- Chaotic (a1,0)
- Chaotic (0,a2)
- Forbidden barrier

Figure 3.13: **Intermittency** in **DWC**.
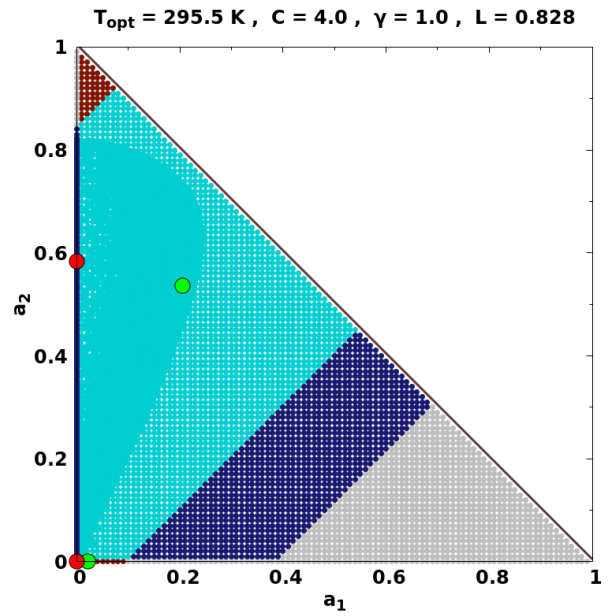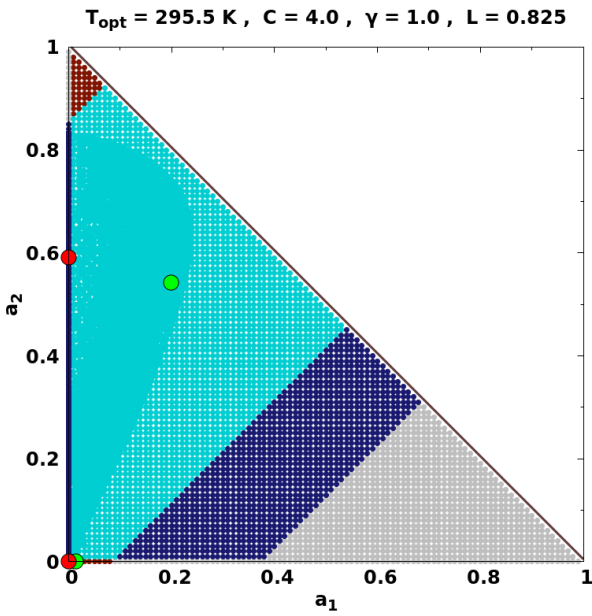
(a) DWC basins of attraction for $C = 4.0$, $\gamma = 1.0$ and $L = 0.825$.

(b) DWC basins of attraction for $C = 4.0$, $\gamma = 1.0$ and $L = 0.828$.
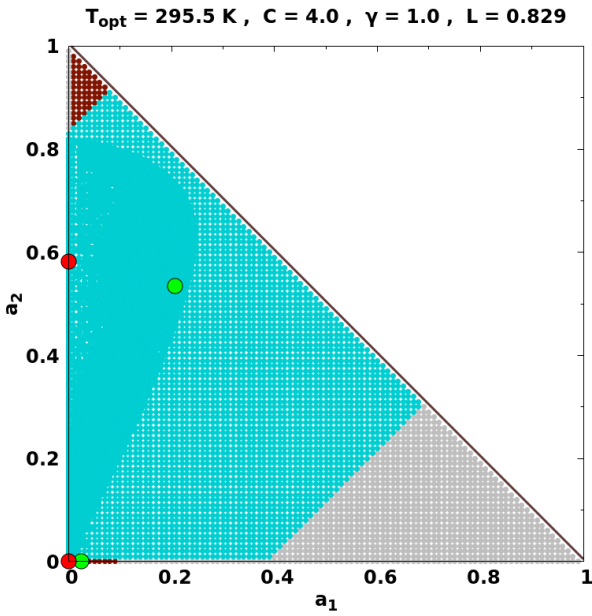
(c) DWC basins of attraction for $C = 4.0$, $\gamma = 1.0$ and $L = 0.829$.

Figure 3.14: **Intermittency** in **DWC**.

T_opt = 295.5 K , C = 4.0 , γ = 1.0 , L = 0.830

(a) DWC basins of attraction for $C = 4.0$, $\gamma = 1.0$ and $L = 0.830$.

T_opt = 295.5 K , C = 4.0 , γ = 1.0 , L = 0.831
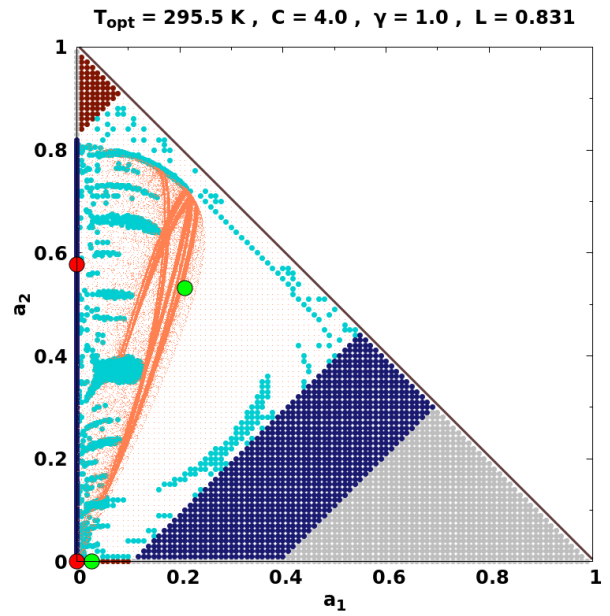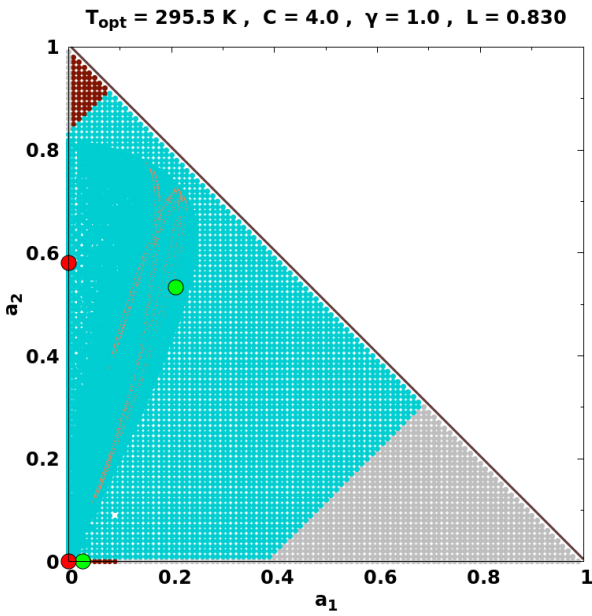
(b) DWC basins of attraction for $C = 4.0$, $\gamma = 1.0$ and $L = 0.831$.

T_opt = 295.5 K , C = 4.0 , γ = 1.0 , L = 0.832
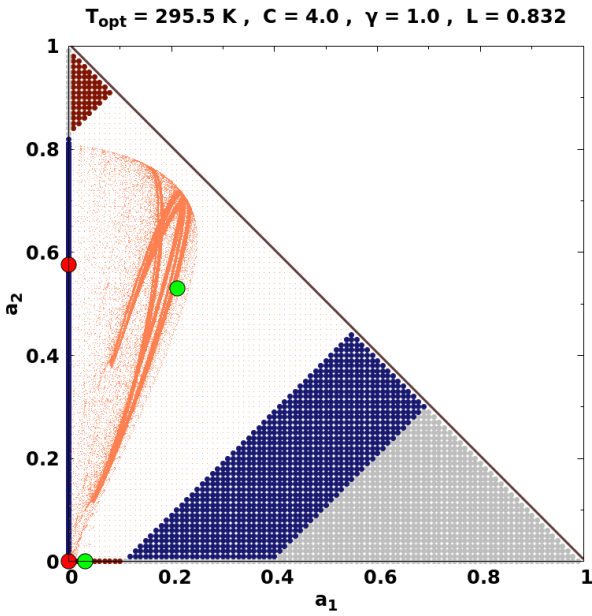
(c) DWC basins of attraction for $C = 4.0$, $\gamma = 1.0$ and $L = 0.832$.

- ● Stable node
- ● Semistable node
- ● Unstable node
- Null (0,0)
- FP not null
- Periodic
- Quasiperiodic
- Chaotic (a1,a2)
- Chaotic (a1,0)
- Chaotic (0,a2)
- Forbidden barrier

Figure 3.15: **Intermittency** in **DWC**.

(a) DWC bifurcation for $C = 4.0$ and $\gamma = 1.0$.

(b) DWC orbits diagram for $C = 4.0$ and $\gamma = 1.0$.

(c) DWC temperature T mean for $C = 4.0$ and $\gamma = 1.0$.

- ● Stable node
- ● Semistable node
- ● Unstable node
- ▢ Null (0,0)
- ▪ FP not null
- ▢ Periodic
- ▢ Quasiperiodic
- ▪ Chaotic (a1,a2)
- ▪ Chaotic (a1,0)
- ▪ Chaotic (0,a2)
- ▬ Forbidden barrier
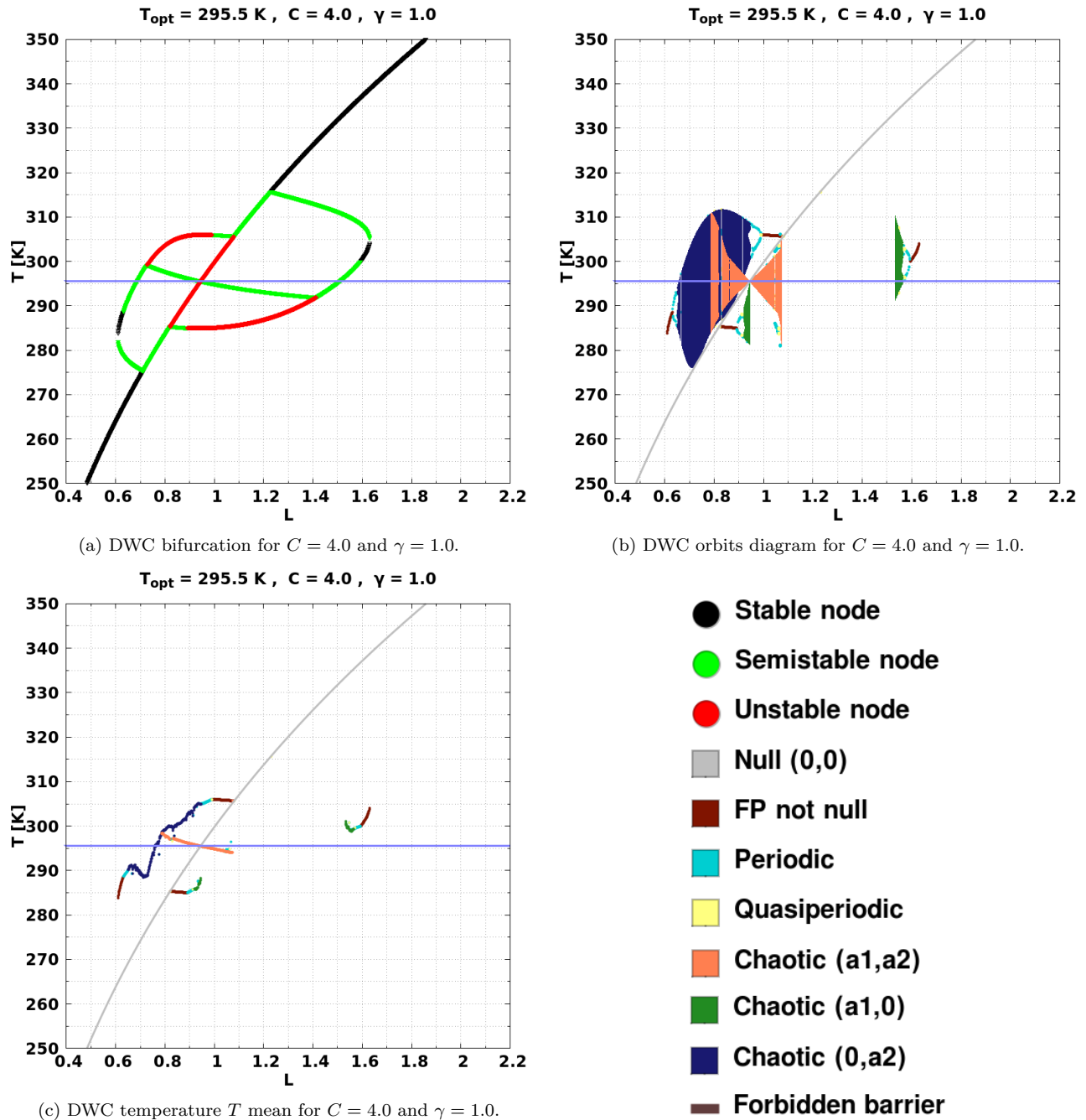
Figure 3.16: **Orbits diagram** and the corresponding temperature T mean for **DWC** for $C = 4.0$ and $\gamma = 1.0$. **Blue** line corresponds to the value of $T_{opt} = 295.5$ K.

3.5.1 Redefining Homeostasis

As it was remarked in **subsection 2.3.3**, **homeostasis** was related by Lovelock to a stable steady state where environmental conditions return after any perturbation which, in the absence of the homeostasis mechanism, would yield to environmental conditions not suitable for life. In this sense, when Zeng found evidence of chaos in Daisyworld (using modified model), he said about homeostasis:

> *These results show that stable climatic conditions are not always maintained in Daisyworld. (…), the conclusion of Watson and Lovelock (1983), based on the differential equation (**Equation 2.10**), that Daisyworld always shows greater stability with daisies present, is not a general result.*

<div align="right">— Zeng [2].</div>

Clearly, Zeng was thinking about chaos as a dynamic regime where steady states no longer exist and that has aperiodic long-term behaviour and sensitivity to initial conditions, so being unpredictable, and thus, chaos itself would prevent homeostasis as it was understood by Lovelock (**Concept 1**) and Jascourt and Raymond, and even Nevison (**subsection 2.5.1**). Nevertheless, due to the existence in **population phase space** of **strange attractors** that maintain all trajectories bounded, so bounding the temperatures accessible by the system too and the fact that populations do not extinct for long time (in generation time scale) despite of being in **chaotic** regime –it was 2×10^6 generations for our simulations–, we can conclude that:

Conclusion 5

In **DWC**, there exists a bounded set of accessible temperatures that are completely different of the temperatures of a dead planet and which are visited aperiodically by chaotic trajectories without get extinct, so providing environmental conditions needed to keep planet habitable.

And this pose the necessity of redefining what has to be understood by **homeostasis**:

Concept 3

Biological homeostasis of the global environment must be understood as the biologically originated mechanism by which environmental conditions are shifted from nonsuitable values for life to other values that are bounded between life suitable values.

These life suitable values can correspond to:

- **Equilibrium states:** where the regulatory agents are **stable fixed points**.

- **Periodic or quasiperiodic states:** where the regulatory agents are **limit cycles** –or **periodic orbits**–, and **toroidal trajectories.**

- **Chaotic states:** where the regulatory agents are **chaotic attractors** that, although they originate long-term irregular behaviour, they still regulating the system and allow the planet to remain habitable.

Thus, this concept includes the idea that **chaotic dynamics** regulates climate to irregular states which being habitables, still exhibit homeostasis. In this sense, a **strange attractor** also represents **homeostasis**, and thus **homeostasis** becomes in a **robust property** of **Daisyworld model**, no matter if we refer to **DWL** or **DWC** model.

3.5.2 Global extinctions in DWC

In **Figure 3.16b** and **Figure 3.16c** there are evident anomalies that we did not expect: coexistence of multiple regimes described in **section 3.5** has disappeared and it has only remained **Null** regime, corresponding to a **dead planet**. Thus, for **DWC**, any initial condition for population of any species is inexorably destined to die, and this happens for L values where **DWL** predicts a steady value for life.

We have found that this behaviour happens between $L = 1.082$ and $L = 1.532$ including these values. We have framed this region by a **dashed red** line in **Figure 3.17**. From **Figure 3.17a**, we can infer that this behaviour cannot be described from linearization around fixed points since there are some L values, from $L = 1.082$ and $L = 1.231$, for which this behaviour happens despite the fixed point $(0, 0)$ is not stable. The value of $L = 1.231$ is a critical point where a **saddle-node bifurcation** occurs and a new **semistable node** in axis a_1 emerges and **semistable node** at origin $(0, 0)$ becomes **stable**.

Until now, we have concluded that given the possibility of multiple stable long term behaviours that there exist in **DWC**, the system also have multiple choices for evolving depending on how basins of attraction in **population phase space** changes and the location of the system in **population phase space** when L effectively changes (**Conclusion 3**). Nevertheless, in this region, the system only has one choice: **extinction**, thus **homeostasis** disappears too.

Last fact makes us think about two primary questions:

Q-1 How coexistence of multiple dynamic regimes disappears?

Q-2 How coexistence of multiple dynamic regimes reappears for $L = 1.533$?

In **Figure 3.18**, **Figure 3.19** and **Figure 3.20** we can follow all **basins of attraction** transformations carried out in transition from **coexistence of multiple dynamic regimes** to **extinction only**. Omitting possible numerical errors in the classification of the **basins of attraction** due to the limited length of the time series we used, we can see that instabilities in **population phase space** –marked by existence of **chaos**, i.e. existence of sensitivity of initial conditions– begin to be replaced by **FP not null** basin (**Figure 3.19d** and **Figure 3.20a**), until this latter is finally replaced by **Null** basin covering all **population phase space** (**Figure 3.20c** and **Figure 3.20d**). Its easy to corroborate that the transition seen corresponds to a **saddle node bifurcation** performed between the **semistable node** in axis a_2 and the **unstable node** at origin $(0, 0)$: the **semistable node** collides with origin ($L = 1.082$, **Figure 3.20c**), whereupon **unstable node** at origin $(0, 0)$ turns into a **semistable node** ($L = 1.083$, **Figure 3.20d**). Then, $L = 1.083$ is the **critical point** for the bifurcation described, and for answering **Q-1**:

Even though the origin $(0,0)$ does not turn into a **stable node** until **critical point** $L = 1.231$ is reached, two sources of instabilities have been lost –two **unstable manifolds**, one from **semistable node** in axis a_2 and another from **unstable node**, where the latter is replaced by a **stable manifold** giving birth to the **semistable node** at origin–.

We have noted before that in $L = 1.231$ another **saddle-node bifurcation** occurs, giving birth to a new **semistable node** in axis a_1 and the **semistable node** at origin $(0,0)$ becomes **stable** (**Figure 3.21**). Furthermore, from **Figure 3.20**, **Figure 3.21** and **Figure 3.22**, we can infer that there is another bifurcation in process between the **semistable node** inside **population phase space**, where both species coexist, and the **unstable node** in axis a_1. The **critical point** for this bifurcation is $L = 1.427$ (**Figure 3.22c**), and after it happens, the **unstable node** turns into a **semistable node**, then reducing even more the instabilities in **population phase space**. Then, looking back on **Q-2**, **how chaos and other dynamical regimes are reborn?**. From **Figure 3.22c** and **Figure 3.22d**, it is clear that two **semistable nodes** in axis a_1 are left, but interestingly, one moves toward the other, and when they are near enough, **chaos** emerges again (**Figure 3.23**). Then:

(a) DWC bifurcation for $C = 4.0$ and $\gamma = 1.0$.

(b) DWC orbits diagram for $C = 4.0$ and $\gamma = 1.0$.

(c) DWC temperature T mean for $C = 4.0$ and $\gamma = 1.0$.

Stable node

Semistable node

Unstable node

Null (0,0)

FP not null

Periodic

Quasiperiodic

Chaotic (a1,a2)

Chaotic (a1,0)

Chaotic (0,a2)

Forbidden barrier
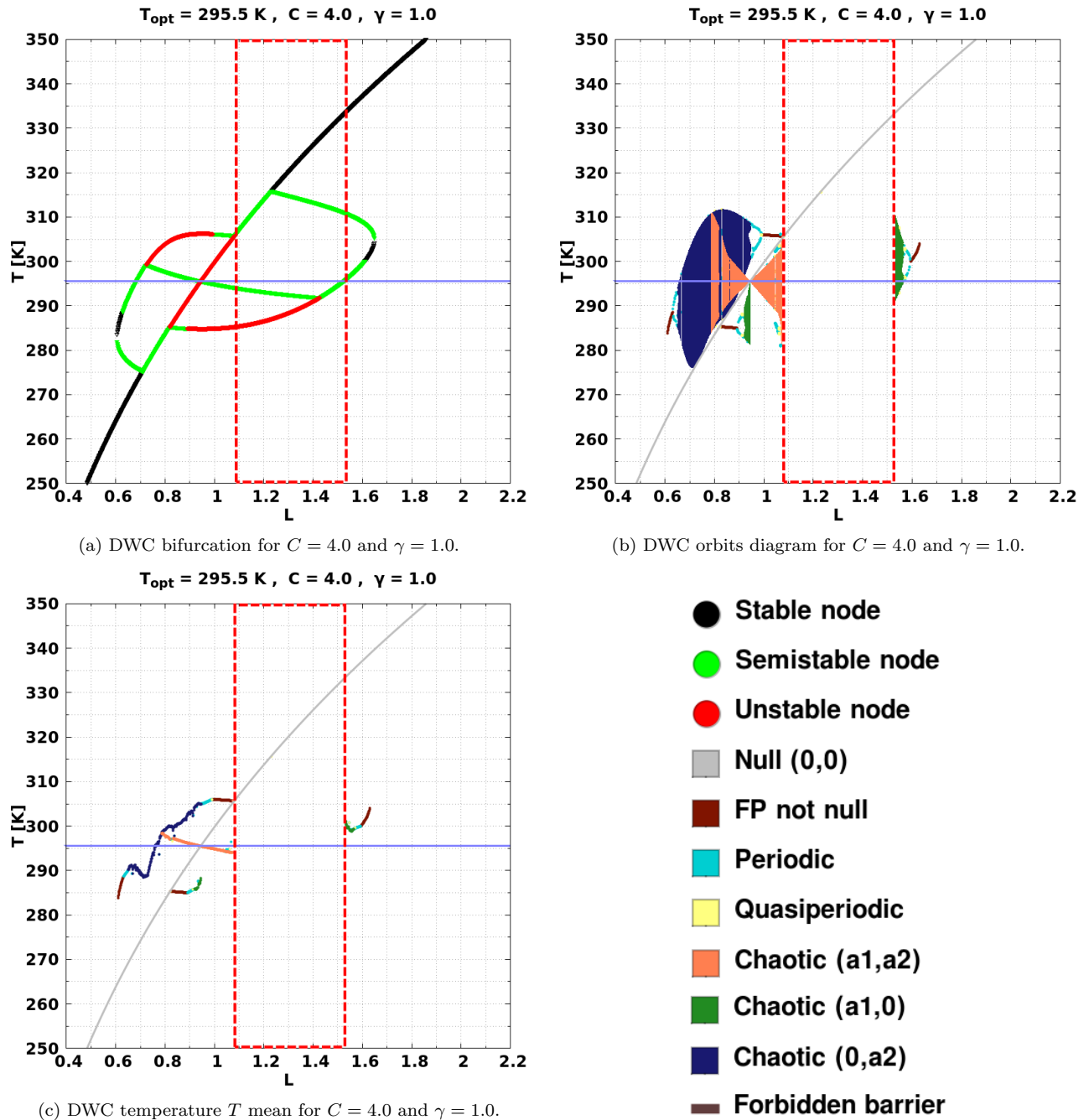
Figure 3.17: Asymptotic **extinction** evidence in **Orbits diagram** and the corresponding temperature T mean for **DWC** for $C = 4.0$ and $\gamma = 1.0$. **Blue** line corresponds to the value of $T_{opt} = 295.5$ K. **Dashed red** line delimits the region where **extinction occurs.**

T_opt = 295.5 K , C = 4.0 , γ = 1.0 , L = 1.072

T_opt = 295.5 K , C = 4.0 , γ = 1.0 , L = 1.073
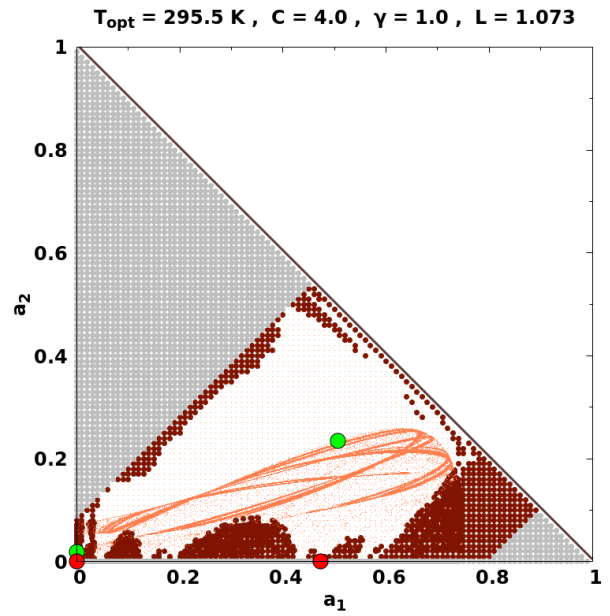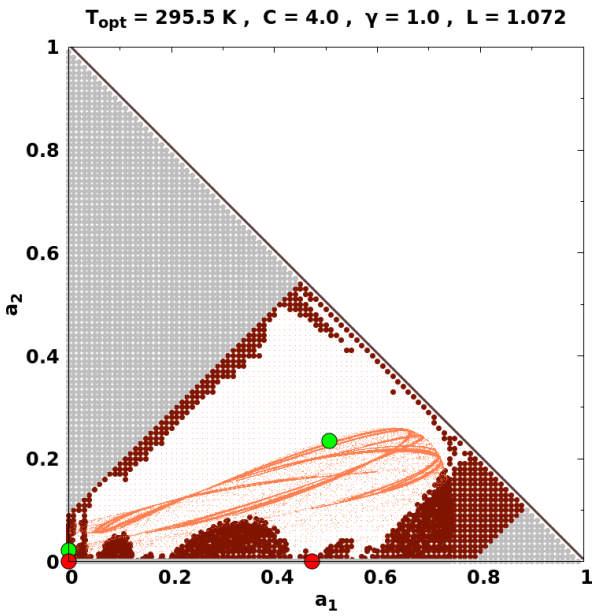
(a) DWC basins of attraction for $C = 4.0$, $\gamma = 1.0$ and $L = 1.072$.

(b) DWC basins of attraction for $C = 4.0$, $\gamma = 1.0$ and $L = 1.073$.

T_opt = 295.5 K , C = 4.0 , γ = 1.0 , L = 1.074

T_opt = 295.5 K , C = 4.0 , γ = 1.0 , L = 1.075
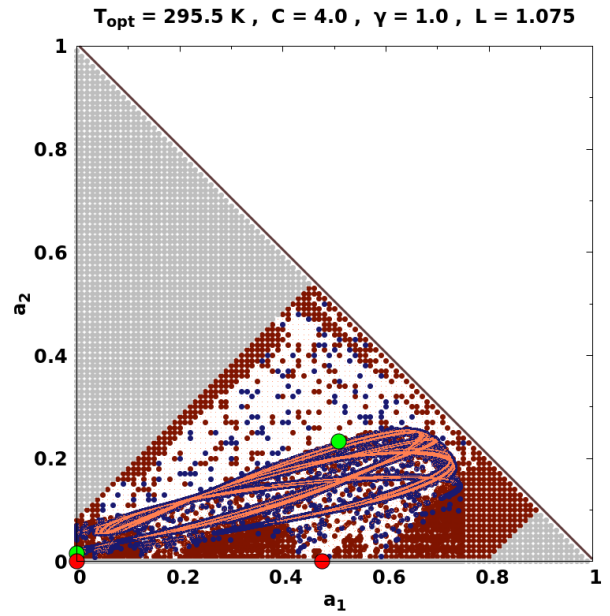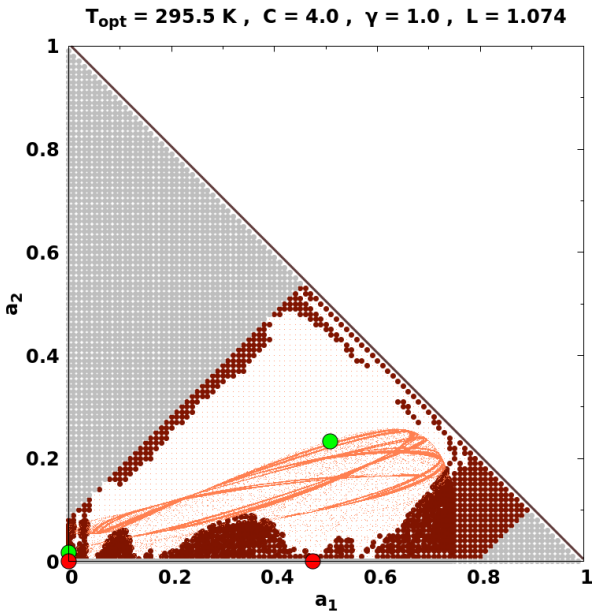
(c) DWC basins of attraction for $C = 4.0$, $\gamma = 1.0$ and $L = 1.074$.

(d) DWC basins of attraction for $C = 4.0$, $\gamma = 1.0$ and $L = 1.075$.

- ● Stable node
- ● Semistable node
- ● Unstable node
- ▬ Forbidden barrier
- ▬ Null (0,0)
- ▬ FP not null
- ▬ Periodic
- ▬ Quasiperiodic
- ▬ Chaotic (a1,a2)
- ▬ Chaotic (a1,0)
- ▬ Chaotic (0,a2)

Figure 3.18: **DWC extinction exploration** from analysis of **basins of attraction** for $C = 4.0$, $\gamma = 1.0$ and next L values: $L = 1.072$ / $L = 1.073$ / $L = 1.074$ / $L = 1.075$.
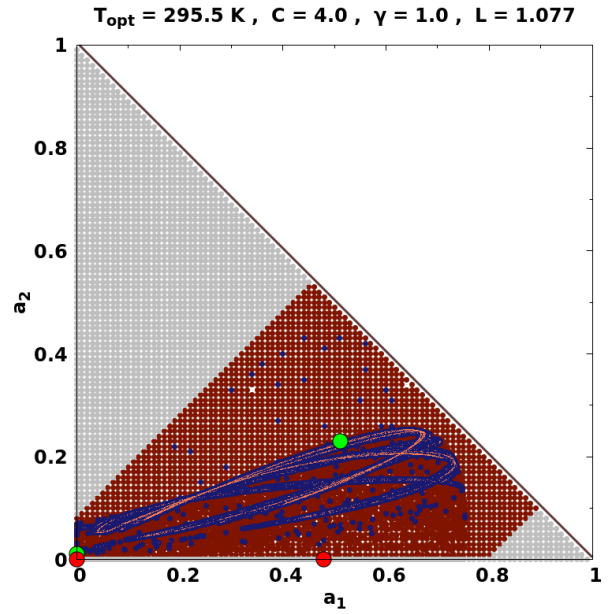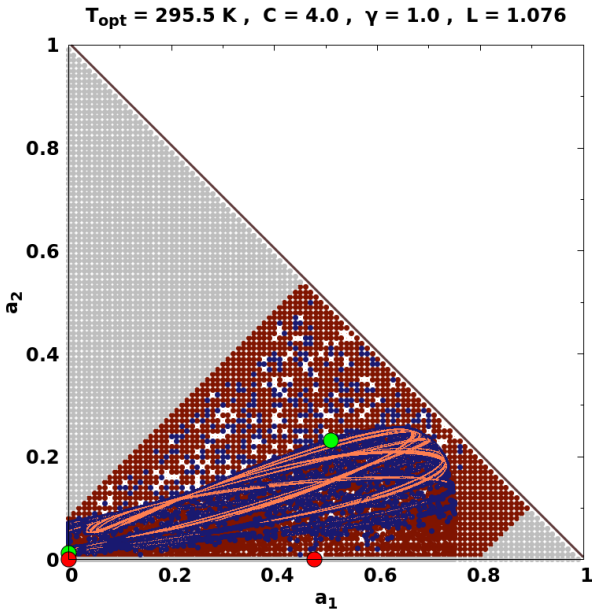
(a) DWC basins of attraction for $C = 4.0$, $\gamma = 1.0$ and $L = 1.076$.

(b) DWC basins of attraction for $C = 4.0$, $\gamma = 1.0$ and $L = 1.077$.
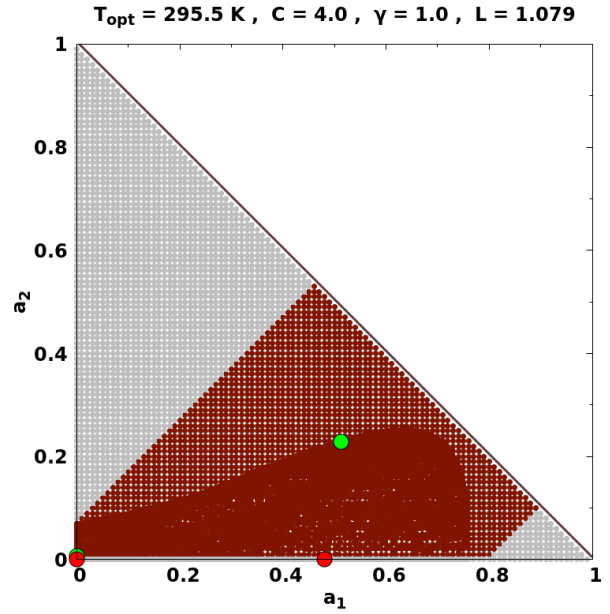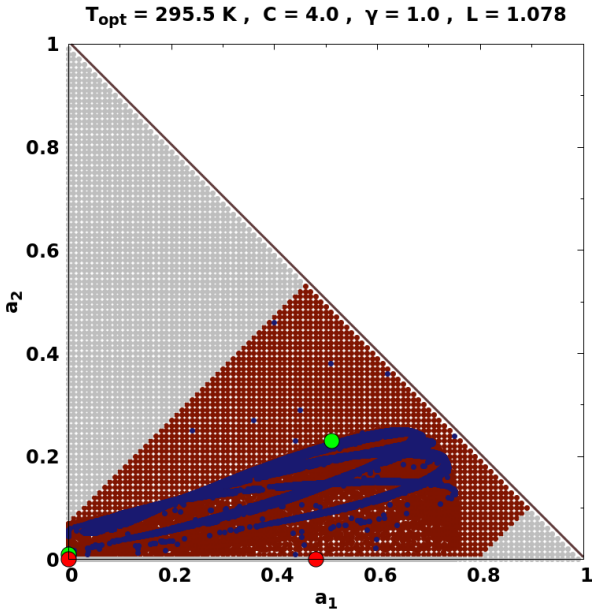
(c) DWC basins of attraction for $C = 4.0$, $\gamma = 1.0$ and $L = 1.078$.

(d) DWC basins of attraction for $C = 4.0$, $\gamma = 1.0$ and $L = 1.079$.
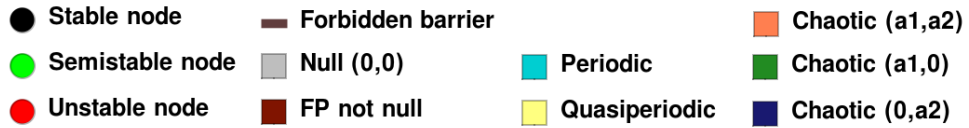
Figure 3.19: **DWC extinction exploration** from analysis of **basins of attraction** for $C = 4.0$, $\gamma = 1.0$ and next L values: $L = 1.076$ / $L = 1.077$ / $L = 1.078$ / $L = 1.079$.
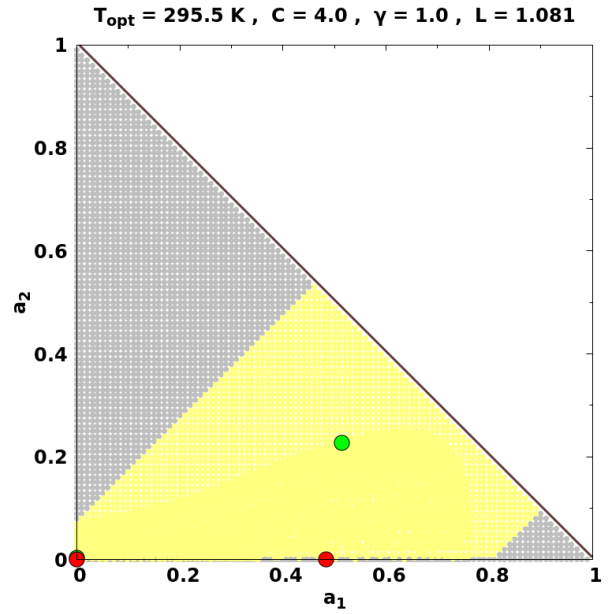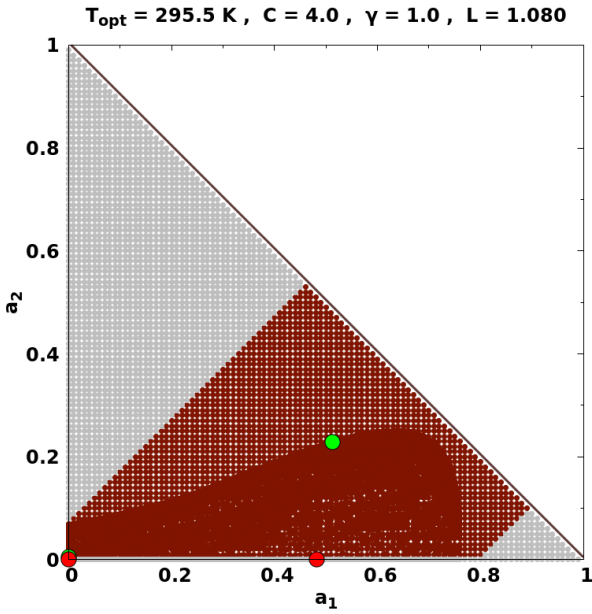
(a) DWC basins of attraction for $C = 4.0$, $\gamma = 1.0$ and $L = 1.080$.   (b) DWC basins of attraction for $C = 4.0$, $\gamma = 1.0$ and $L = 1.081$.
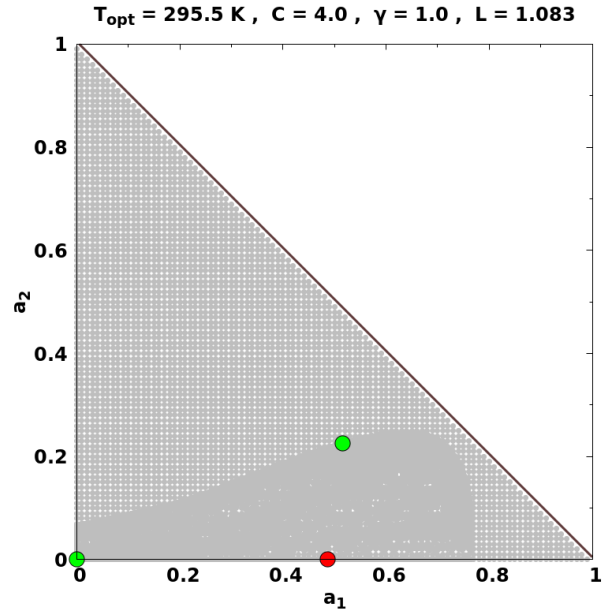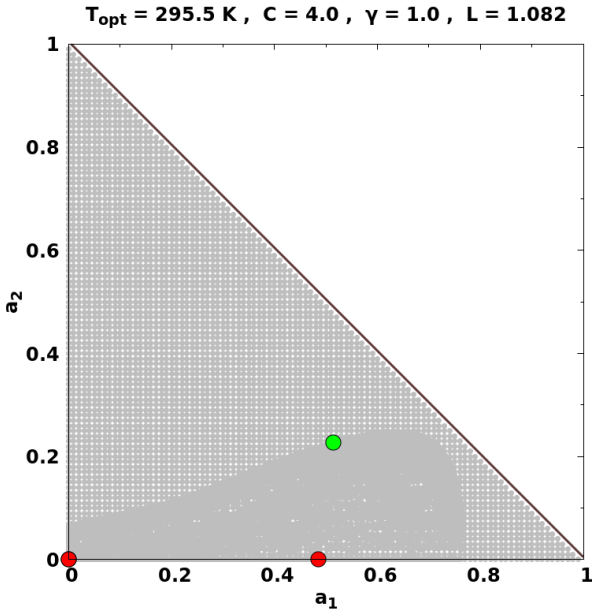
(c) DWC basins of attraction for $C = 4.0$, $\gamma = 1.0$ and $L = 1.082$.   (d) DWC basins of attraction for $C = 4.0$, $\gamma = 1.0$ and $L = 1.083$.

Figure 3.20: **DWC exploration of extinction** from analysis of **basins of attraction** for $C = 4.0$, $\gamma = 1.0$ and next L values: $L = 1.080$ / $L = 1.081$ / $L = 1.082$ / $L = 1.083$.
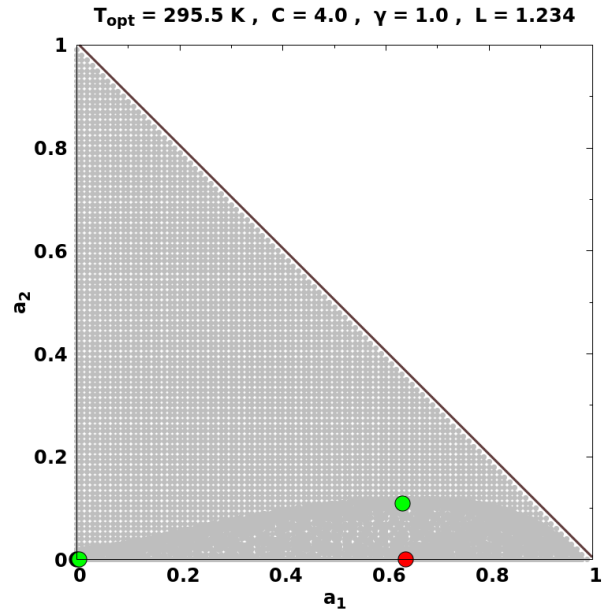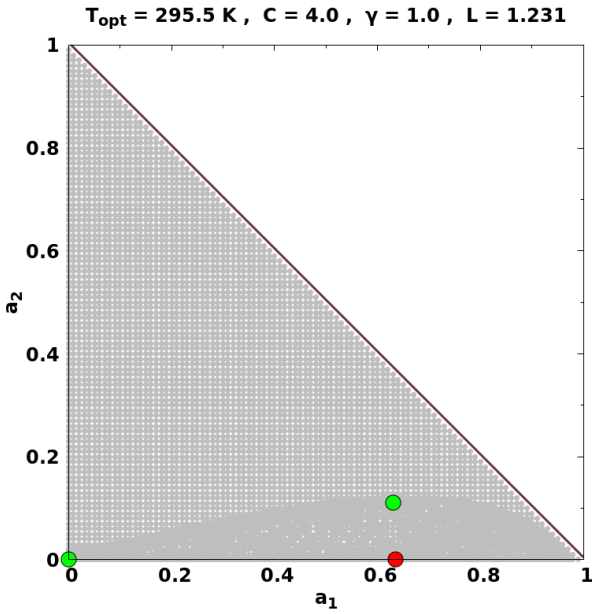
(a) DWC basins of attraction for $C = 4.0$, $\gamma = 1.0$ and $L = 1.231$.
(b) DWC basins of attraction for $C = 4.0$, $\gamma = 1.0$ and $L = 1.234$.
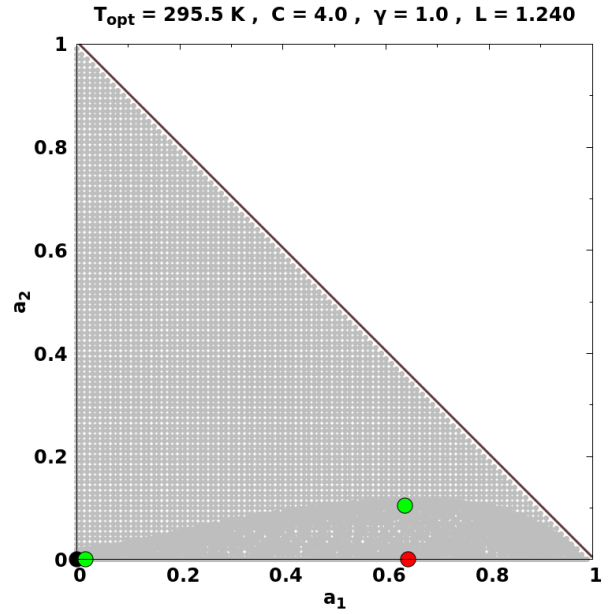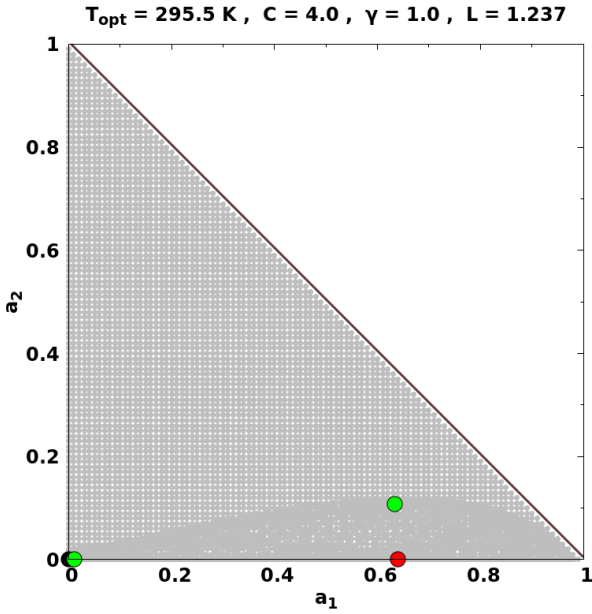
(c) DWC basins of attraction for $C = 4.0$, $\gamma = 1.0$ and $L = 1.237$.
(d) DWC basins of attraction for $C = 4.0$, $\gamma = 1.0$ and $L = 1.240$.

Figure 3.21: **DWC exploration of bifurcation at origin** from analysis of **basins of attraction** for $C = 4.0$, $\gamma = 1.0$ and next L values: $L = 1.231$ / $L = 1.234$ / $L = 1.237$ / $L = 1.240$.
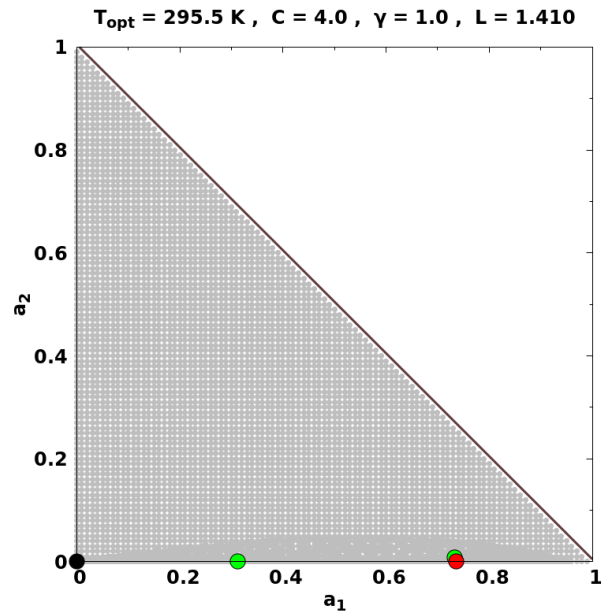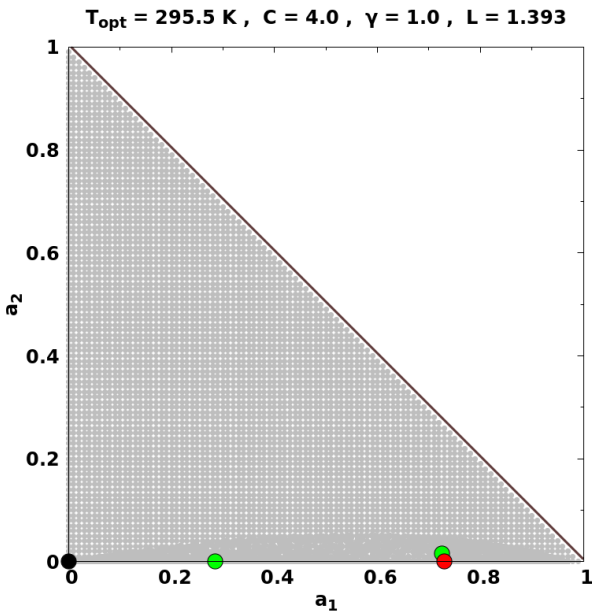
(a) DWC basins of attraction for $C = 4.0$, $\gamma = 1.0$ and $L = 1.393$.

(b) DWC basins of attraction for $C = 4.0$, $\gamma = 1.0$ and $L = 1.410$.
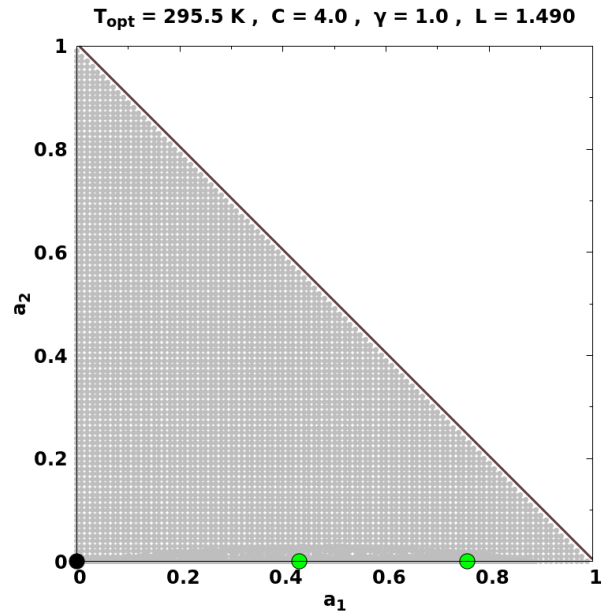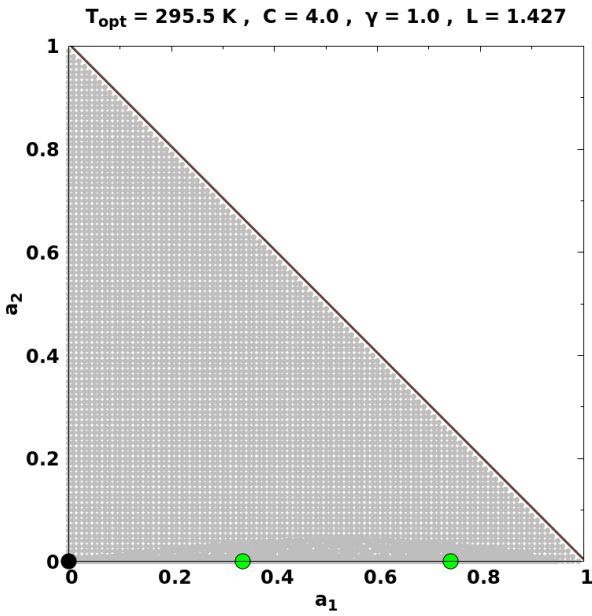
(c) DWC basins of attraction for $C = 4.0$, $\gamma = 1.0$ and $L = 1.427$.

(d) DWC basins of attraction for $C = 4.0$, $\gamma = 1.0$ and $L = 1.490$.

Figure 3.22: **DWC exploration of bifurcations** from analysis of **basins of attraction** for $C = 4.0$, $\gamma = 1.0$ and next L values: $L = 1.393$ / $L = 1.410$ / $L = 1.427$ / $L = 1.490$.
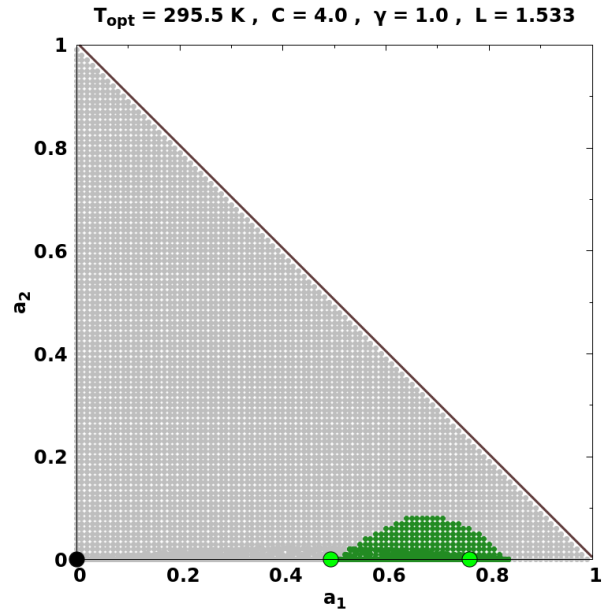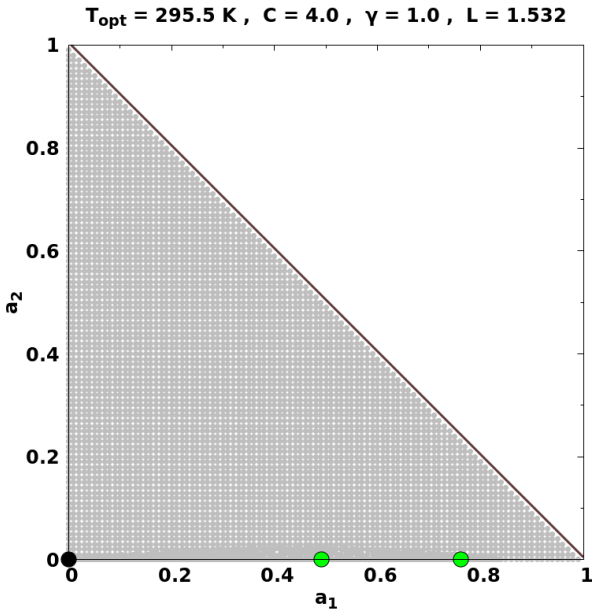
(a) DWC basins of attraction for $C = 4.0$, $\gamma = 1.0$ and $L = 1.532$.

(b) DWC basins of attraction for $C = 4.0$, $\gamma = 1.0$ and $L = 1.533$.
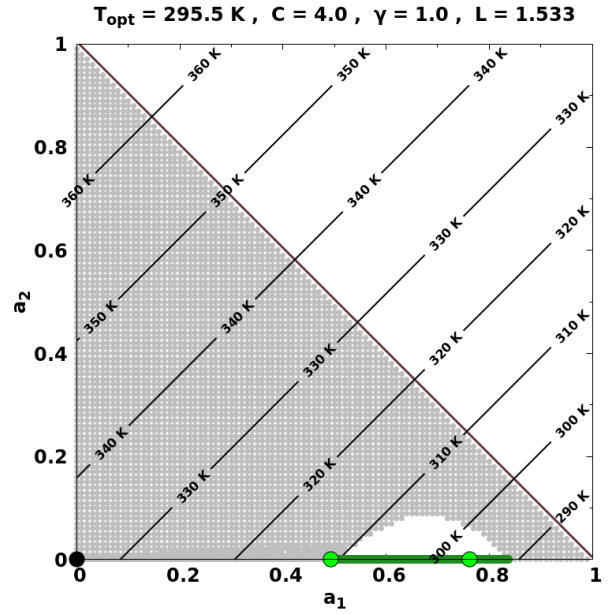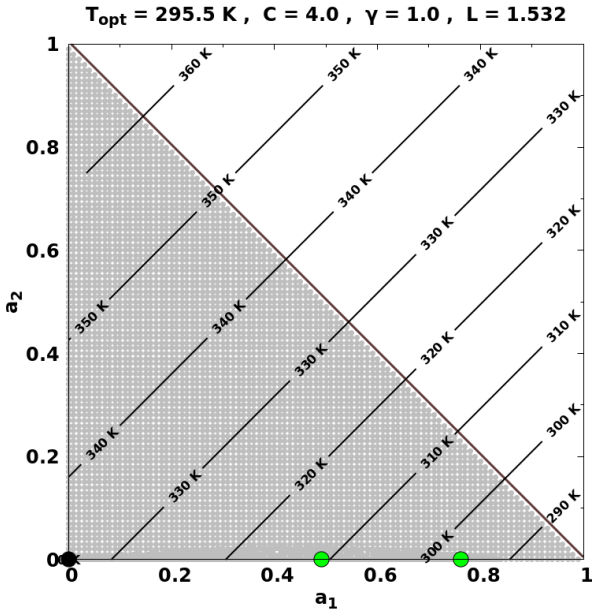
(c) DWC asymptotic state for $C = 4.0$, $\gamma = 1.0$ and $L = 1.532$, besides to temperature T contour lines.

(d) DWC asymptotic state for $C = 4.0$, $\gamma = 1.0$ and $L = 1.533$, besides to temperature T contour lines.

Figure 3.23: **DWC analysis of chaos rebirth** using **basins of attraction** for $C = 4.0$, $\gamma = 1.0$ and next L values: $L = 1.532$ / $L = 1.533$ and the corresponding asymtotic state, besides temperature T contour lines.

3.5.3 Overpopulation in DWC

We also wanted to see the effect of changing parameters C and γ over whole dynamics. In **Appendix A**, we can find the whole set of **orbit diagrams** we have produced in this study besides their corresponding **temperature T mean** and **bifurcation diagrams**. We have extracted some of them because of their perplexing behaviour; next we explain it. From **Figure 3.24** it can be seen that <u>the system surpasses forbidden barrier</u>, despite constraint **Equation 2.9**. **How could it be possible?**
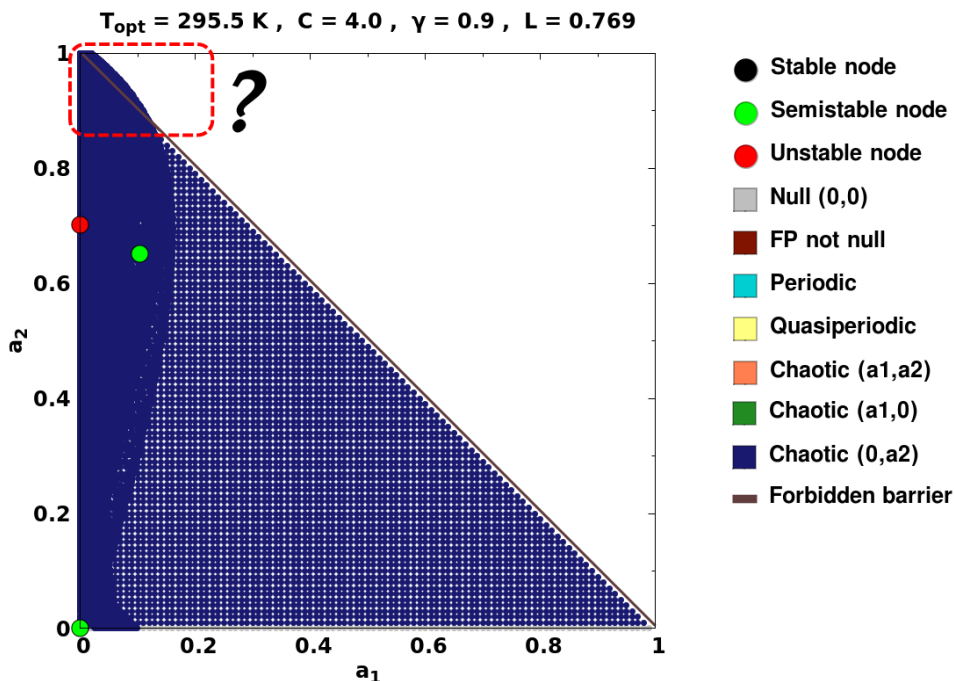
Figure 3.24: DWC basins of attraction for $C = 4.0$, $\gamma = 0.9$ and $L = 0.769$. Dashed red line delimits the region where <u>the system surpasses forbidden barrier</u>. A **question mark** has been added to denote how shaking is this behaviour.

In order to investigate this behaviour, we decided to modify classification given in **section 3.5** adding next class:

- **Overpopulation:** it corresponds to the set of points which belong to any of the **dynamical regimes** identified in **section 3.5**, but that evolve <u>surpassing the barrier towards forbidden values</u>; i.e. which fulfill sometime the condition:

$$p < (a_1 + a_2) \tag{3.8}$$

Figure 3.25 shows the result of this classification. We must emphasize that **Overpopulation** classification was performed after the **dynamical regimes** classification, so a point belonging to the **basin of attraction** of any **dynamical regime** can be classified as belonging to the **Overpopulation** class if the time series generated from it fulfills the condition imposed by **Equation 3.8** at some point in time violating **Equation 2.9**. In order to sketch up the **asymptotic states** of **Figure 3.25b**, we plotted the whole **basin of attraction** for **Null**

regime, above it we plotted the whole **Overpopulation** set of points and then we added temperature T contour lines and the **chaotic attractors** generated with a random initial condition for each **chaotic regime** (for a transient time of 1×10^6 generations and then for an asymptotic time of 1×10^6 generations). According to the results, it is clear that the condition **Equation 3.8** was fulfilled in the **transient**.
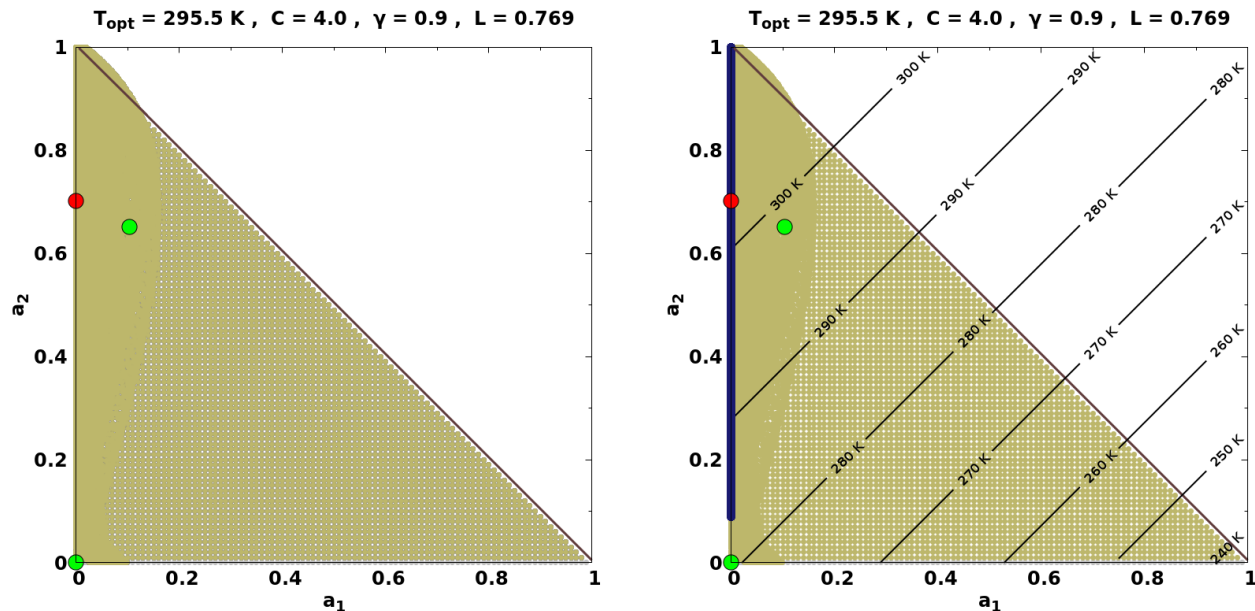
(a) DWC basins of attraction for $C = 4.0$, $\gamma = 0.9$ and $L = 0.769$. **Overpopulation** class has been added.

(b) DWC asymptotic state for $C = 4.0$, $\gamma = 0.9$ and $L = 0.769$, besides to temperature T contour lines.

● Stable node	▬ Forbidden barrier	▮ FP not null	▮ Chaotic (a1,a2)
● Semistable node	▮ Overpopulation	▮ Periodic	▮ Chaotic (a1,0)
● Unstable node	▯ Null (0,0)	▯ Quasiperiodic	▮ Chaotic (0,a2)
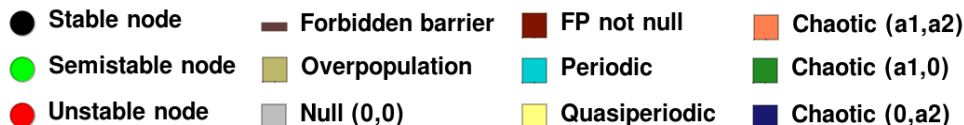
Figure 3.25: **DWC** basins of attraction and asymptotic state for $C = 4.0$, $\gamma = 0.9$ and $L = 0.769$. **Overpopulation** class has been added.

From the knowledge of the **logistic map** $x_{n+1} = r \ x_n(1 - x_n)$, we do know that r must be restricted to the interval $[0, 4]$ so that x_{n+1} maps the interval $0 \leq x \leq 1$. When $r > 4$, one can obtain $x_n > 1$ for some n, and then this leads the subsequent iterations to diverge toward $-\infty$. Biologically, this means the population goes extinct [50]. If this were the case for our map, then our system would have been mapped to zero, but this did not happen. Then the next question about stability of the system was raised: **How one can be sure that the system doesn't blow up –i.e. values of a_i go to infinity ($\pm\infty$)– for a given set of parameter values or a set of initial conditions?**. To address this question, we recall that one can speak of **conservative** and **dissipative maps**. A **conservative map** is one that preserves **phase space volume** as it iterates. A map is volume preserving if the magnitud of the determinant of its Jacobian matrix is one, i.e. $|\boldsymbol{J}| = \mathbf{1}$. On the other hand, if $|\boldsymbol{J}| < \mathbf{1}$ in some regions, then it corresponds to a **dissipative map**, and typically it can have **attractors**, thus it do not blow up [51]. We sketched up the distribution of the determinant of the jacobian matrix $|J|$ of the system and the corresponding contour lines (**Figure 3.26**).
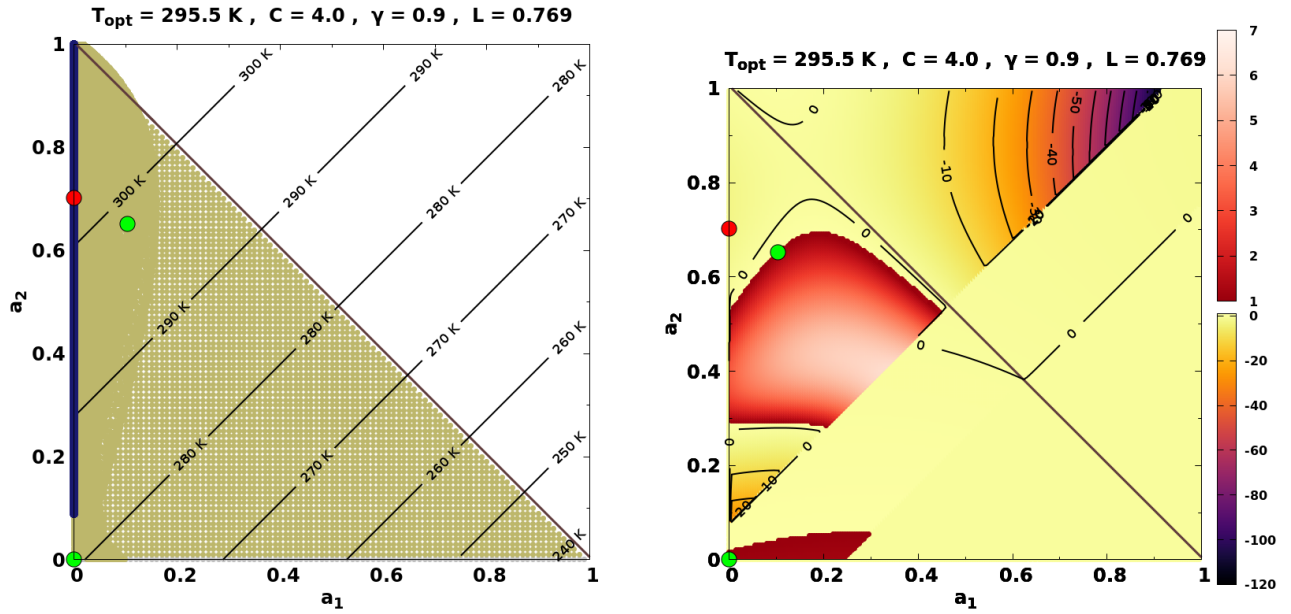
(a) DWC asymptotic state for $C = 4.0$, $\gamma = 0.9$ and $L = 0.769$, besides to temperature T contour lines.

(b) DWC distribution of determinant of jacobian matrix $|J|$ of the system for $C = 4.0$, $\gamma = 0.9$ and $L = 0.769$.

● Stable node   ▬ Forbidden barrier   ■ FP not null   ■ Chaotic (a1,a2)

● Semistable node   ■ Overpopulation   ■ Periodic   ■ Chaotic (a1,0)

● Unstable node   ■ Null (0,0)   ■ Quasiperiodic   ■ Chaotic (0,a2)

Figure 3.26: **DWC** asymptotic state and distribution of determinant of jacobian matrix $|J|$ of the system for $C = 4.0$, $\gamma = 0.9$ and $L = 0.769$. In **(b)**, two colormaps have been added: **dark red colormap** denotes the region where the system has $|J| > 1$, whilst **colormap** from **black** to **yellow** denotes the region where the system has $|J| < 1$.

We have found that, although the system fulfills **Equation 3.8**, the system has regions with $|J| < 1$, thus it must have an **attractor set** that doesn't allow the system to blow up towards infinity. This suggests that, unlike **logistic map** where the system tends to $-\infty$ when $r > 4$, our system has the property of asymptotically trap tajectories in an **attractor set** although the combination of parameters (C, α) is such that in some time the system can surpass the forbidden barrier.

Conclusion 8

Although **Overpopulation** exists in **DWC**, the system never blows up, since distribution of determinant of jacobian matrix $|J|$ shows that the system is characterized by having regions with $|J| < 1$, and although it surpasses **forbidden barrier**, the system is pulled back to the **attracting set** which is **chaotic**.

Finally, we must remark that in this simulation there is not any numerical error caused by discretization, then the only error left would be floating-point arithmetic, however the functions involved in this system are so simple (parables) that one can discard this behaviour is

originated from this errors. It isn't an equation artefact either.

Conclusion 9: Overpopulation in DWC

The system has a topological structure (chaotic attractor) that is able to soften catastrophical effects of overpopulation in such a manner that the system doesn't collapse in front of overpopulation (for some set of parameters, because there are other sets for which there exists massive extinction).

Too many models, as logistic map, fails when it is taken to their limits (in this case overpopulation), but this system is different.

All information seen until now in this subsection is summarized graphically in **Figure 3.27**. In addition, we sketched up the **orbits diagram** and the corresponding temperatures T mean for $C = 4.0$ and $\gamma = 0.9$ (**Figure 3.28**). In that graphic, those values of L where **Overpopulation** occurs, are marked by a vertical line with its corresponding color.
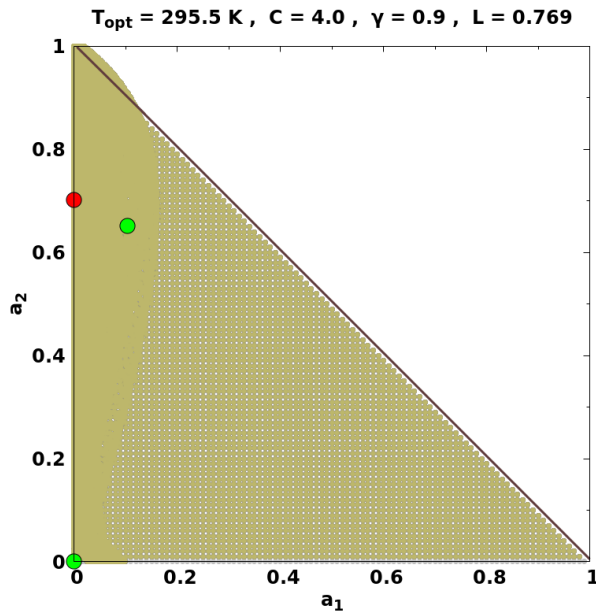
(a) DWC basins of attraction for $C = 4.0$, $\gamma = 0.9$ and $L = 0.769$. **Overpopulation** class has been added.
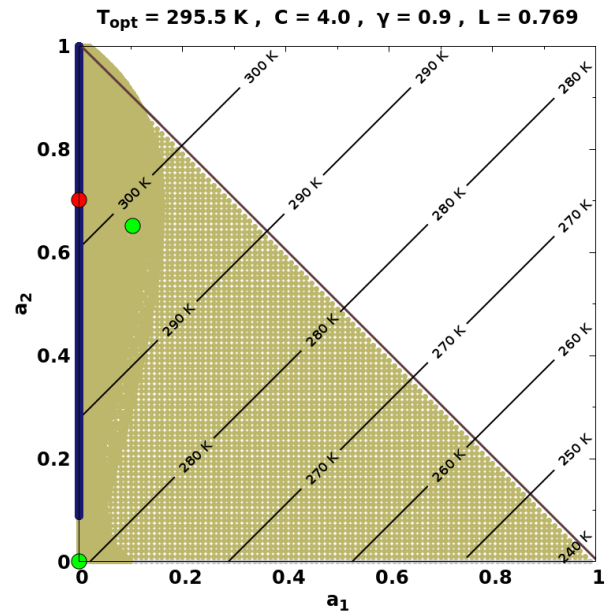
(b) DWC asymptotic state for $C = 4.0$, $\gamma = 0.9$ and $L = 0.769$, besides to temperature T contour lines.
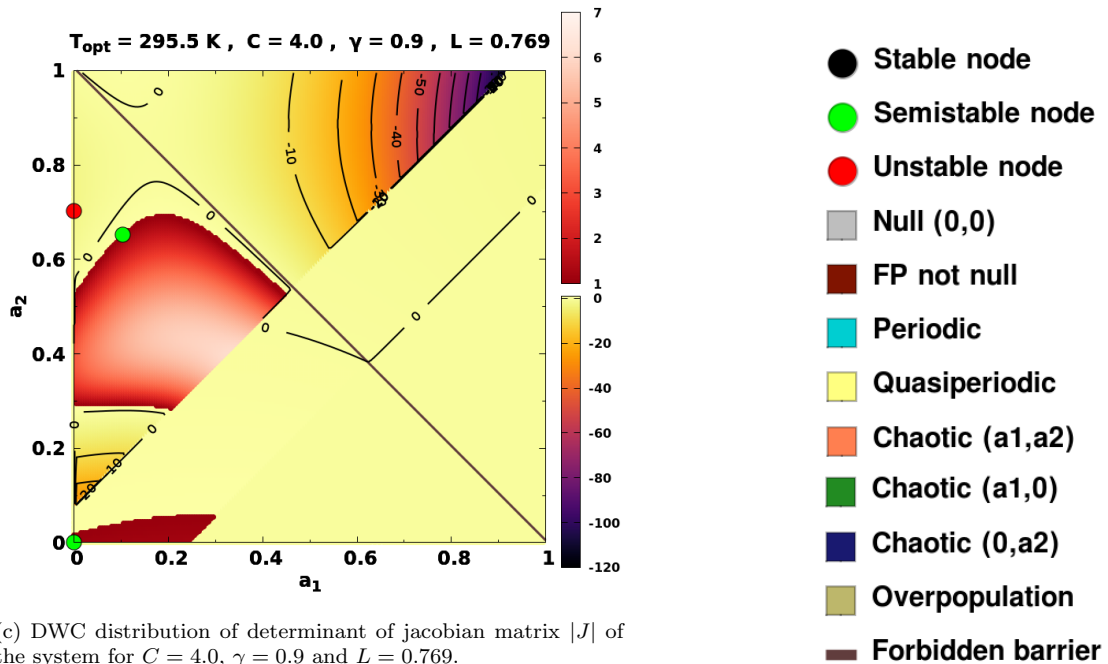
(c) DWC distribution of determinant of jacobian matrix $|J|$ of the system for $C = 4.0$, $\gamma = 0.9$ and $L = 0.769$.

Figure 3.27: **DWC** basins of attraction and asymptotic state for $C = 4.0$, $\gamma = 0.9$ and $L = 0.769$, besides the corresponding distribution of deterinant of jacobian matrix $|J|$ of the system. In **(c)**, two colormaps have been added: **dark red colormap** denotes the region where the system has $|J| > 1$, whilst **colormap** from **black** to **yellow** denotes the region where the system has $|J| < 1$.

(a) DWC bifurcation for $C = 4.0$ and $\gamma = 0.9$.

(b) DWC orbits diagram for $C = 4.0$ and $\gamma = 0.9$.

(c) DWC temperature T mean for $C = 4.0$ and $\gamma = 0.9$.

Legend:

- ● Stable node
- ● Semistable node
- ● Unstable node
- ▢ Null (0,0)
- ▮ FP not null
- ▮ Periodic
- ▢ Quasiperiodic
- ▮ Chaotic (a1,a2)
- ▮ Chaotic (a1,0)
- ▮ Chaotic (0,a2)
- ▮ Overpopulation
- ▬ Forbidden barrier
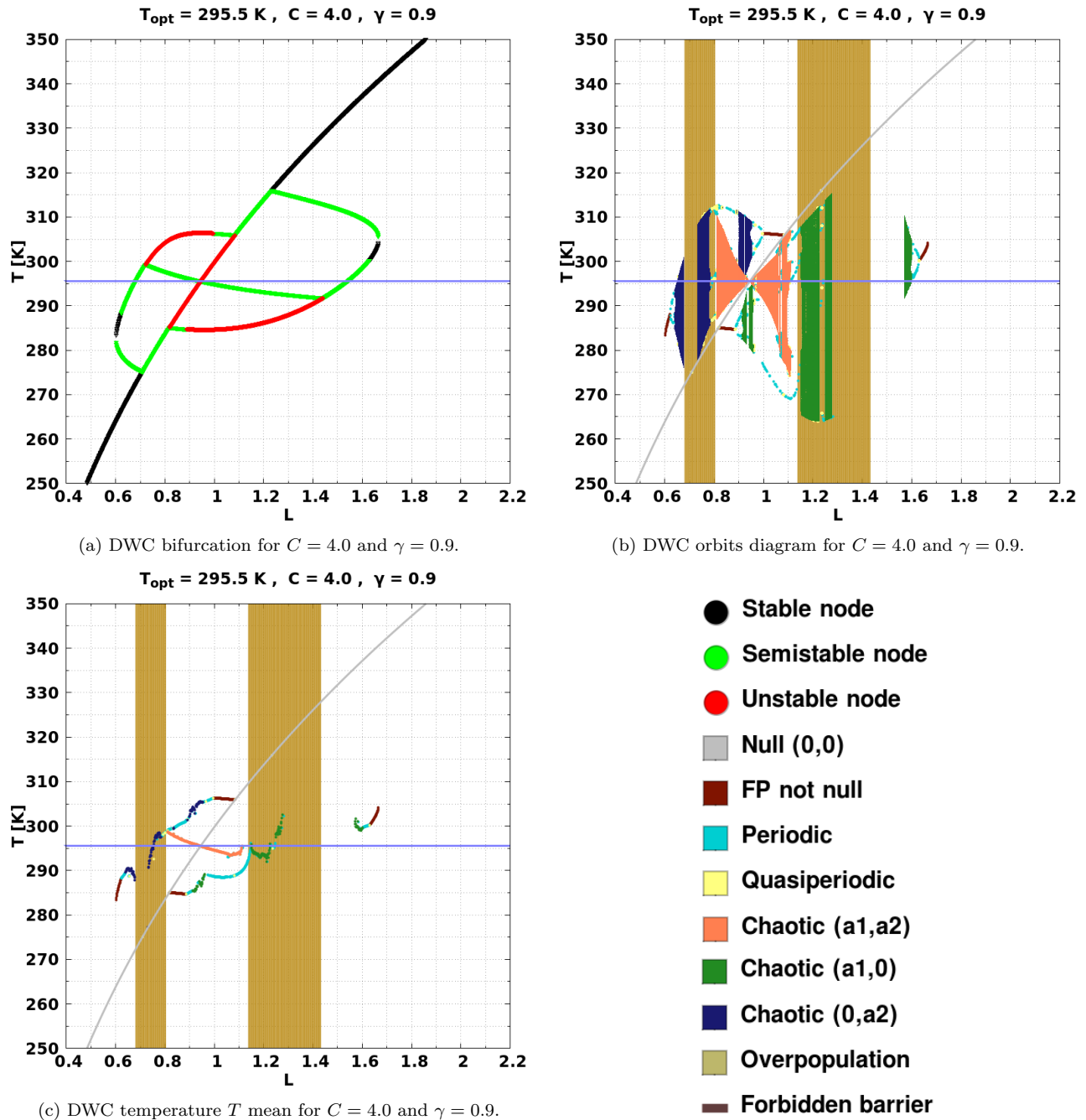
Figure 3.28: **Orbits diagram** and the corresponding temperature T mean for **DWC** for $C = 4.0$ and $\gamma = 0.9$. **Blue** line corresponds to the value of $T_{opt} = 295.5$ K. Finally, those values of L where **Overpopulation** occurs, are marked by a vertical line with its corresponding color.

The complete set of **orbits diagrams** investigated can be found in **Appendix A**. We wanted to see how is **Overpopulation** when **Chaotic (a_1, a_2)** is present. With this in mind, we chose to sketched up all the results of this subsection again, but for $C = 3.0$, $\gamma = 0.2$ and $L = 1.080$. We iterated the system from the initial conditions $a_{1;\,0} = 0.5$ and $a_{2;\,0} = 0.2$, for a transient time of 1×10^6 generations and then for an asymptotic time of 1×10^6 generations. Part of the time series produced can be seen in **Figure 3.29**.

Using the algorithm of **the largest Lyapunov exponent $\lambda_{\mathbf{max}}$** [41], we found that $\lambda_{\max} = 0.1619$ which is a firm sign of **chaos**. In addition we plotted the **power spectrum** for both time series –that of a_1 and that of a_2–. The result can be seen in **Figure 3.30**, and it is clear that it correspond to a chaotic-like spectrum. Now, we can firmly assess that the time series produced is **chaotic** and so, **chaos** belongs to **DWC** dynamics. The presumed chaotic attractor is plotted in **Figure 3.7**, and we used **box counting** method [42] to compute an estimate of its **fractal dimension ν**. We found that $\nu = 1.585$ (**??**), which corresponds to the dimension of a **fractal set**, so confirming the existence of a **strange attractor**.
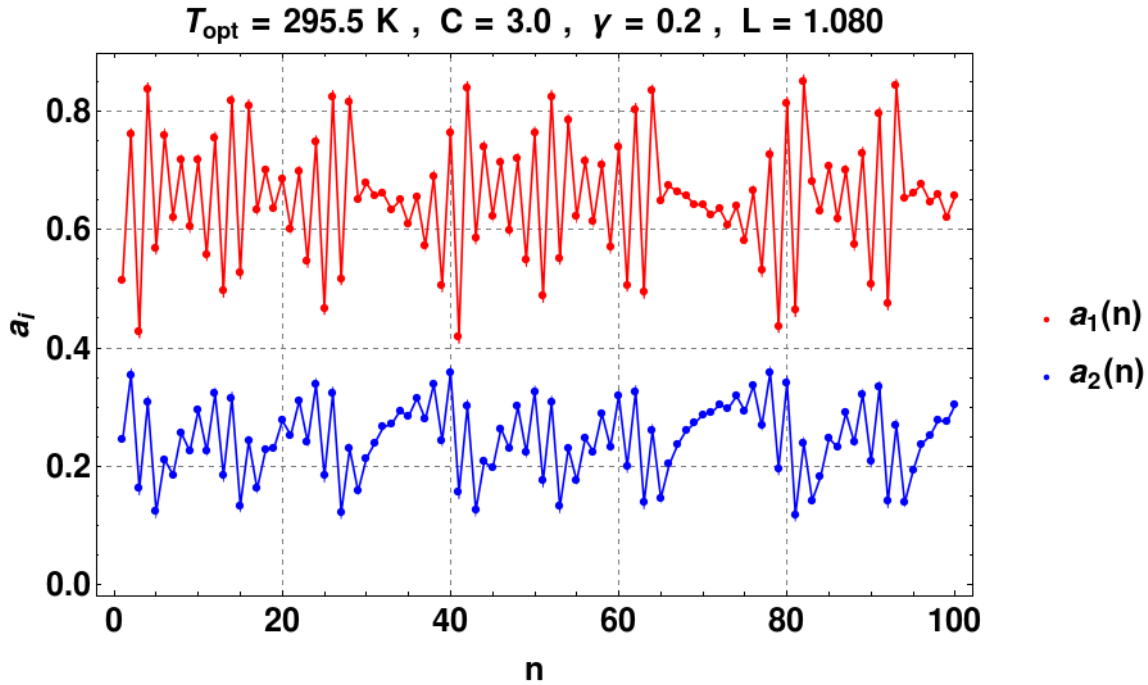
Figure 3.29: DWC time series for $C = 3.0$, $\gamma = 0.2$ and $L = 1.080$ after a transient time of 1×10^6 generations has passed. The initial conditions were $a_{1;\,0} = 0.5$ and $a_{2;\,0} = 0.2$.
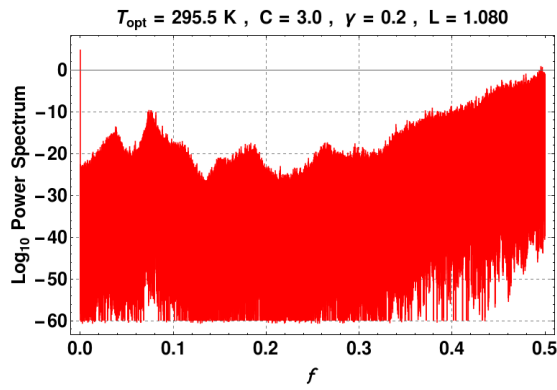
(a) DWC asymptotic state for $C = 4.0$, $\gamma = 1.0$ and $L = 0.800$, besides to temperature T contour lines.
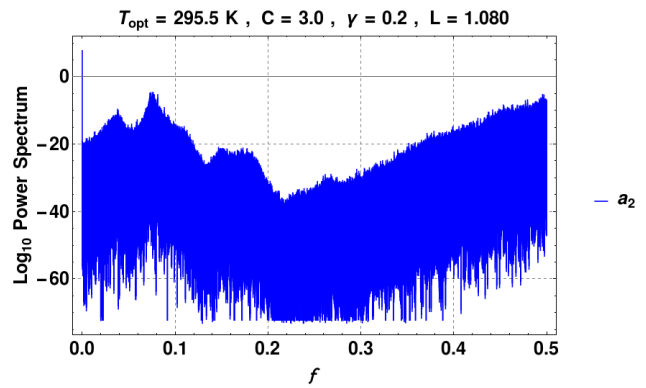
(b) DWC power spectrum of a_2 time series.

Figure 3.30: DWC power spectrum for time series of **Figure 3.29**.
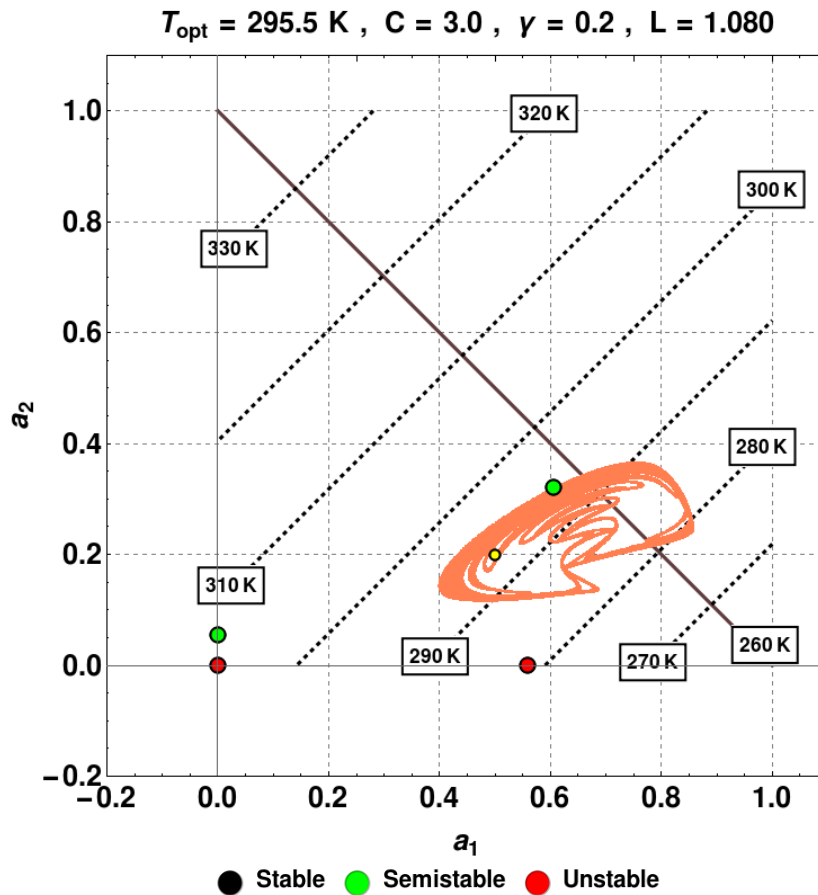
Figure 3.31: DWC asymtotic state in population phase space for $C = 3.0$, $\gamma = 0.2$ and $L = 1.080$. The initial conditions were $a_{1;\,0} = 0.5$ and $a_{2;\,0} = 0.2$ (this initial condition is marked with a **yellow dot**). The structure which appears in this figure may be a **strange attractor** with **fractal dimension $\nu = 1.585$**.

Figure 3.32 shows **basins of attraction** for the parameters values $C = 3.0$, $\gamma = 0.2$ and $L = 1.080..$ It is interesting that, opposite to what happens in **Figure 3.24**, the **chaotic attractor** is not limited to allowed region in **population phase space**, but it surpasses **forbidden barrier**. Then **Overpopulation** is not limited only to **transient** but it could also occurs **asymptotically**, and from **Figure 3.34c**, we can ensure that the system never blows up.

Now, taking a deep look into both **Figure 3.32** and **Figure 3.24**, we can figure out that they look somewhat different from **Figure 3.9b**. Indeed, **basins of attraction** evidenced in **Figure 3.9b** has been lost in **Figure 3.32** and **Figure 3.24**, where we suppose that somehow instabilities are as big as capable to destroy all **internal structure** of **population phase space**, and then all allowed space –except the axes a_1 and a_2–, becomes part of some **Chaotic** regime. This behaviour contradicts **Conclusion 1**, so it should be written as:

> ### Conclusion 10
>
> For some parameter values there is a strong relationship between **basins of attraction** shape and β variable, but there are some parameters values which produce instabilities in the system as big as to destroy **basins of attraction shape** and the whole system –except maybe the axes a_1 and a_2–, becomes **Chaotic**.

In order to corroborate this conclusion, we examined β_i contour lines in **Figure 3.33**, and we found it is reaffirmed.
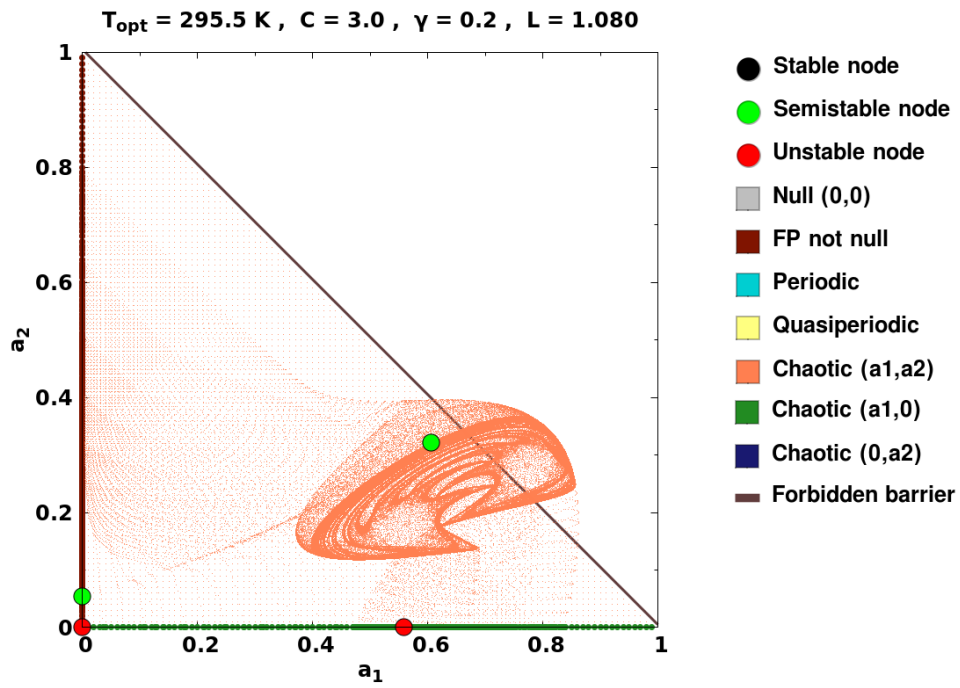
Figure 3.32: DWC basins of attraction for $C = 3.0$, $\gamma = 0.2$ and $L = 1.080$. The region where the system surpasses forbidden barrier is evident.
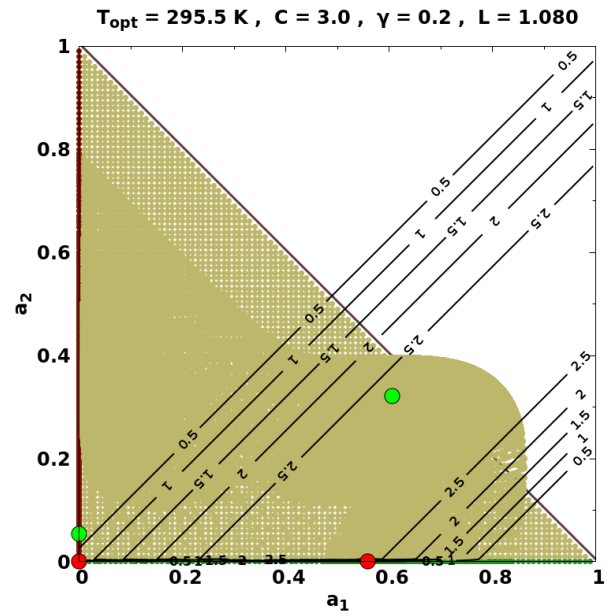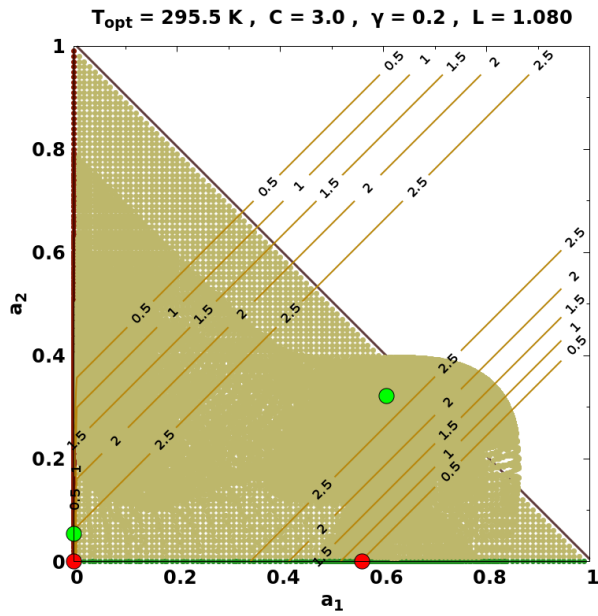
(a) DWC basins of attraction for $C = 3.0$, $\gamma = 0.2$ and $L = 1.080$ besides β_1 contour lines. **Overpopulation** class has been added.

(b) DWC basins of attraction for $C = 3.0$, $\gamma = 0.2$ and $L = 1.080$ besides β_2 contour lines. **Overpopulation** class has been added.

● Stable node	▬ Forbidden barrier	■ FP not null	■ Chaotic (a1,a2)
● Semistable node	▨ Overpopulation	■ Periodic	■ Chaotic (a1,0)
● Unstable node	▨ Null (0,0)	■ Quasiperiodic	■ Chaotic (0,a2)

Figure 3.33: **DWC** basins of attraction and β_i contour lines for $C = 4.0$, $\gamma = 0.9$ and $L = 0.769$. **Overpopulation** class has been added.
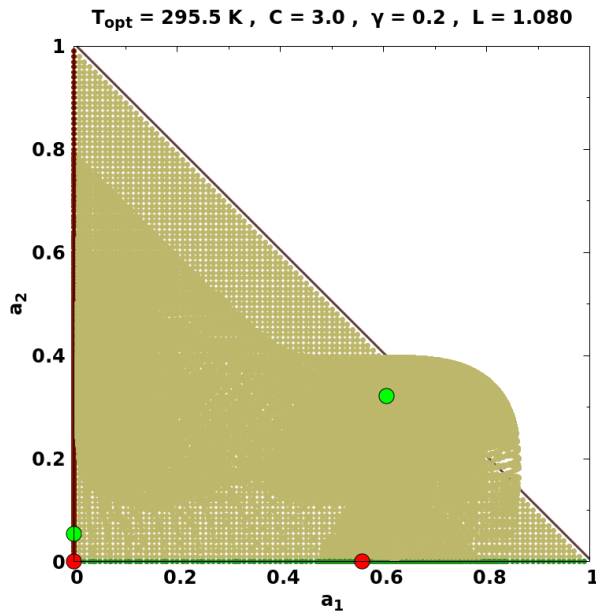
(a) DWC basins of attraction for $C = 3.0$, $\gamma = 0.2$ and $L = 1.080$. **Overpopulation** class has been added.
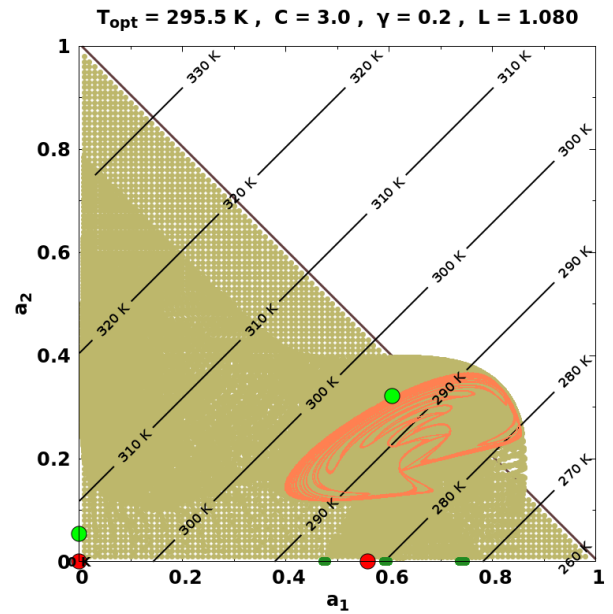
(b) DWC asymptotic state for $C = 3.0$, $\gamma = 0.2$ and $L = 1.080$, besides to temperature T contour lines.
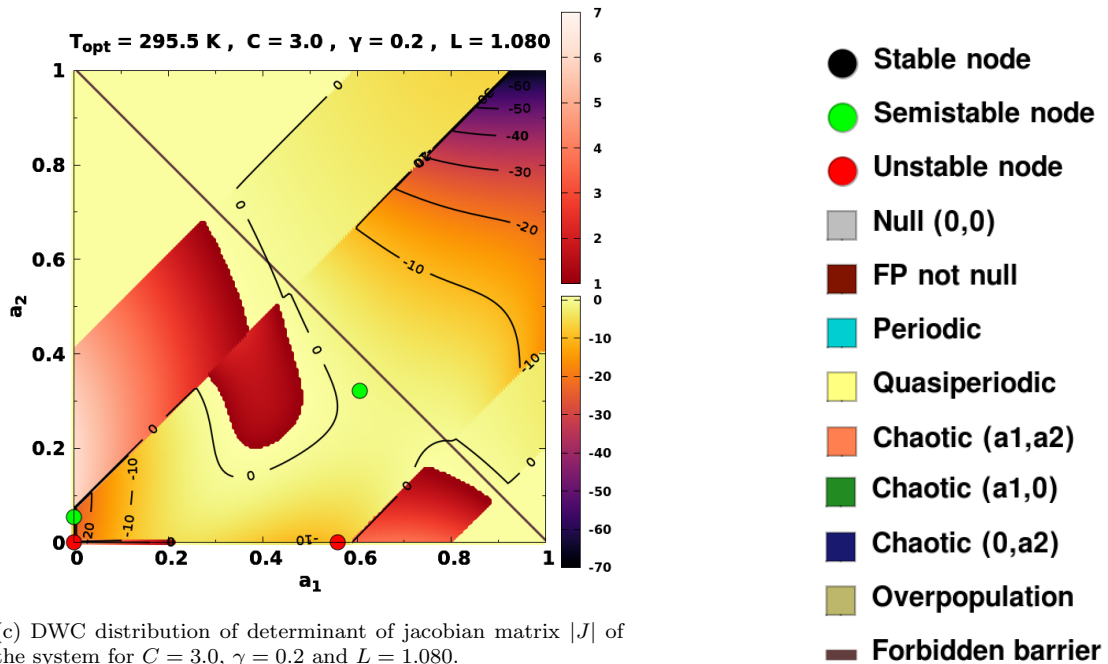
(c) DWC distribution of determinant of jacobian matrix $|J|$ of the system for $C = 3.0$, $\gamma = 0.2$ and $L = 1.080$.

Figure 3.34: **DWC** basins of attraction and asymptotic state for $C = 3.0$, $\gamma = 0.2$ and $L = 1.080$, besides the corresponding distribution of deterinant of jacobian matrix $|J|$ of the system. In **(c)**, two colormaps have been added: **dark red colormap** denotes the region where the system has $|\boldsymbol{J}| > 1$, whilst **colormap** from **black** to **yellow** denotes the region where the system has $|\boldsymbol{J}| < 1$.

Conclusions

We have studied ideas from the work by Zeng et al. and Jascourt et al. regarding the formulation of Daisyworld and its implications. We have found that **Daisyworld** can be represented by two types of models: **DWL** –the original formulation by Lovelock– and **DWC** –proposed in this work–. The dynamics of **DWL** is characterized by being governed by dynamics of fixed points and saddle-node bifurcations. In contrast, because it is an iterated map, **DWC** is governed by more complex dynamics, which include **Chaos** born by **period doubling** as **main route to chaos** (**Conclusion 4**). We have found evidence of complex **intermittency** in DWC, where **chaos** is interspersed with **periodic** oscillations (see **Figure 3.13**, **Figure 3.14** and **Figure 3.15**). We have also found evidence of **multifractality** in DWC, where multifractal dynamics has biological origin (**Conclusion 2**). In addition, we also found that there is a strong relationship between the shape of the **basins of attraction** and the growth rate of the flowers β, which provides the coupling between environment and population dynamics, but there are some environmental conditions where instabilities are as big as destroying that coupling (**Conclusion 10**). Having said this, we conclude that **DWC is highly complex** (**Conclusion 3**) and this makes system to become too delicate, and combining increments of L and changes in basins of attraction would, for example, lead the system to extinct if it accidentally falls in the basin of attraction of extinction when L effectively changes.

Remember from **Concept 1** that:

> **Biological homeostasis of the global environment** is understood –by Lovelock– as the mechanism by which, under forcings which would cause environmental conditions nonsuitable for life, the environmental conditions are set down in a steady state to life suitable values.

Nevertheless, the behaviours described do not imply that homeostasis has been lost. Indeed, there exists a bounded set of **accesible temperatures** which are visited by **chaotic trajectories** and are completely different to those of a dead planet, thus providing environmental conditions needed to keep the planet habitable (**Conclusion 5**). This lead us to redefine **homeostasis** in **Gaia theory** context as **Concept 3**:

Biological homeostasis of the global environment must be understood as the biologically originated mechanism by which environmental conditions are shifted from nonsuitable values for life to other values that are bounded between life suitable values.

These life suitable values can correspond to:

- **Equilibrium states:** where the regulatory agents are **stable fixed points**.

- **Periodic or quasiperiodic states:** where the regulatory agents are **limit cycles** –or **periodic orbits**–, and **toroidal trajectories.**

- **Chaotic states:** where the regulatory agents are **chaotic attractors** that, although they originate long-term irregular behaviour, they still regulating the system and allow the planet to remain habitable.

Thus, this concept includes the idea that **chaotic dynamics** regulates climate to irregular states which being habitables, still exhibit homeostasis. In this sense, a **strange attractor** also represents **homeostasis**, and thus **homeostasis** becomes in a **robust property** of **Daisyworld model**, no matter if we refer to **DWL** or **DWC** model.

But the complexity in **DWC** also involves other unexpected behaviours such as **global extinctions** (Conclusion 6 and Conclusion 7), which happens for some values of luminosity of the star. In these cases any initial population of any of the species eventually goes to zero, i.e. goes extinct, in contrast to what is predicted by **DWL** where these values of luminosity can have steady values for life.

Finally, we also have found a last interesting behaviour in **DWC** which we have called **Overpopulation**, where population values exceed the allowed values imposed by environmental constraints, but this doens't lead to extinction. Turning back to Conclusion 8, we recall that for the **logistic map**, the model becomes biologically nonsense for $4 < r$. So, **does Overpopulation make biological sense for DWC?** Evidently, **Overpopulation** is a theoretical problem of the mathematical model used, since from our point of view, this behaviour would lead to catastrophes. However, since the system never blows up (solutions stay bounded), we believe that the **Overpopulation** problem can be treated without discarding the model altogether. In fact, the topological structure of the system when **Overpopulation** occurs deserves deeper investigation in order to gain better insight of the implications for **climate systems**, including ours.

All the research associated to **Daisyworld**, including our own results, suggests that **Gaia theory** involves more complexities than those reported until now. This shows that there is much more work to do that could be helpful in the context of **climate systems**, **exoplanets** and **habitable zones**, and even **climate theory applied to the Earth**, including **climate**

change.

Appendices

Appendix A

DWC - Full set of orbits diagrams

(a) DWC bifurcation for $C = 1.0$ and $\gamma = 0.1$.

(b) DWC orbits diagram for $C = 1.0$ and $\gamma = 0.1$.

(c) DWC temperature T mean for $C = 1.0$ and $\gamma = 0.1$.
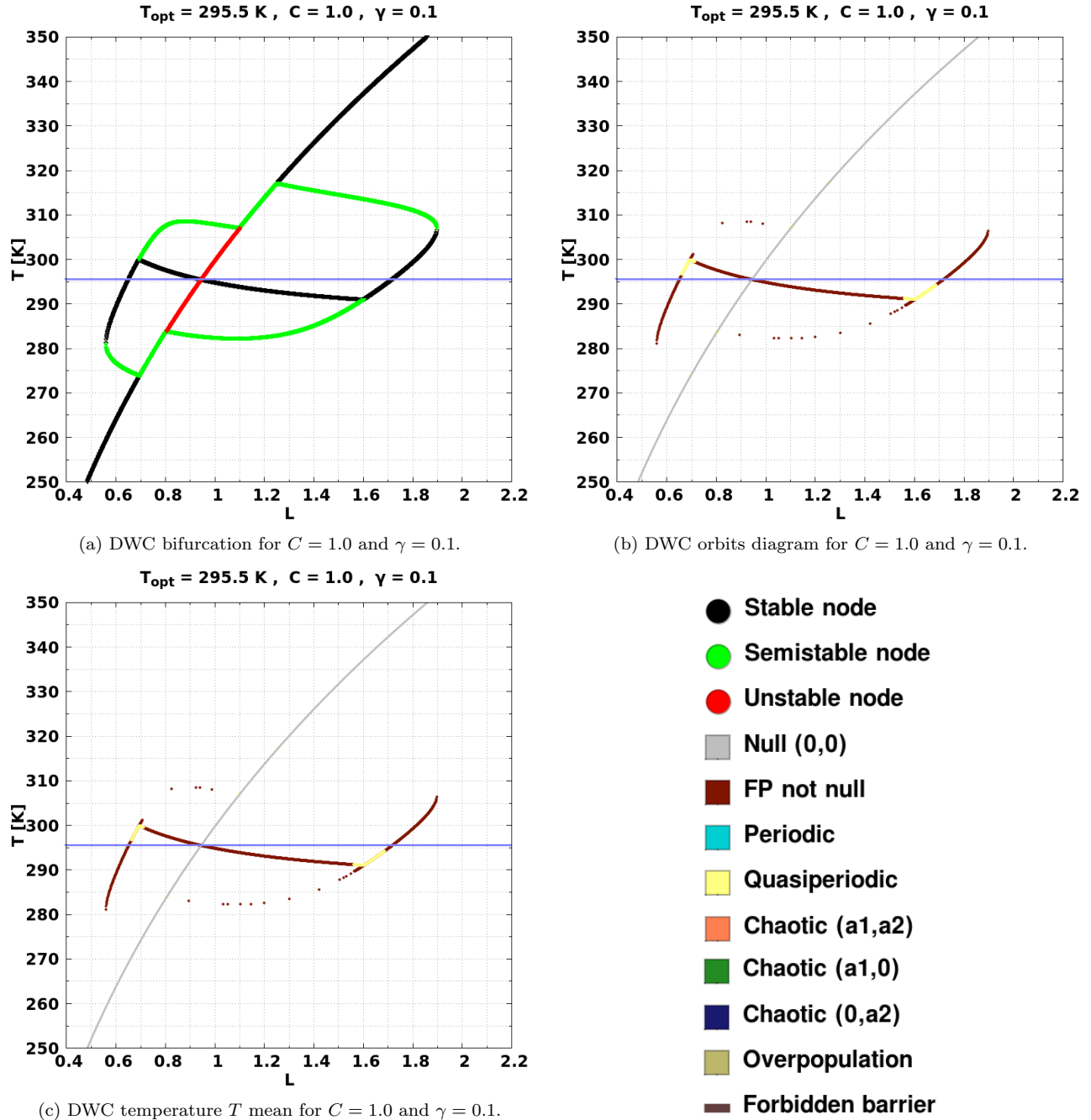
Figure A.1: **Orbits diagram** and the corresponding temperature T mean for **DWC** for $C = 1.0$ and $\gamma = 0.1$. **Blue** line corresponds to the value of $T_{opt} = 295.5$ K. Finally, those values of L where **Overpopulation** occurs, are marked by a vertical line with its corresponding color.
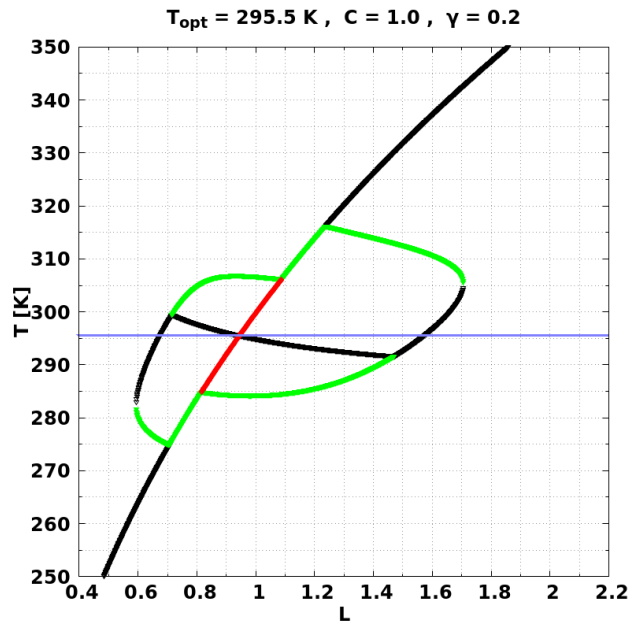
(a) DWC bifurcation for $C = 1.0$ and $\gamma = 0.2$.
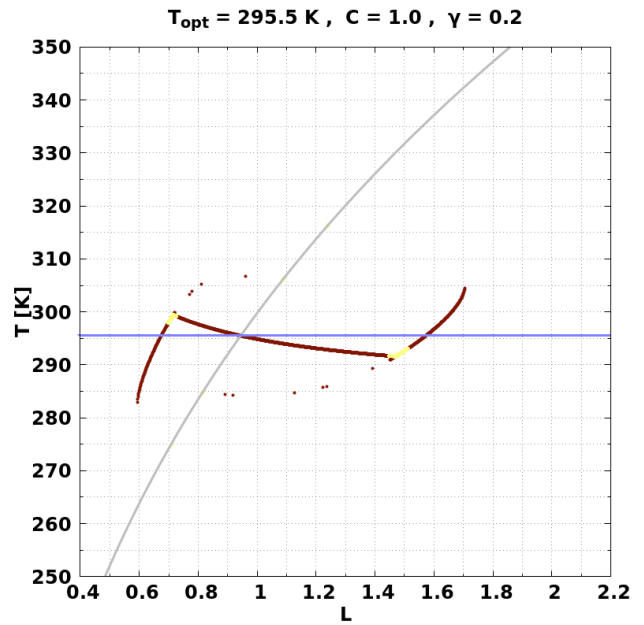
(b) DWC orbits diagram for $C = 1.0$ and $\gamma = 0.2$.
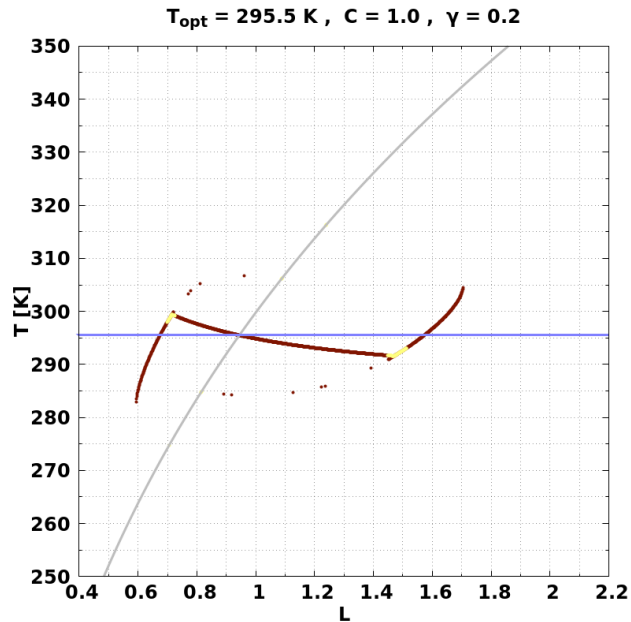
(c) DWC temperature T mean for $C = 1.0$ and $\gamma = 0.2$.

Figure A.2: **Orbits diagram** and the corresponding temperature T mean for **DWC** for $C = 1.0$ and $\gamma = 0.2$. **Blue** line corresponds to the value of $T_{opt} = 295.5$ K. Finally, those values of L where **Overpopulation** occurs, are marked by a vertical line with its corresponding color.
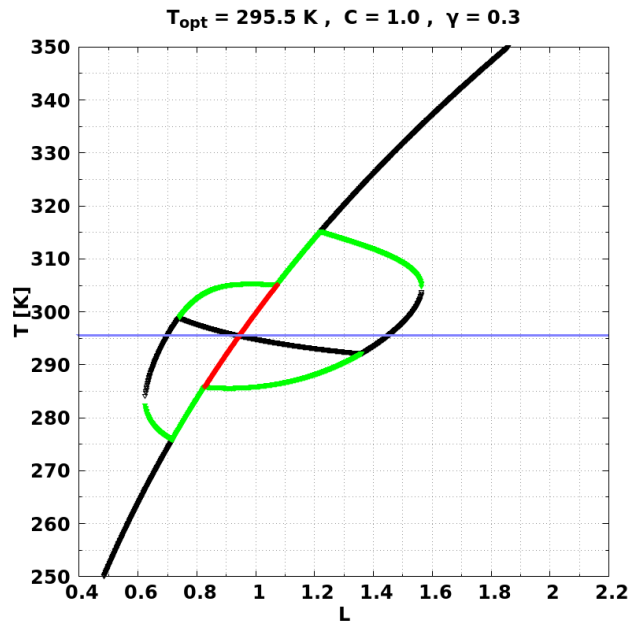
(a) DWC bifurcation for $C = 1.0$ and $\gamma = 0.3$.
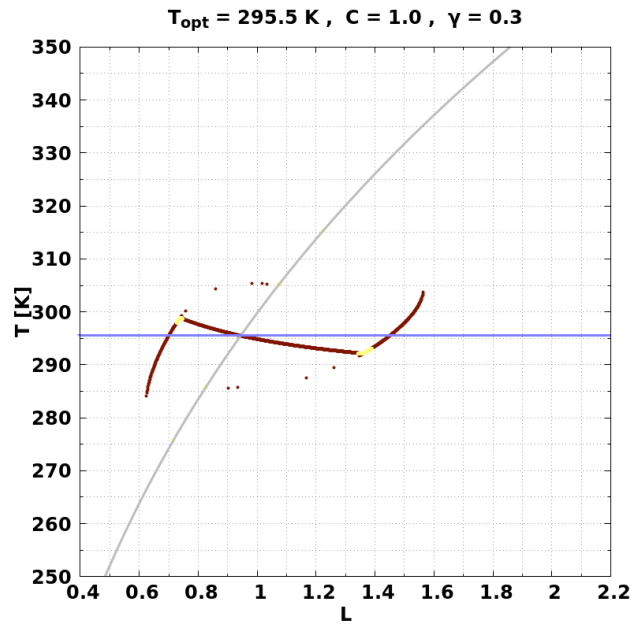
(b) DWC orbits diagram for $C = 1.0$ and $\gamma = 0.3$.
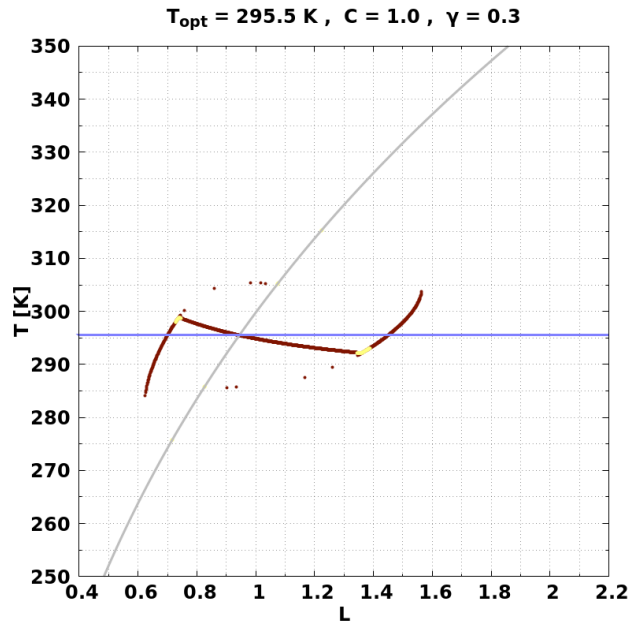
(c) DWC temperature T mean for $C = 1.0$ and $\gamma = 0.3$.

Figure A.3: **Orbits diagram** and the corresponding temperature T mean for **DWC** for $C = 1.0$ and $\gamma = 0.3$. **Blue** line corresponds to the value of $T_{opt} = 295.5$ K. Finally, those values of L where **Overpopulation** occurs, are marked by a vertical line with its corresponding color.
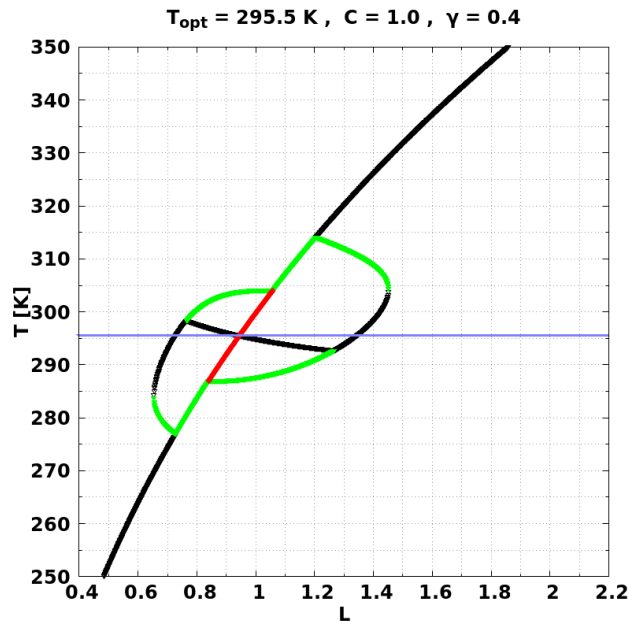
(a) DWC bifurcation for $C = 1.0$ and $\gamma = 0.4$.
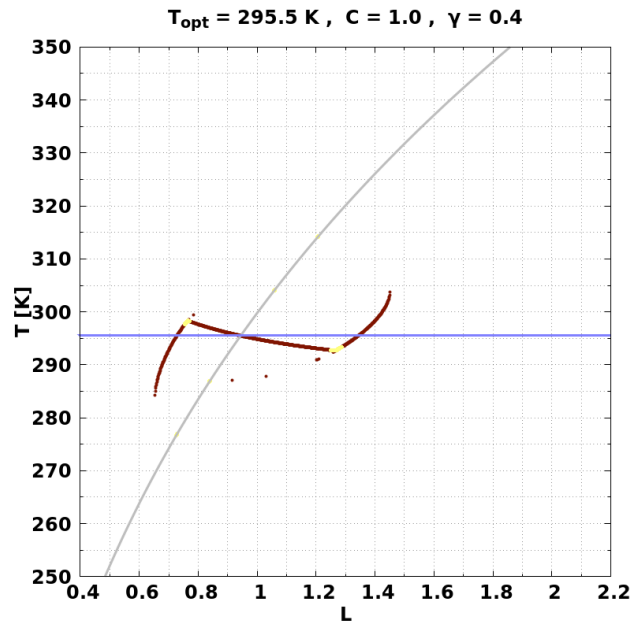
(b) DWC orbits diagram for $C = 1.0$ and $\gamma = 0.4$.
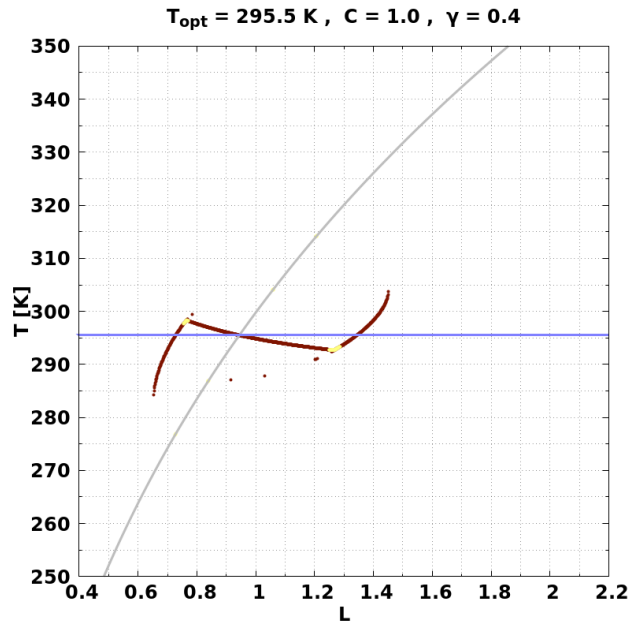
(c) DWC temperature T mean for $C = 1.0$ and $\gamma = 0.4$.

Figure A.4: **Orbits diagram** and the corresponding temperature T mean for **DWC** for $C = 1.0$ and $\gamma = 0.4$. **Blue** line corresponds to the value of $T_{opt} = 295.5$ K. Finally, those values of L where **Overpopulation** occurs, are marked by a vertical line with its corresponding color.
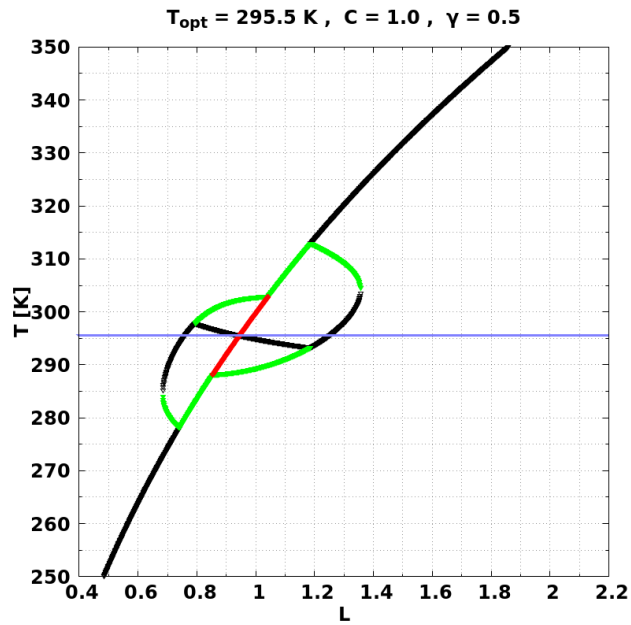
(a) DWC bifurcation for $C = 1.0$ and $\gamma = 0.5$.
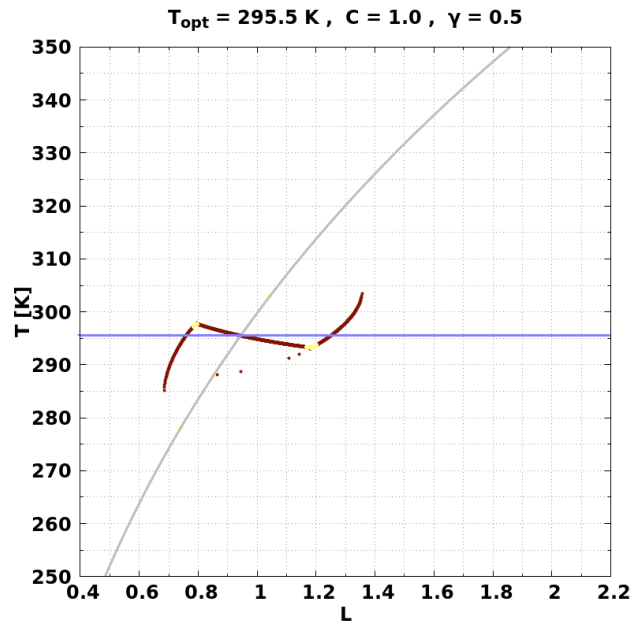
(b) DWC orbits diagram for $C = 1.0$ and $\gamma = 0.5$.
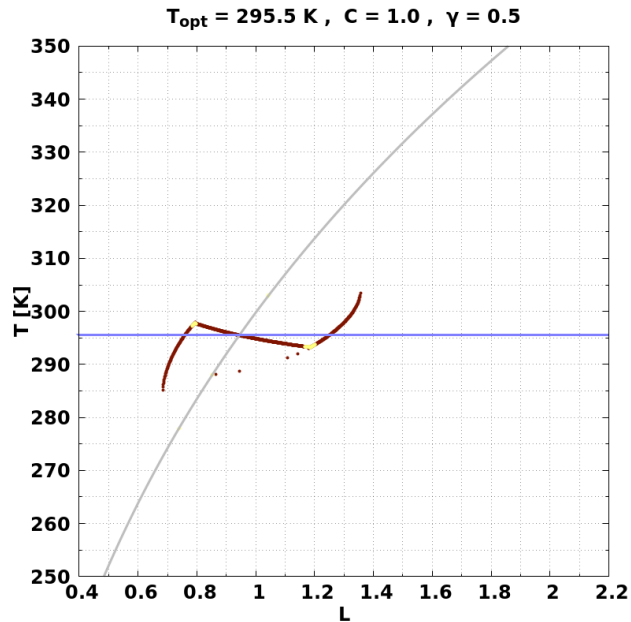
(c) DWC temperature T mean for $C = 1.0$ and $\gamma = 0.5$.

Legend:
- Stable node
- Semistable node
- Unstable node
- Null (0,0)
- FP not null
- Periodic
- Quasiperiodic
- Chaotic (a1,a2)
- Chaotic (a1,0)
- Chaotic (0,a2)
- Overpopulation
- Forbidden barrier

Figure A.5: **Orbits diagram** and the corresponding temperature T mean for **DWC** for $C = 1.0$ and $\gamma = 0.5$. **Blue** line corresponds to the value of $T_{opt} = 295.5$ K. Finally, those values of L where **Overpopulation** occurs, are marked by a vertical line with its corresponding color.
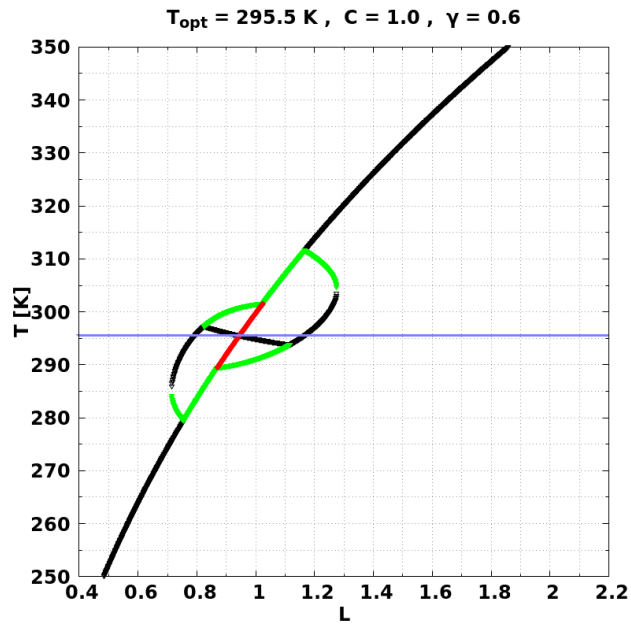
(a) DWC bifurcation for $C = 1.0$ and $\gamma = 0.6$.
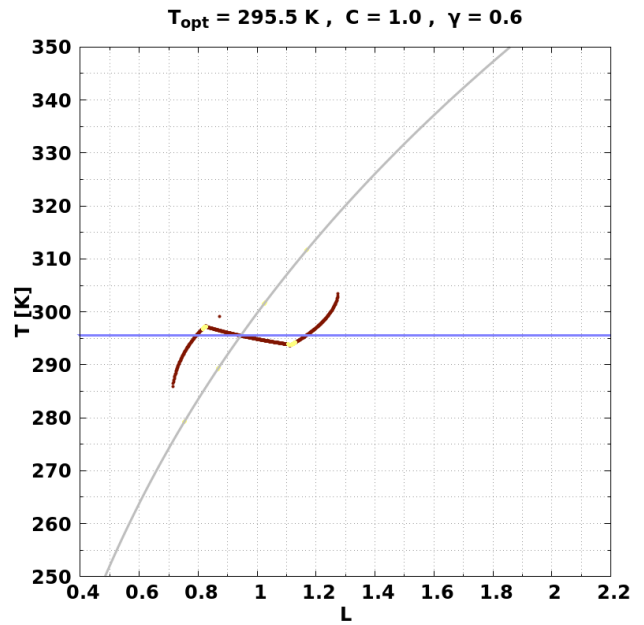
(b) DWC orbits diagram for $C = 1.0$ and $\gamma = 0.6$.
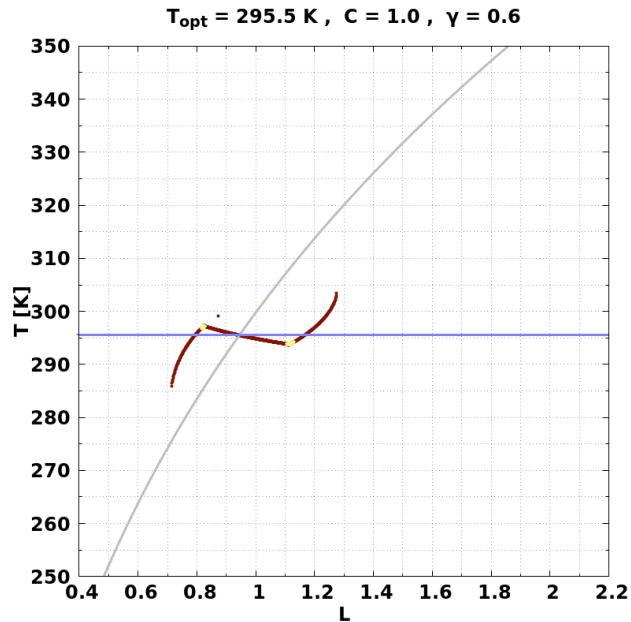
(c) DWC temperature T mean for $C = 1.0$ and $\gamma = 0.6$.

- ● Stable node
- ● Semistable node
- ● Unstable node
- ▦ Null (0,0)
- ▪ FP not null
- ▪ Periodic
- ▪ Quasiperiodic
- ▪ Chaotic (a1,a2)
- ▪ Chaotic (a1,0)
- ▪ Chaotic (0,a2)
- ▪ Overpopulation
- ▬ Forbidden barrier

Figure A.6: **Orbits diagram** and the corresponding temperature T mean for **DWC** for $C = 1.0$ and $\gamma = 0.6$. **Blue** line corresponds to the value of $T_{opt} = 295.5$ K. Finally, those values of L where **Overpopulation** occurs, are marked by a vertical line with its corresponding color.
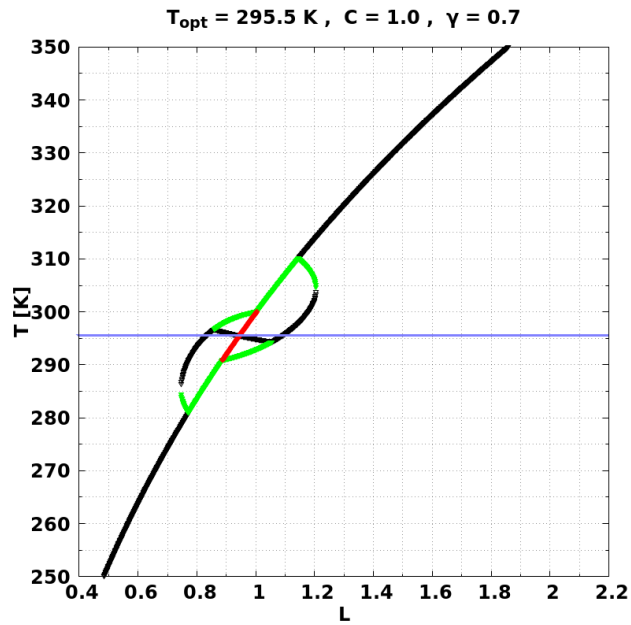
(a) DWC bifurcation for $C = 1.0$ and $\gamma = 0.7$.
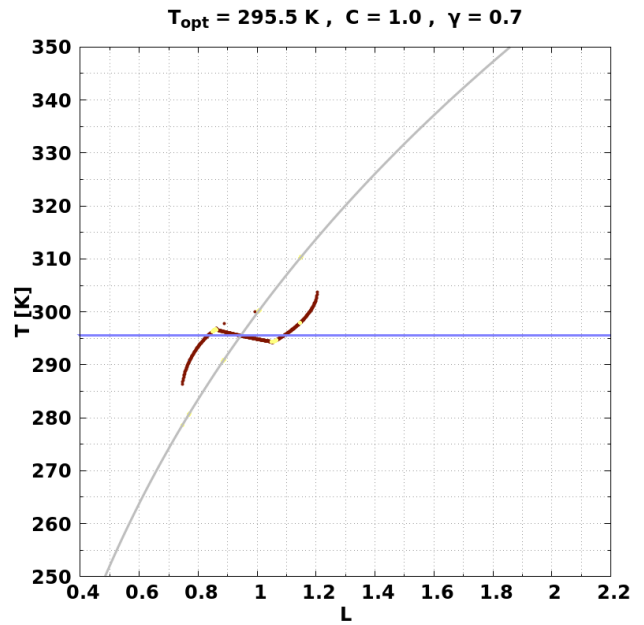
(b) DWC orbits diagram for $C = 1.0$ and $\gamma = 0.7$.
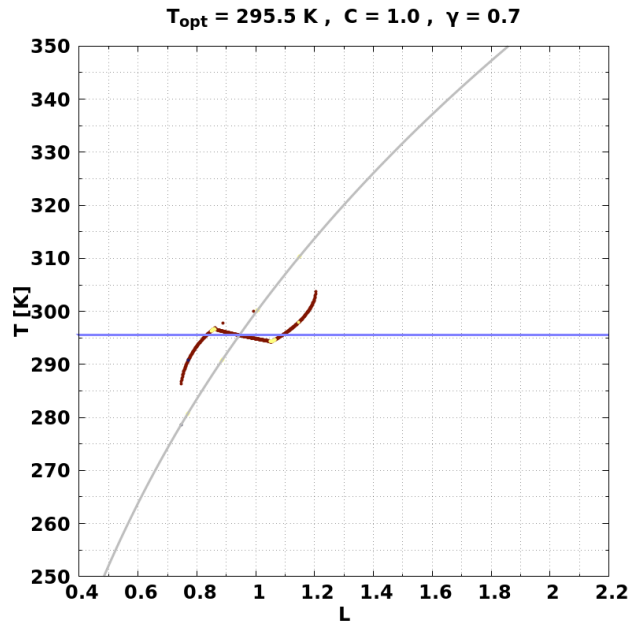
(c) DWC temperature T mean for $C = 1.0$ and $\gamma = 0.7$.

● Stable node
● Semistable node
● Unstable node
▨ Null (0,0)
▨ FP not null
▨ Periodic
▨ Quasiperiodic
▨ Chaotic (a1,a2)
▨ Chaotic (a1,0)
▨ Chaotic (0,a2)
▨ Overpopulation
▬ Forbidden barrier

Figure A.7: **Orbits diagram** and the corresponding temperature T mean for **DWC** for $C = 1.0$ and $\gamma = 0.7$. **Blue** line corresponds to the value of $T_{opt} = 295.5$ K. Finally, those values of L where **Overpopulation** occurs, are marked by a vertical line with its corresponding color.
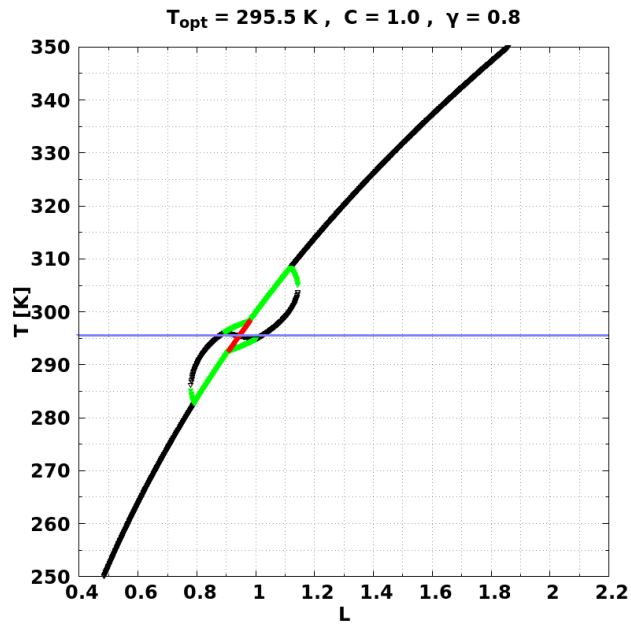
(a) DWC bifurcation for $C = 1.0$ and $\gamma = 0.8$.
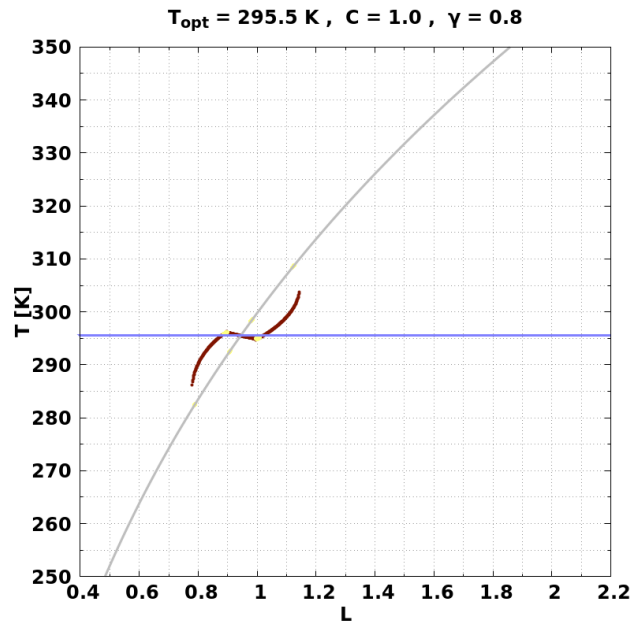
(b) DWC orbits diagram for $C = 1.0$ and $\gamma = 0.8$.
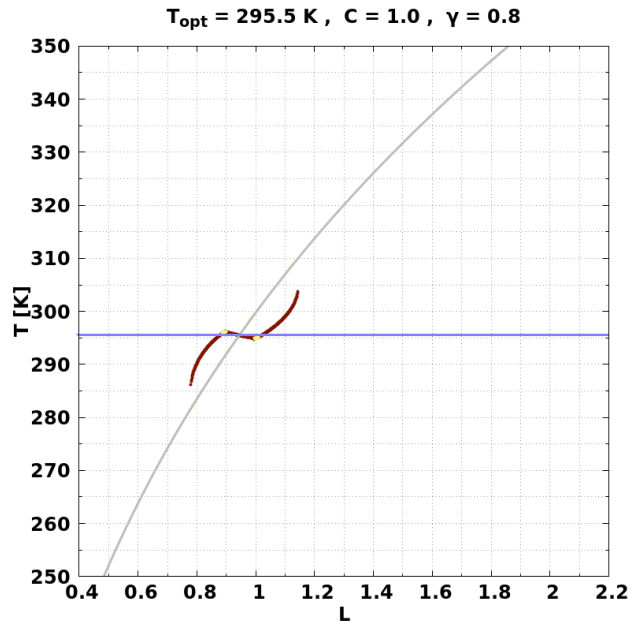
(c) DWC temperature T mean for $C = 1.0$ and $\gamma = 0.8$.

Figure A.8: **Orbits diagram** and the corresponding temperature T mean for **DWC** for $C = 1.0$ and $\gamma = 0.8$. **Blue** line corresponds to the value of $T_{opt} = 295.5$ K. Finally, those values of L where **Overpopulation** occurs, are marked by a vertical line with its corresponding color.
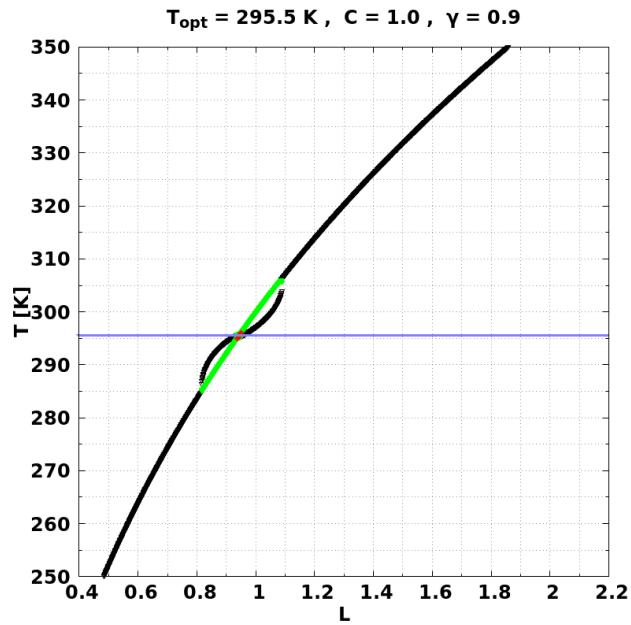
(a) DWC bifurcation for $C = 1.0$ and $\gamma = 0.9$.
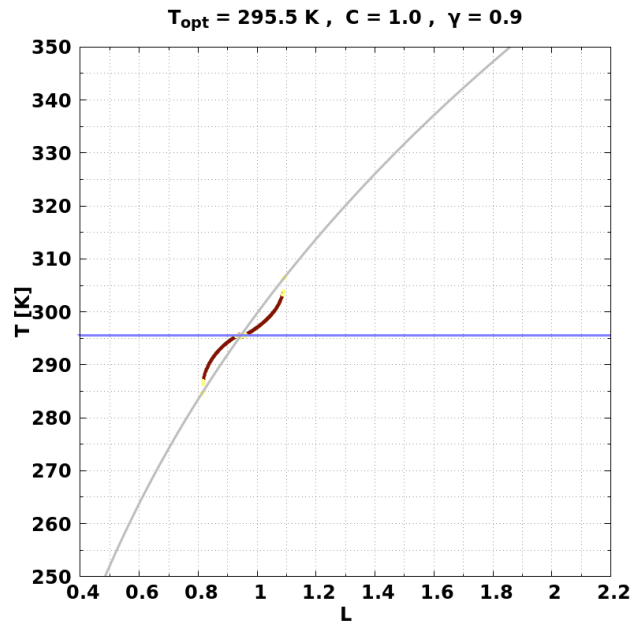
(b) DWC orbits diagram for $C = 1.0$ and $\gamma = 0.9$.
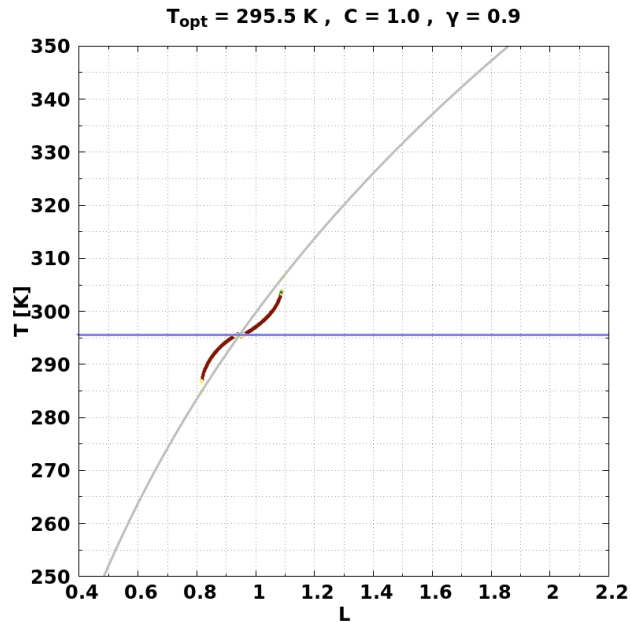
(c) DWC temperature T mean for $C = 1.0$ and $\gamma = 0.9$.

Figure A.9: **Orbits diagram** and the corresponding temperature T mean for **DWC** for $C = 1.0$ and $\gamma = 0.9$. **Blue** line corresponds to the value of $T_{opt} = 295.5$ K. Finally, those values of L where **Overpopulation** occurs, are marked by a vertical line with its corresponding color.
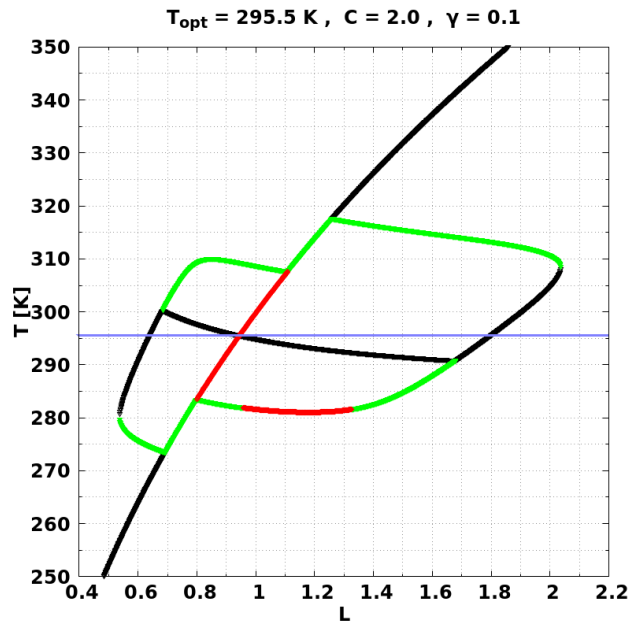
(a) DWC bifurcation for $C = 2.0$ and $\gamma = 0.1$.
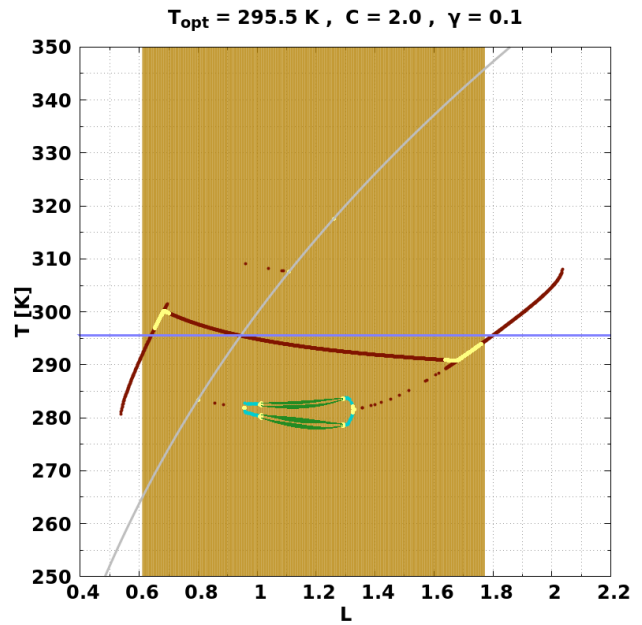
(b) DWC orbits diagram for $C = 2.0$ and $\gamma = 0.1$.
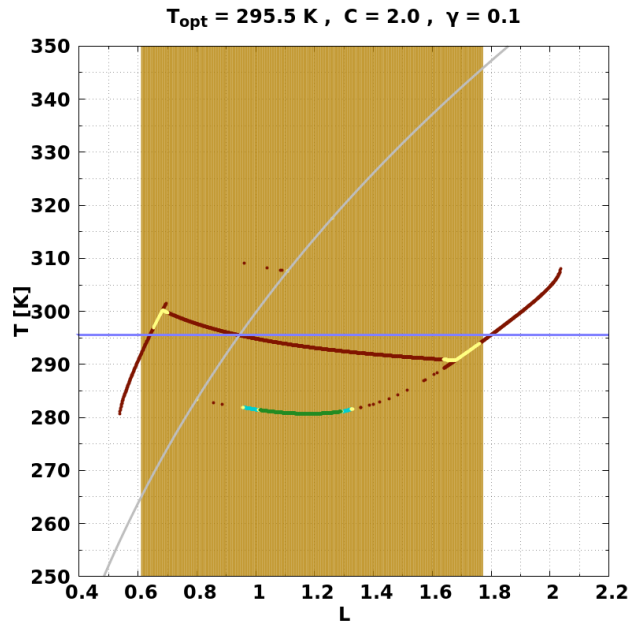
(c) DWC temperature T mean for $C = 2.0$ and $\gamma = 0.1$.

- ● Stable node
- ● Semistable node
- ● Unstable node
- ▨ Null (0,0)
- ▉ FP not null
- ▢ Periodic
- ▢ Quasiperiodic
- ▢ Chaotic (a1,a2)
- ▉ Chaotic (a1,0)
- ▉ Chaotic (0,a2)
- ▨ Overpopulation
- ▬ Forbidden barrier

Figure A.10: **Orbits diagram** and the corresponding temperature T mean for **DWC** for $C = 2.0$ and $\gamma = 0.1$. **Blue** line corresponds to the value of $T_{opt} = 295.5$ K. Finally, those values of L where **Overpopulation** occurs, are marked by a vertical line with its corresponding color.
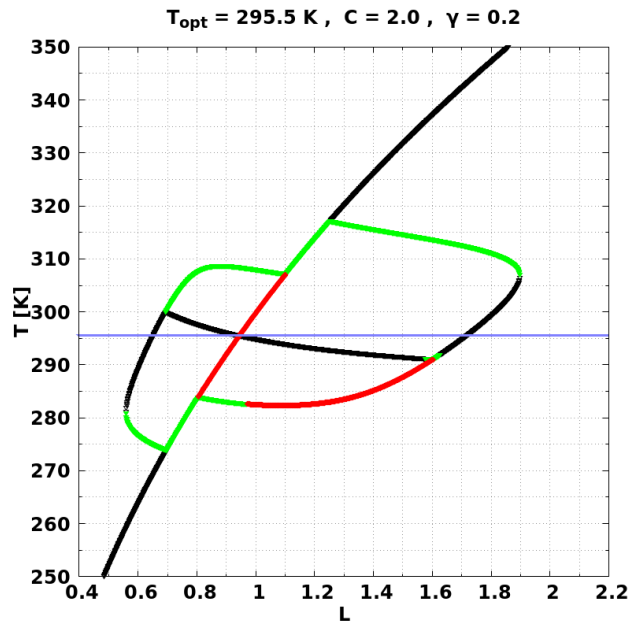
(a) DWC bifurcation for $C = 2.0$ and $\gamma = 0.2$.
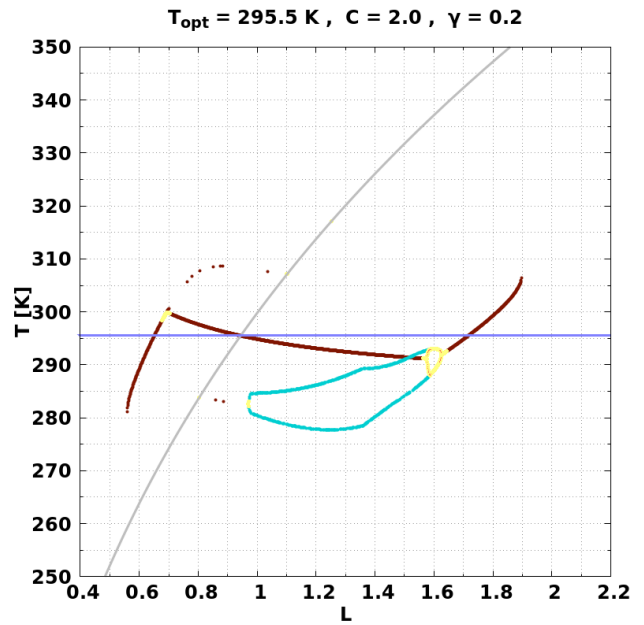
(b) DWC orbits diagram for $C = 2.0$ and $\gamma = 0.2$.
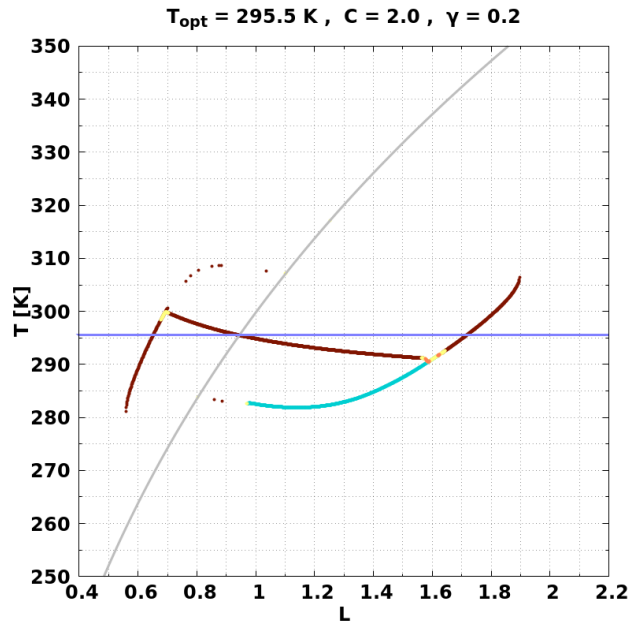
(c) DWC temperature T mean for $C = 2.0$ and $\gamma = 0.2$.

Figure A.11: **Orbits diagram** and the corresponding temperature T mean for **DWC** for $C = 2.0$ and $\gamma = 0.2$. **Blue** line corresponds to the value of $T_{opt} = 295.5$ K. Finally, those values of L where **Overpopulation** occurs, are marked by a vertical line with its corresponding color.

(a) DWC bifurcation for $C = 2.0$ and $\gamma = 0.3$.

(b) DWC orbits diagram for $C = 2.0$ and $\gamma = 0.3$.

(c) DWC temperature T mean for $C = 2.0$ and $\gamma = 0.3$.

Legend:
- Stable node
- Semistable node
- Unstable node
- Null (0,0)
- FP not null
- Periodic
- Quasiperiodic
- Chaotic (a1,a2)
- Chaotic (a1,0)
- Chaotic (0,a2)
- Overpopulation
- Forbidden barrier
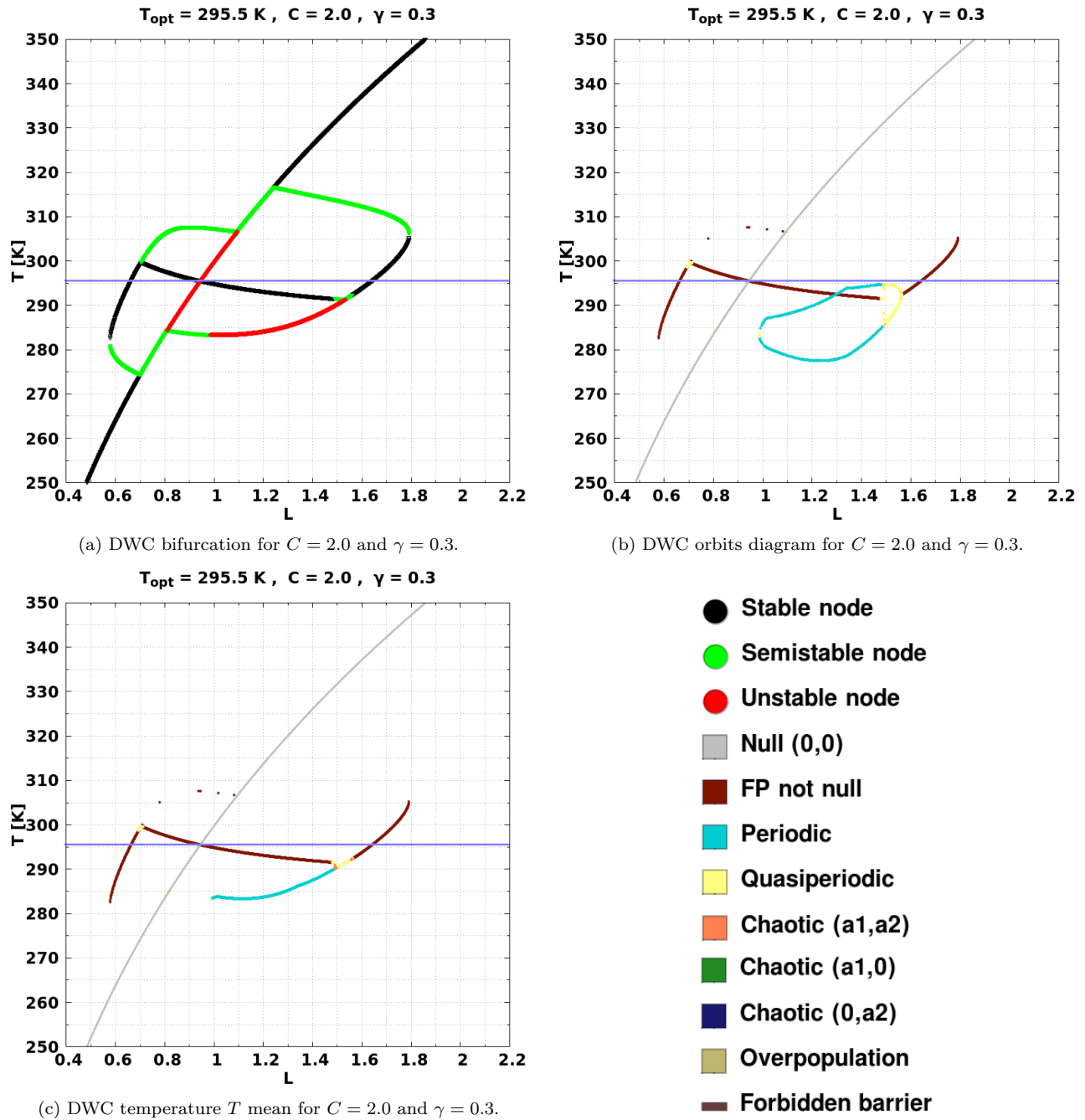
Figure A.12: **Orbits diagram** and the corresponding temperature T mean for **DWC** for $C = 2.0$ and $\gamma = 0.3$. **Blue** line corresponds to the value of $T_{opt} = 295.5$ K. Finally, those values of L where **Overpopulation** occurs, are marked by a vertical line with its corresponding color.
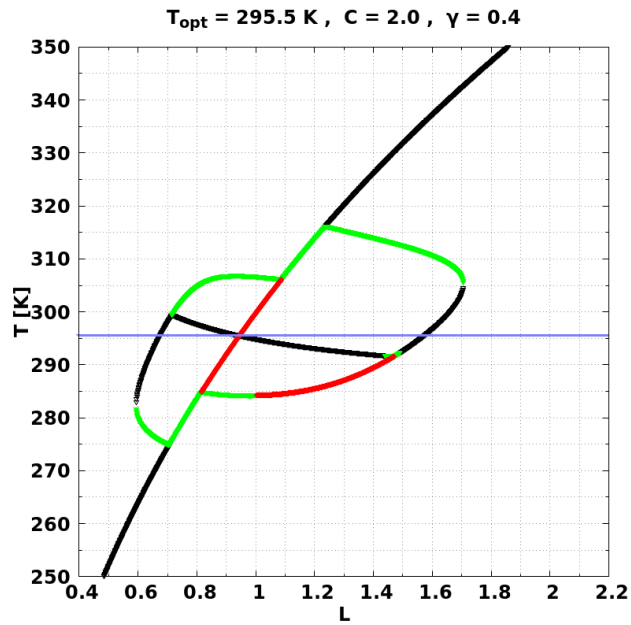
(a) DWC bifurcation for $C = 2.0$ and $\gamma = 0.4$.
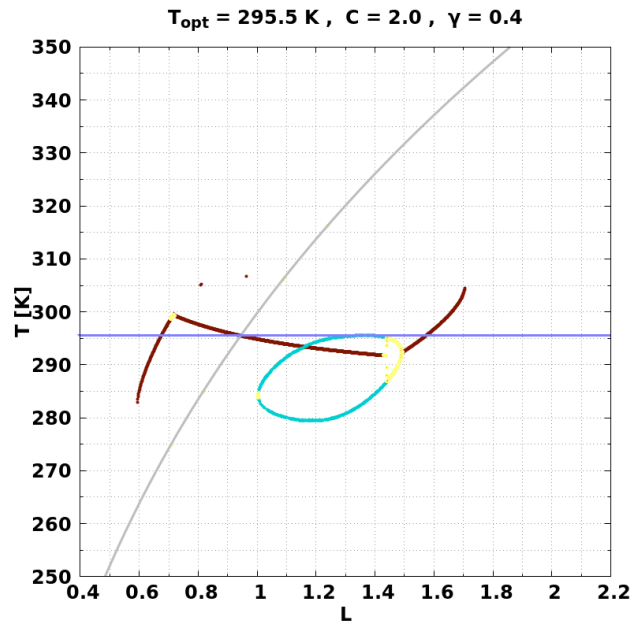
(b) DWC orbits diagram for $C = 2.0$ and $\gamma = 0.4$.
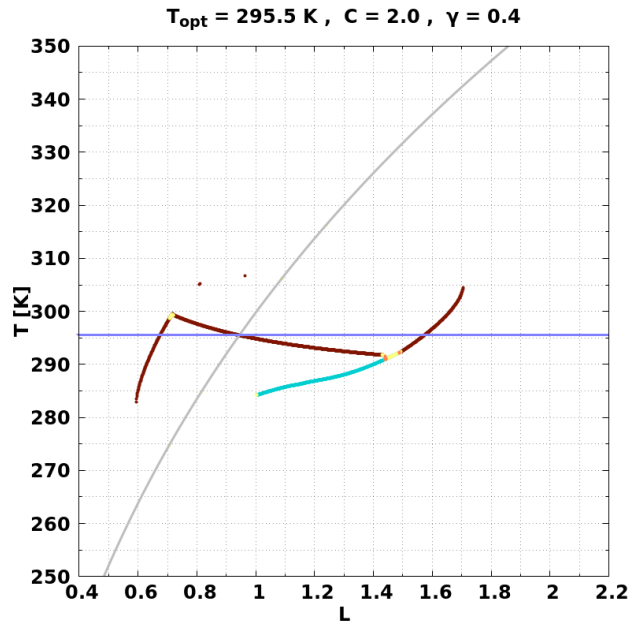
(c) DWC temperature T mean for $C = 2.0$ and $\gamma = 0.4$.

Figure A.13: **Orbits diagram** and the corresponding temperature T mean for **DWC** for $C = 2.0$ and $\gamma = 0.4$. **Blue** line corresponds to the value of $T_{opt} = 295.5$ K. Finally, those values of L where **Overpopulation** occurs, are marked by a vertical line with its corresponding color.
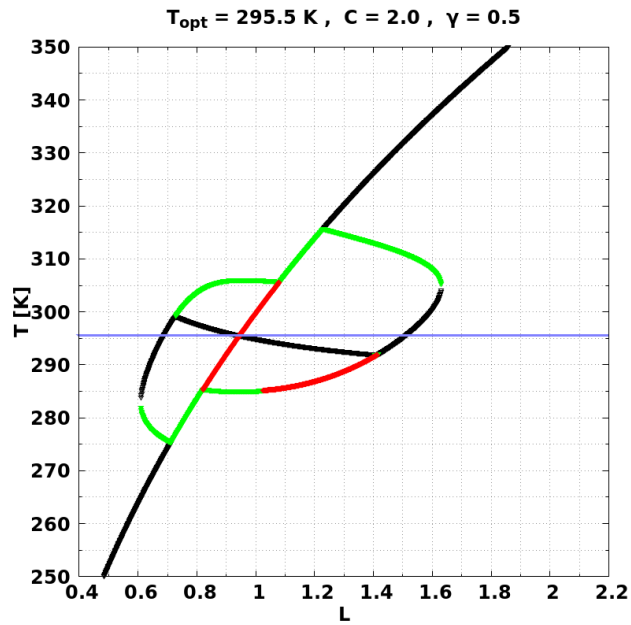
(a) DWC bifurcation for $C = 2.0$ and $\gamma = 0.5$.
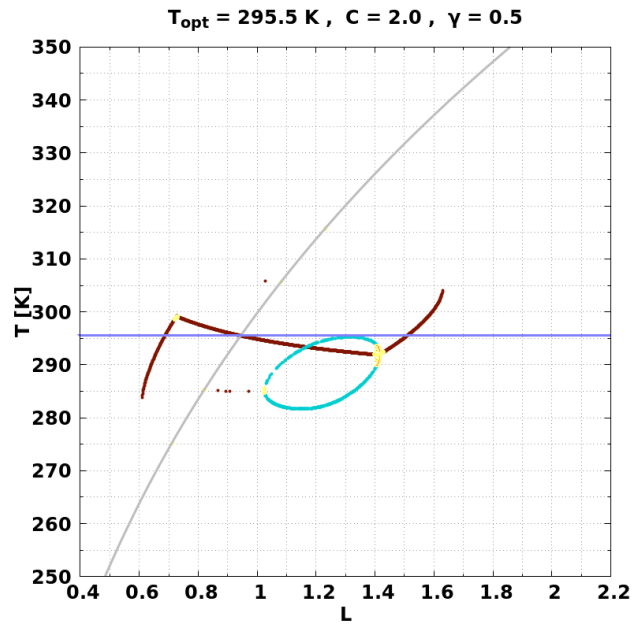
(b) DWC orbits diagram for $C = 2.0$ and $\gamma = 0.5$.
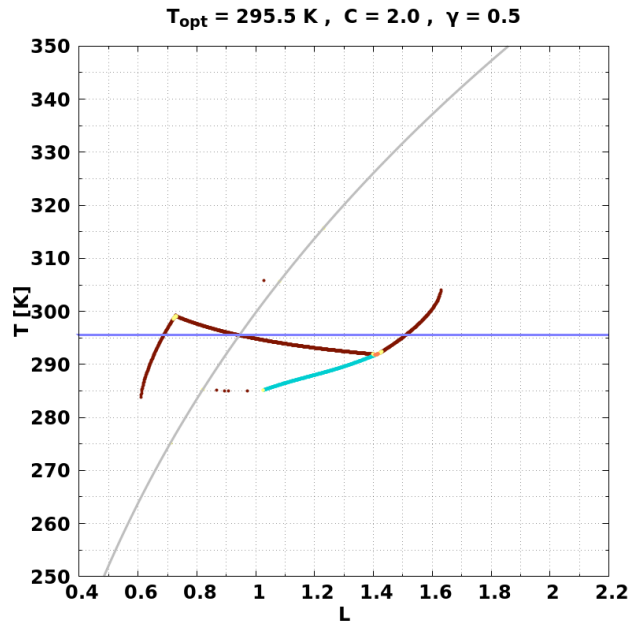
(c) DWC temperature T mean for $C = 2.0$ and $\gamma = 0.5$.

Legend:
- Stable node
- Semistable node
- Unstable node
- Null (0,0)
- FP not null
- Periodic
- Quasiperiodic
- Chaotic (a1,a2)
- Chaotic (a1,0)
- Chaotic (0,a2)
- Overpopulation
- Forbidden barrier

Figure A.14: **Orbits diagram** and the corresponding temperature T mean for **DWC** for $C = 2.0$ and $\gamma = 0.5$. **Blue** line corresponds to the value of $T_{opt} = 295.5$ K. Finally, those values of L where **Overpopulation** occurs, are marked by a vertical line with its corresponding color.
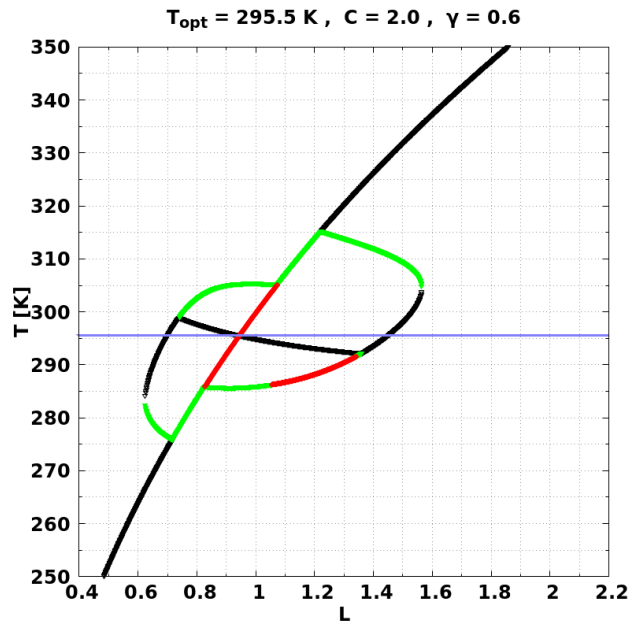
(a) DWC bifurcation for $C = 2.0$ and $\gamma = 0.6$.
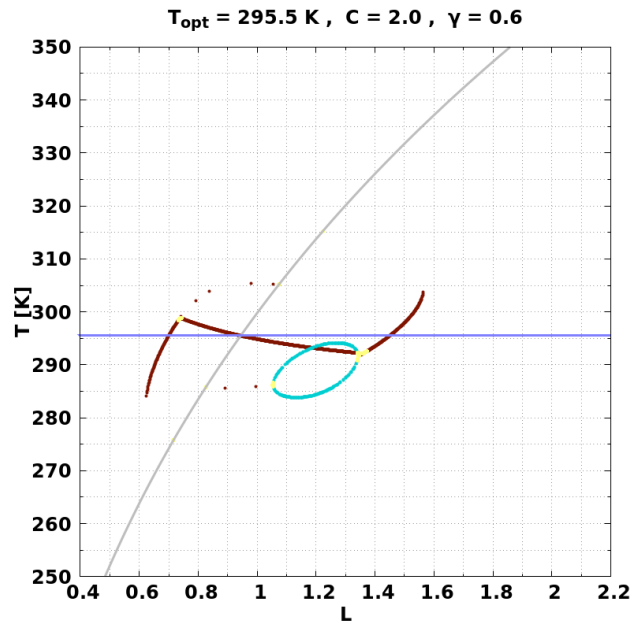
(b) DWC orbits diagram for $C = 2.0$ and $\gamma = 0.6$.
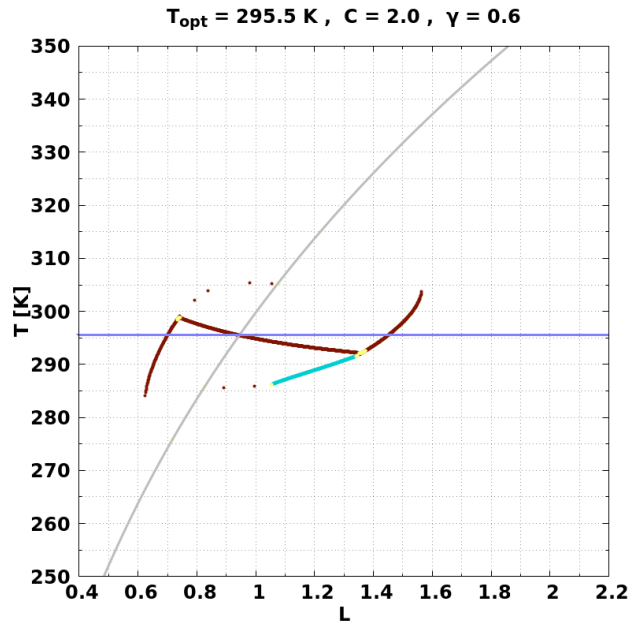
(c) DWC temperature T mean for $C = 2.0$ and $\gamma = 0.6$.

Figure A.15: **Orbits diagram** and the corresponding temperature T mean for **DWC** for $C = 2.0$ and $\gamma = 0.6$. **Blue** line corresponds to the value of $T_{opt} = 295.5$ K. Finally, those values of L where **Overpopulation** occurs, are marked by a vertical line with its corresponding color.
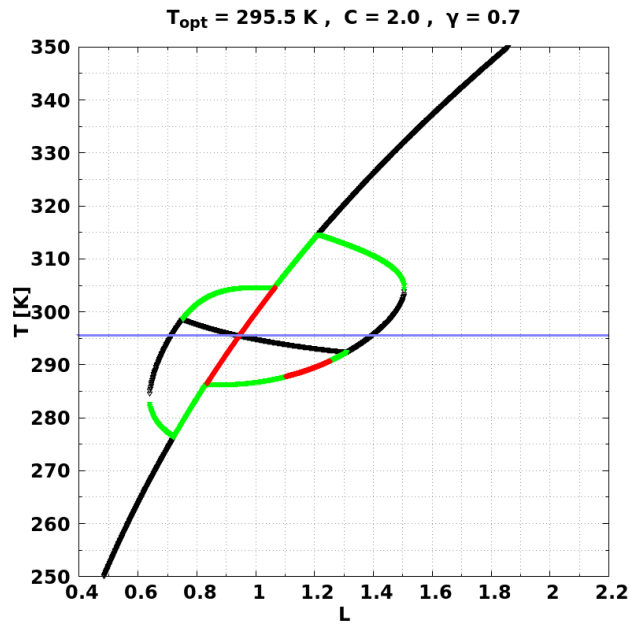
(a) DWC bifurcation for $C = 2.0$ and $\gamma = 0.7$.
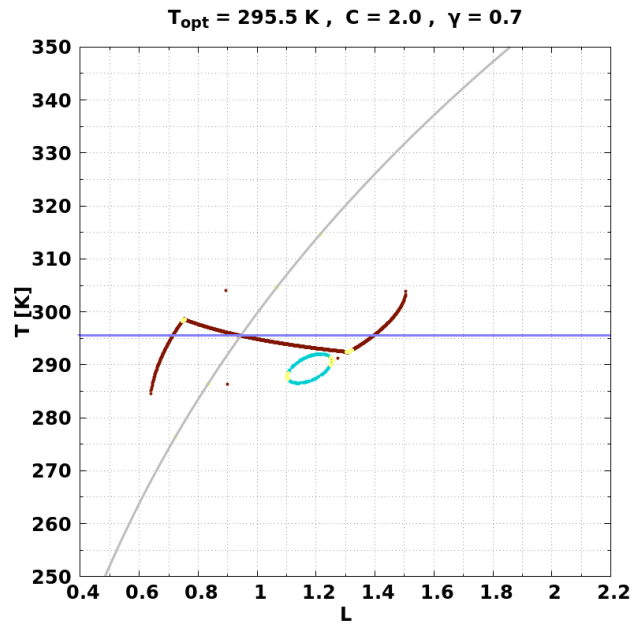
(b) DWC orbits diagram for $C = 2.0$ and $\gamma = 0.7$.
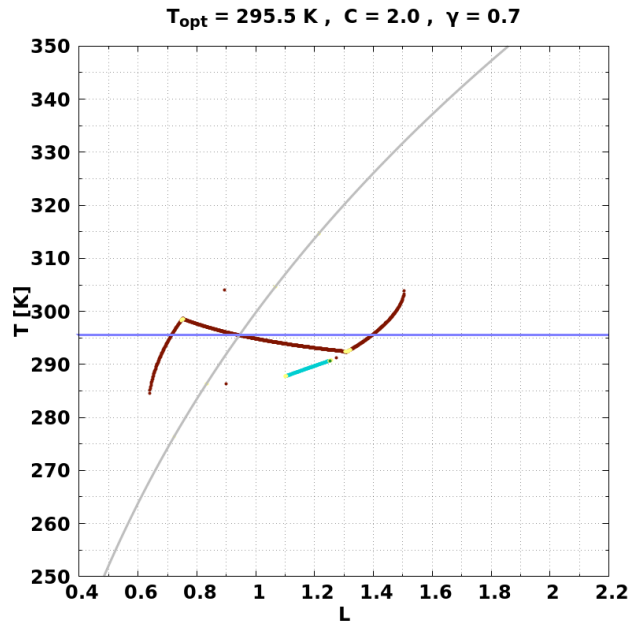
(c) DWC temperature T mean for $C = 2.0$ and $\gamma = 0.7$.

Figure A.16: **Orbits diagram** and the corresponding temperature T mean for **DWC** for $C = 2.0$ and $\gamma = 0.7$. **Blue** line corresponds to the value of $T_{opt} = 295.5$ K. Finally, those values of L where **Overpopulation** occurs, are marked by a vertical line with its corresponding color.
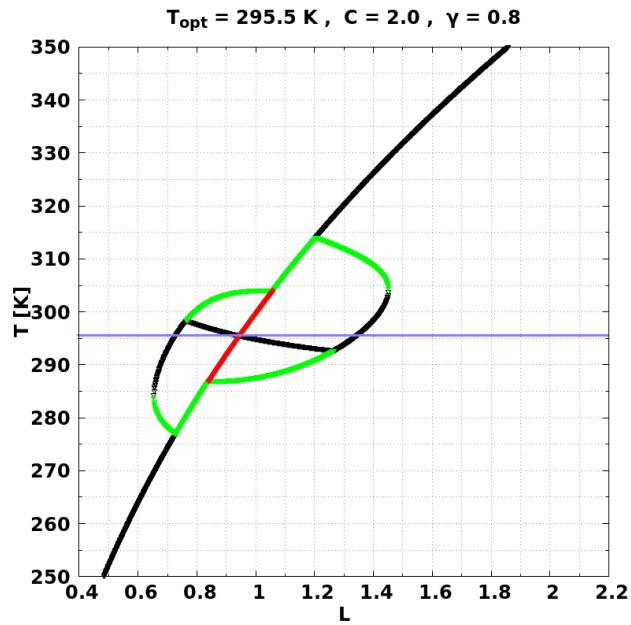
(a) DWC bifurcation for $C = 2.0$ and $\gamma = 0.8$.
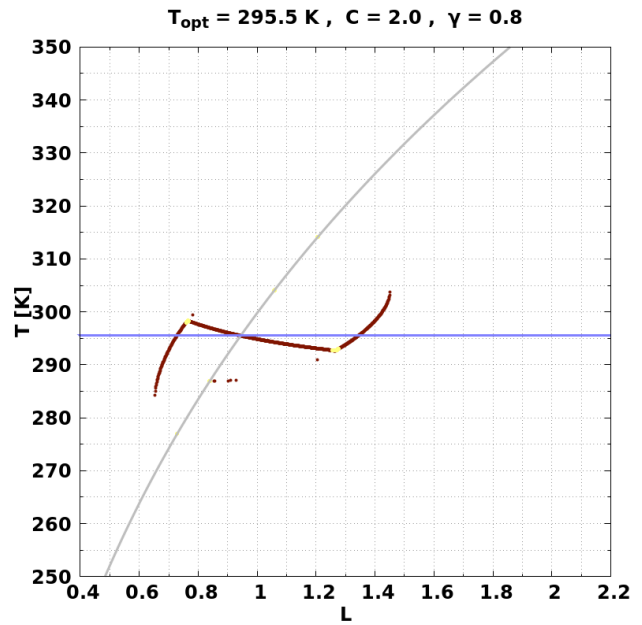
(b) DWC orbits diagram for $C = 2.0$ and $\gamma = 0.8$.
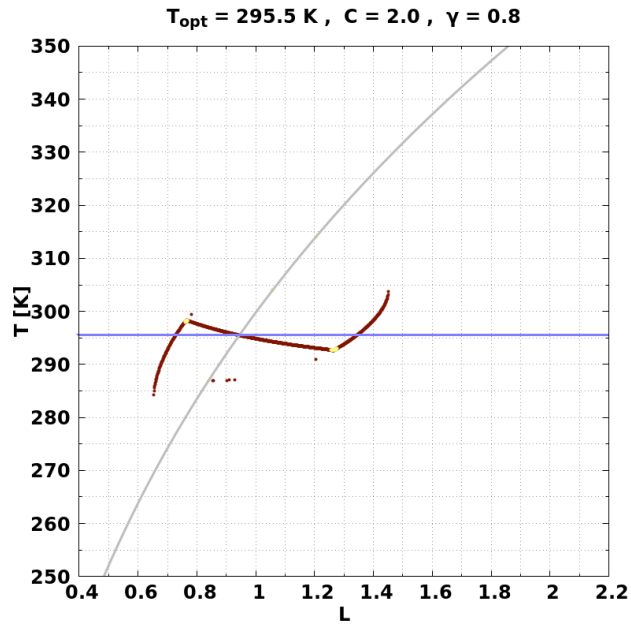
(c) DWC temperature T mean for $C = 2.0$ and $\gamma = 0.8$.

Figure A.17: **Orbits diagram** and the corresponding temperature T mean for **DWC** for $C = 2.0$ and $\gamma = 0.8$. **Blue** line corresponds to the value of $T_{opt} = 295.5$ K. Finally, those values of L where **Overpopulation** occurs, are marked by a vertical line with its corresponding color.
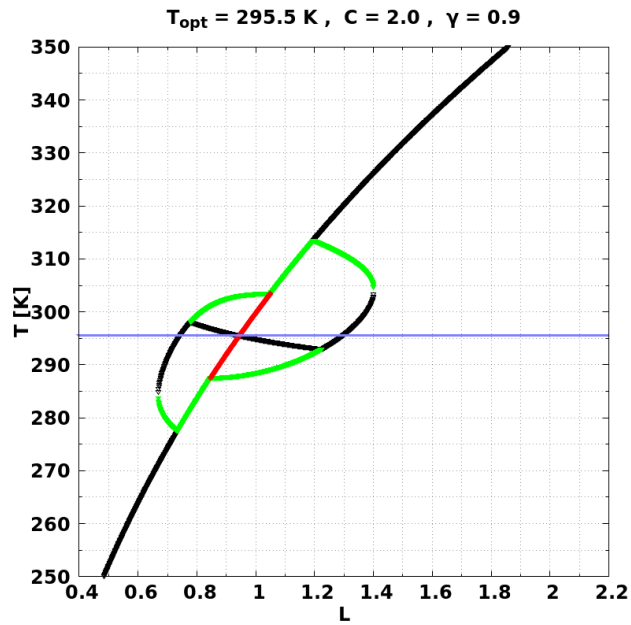
(a) DWC bifurcation for $C = 2.0$ and $\gamma = 0.9$.
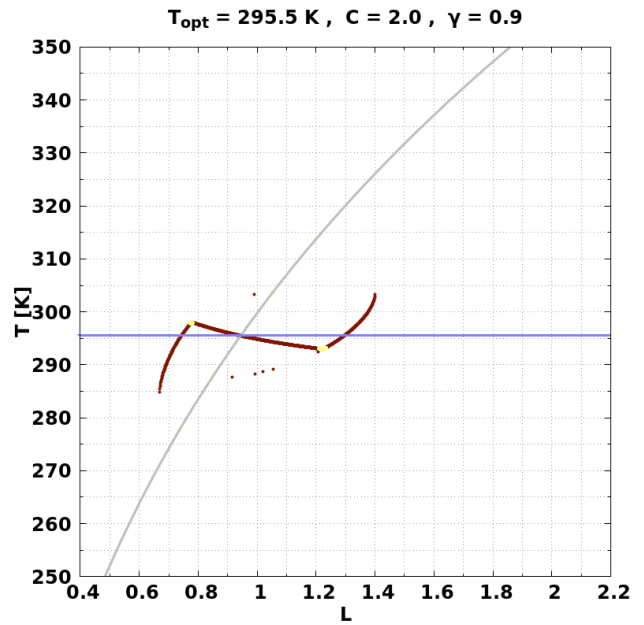
(b) DWC orbits diagram for $C = 2.0$ and $\gamma = 0.9$.
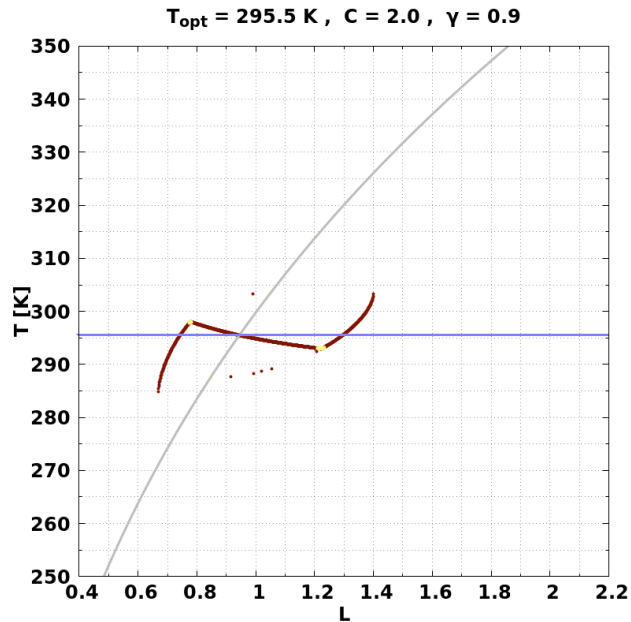
(c) DWC temperature T mean for $C = 2.0$ and $\gamma = 0.9$.

Figure A.18: **Orbits diagram** and the corresponding temperature T mean for **DWC** for $C = 2.0$ and $\gamma = 0.9$. **Blue** line corresponds to the value of $T_{opt} = 295.5$ K. Finally, those values of L where **Overpopulation** occurs, are marked by a vertical line with its corresponding color.
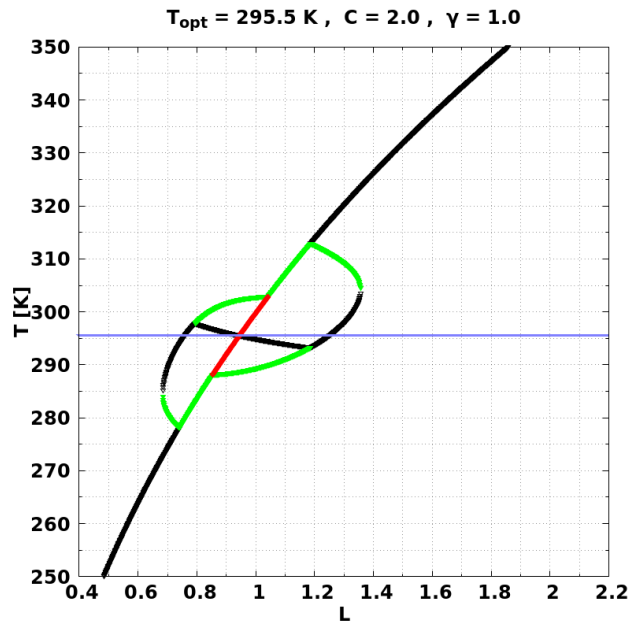
(a) DWC bifurcation for $C = 2.0$ and $\gamma = 1.0$.
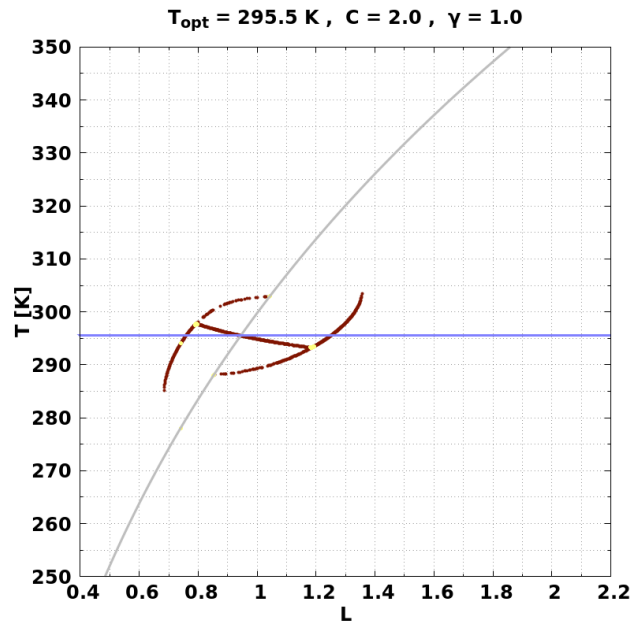
(b) DWC orbits diagram for $C = 2.0$ and $\gamma = 1.0$.
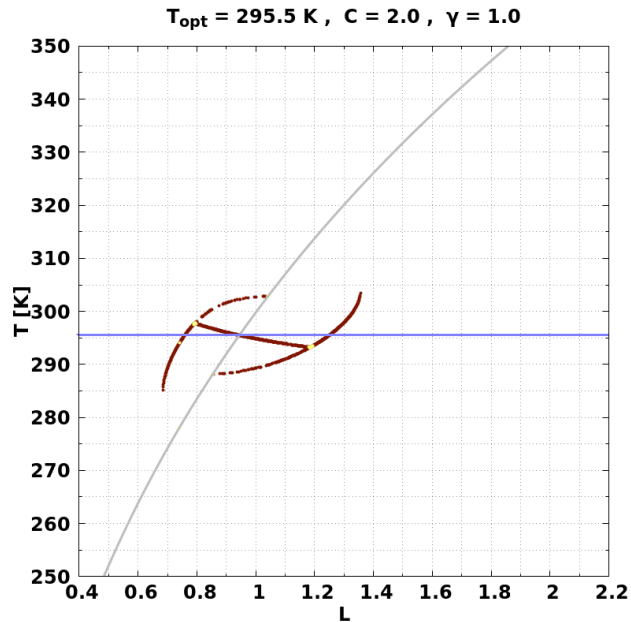
(c) DWC temperature T mean for $C = 2.0$ and $\gamma = 1.0$.

Figure A.19: **Orbits diagram** and the corresponding temperature T mean for **DWC** for $C = 2.0$ and $\gamma = 1.0$. **Blue** line corresponds to the value of $T_{opt} = 295.5$ K. Finally, those values of L where **Overpopulation** occurs, are marked by a vertical line with its corresponding color.
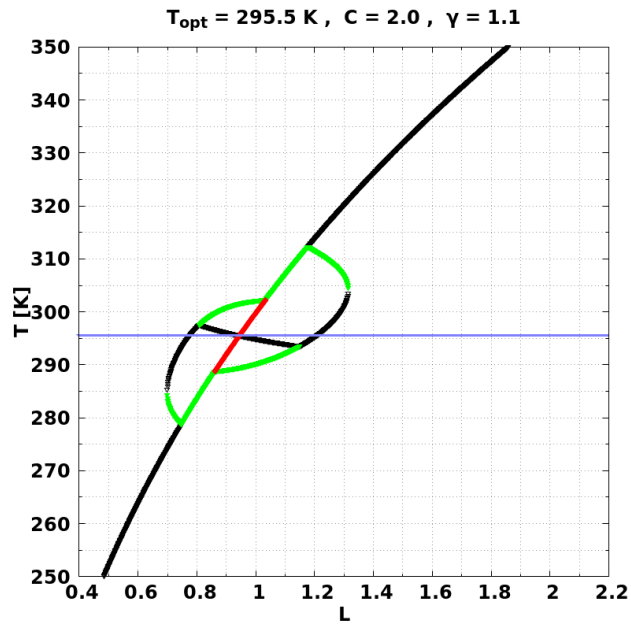
(a) DWC bifurcation for $C = 2.0$ and $\gamma = 1.1$.
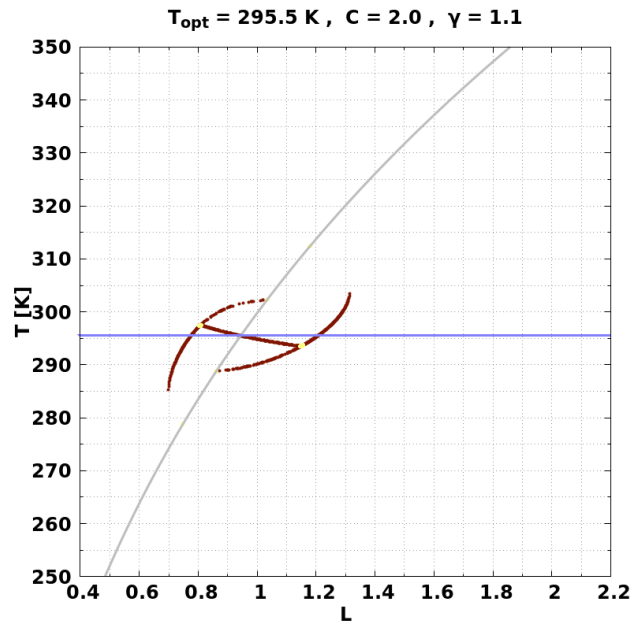
(b) DWC orbits diagram for $C = 2.0$ and $\gamma = 1.1$.
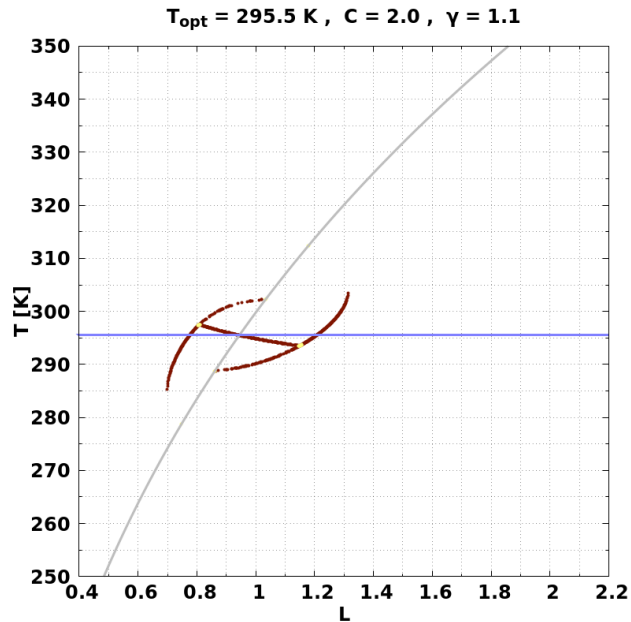
(c) DWC temperature T mean for $C = 2.0$ and $\gamma = 1.1$.

Figure A.20: **Orbits diagram** and the corresponding temperature T mean for **DWC** for $C = 2.0$ and $\gamma = 1.1$. **Blue** line corresponds to the value of $T_{opt} = 295.5$ K. Finally, those values of L where **Overpopulation** occurs, are marked by a vertical line with its corresponding color.
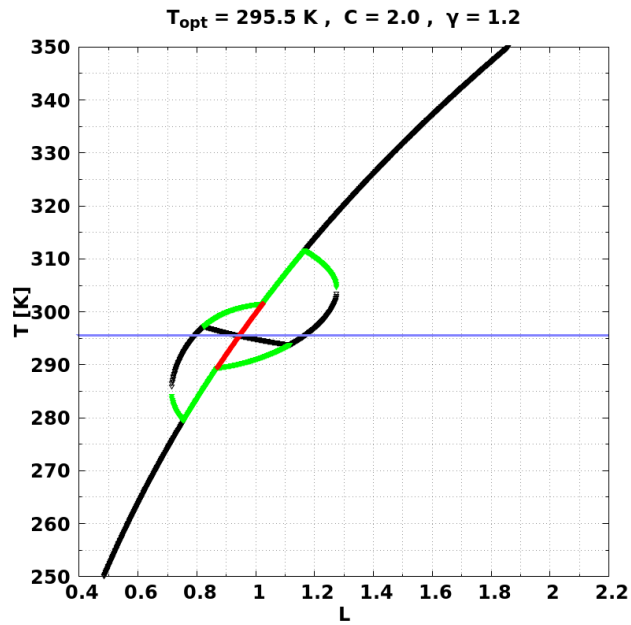
(a) DWC bifurcation for $C = 2.0$ and $\gamma = 1.2$.
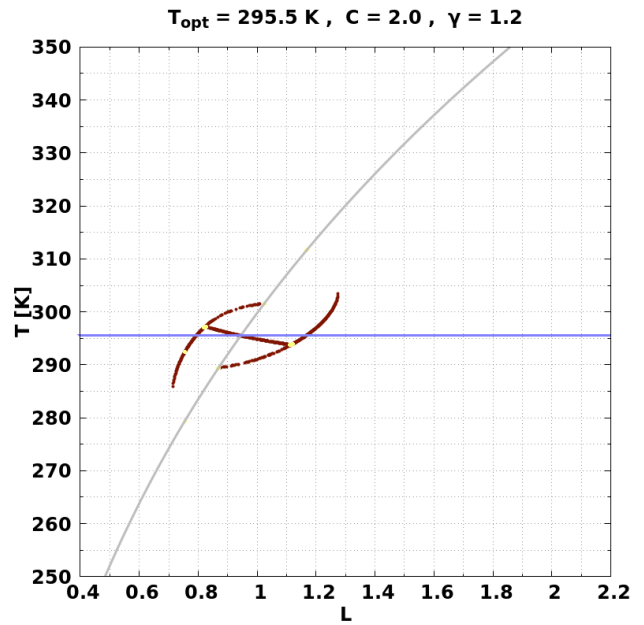
(b) DWC orbits diagram for $C = 2.0$ and $\gamma = 1.2$.
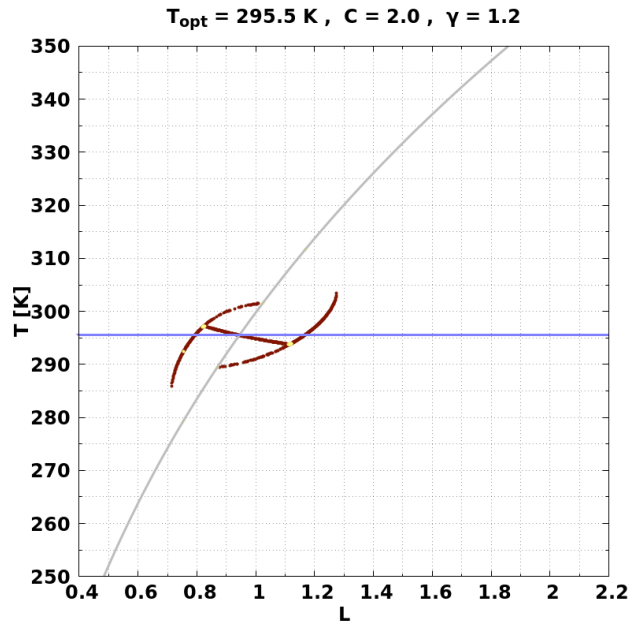
(c) DWC temperature T mean for $C = 2.0$ and $\gamma = 1.2$.

Figure A.21: **Orbits diagram** and the corresponding temperature T mean for **DWC** for $C = 2.0$ and $\gamma = 1.2$. **Blue** line corresponds to the value of $T_{opt} = 295.5$ K. Finally, those values of L where **Overpopulation** occurs, are marked by a vertical line with its corresponding color.
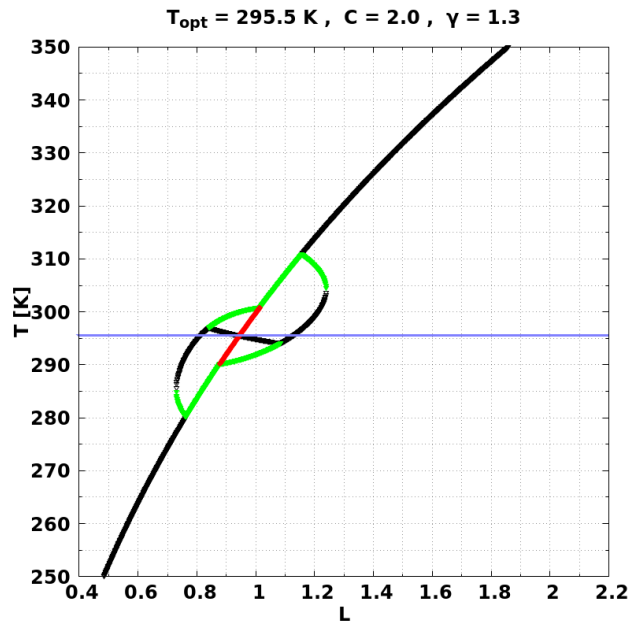
(a) DWC bifurcation for $C = 2.0$ and $\gamma = 1.3$.
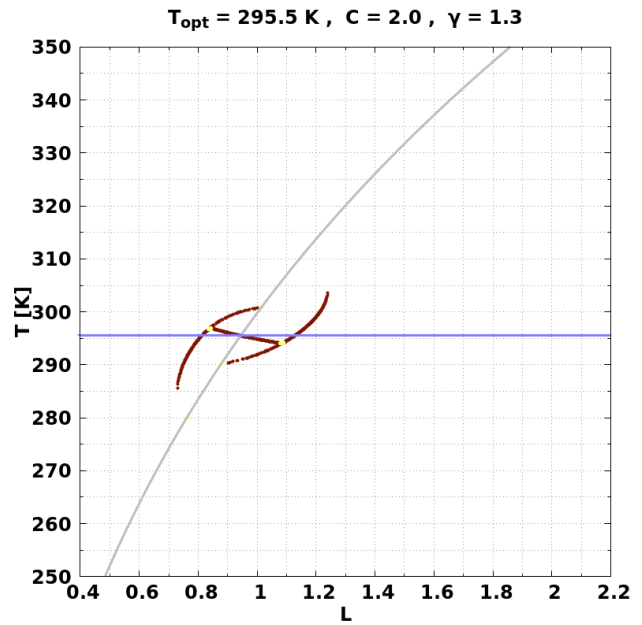
(b) DWC orbits diagram for $C = 2.0$ and $\gamma = 1.3$.
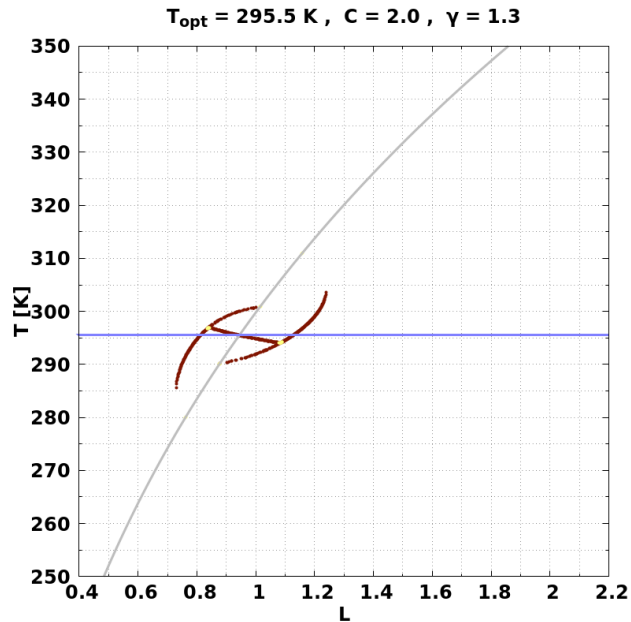
(c) DWC temperature T mean for $C = 2.0$ and $\gamma = 1.3$.

Figure A.22: **Orbits diagram** and the corresponding temperature T mean for **DWC** for $C = 2.0$ and $\gamma = 1.3$. **Blue** line corresponds to the value of $T_{opt} = 295.5$ K. Finally, those values of L where **Overpopulation** occurs, are marked by a vertical line with its corresponding color.
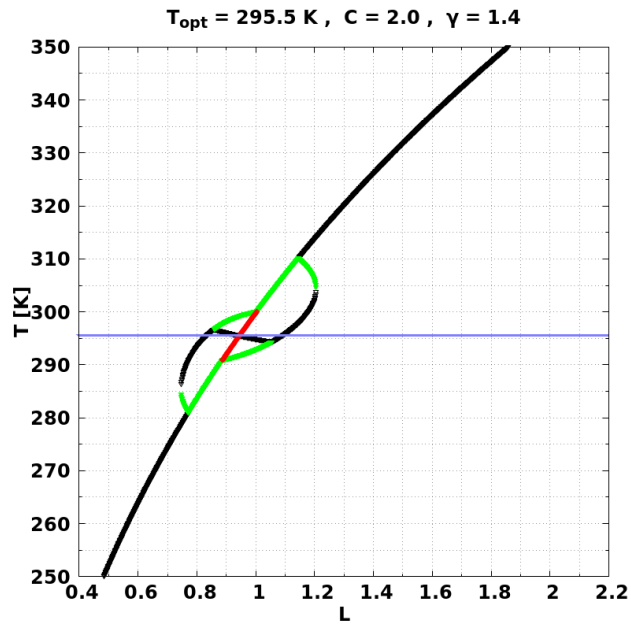
(a) DWC bifurcation for $C = 2.0$ and $\gamma = 1.4$.
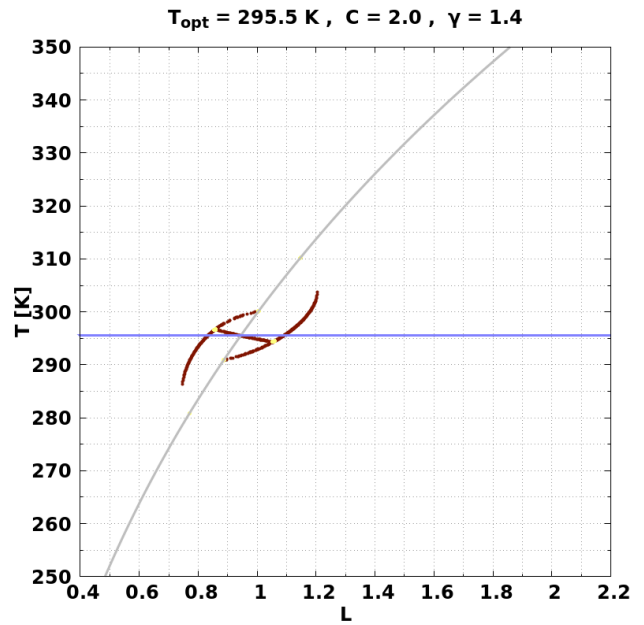
(b) DWC orbits diagram for $C = 2.0$ and $\gamma = 1.4$.
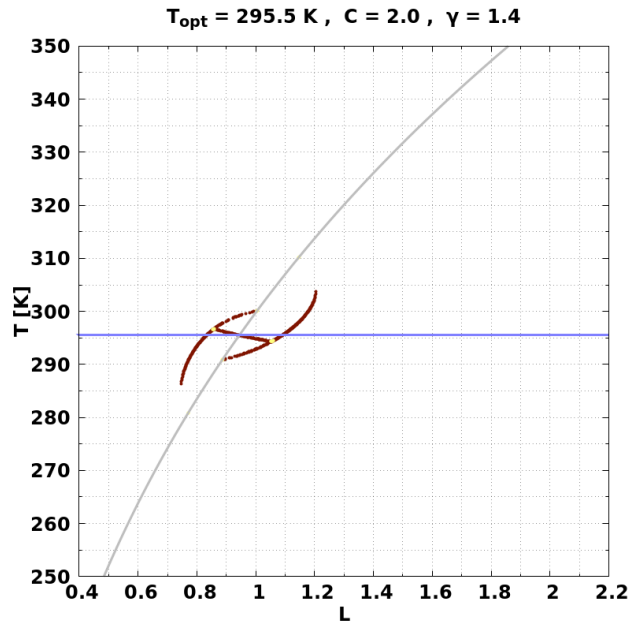
(c) DWC temperature T mean for $C = 2.0$ and $\gamma = 1.4$.

Figure A.23: **Orbits diagram** and the corresponding temperature T mean for **DWC** for $C = 2.0$ and $\gamma = 1.4$. **Blue** line corresponds to the value of $T_{opt} = 295.5$ K. Finally, those values of L where **Overpopulation** occurs, are marked by a vertical line with its corresponding color.
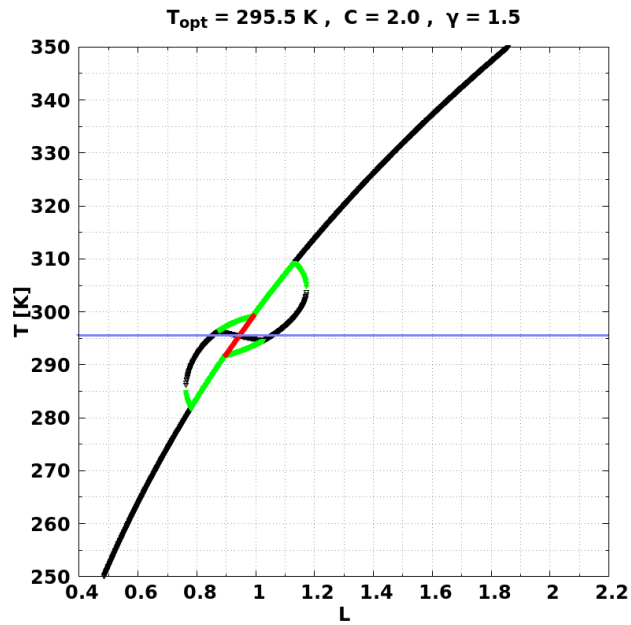
(a) DWC bifurcation for $C = 2.0$ and $\gamma = 1.5$.
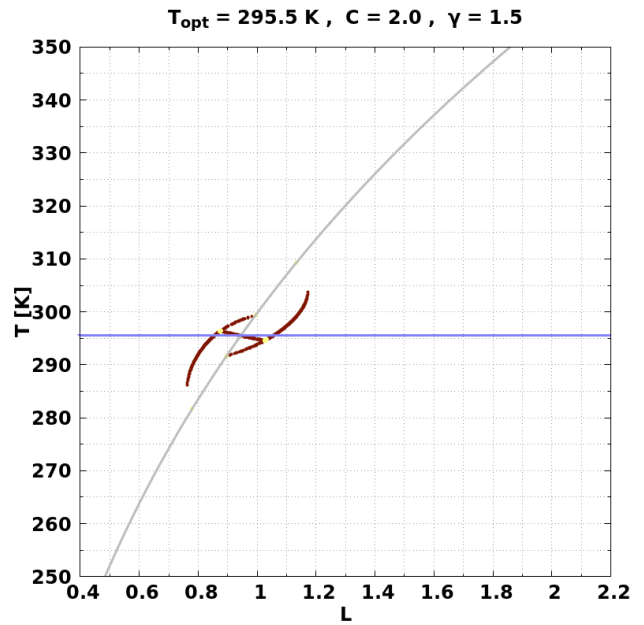
(b) DWC orbits diagram for $C = 2.0$ and $\gamma = 1.5$.
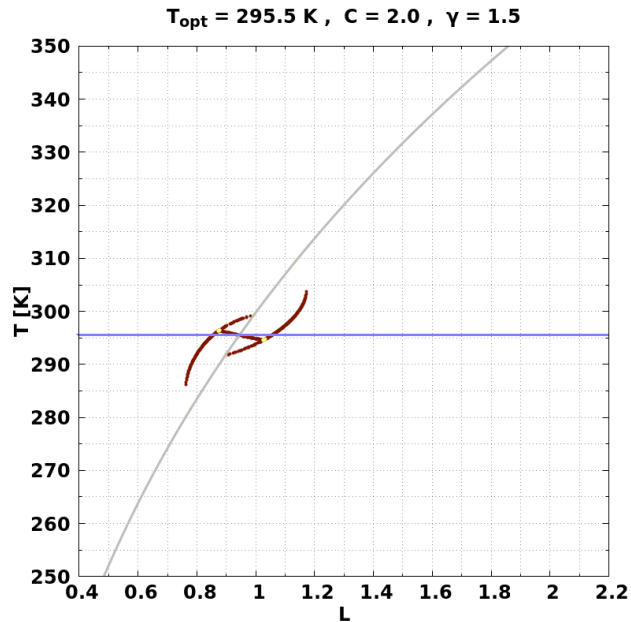
(c) DWC temperature T mean for $C = 2.0$ and $\gamma = 1.5$.

Figure A.24: **Orbits diagram** and the corresponding temperature T mean for **DWC** for $C = 2.0$ and $\gamma = 1.5$. **Blue** line corresponds to the value of $T_{opt} = 295.5$ K. Finally, those values of L where **Overpopulation** occurs, are marked by a vertical line with its corresponding color.
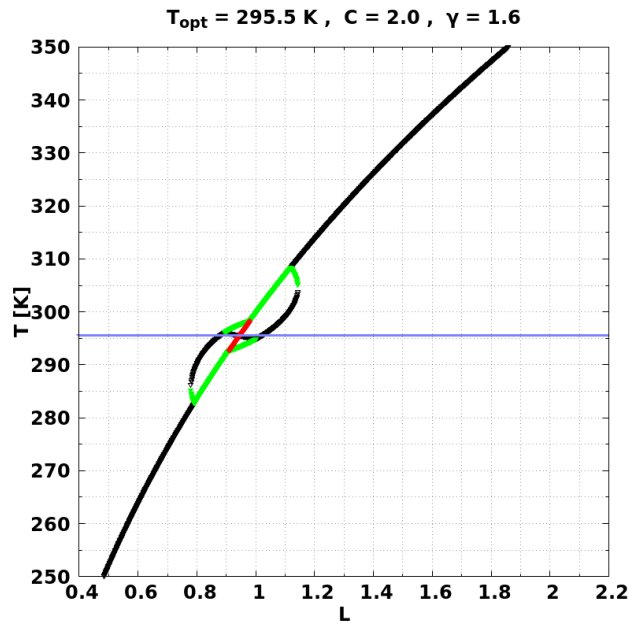
(a) DWC bifurcation for $C = 2.0$ and $\gamma = 1.6$.
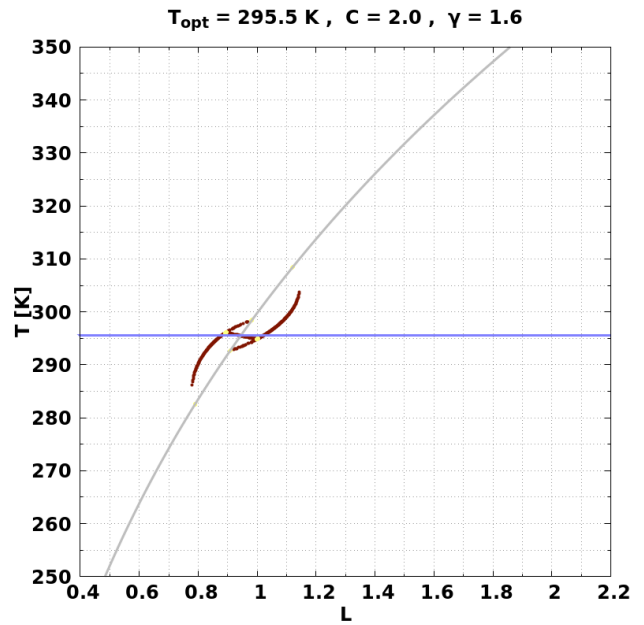
(b) DWC orbits diagram for $C = 2.0$ and $\gamma = 1.6$.
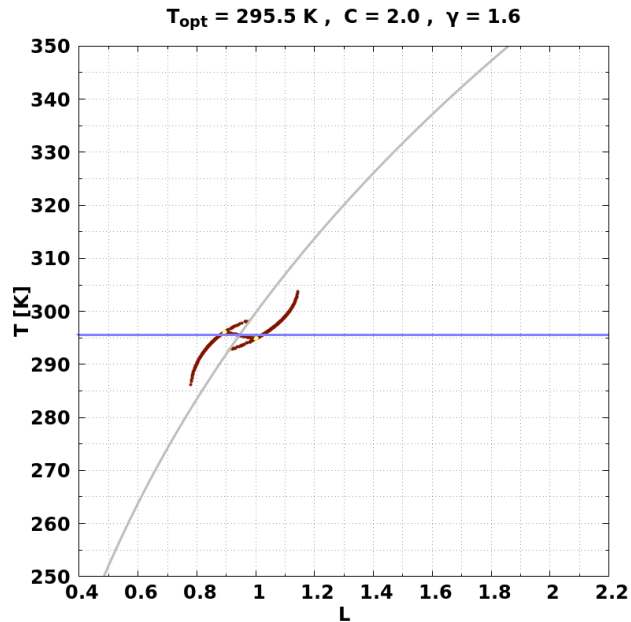
(c) DWC temperature T mean for $C = 2.0$ and $\gamma = 1.6$.

Figure A.25: **Orbits diagram** and the corresponding temperature T mean for **DWC** for $C = 2.0$ and $\gamma = 1.6$. **Blue** line corresponds to the value of $T_{opt} = 295.5$ K. Finally, those values of L where **Overpopulation** occurs, are marked by a vertical line with its corresponding color.
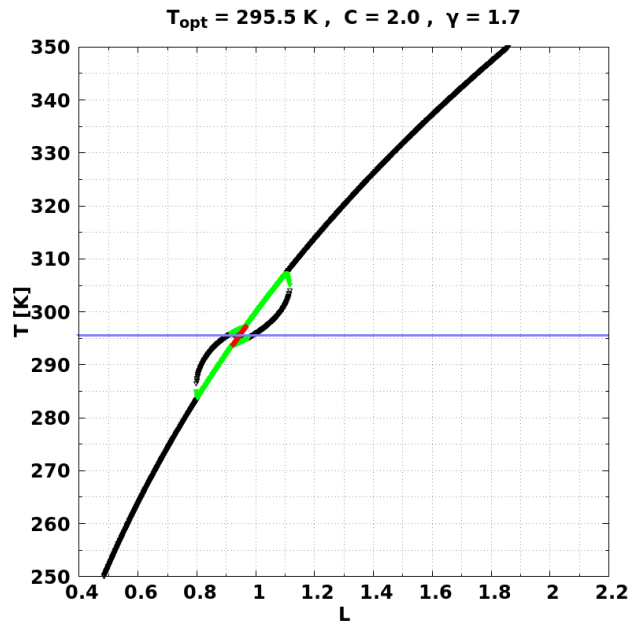
(a) DWC bifurcation for $C = 2.0$ and $\gamma = 1.7$.
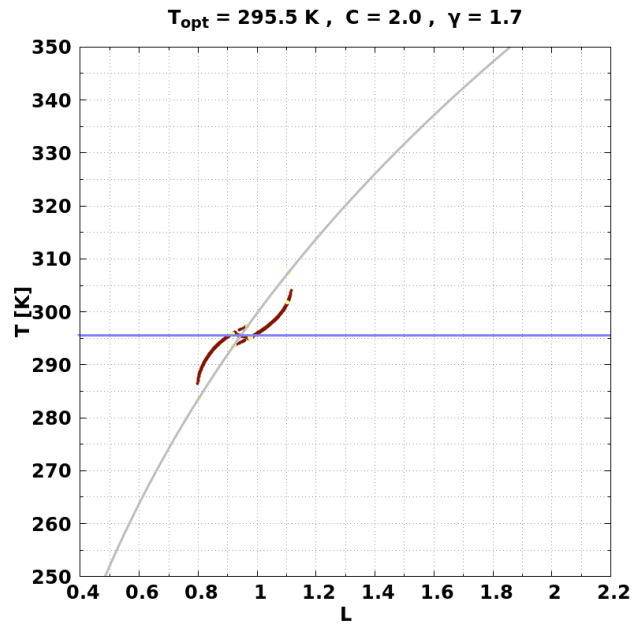
(b) DWC orbits diagram for $C = 2.0$ and $\gamma = 1.7$.
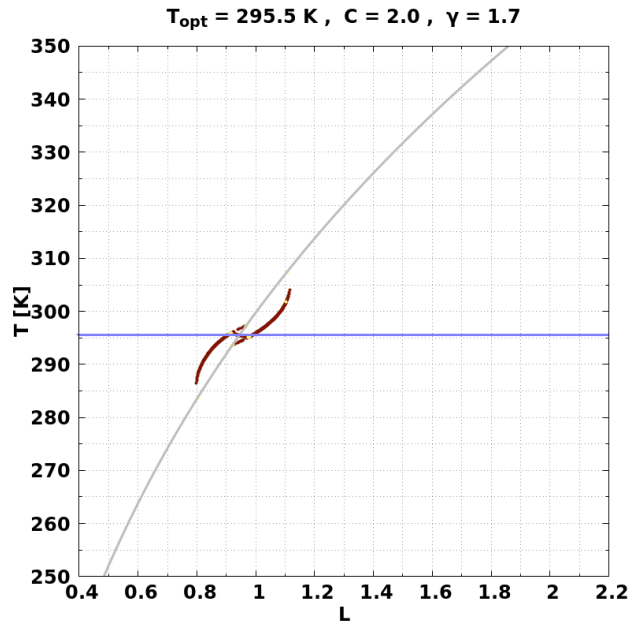
(c) DWC temperature T mean for $C = 2.0$ and $\gamma = 1.7$.

Figure A.26: **Orbits diagram** and the corresponding temperature T mean for **DWC** for $C = 2.0$ and $\gamma = 1.7$. **Blue** line corresponds to the value of $T_{opt} = 295.5$ K. Finally, those values of L where **Overpopulation** occurs, are marked by a vertical line with its corresponding color.
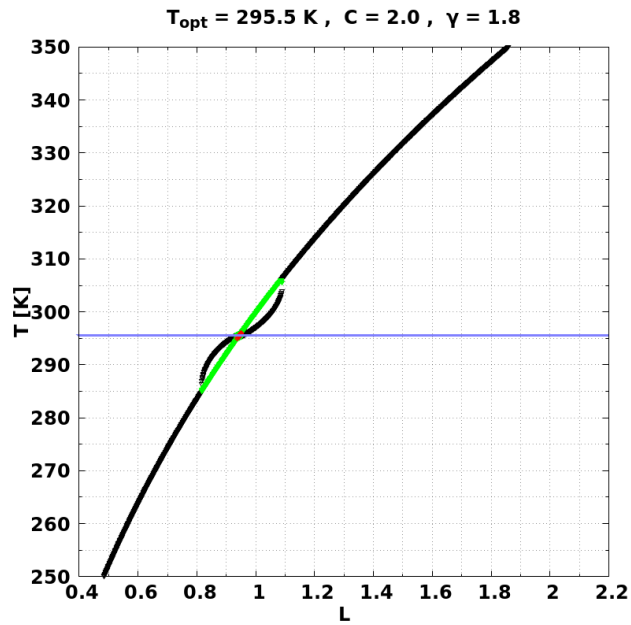
(a) DWC bifurcation for $C = 2.0$ and $\gamma = 1.8$.
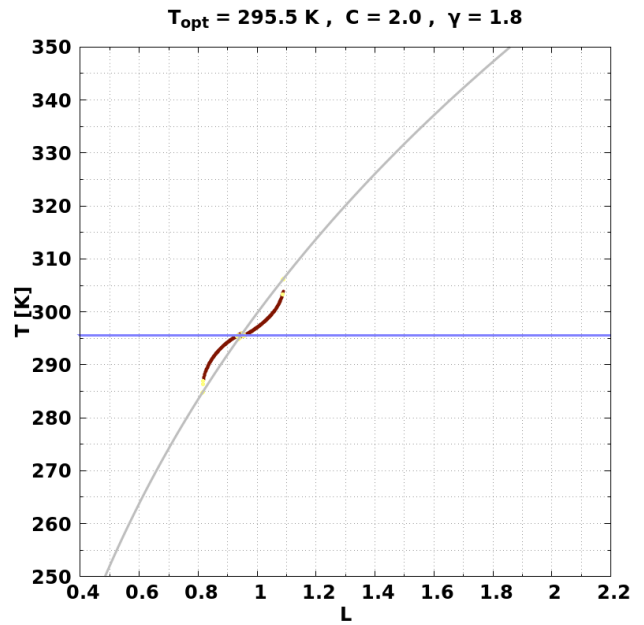
(b) DWC orbits diagram for $C = 2.0$ and $\gamma = 1.8$.
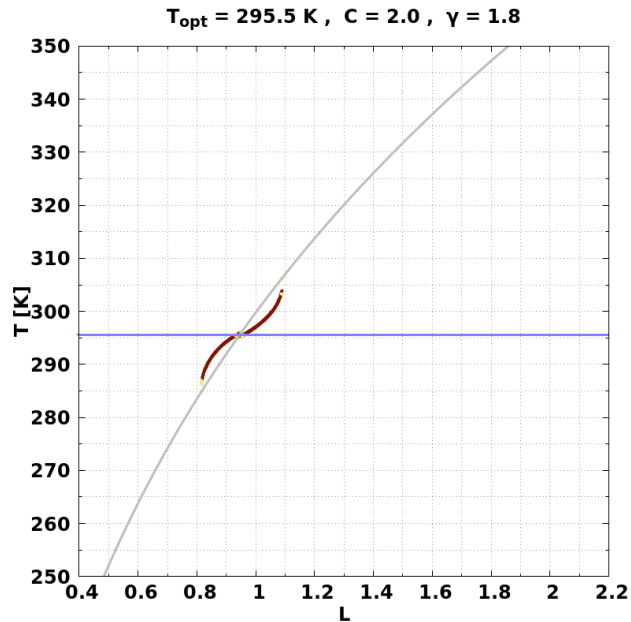
(c) DWC temperature T mean for $C = 2.0$ and $\gamma = 1.8$.

Figure A.27: **Orbits diagram** and the corresponding temperature T mean for **DWC** for $C = 2.0$ and $\gamma = 1.8$. **Blue** line corresponds to the value of $T_{opt} = 295.5$ K. Finally, those values of L where **Overpopulation** occurs, are marked by a vertical line with its corresponding color.
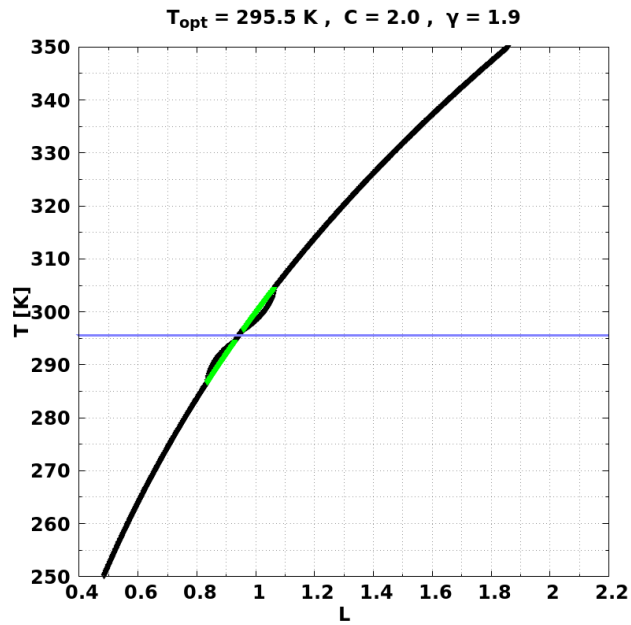
(a) DWC bifurcation for $C = 2.0$ and $\gamma = 1.9$.
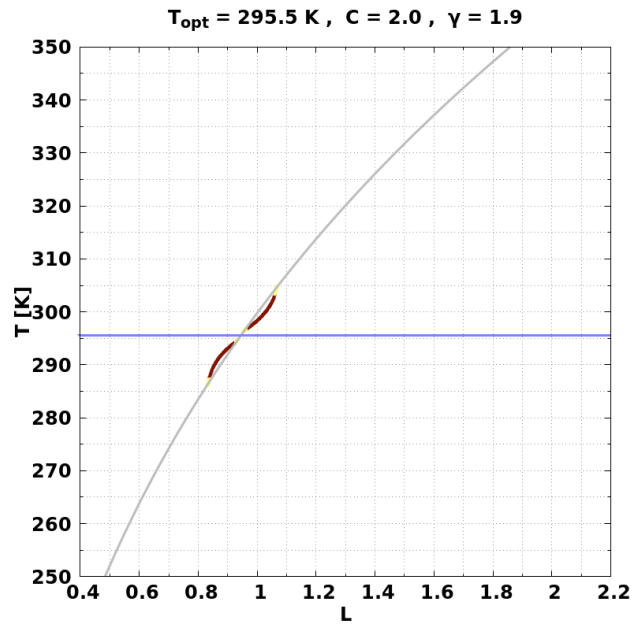
(b) DWC orbits diagram for $C = 2.0$ and $\gamma = 1.9$.
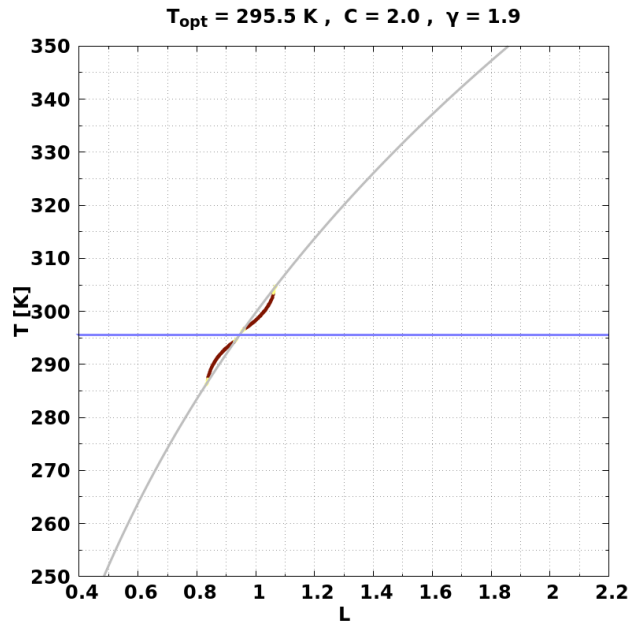
(c) DWC temperature T mean for $C = 2.0$ and $\gamma = 1.9$.

Figure A.28: **Orbits diagram** and the corresponding temperature T mean for **DWC** for $C = 2.0$ and $\gamma = 1.9$. **Blue** line corresponds to the value of $T_{opt} = 295.5$ K. Finally, those values of L where **Overpopulation** occurs, are marked by a vertical line with its corresponding color.
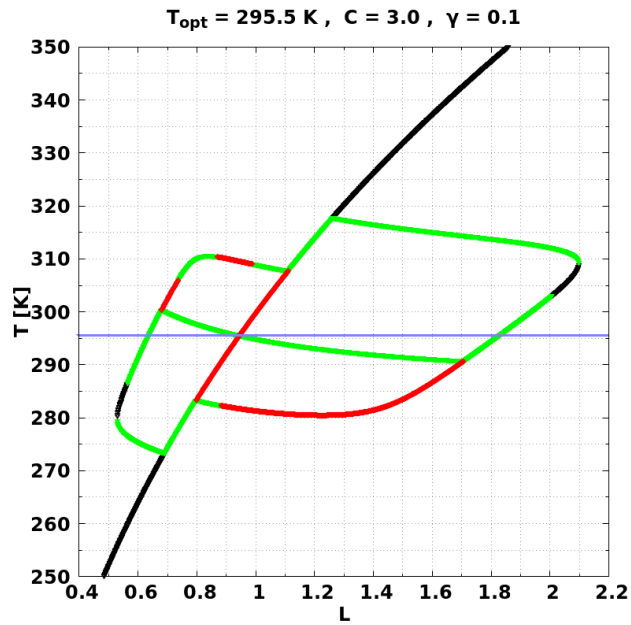
(a) DWC bifurcation for $C = 3.0$ and $\gamma = 0.1$.
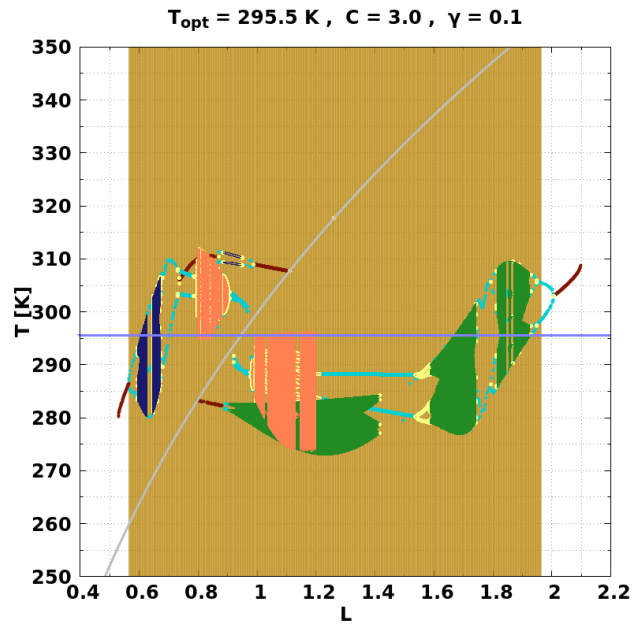
(b) DWC orbits diagram for $C = 3.0$ and $\gamma = 0.1$.
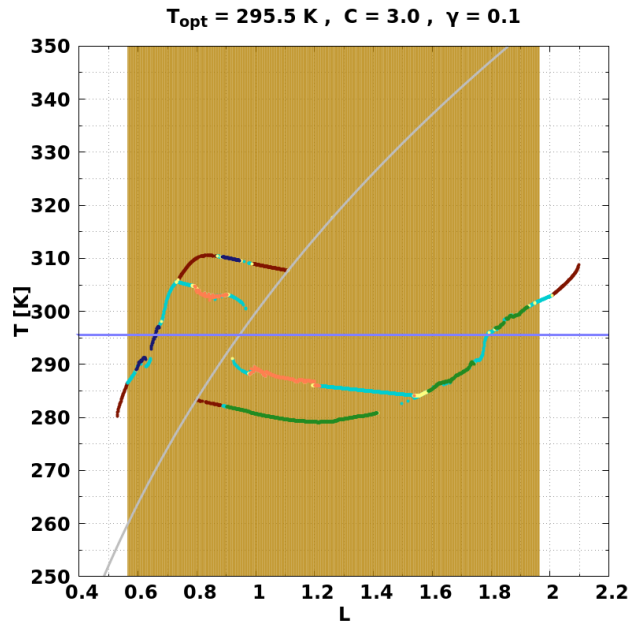
(c) DWC temperature T mean for $C = 3.0$ and $\gamma = 0.1$.

Figure A.29: **Orbits diagram** and the corresponding temperature T mean for **DWC** for $C = 3.0$ and $\gamma = 0.1$. **Blue** line corresponds to the value of $T_{opt} = 295.5$ K. Finally, those values of L where **Overpopulation** occurs, are marked by a vertical line with its corresponding color.
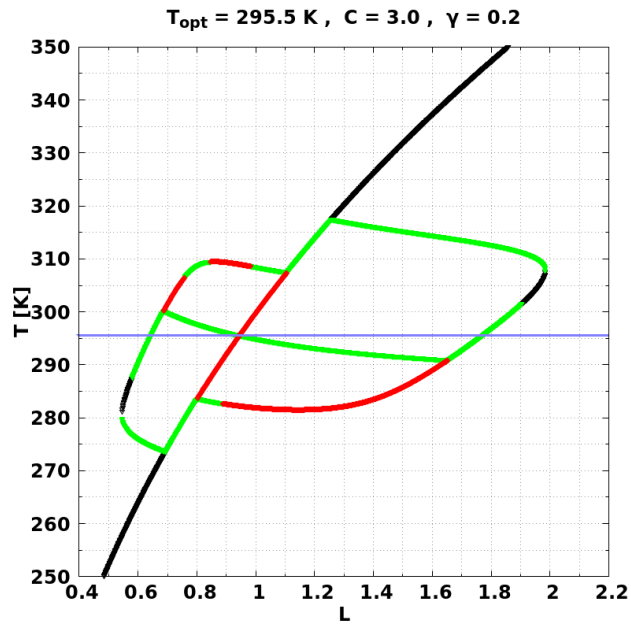
(a) DWC bifurcation for $C = 3.0$ and $\gamma = 0.2$.
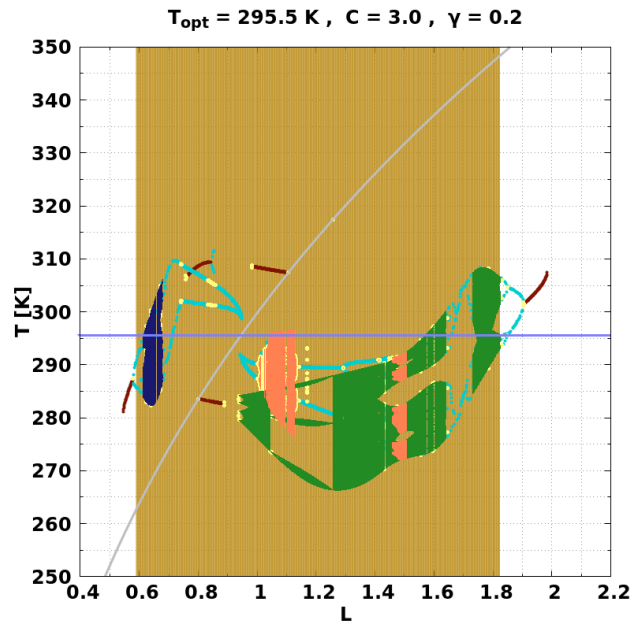
(b) DWC orbits diagram for $C = 3.0$ and $\gamma = 0.2$.
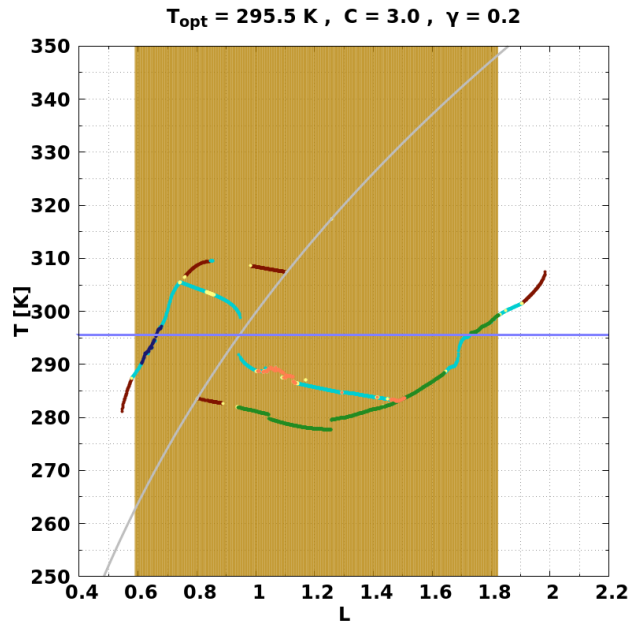
(c) DWC temperature T mean for $C = 3.0$ and $\gamma = 0.2$.

Legend:
- Stable node
- Semistable node
- Unstable node
- Null (0,0)
- FP not null
- Periodic
- Quasiperiodic
- Chaotic (a1,a2)
- Chaotic (a1,0)
- Chaotic (0,a2)
- Overpopulation
- Forbidden barrier

Figure A.30: **Orbits diagram** and the corresponding temperature T mean for **DWC** for $C = 3.0$ and $\gamma = 0.2$. **Blue** line corresponds to the value of $T_{opt} = 295.5$ K. Finally, those values of L where **Overpopulation** occurs, are marked by a vertical line with its corresponding color.
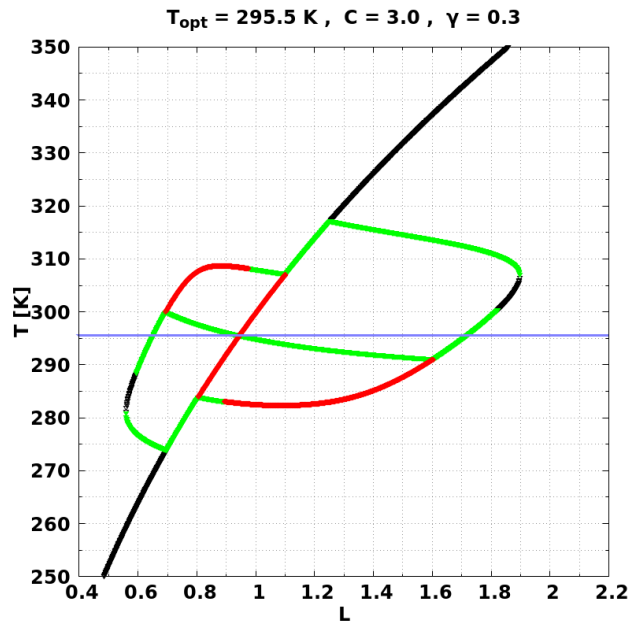
(a) DWC bifurcation for $C = 3.0$ and $\gamma = 0.3$.
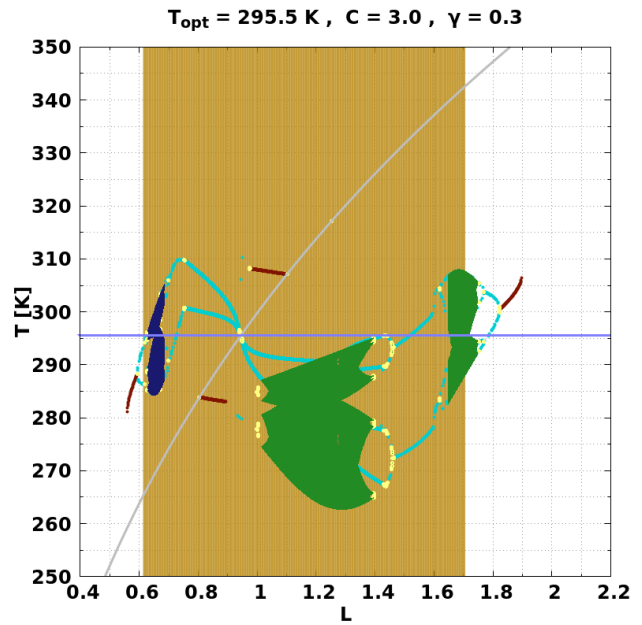
(b) DWC orbits diagram for $C = 3.0$ and $\gamma = 0.3$.
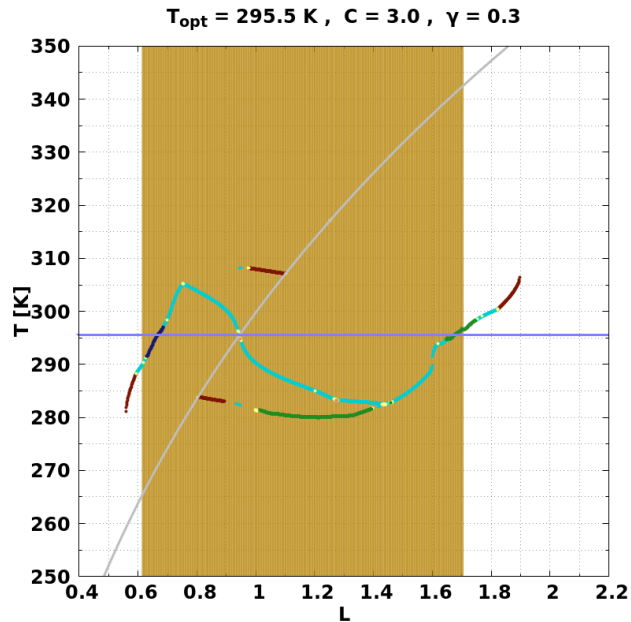
(c) DWC temperature T mean for $C = 3.0$ and $\gamma = 0.3$.

Figure A.31: **Orbits diagram** and the corresponding temperature T mean for **DWC** for $C = 3.0$ and $\gamma = 0.3$. **Blue** line corresponds to the value of $T_{opt} = 295.5$ K. Finally, those values of L where **Overpopulation** occurs, are marked by a vertical line with its corresponding color.

(a) DWC bifurcation for $C = 3.0$ and $\gamma = 0.4$.

(b) DWC orbits diagram for $C = 3.0$ and $\gamma = 0.4$.

(c) DWC temperature T mean for $C = 3.0$ and $\gamma = 0.4$.
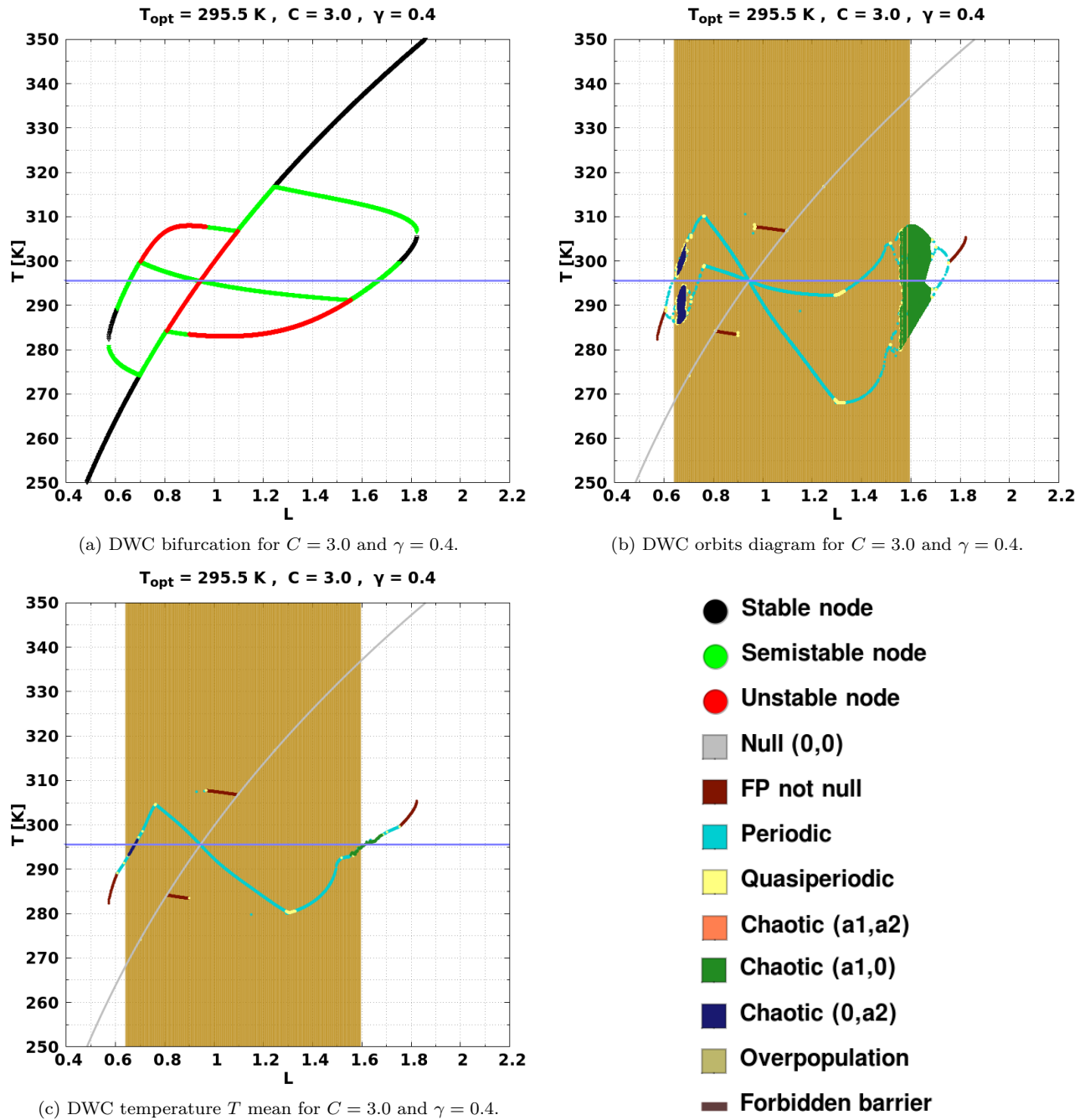
Figure A.32: **Orbits diagram** and the corresponding temperature T mean for **DWC** for $C = 3.0$ and $\gamma = 0.4$. **Blue** line corresponds to the value of $T_{opt} = 295.5$ K. Finally, those values of L where **Overpopulation** occurs, are marked by a vertical line with its corresponding color.
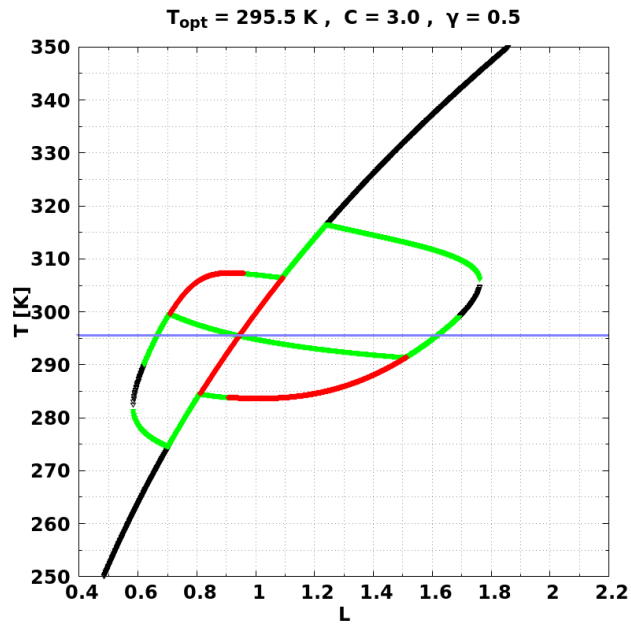
(a) DWC bifurcation for $C = 3.0$ and $\gamma = 0.5$.
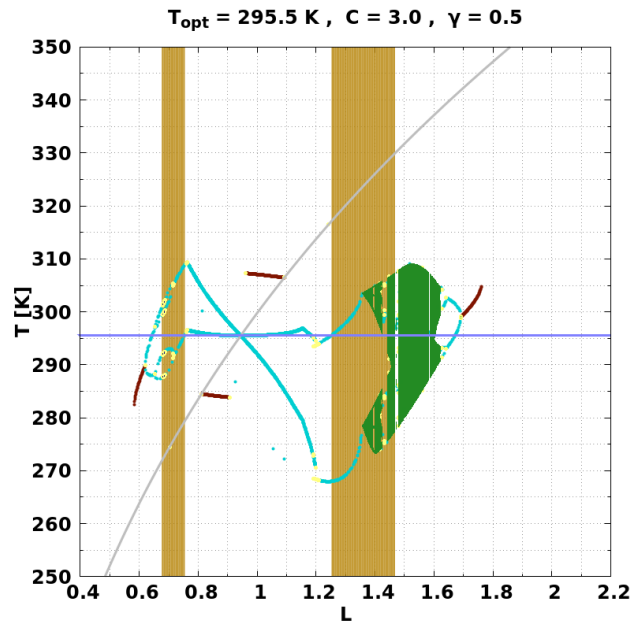
(b) DWC orbits diagram for $C = 3.0$ and $\gamma = 0.5$.
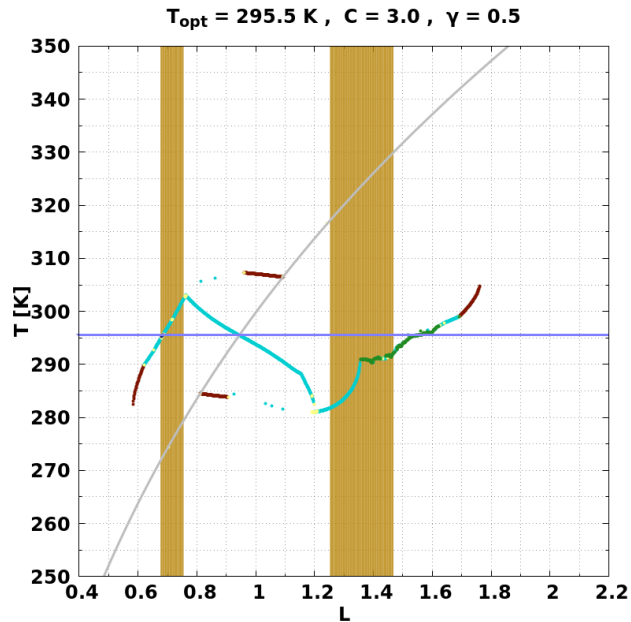
(c) DWC temperature T mean for $C = 3.0$ and $\gamma = 0.5$.

Figure A.33: **Orbits diagram** and the corresponding temperature T mean for **DWC** for $C = 3.0$ and $\gamma = 0.5$. **Blue** line corresponds to the value of $T_{opt} = 295.5$ K. Finally, those values of L where **Overpopulation** occurs, are marked by a vertical line with its corresponding color.
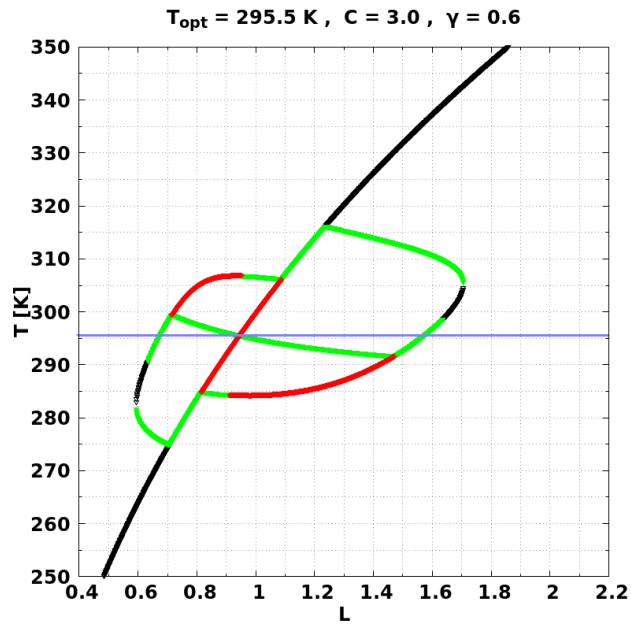
(a) DWC bifurcation for $C = 3.0$ and $\gamma = 0.6$.
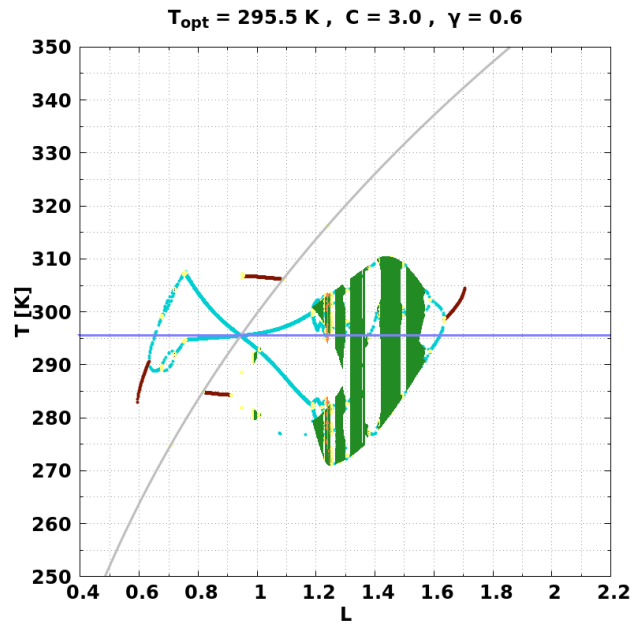
(b) DWC orbits diagram for $C = 3.0$ and $\gamma = 0.6$.
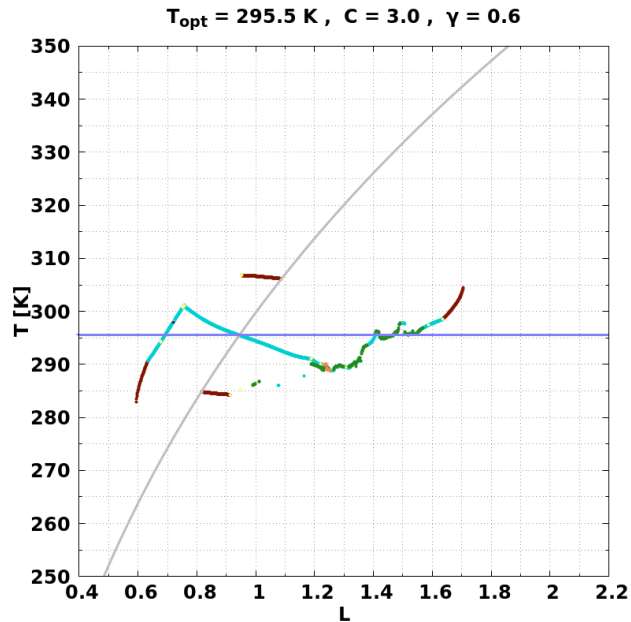
(c) DWC temperature T mean for $C = 3.0$ and $\gamma = 0.6$.

Figure A.34: **Orbits diagram** and the corresponding temperature T mean for **DWC** for $C = 3.0$ and $\gamma = 0.6$. **Blue** line corresponds to the value of $T_{opt} = 295.5$ K. Finally, those values of L where **Overpopulation** occurs, are marked by a vertical line with its corresponding color.
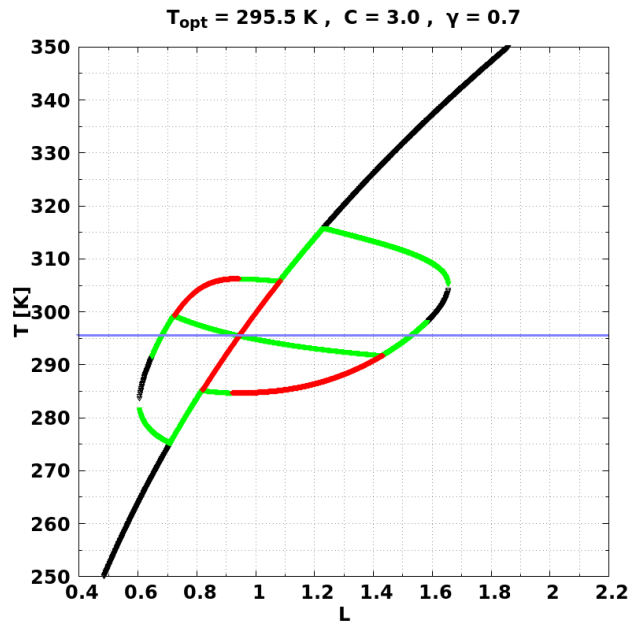
(a) DWC bifurcation for $C = 3.0$ and $\gamma = 0.7$.
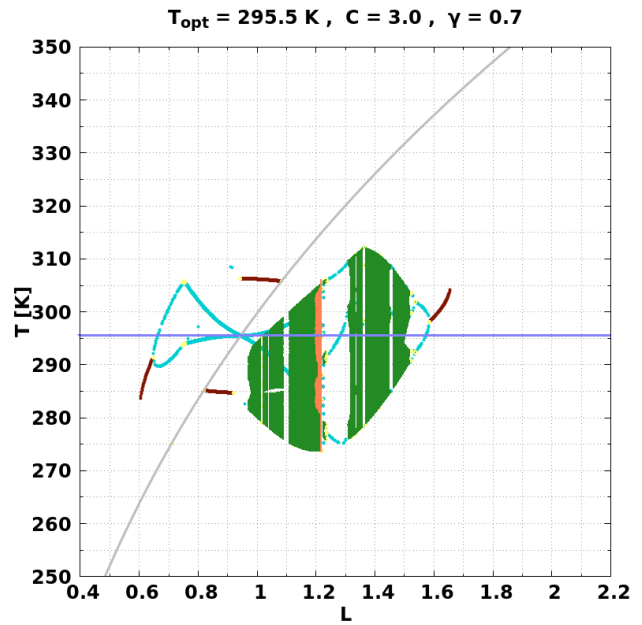
(b) DWC orbits diagram for $C = 3.0$ and $\gamma = 0.7$.
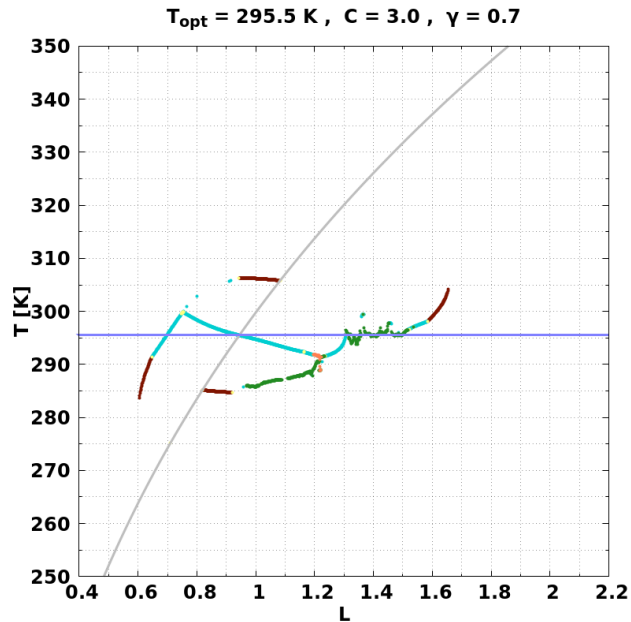
(c) DWC temperature T mean for $C = 3.0$ and $\gamma = 0.7$.

Figure A.35: **Orbits diagram** and the corresponding temperature T mean for **DWC** for $C = 3.0$ and $\gamma = 0.7$. **Blue** line corresponds to the value of $T_{opt} = 295.5$ K. Finally, those values of L where **Overpopulation** occurs, are marked by a vertical line with its corresponding color.
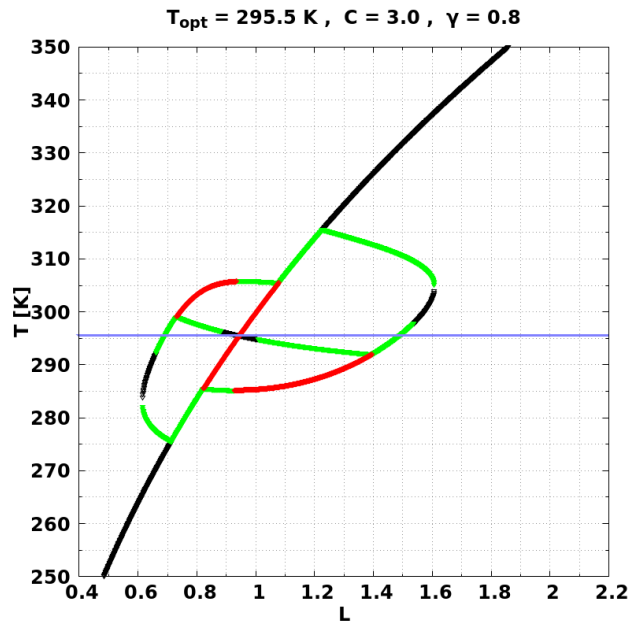
(a) DWC bifurcation for $C = 3.0$ and $\gamma = 0.8$.
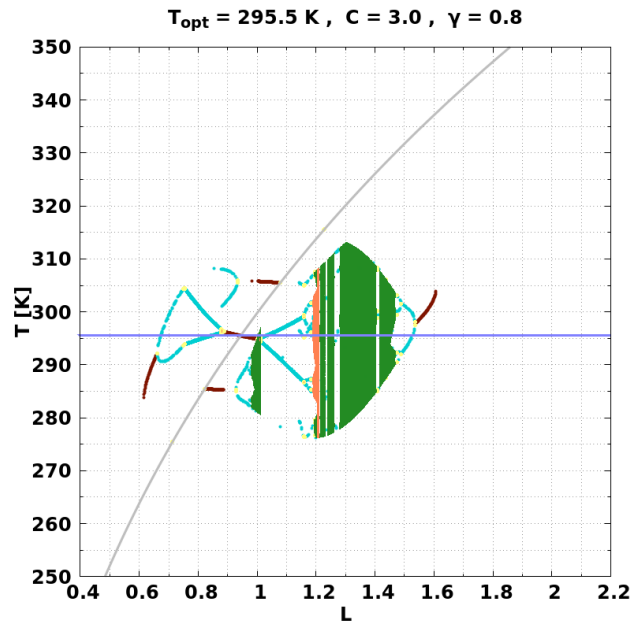
(b) DWC orbits diagram for $C = 3.0$ and $\gamma = 0.8$.
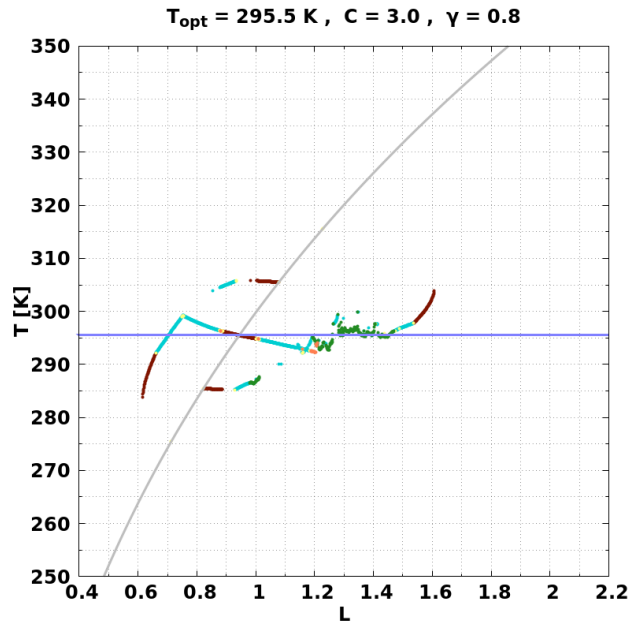
(c) DWC temperature T mean for $C = 3.0$ and $\gamma = 0.8$.

Figure A.36: **Orbits diagram** and the corresponding temperature T mean for **DWC** for $C = 3.0$ and $\gamma = 0.8$. **Blue** line corresponds to the value of $T_{opt} = 295.5$ K. Finally, those values of L where **Overpopulation** occurs, are marked by a vertical line with its corresponding color.
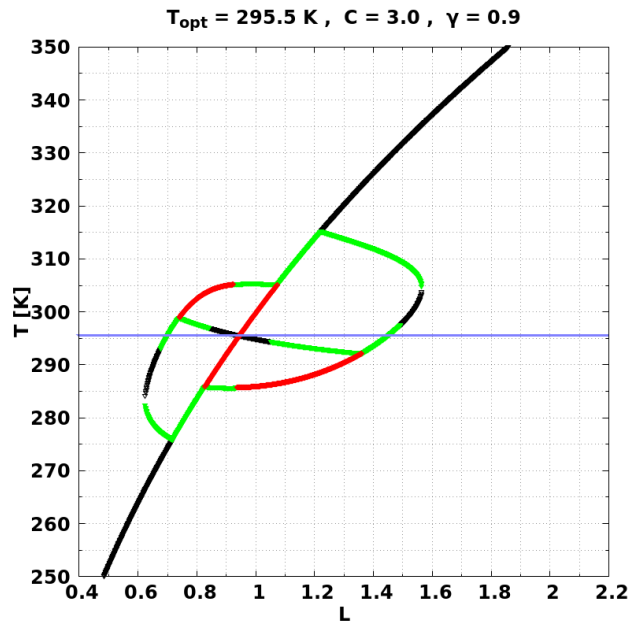
(a) DWC bifurcation for $C = 3.0$ and $\gamma = 0.9$.
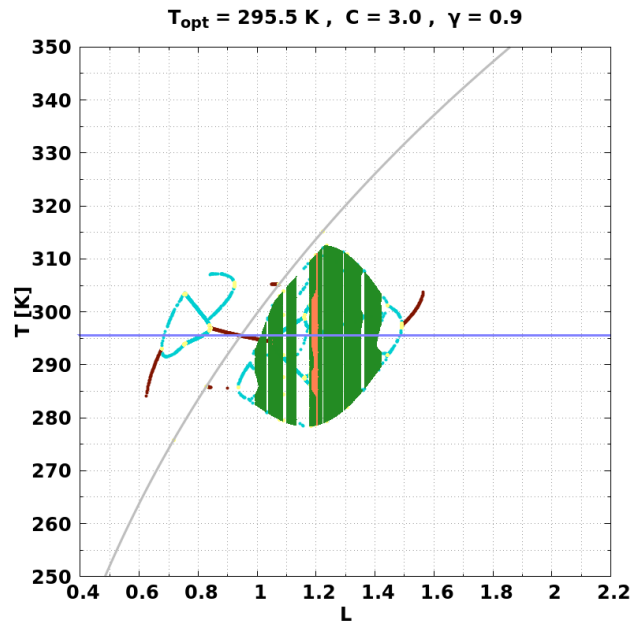
(b) DWC orbits diagram for $C = 3.0$ and $\gamma = 0.9$.
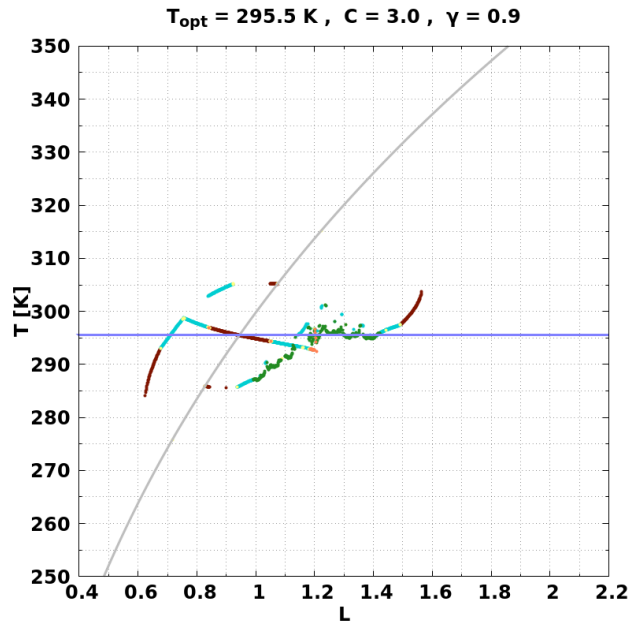
(c) DWC temperature T mean for $C = 3.0$ and $\gamma = 0.9$.

Figure A.37: **Orbits diagram** and the corresponding temperature T mean for **DWC** for $C = 3.0$ and $\gamma = 0.9$. **Blue** line corresponds to the value of $T_{opt} = 295.5$ K. Finally, those values of L where **Overpopulation** occurs, are marked by a vertical line with its corresponding color.
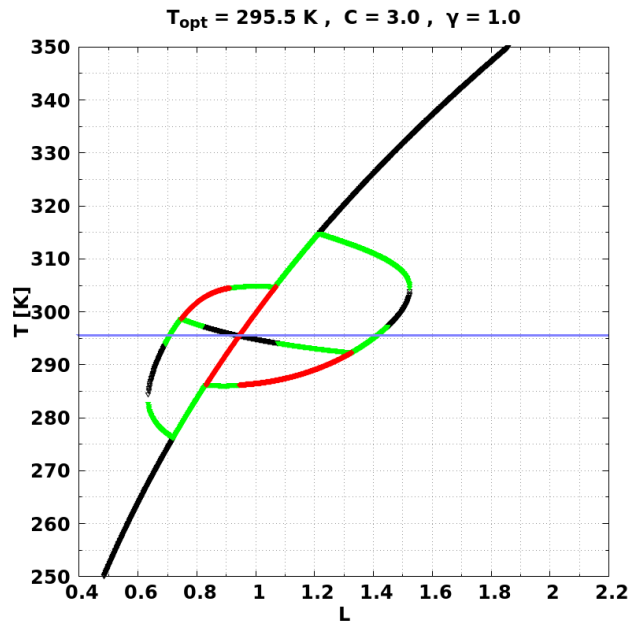
(a) DWC bifurcation for $C = 3.0$ and $\gamma = 1.0$.
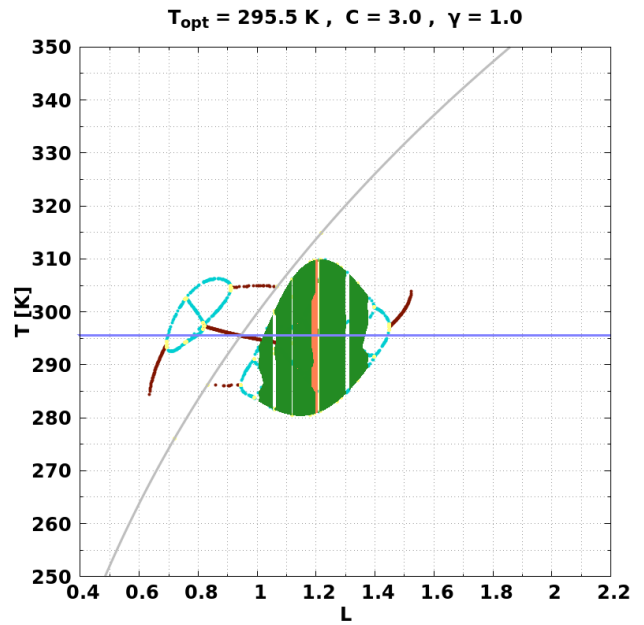
(b) DWC orbits diagram for $C = 3.0$ and $\gamma = 1.0$.
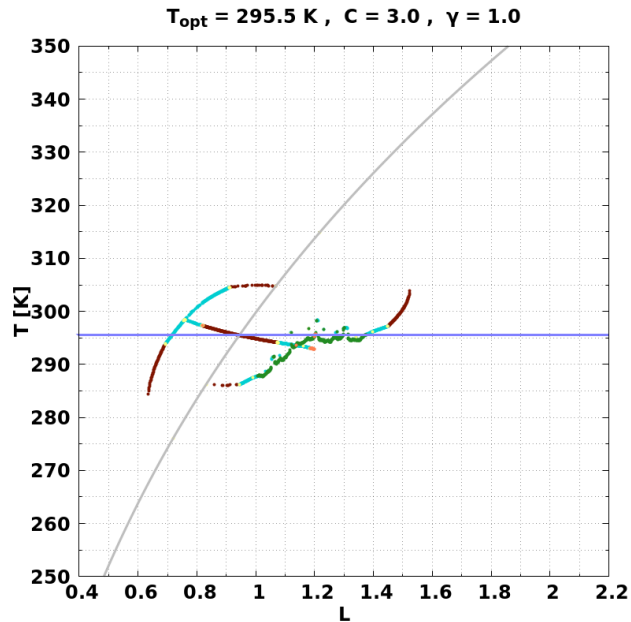
(c) DWC temperature T mean for $C = 3.0$ and $\gamma = 1.0$.

Figure A.38: **Orbits diagram** and the corresponding temperature T mean for **DWC** for $C = 3.0$ and $\gamma = 1.0$. **Blue** line corresponds to the value of $T_{opt} = 295.5$ K. Finally, those values of L where **Overpopulation** occurs, are marked by a vertical line with its corresponding color.
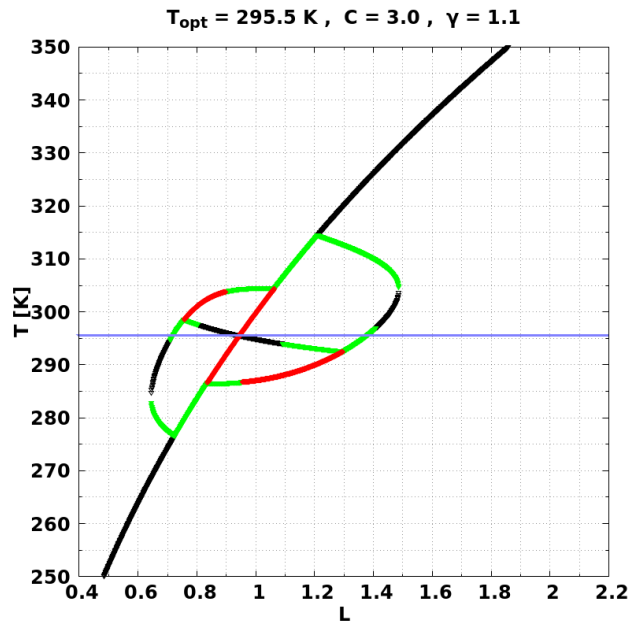
(a) DWC bifurcation for $C = 3.0$ and $\gamma = 1.1$.
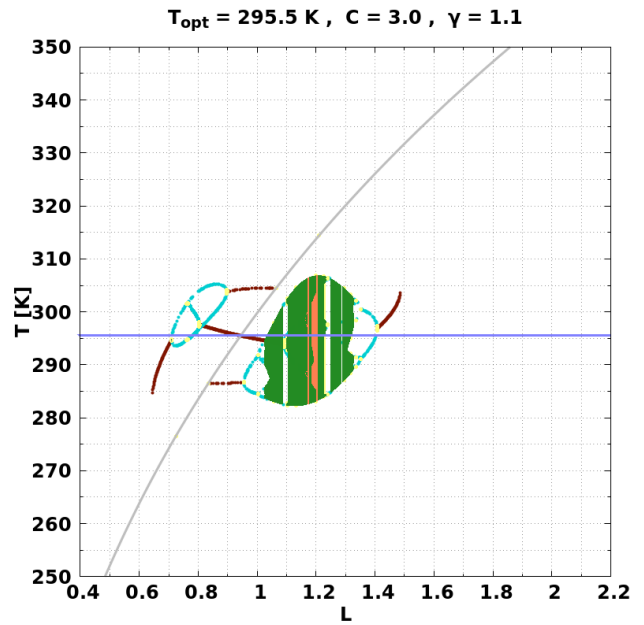
(b) DWC orbits diagram for $C = 3.0$ and $\gamma = 1.1$.
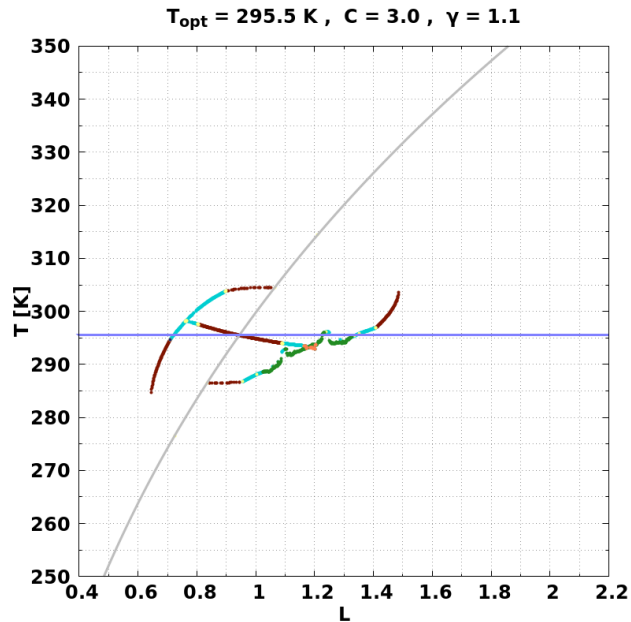
(c) DWC temperature T mean for $C = 3.0$ and $\gamma = 1.1$.

Figure A.39: **Orbits diagram** and the corresponding temperature T mean for **DWC** for $C = 3.0$ and $\gamma = 1.1$. **Blue** line corresponds to the value of $T_{opt} = 295.5$ K. Finally, those values of L where **Overpopulation** occurs, are marked by a vertical line with its corresponding color.
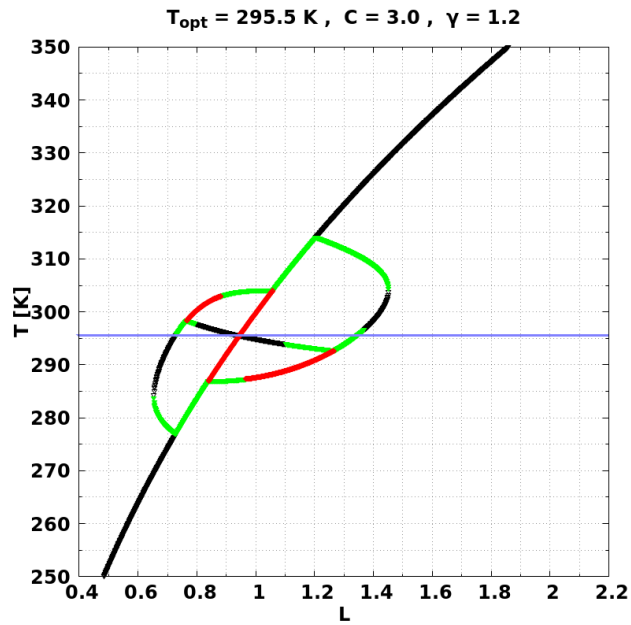
(a) DWC bifurcation for $C = 3.0$ and $\gamma = 1.2$.
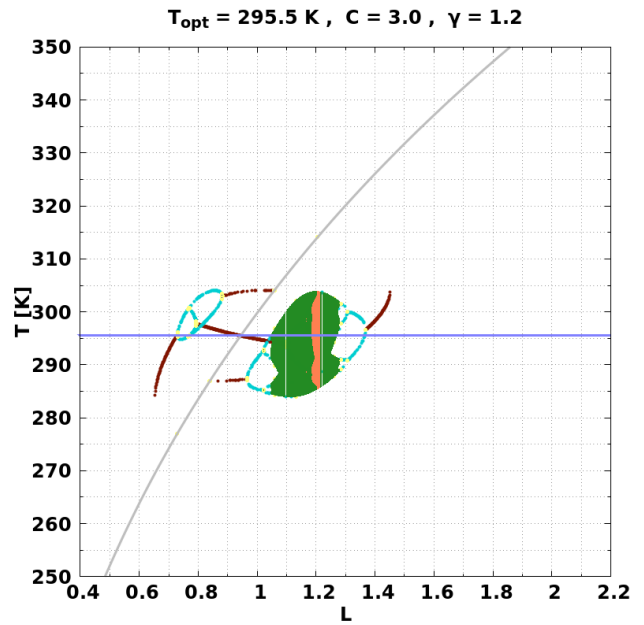
(b) DWC orbits diagram for $C = 3.0$ and $\gamma = 1.2$.
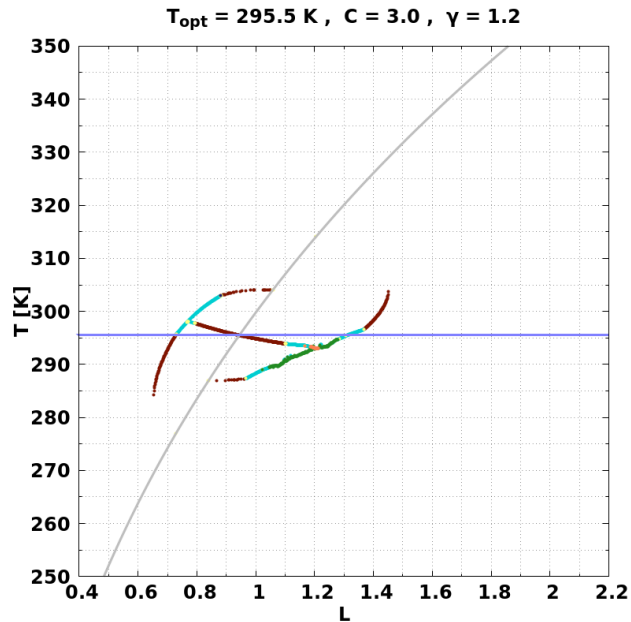
(c) DWC temperature T mean for $C = 3.0$ and $\gamma = 1.2$.

- ● Stable node
- ● Semistable node
- ● Unstable node
- ▨ Null (0,0)
- ▨ FP not null
- ▨ Periodic
- ▨ Quasiperiodic
- ▨ Chaotic (a1,a2)
- ▨ Chaotic (a1,0)
- ▨ Chaotic (0,a2)
- ▨ Overpopulation
- ▬ Forbidden barrier

Figure A.40: **Orbits diagram** and the corresponding temperature T mean for **DWC** for $C = 3.0$ and $\gamma = 1.2$. **Blue** line corresponds to the value of $T_{opt} = 295.5$ K. Finally, those values of L where **Overpopulation** occurs, are marked by a vertical line with its corresponding color.
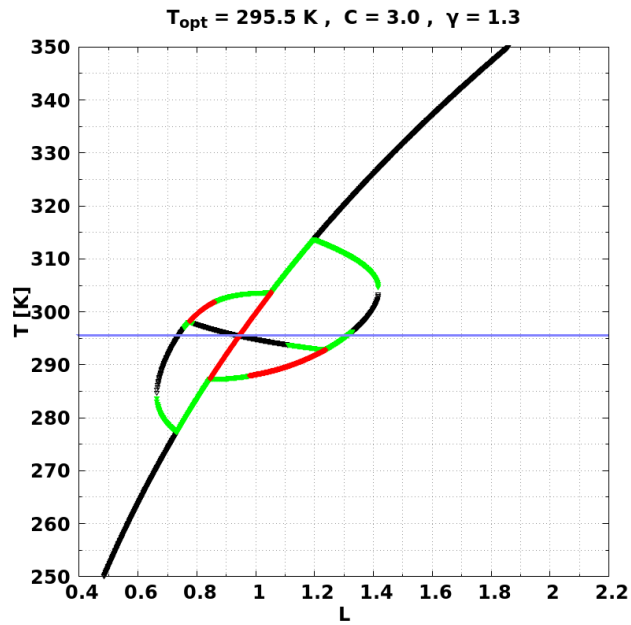
(a) DWC bifurcation for $C = 3.0$ and $\gamma = 1.3$.
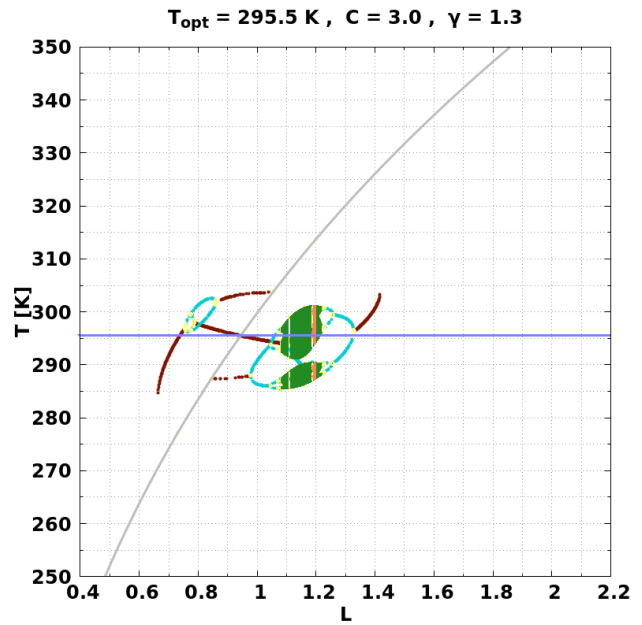
(b) DWC orbits diagram for $C = 3.0$ and $\gamma = 1.3$.
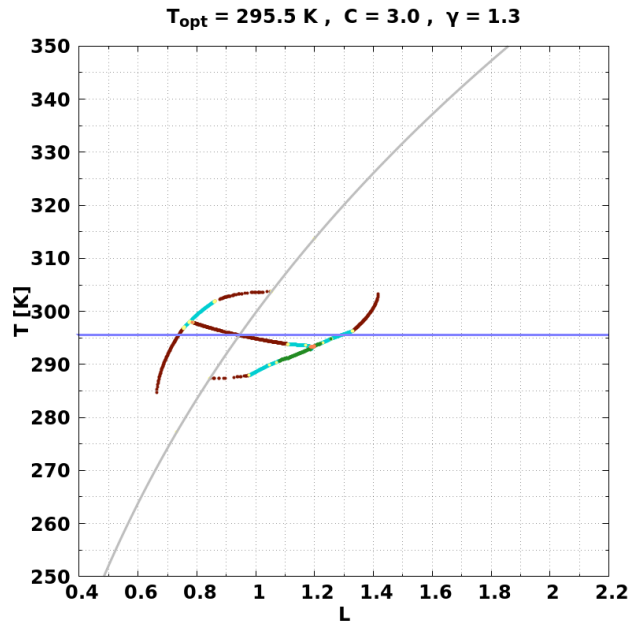
(c) DWC temperature T mean for $C = 3.0$ and $\gamma = 1.3$.

Figure A.41: **Orbits diagram** and the corresponding temperature T mean for **DWC** for $C = 3.0$ and $\gamma = 1.3$. **Blue** line corresponds to the value of $T_{opt} = 295.5$ K. Finally, those values of L where **Overpopulation** occurs, are marked by a vertical line with its corresponding color.
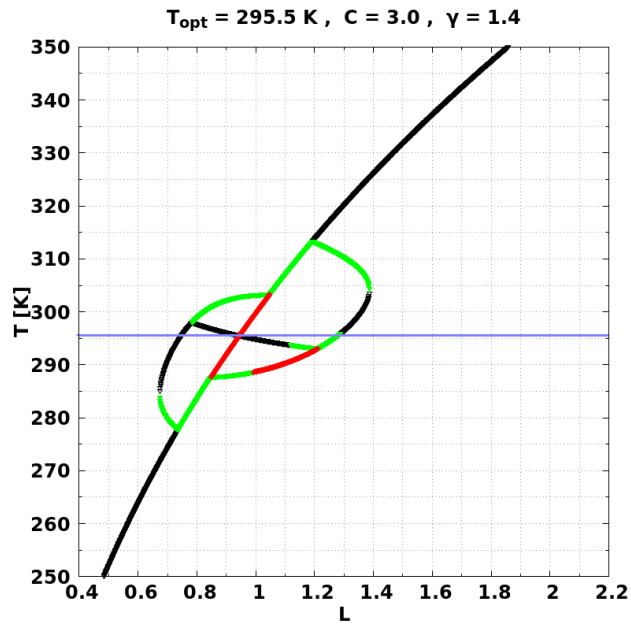
(a) DWC bifurcation for $C = 3.0$ and $\gamma = 1.4$.
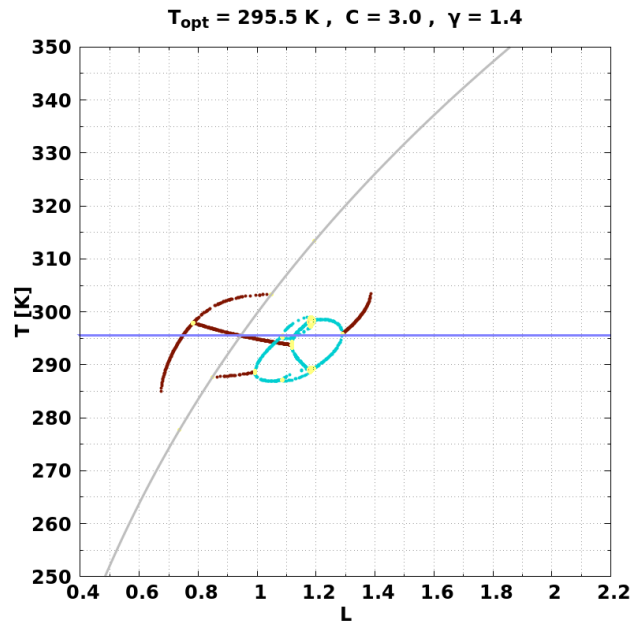
(b) DWC orbits diagram for $C = 3.0$ and $\gamma = 1.4$.
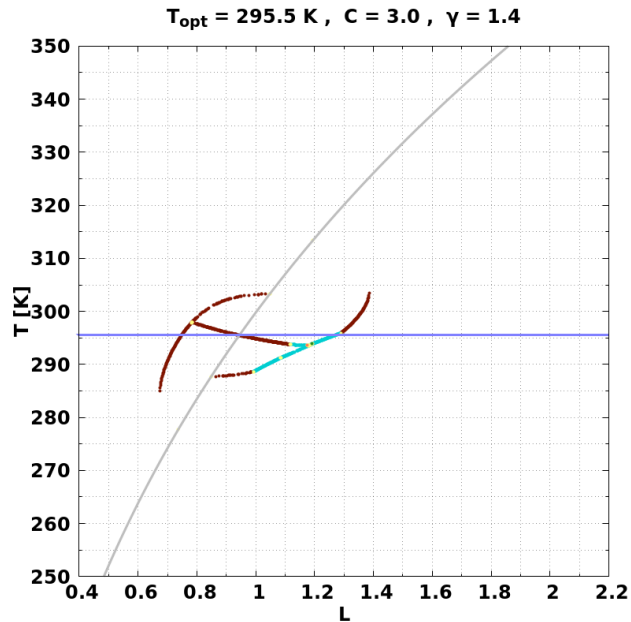
(c) DWC temperature T mean for $C = 3.0$ and $\gamma = 1.4$.

Figure A.42: **Orbits diagram** and the corresponding temperature T mean for **DWC** for $C = 3.0$ and $\gamma = 1.4$. **Blue** line corresponds to the value of $T_{opt} = 295.5$ K. Finally, those values of L where **Overpopulation** occurs, are marked by a vertical line with its corresponding color.
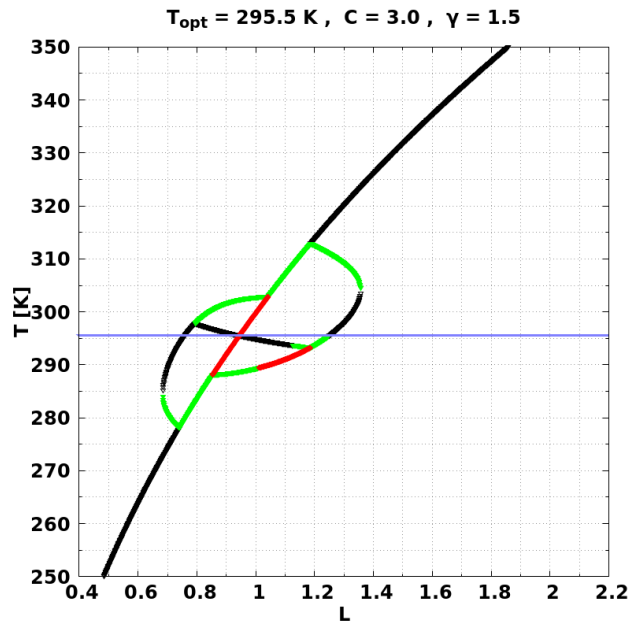
(a) DWC bifurcation for $C = 3.0$ and $\gamma = 1.5$.
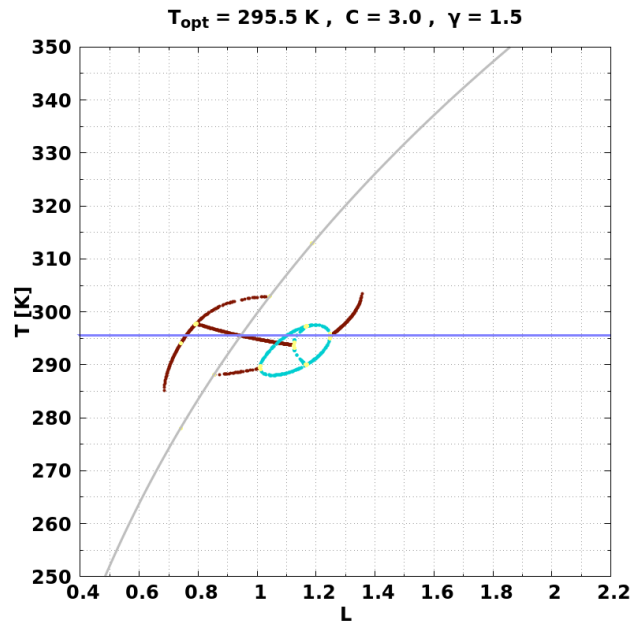
(b) DWC orbits diagram for $C = 3.0$ and $\gamma = 1.5$.
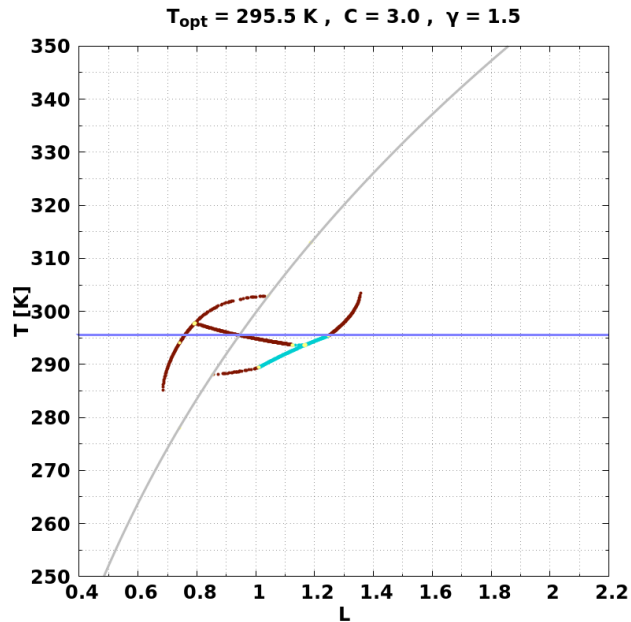
(c) DWC temperature T mean for $C = 3.0$ and $\gamma = 1.5$.

Figure A.43: **Orbits diagram** and the corresponding temperature T mean for **DWC** for $C = 3.0$ and $\gamma = 1.5$. **Blue** line corresponds to the value of $T_{opt} = 295.5$ K. Finally, those values of L where **Overpopulation** occurs, are marked by a vertical line with its corresponding color.
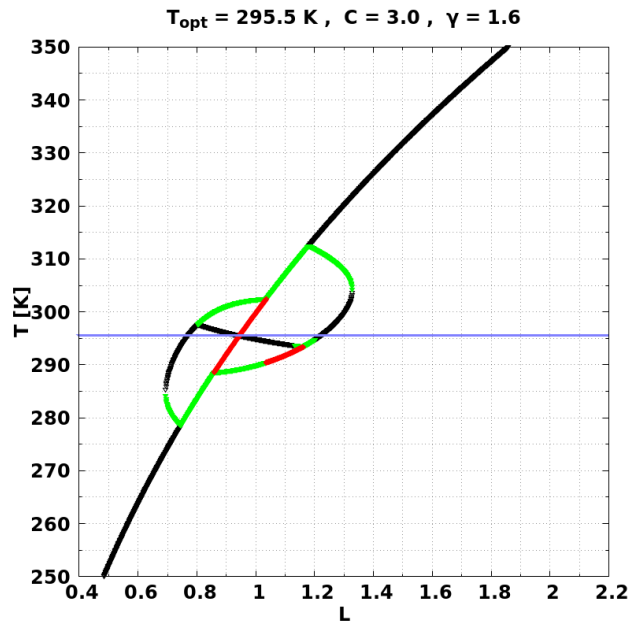
(a) DWC bifurcation for $C = 3.0$ and $\gamma = 1.6$.
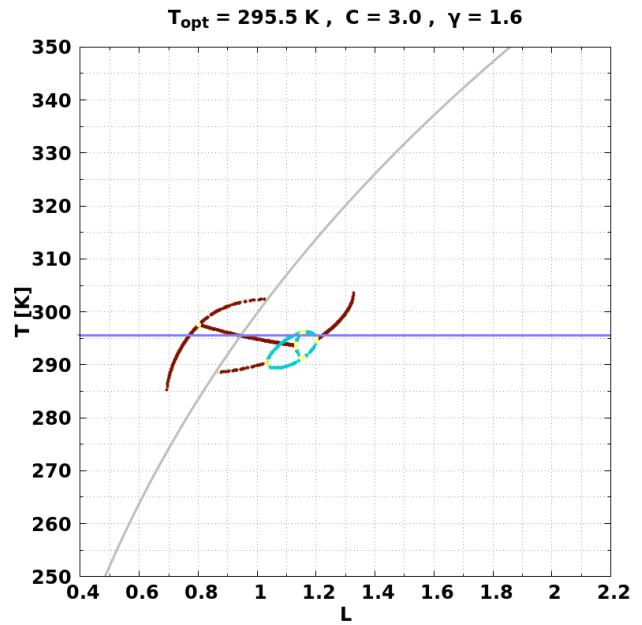
(b) DWC orbits diagram for $C = 3.0$ and $\gamma = 1.6$.
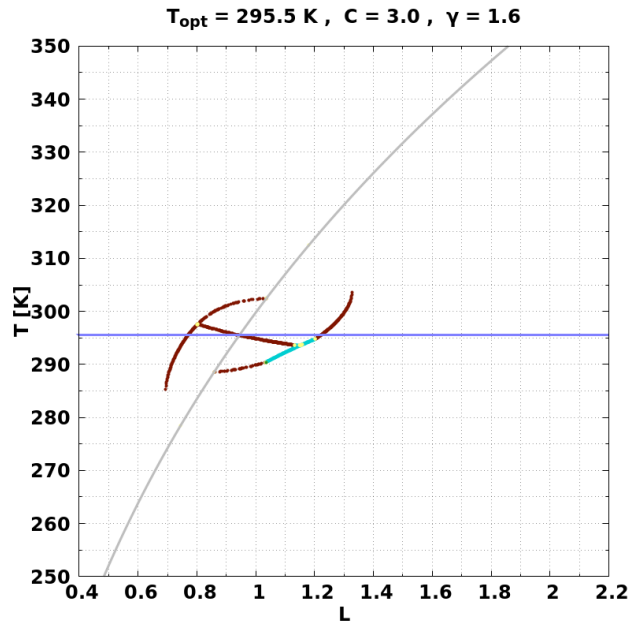
(c) DWC temperature T mean for $C = 3.0$ and $\gamma = 1.6$.

- ● Stable node
- ● Semistable node
- ● Unstable node
- Null (0,0)
- FP not null
- Periodic
- Quasiperiodic
- Chaotic (a1,a2)
- Chaotic (a1,0)
- Chaotic (0,a2)
- Overpopulation
- Forbidden barrier

Figure A.44: **Orbits diagram** and the corresponding temperature T mean for **DWC** for $C = 3.0$ and $\gamma = 1.6$. **Blue** line corresponds to the value of $T_{opt} = 295.5$ K. Finally, those values of L where **Overpopulation** occurs, are marked by a vertical line with its corresponding color.
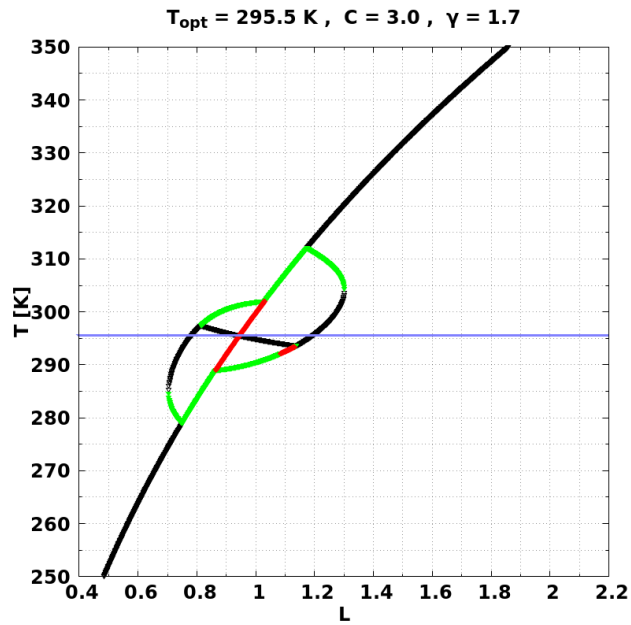
(a) DWC bifurcation for $C = 3.0$ and $\gamma = 1.7$.
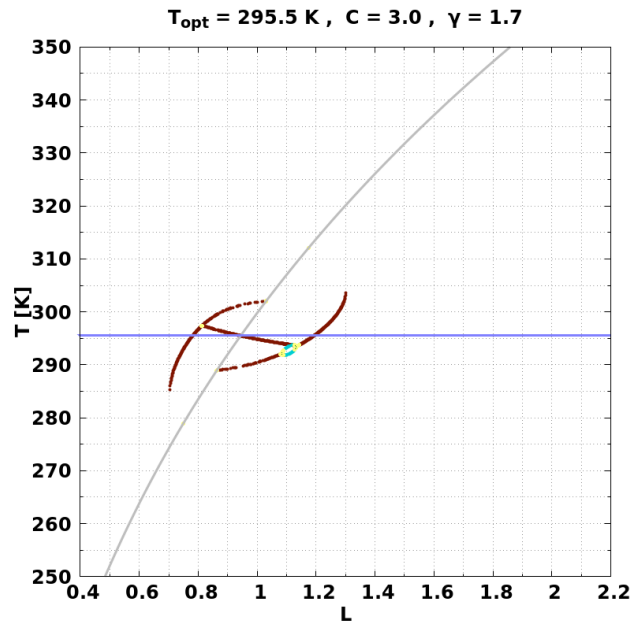
(b) DWC orbits diagram for $C = 3.0$ and $\gamma = 1.7$.
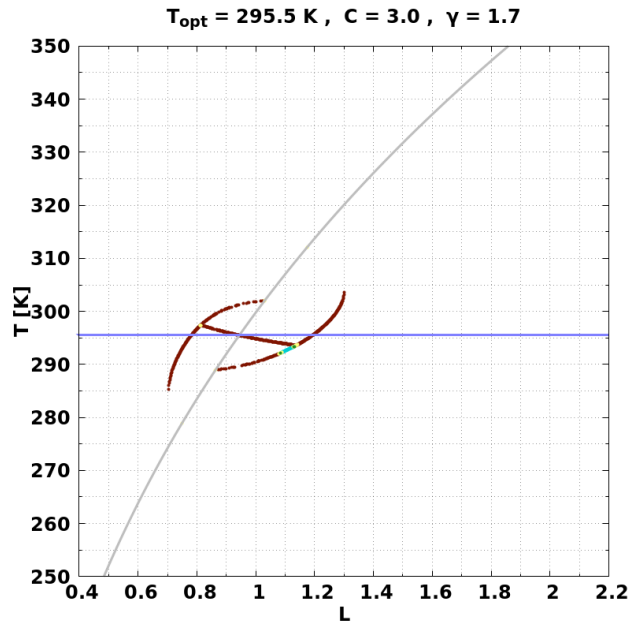
(c) DWC temperature T mean for $C = 3.0$ and $\gamma = 1.7$.

Figure A.45: **Orbits diagram** and the corresponding temperature T mean for **DWC** for $C = 3.0$ and $\gamma = 1.7$. **Blue** line corresponds to the value of $T_{opt} = 295.5$ K. Finally, those values of L where **Overpopulation** occurs, are marked by a vertical line with its corresponding color.
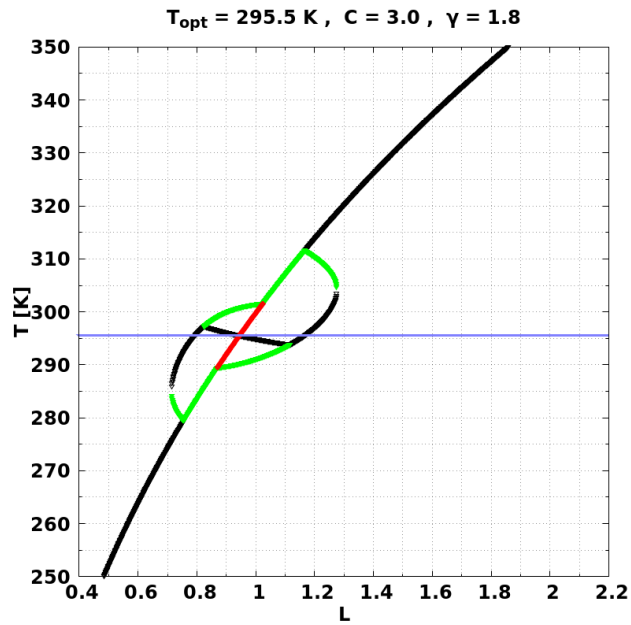
(a) DWC bifurcation for $C = 3.0$ and $\gamma = 1.8$.
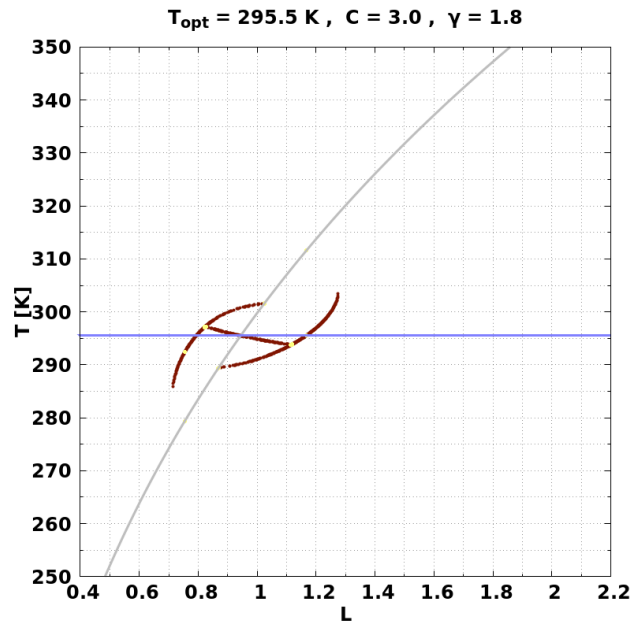
(b) DWC orbits diagram for $C = 3.0$ and $\gamma = 1.8$.
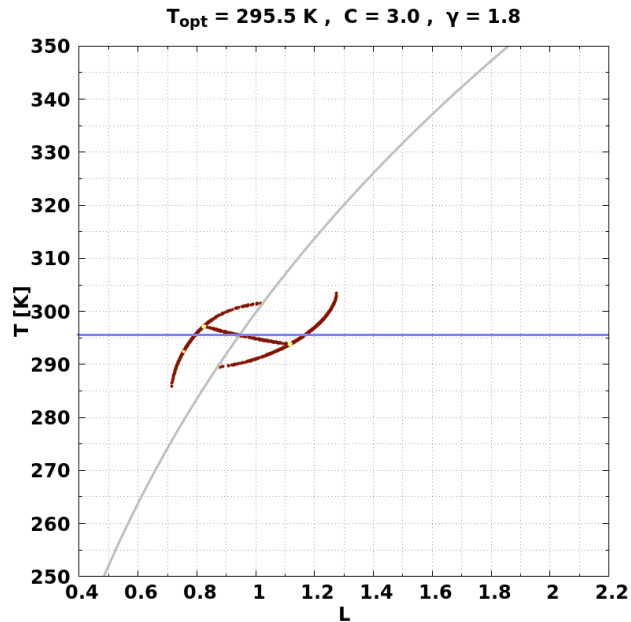
(c) DWC temperature T mean for $C = 3.0$ and $\gamma = 1.8$.

Figure A.46: **Orbits diagram** and the corresponding temperature T mean for **DWC** for $C = 3.0$ and $\gamma = 1.8$. **Blue** line corresponds to the value of $T_{opt} = 295.5$ K. Finally, those values of L where **Overpopulation** occurs, are marked by a vertical line with its corresponding color.
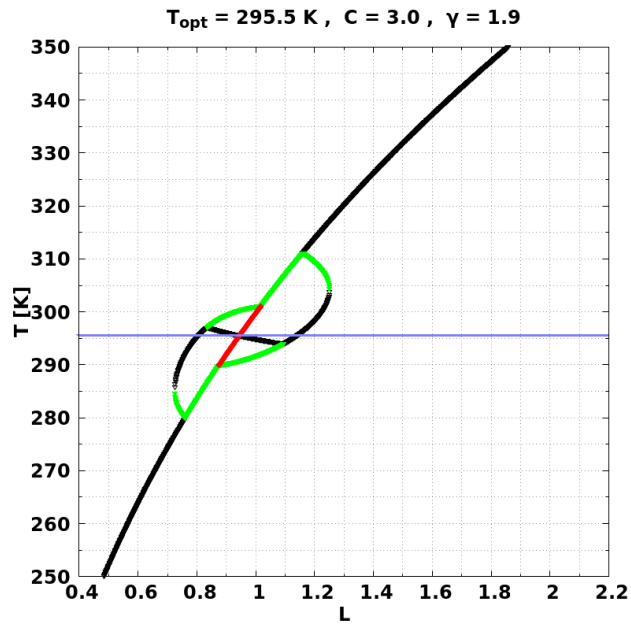
(a) DWC bifurcation for $C = 3.0$ and $\gamma = 1.9$.
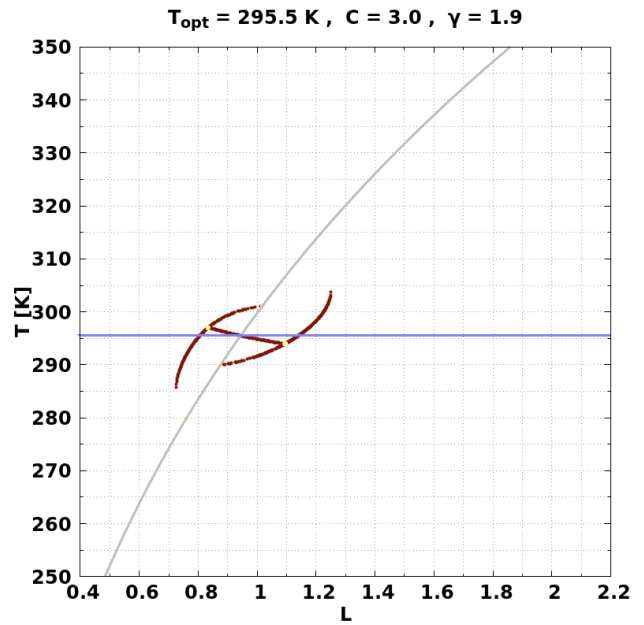
(b) DWC orbits diagram for $C = 3.0$ and $\gamma = 1.9$.
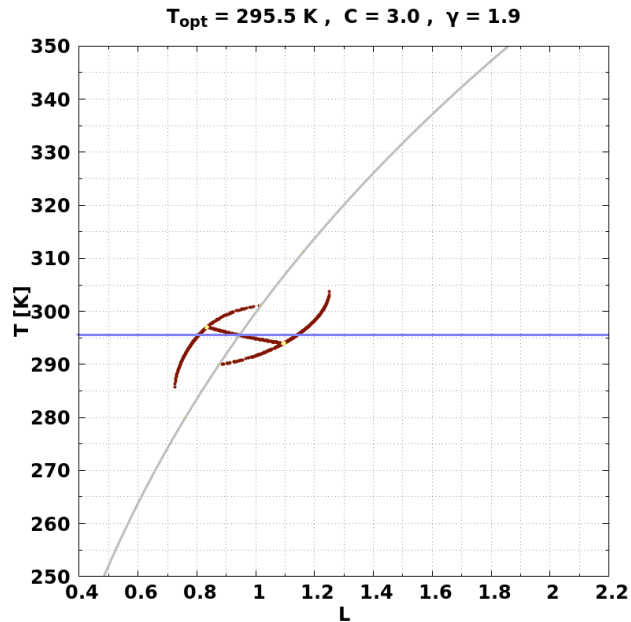
(c) DWC temperature T mean for $C = 3.0$ and $\gamma = 1.9$.

Figure A.47: **Orbits diagram** and the corresponding temperature T mean for **DWC** for $C = 3.0$ and $\gamma = 1.9$. **Blue** line corresponds to the value of $T_{opt} = 295.5$ K. Finally, those values of L where **Overpopulation** occurs, are marked by a vertical line with its corresponding color.
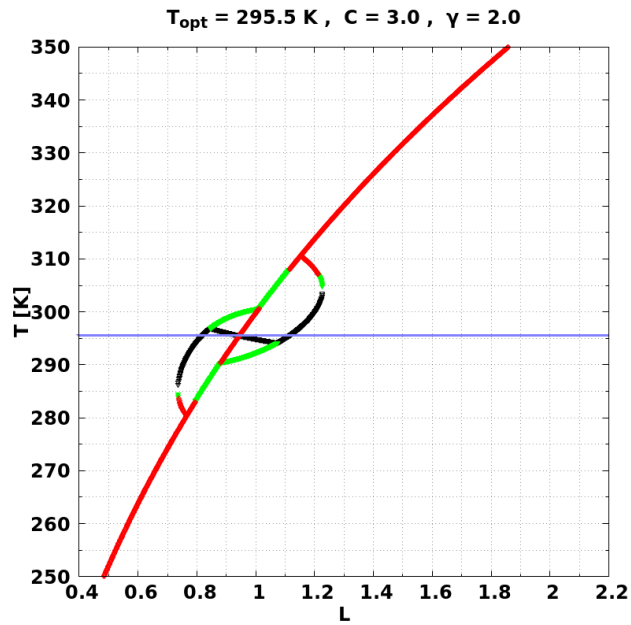
(a) DWC bifurcation for $C = 3.0$ and $\gamma = 2.0$.
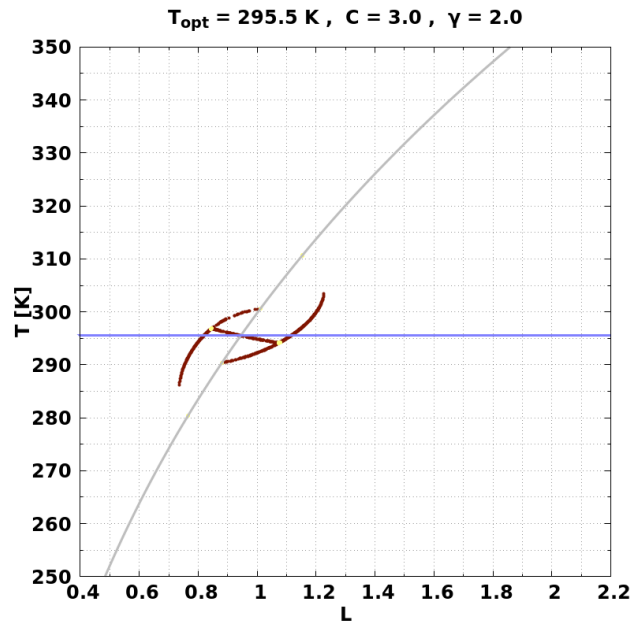
(b) DWC orbits diagram for $C = 3.0$ and $\gamma = 2.0$.
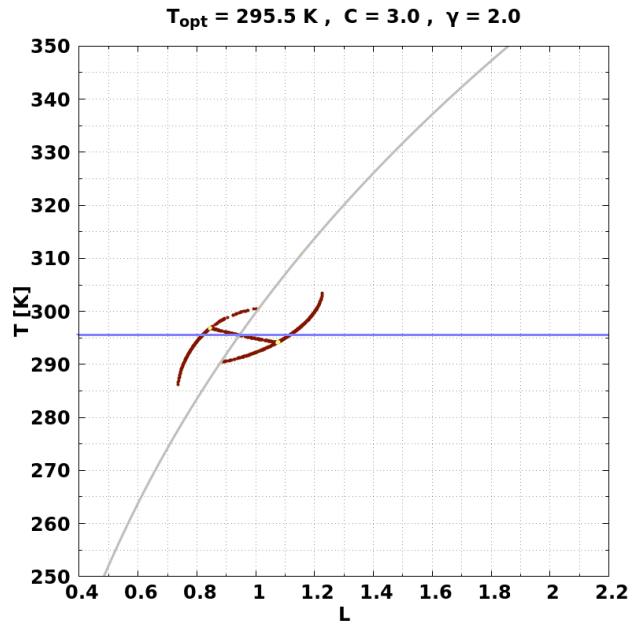
(c) DWC temperature T mean for $C = 3.0$ and $\gamma = 2.0$.

Figure A.48: **Orbits diagram** and the corresponding temperature T mean for **DWC** for $C = 3.0$ and $\gamma = 2.0$. **Blue** line corresponds to the value of $T_{opt} = 295.5$ K. Finally, those values of L where **Overpopulation** occurs, are marked by a vertical line with its corresponding color.
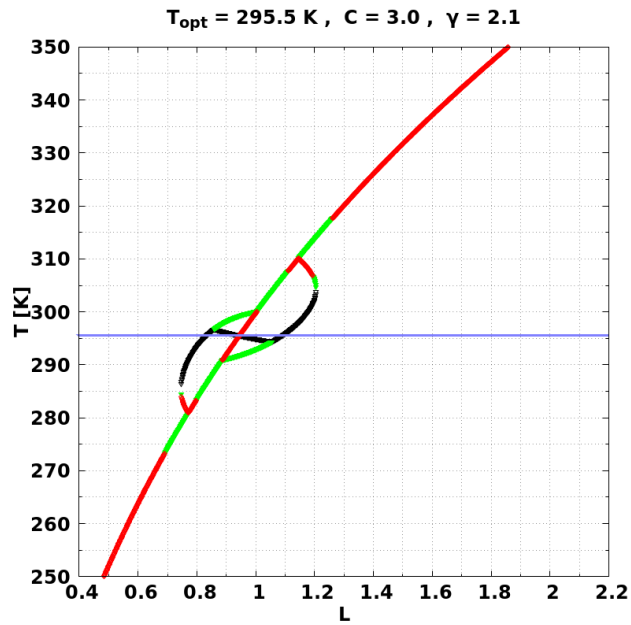
(a) DWC bifurcation for $C = 3.0$ and $\gamma = 2.1$.
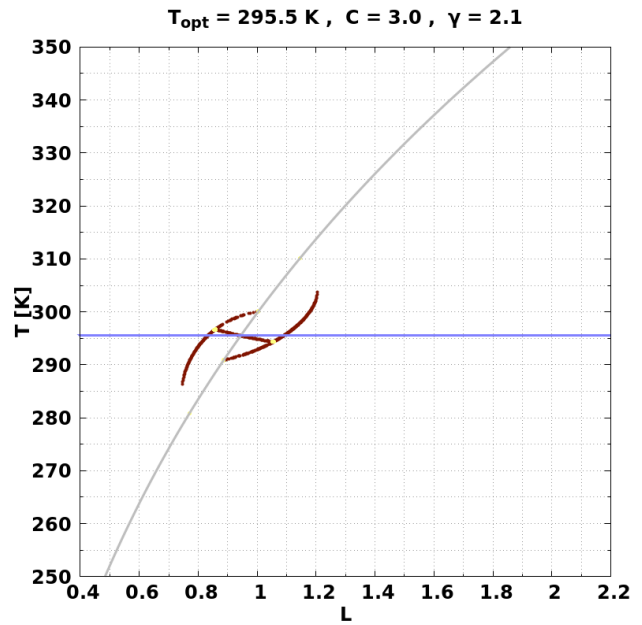
(b) DWC orbits diagram for $C = 3.0$ and $\gamma = 2.1$.
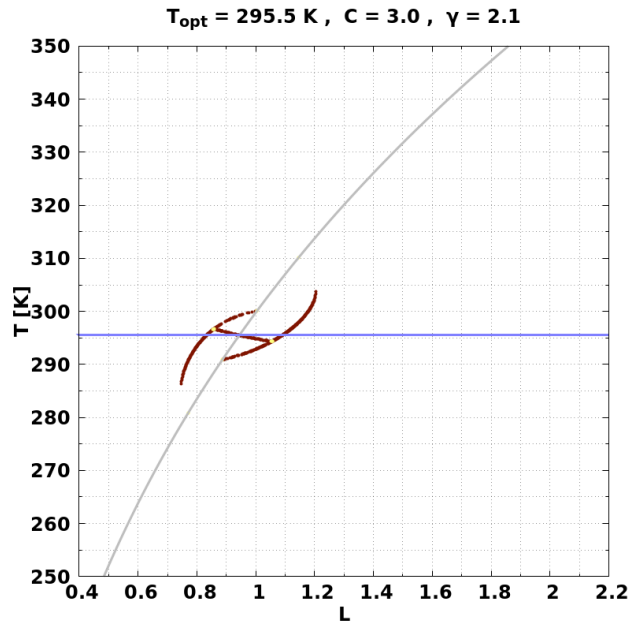
(c) DWC temperature T mean for $C = 3.0$ and $\gamma = 2.1$.

Figure A.49: **Orbits diagram** and the corresponding temperature T mean for **DWC** for $C = 3.0$ and $\gamma = 2.1$. **Blue** line corresponds to the value of $T_{opt} = 295.5$ K. Finally, those values of L where **Overpopulation** occurs, are marked by a vertical line with its corresponding color.
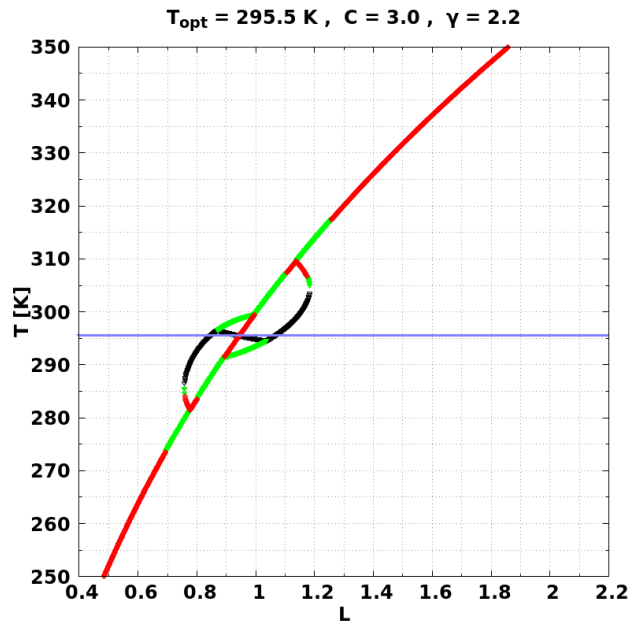
(a) DWC bifurcation for $C = 3.0$ and $\gamma = 2.2$.
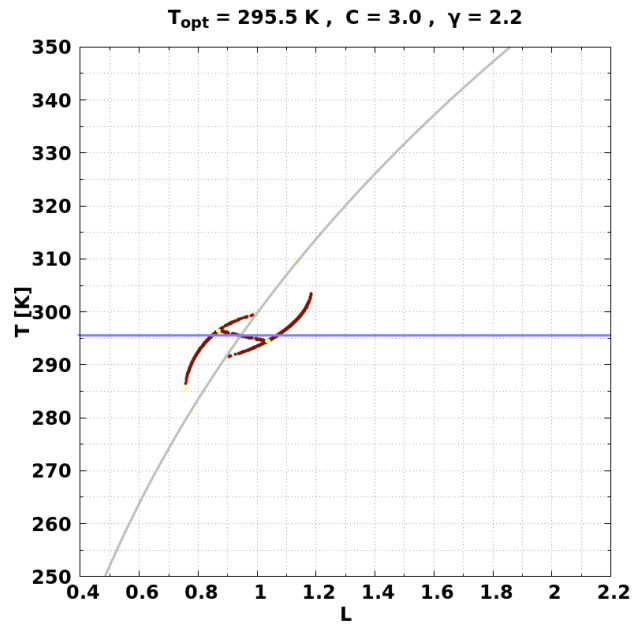
(b) DWC orbits diagram for $C = 3.0$ and $\gamma = 2.2$.
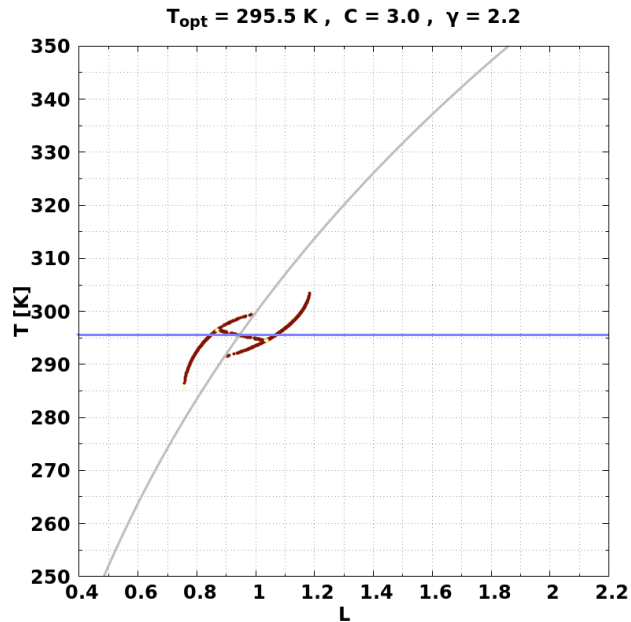
(c) DWC temperature T mean for $C = 3.0$ and $\gamma = 2.2$.

Legend:
- ● Stable node
- ● Semistable node
- ● Unstable node
- ▪ Null (0,0)
- ▪ FP not null
- ▪ Periodic
- ▪ Quasiperiodic
- ▪ Chaotic (a1,a2)
- ▪ Chaotic (a1,0)
- ▪ Chaotic (0,a2)
- ▪ Overpopulation
- ▬ Forbidden barrier

Figure A.50: **Orbits diagram** and the corresponding temperature T mean for **DWC** for $C = 3.0$ and $\gamma = 2.2$. **Blue** line corresponds to the value of $T_{opt} = 295.5$ K. Finally, those values of L where **Overpopulation** occurs, are marked by a vertical line with its corresponding color.
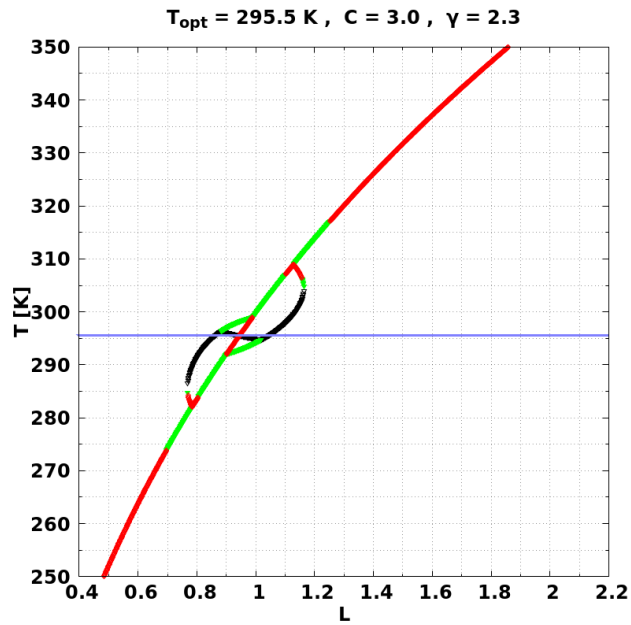
(a) DWC bifurcation for $C = 3.0$ and $\gamma = 2.3$.
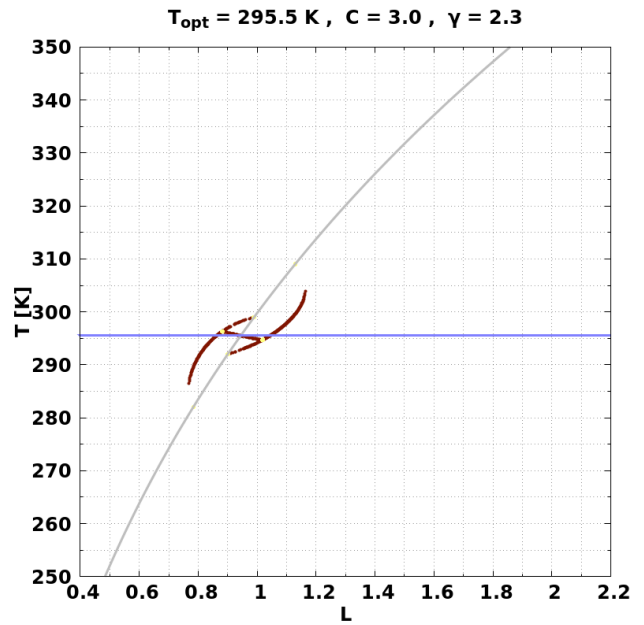
(b) DWC orbits diagram for $C = 3.0$ and $\gamma = 2.3$.
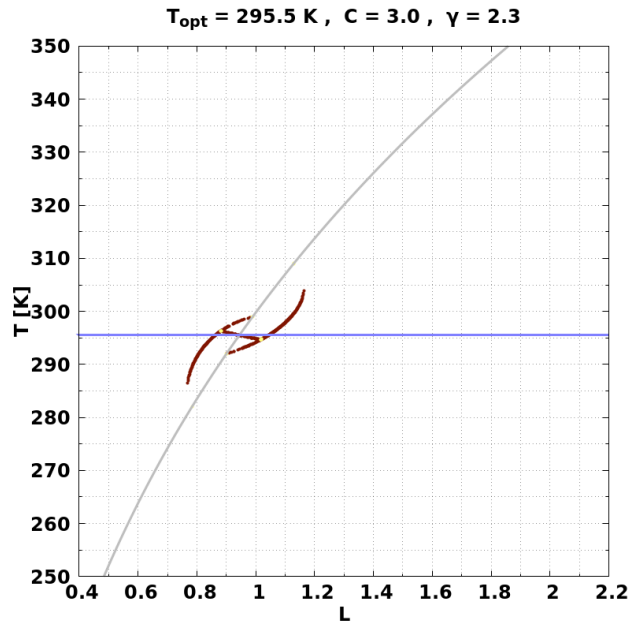
(c) DWC temperature T mean for $C = 3.0$ and $\gamma = 2.3$.

Figure A.51: **Orbits diagram** and the corresponding temperature T mean for **DWC** for $C = 3.0$ and $\gamma = 2.3$. **Blue** line corresponds to the value of $T_{opt} = 295.5$ K. Finally, those values of L where **Overpopulation** occurs, are marked by a vertical line with its corresponding color.
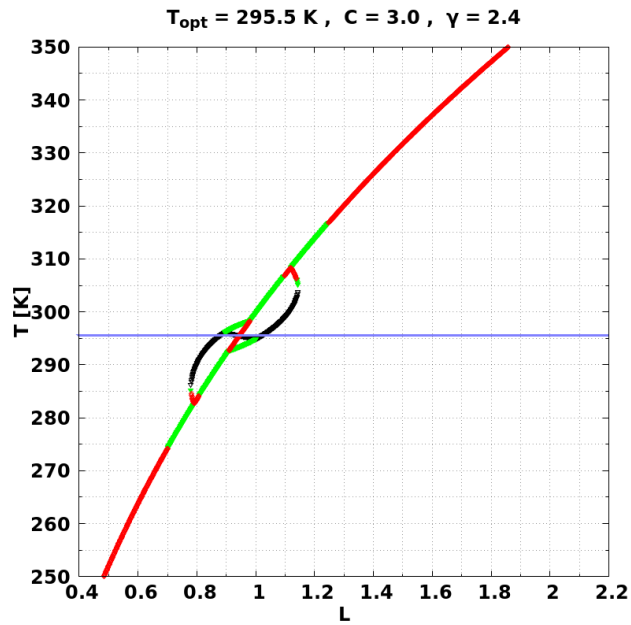
(a) DWC bifurcation for $C = 3.0$ and $\gamma = 2.4$.
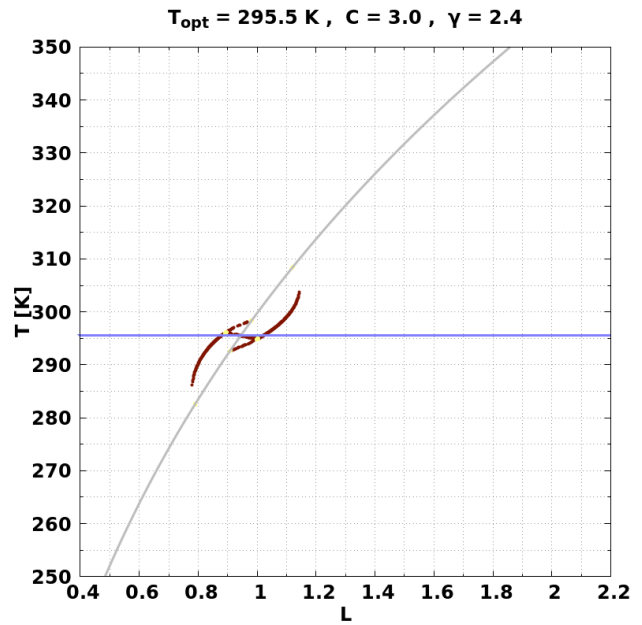
(b) DWC orbits diagram for $C = 3.0$ and $\gamma = 2.4$.
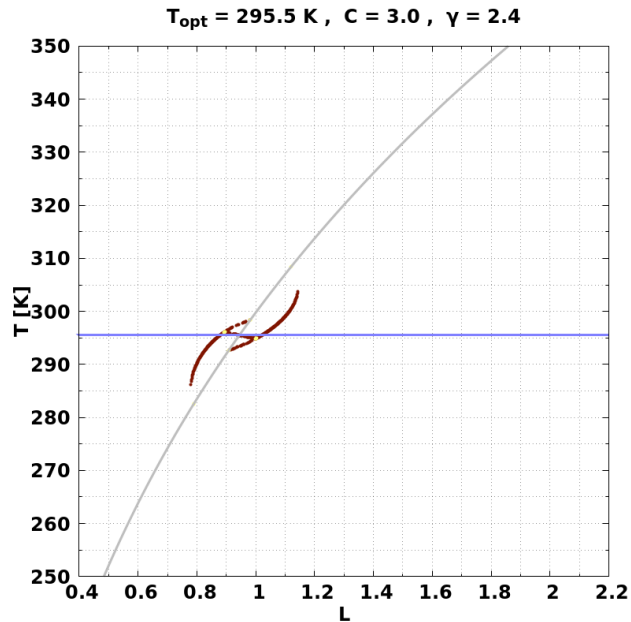
(c) DWC temperature T mean for $C = 3.0$ and $\gamma = 2.4$.

Figure A.52: **Orbits diagram** and the corresponding temperature T mean for **DWC** for $C = 3.0$ and $\gamma = 2.4$. **Blue** line corresponds to the value of $T_{opt} = 295.5$ K. Finally, those values of L where **Overpopulation** occurs, are marked by a vertical line with its corresponding color.
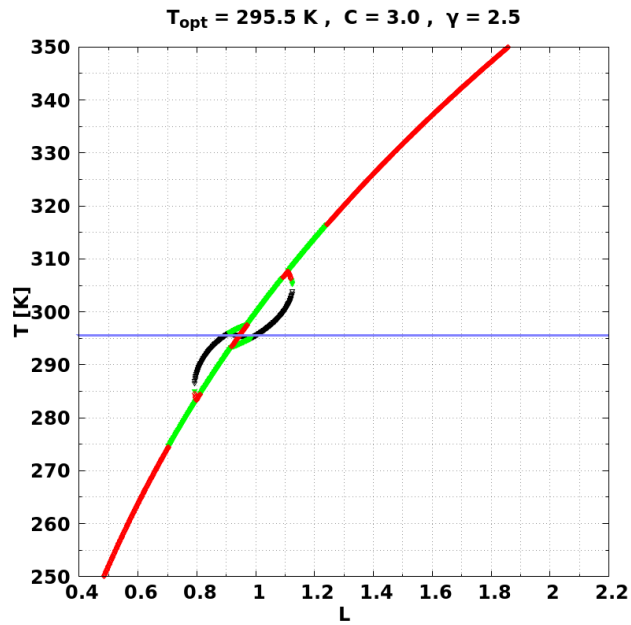
(a) DWC bifurcation for $C = 3.0$ and $\gamma = 2.5$.
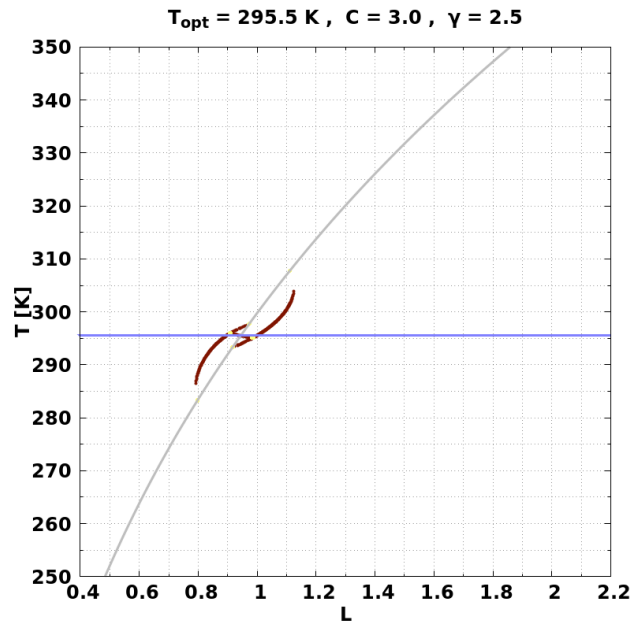
(b) DWC orbits diagram for $C = 3.0$ and $\gamma = 2.5$.
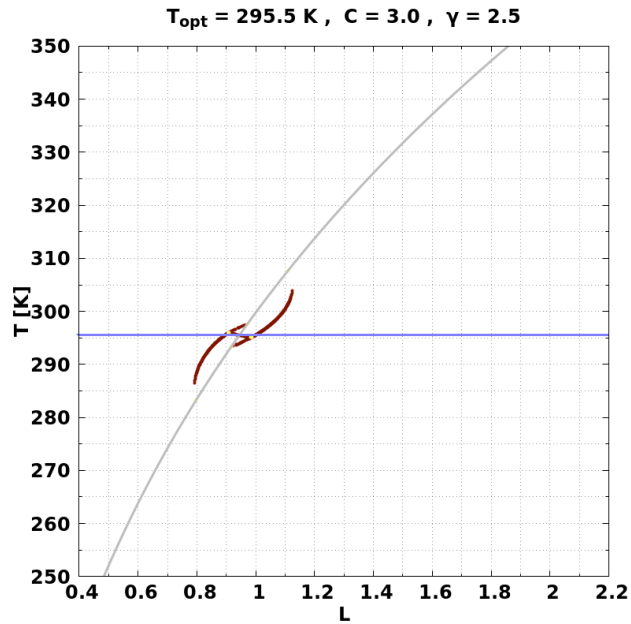
(c) DWC temperature T mean for $C = 3.0$ and $\gamma = 2.5$.

Legend:
- ● Stable node
- ● Semistable node
- ● Unstable node
- ▪ Null (0,0)
- ▪ FP not null
- ▪ Periodic
- ▪ Quasiperiodic
- ▪ Chaotic (a1,a2)
- ▪ Chaotic (a1,0)
- ▪ Chaotic (0,a2)
- ▪ Overpopulation
- ▬ Forbidden barrier

Figure A.53: **Orbits diagram** and the corresponding temperature T mean for **DWC** for $C = 3.0$ and $\gamma = 2.5$. **Blue** line corresponds to the value of $T_{opt} = 295.5$ K. Finally, those values of L where **Overpopulation** occurs, are marked by a vertical line with its corresponding color.
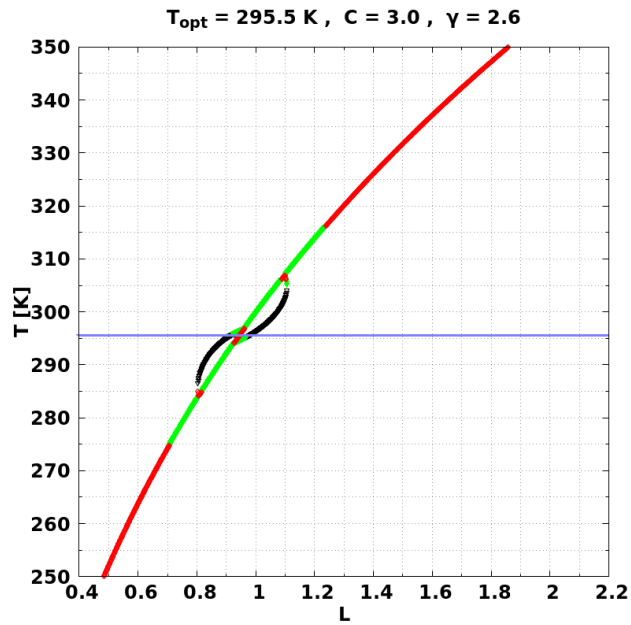
(a) DWC bifurcation for $C = 3.0$ and $\gamma = 2.6$.
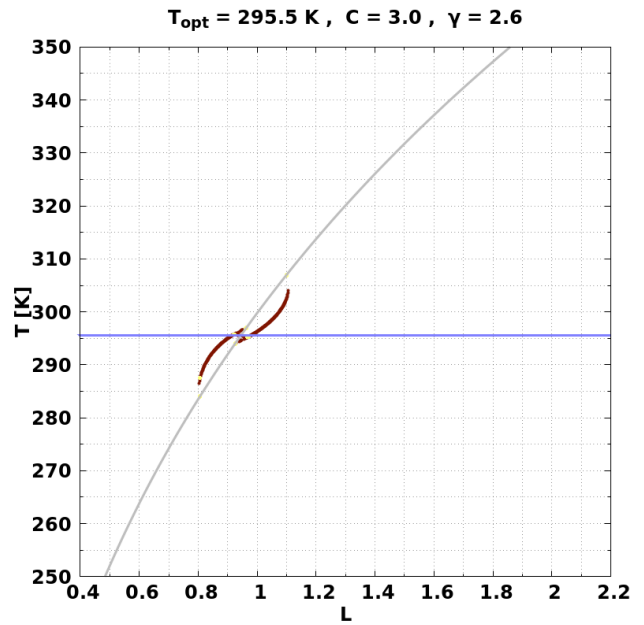
(b) DWC orbits diagram for $C = 3.0$ and $\gamma = 2.6$.
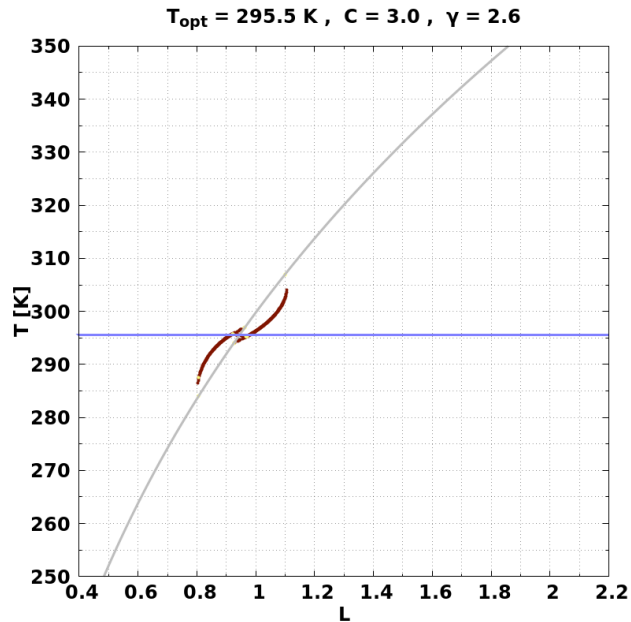
(c) DWC temperature T mean for $C = 3.0$ and $\gamma = 2.6$.

Legend:
- Stable node
- Semistable node
- Unstable node
- Null (0,0)
- FP not null
- Periodic
- Quasiperiodic
- Chaotic (a1,a2)
- Chaotic (a1,0)
- Chaotic (0,a2)
- Overpopulation
- Forbidden barrier

Figure A.54: **Orbits diagram** and the corresponding temperature T mean for **DWC** for $C = 3.0$ and $\gamma = 2.6$. **Blue** line corresponds to the value of $T_{opt} = 295.5$ K. Finally, those values of L where **Overpopulation** occurs, are marked by a vertical line with its corresponding color.
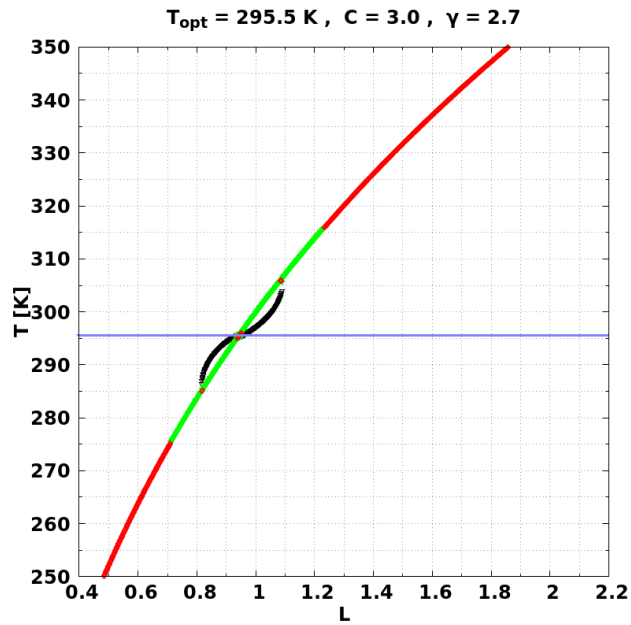
(a) DWC bifurcation for $C = 3.0$ and $\gamma = 2.7$.
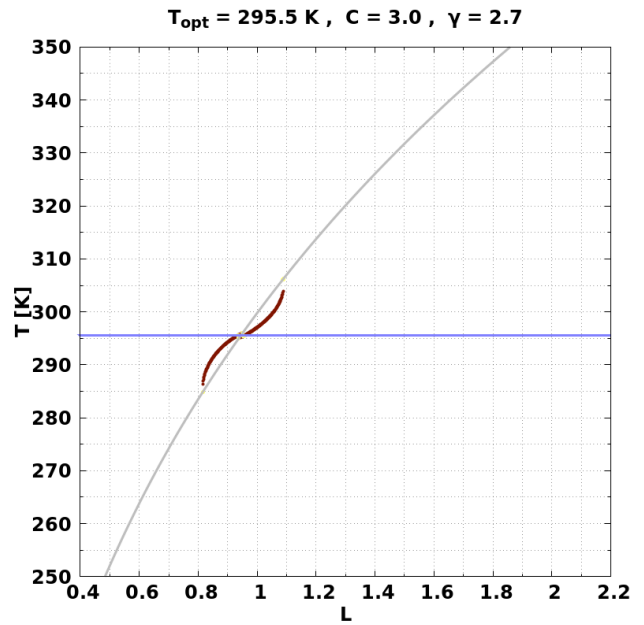
(b) DWC orbits diagram for $C = 3.0$ and $\gamma = 2.7$.
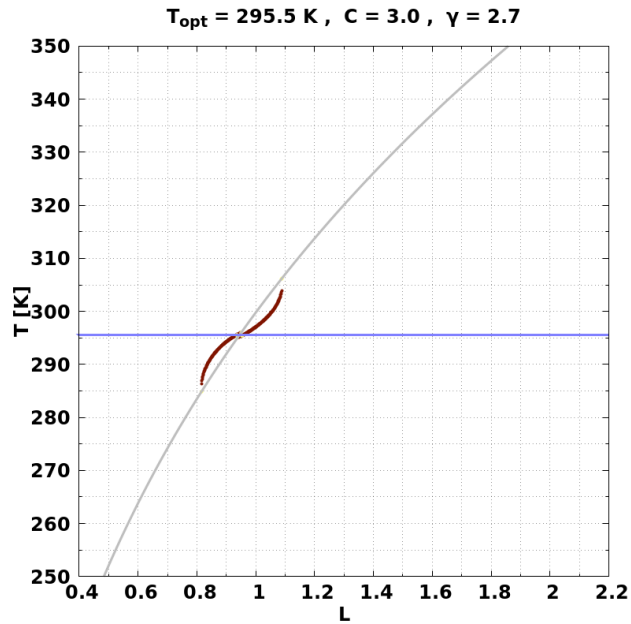
(c) DWC temperature T mean for $C = 3.0$ and $\gamma = 2.7$.

Figure A.55: **Orbits diagram** and the corresponding temperature T mean for **DWC** for $C = 3.0$ and $\gamma = 2.7$. **Blue** line corresponds to the value of $T_{opt} = 295.5$ K. Finally, those values of L where **Overpopulation** occurs, are marked by a vertical line with its corresponding color.
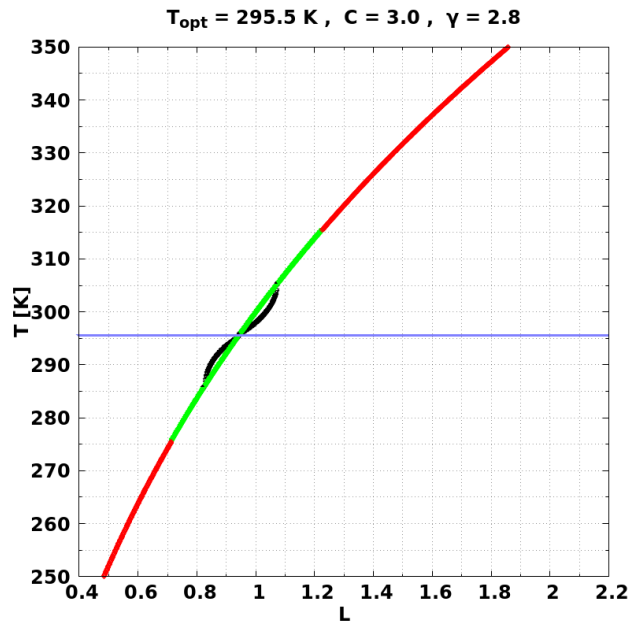
(a) DWC bifurcation for $C = 3.0$ and $\gamma = 2.8$.
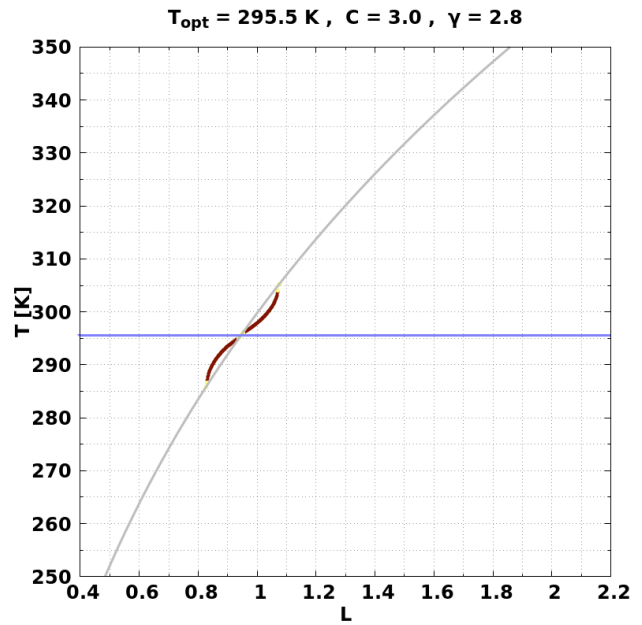
(b) DWC orbits diagram for $C = 3.0$ and $\gamma = 2.8$.
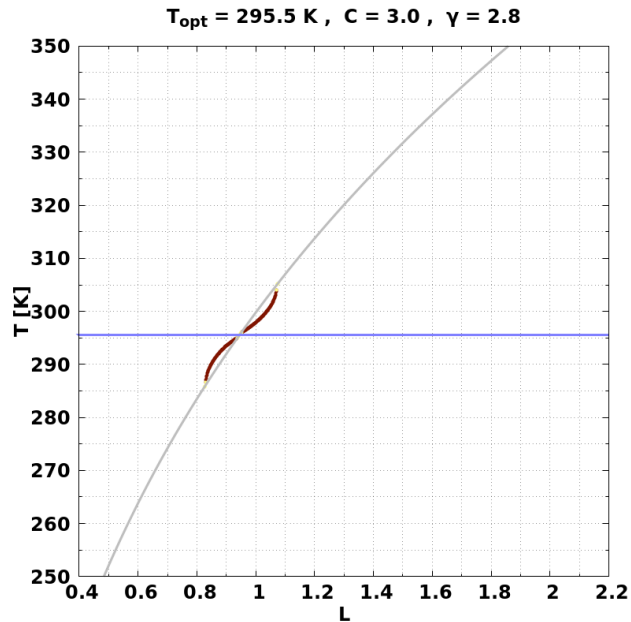
(c) DWC temperature T mean for $C = 3.0$ and $\gamma = 2.8$.

Figure A.56: **Orbits diagram** and the corresponding temperature T mean for **DWC** for $C = 3.0$ and $\gamma = 2.8$. **Blue** line corresponds to the value of $T_{opt} = 295.5$ K. Finally, those values of L where **Overpopulation** occurs, are marked by a vertical line with its corresponding color.
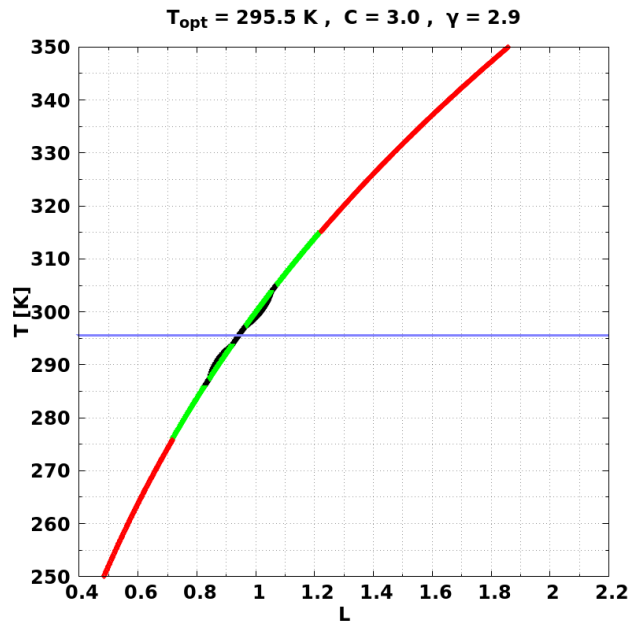
(a) DWC bifurcation for $C = 3.0$ and $\gamma = 2.9$.
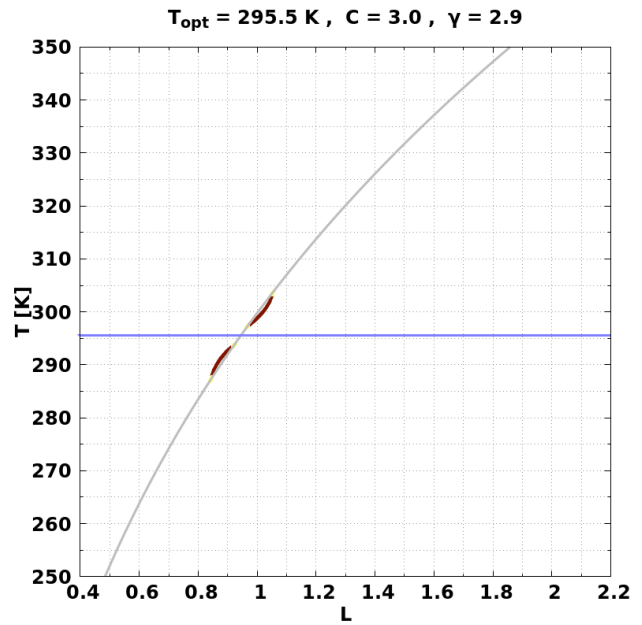
(b) DWC orbits diagram for $C = 3.0$ and $\gamma = 2.9$.
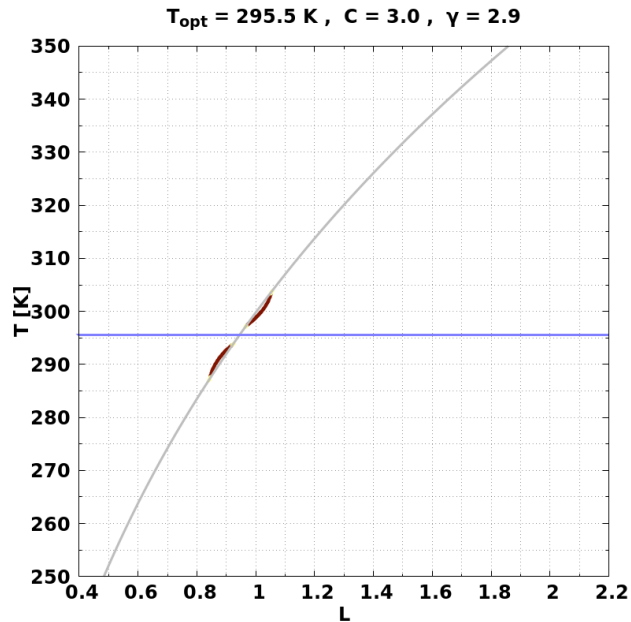
(c) DWC temperature T mean for $C = 3.0$ and $\gamma = 2.9$.

Legend:
- Stable node (black)
- Semistable node (green)
- Unstable node (red)
- Null (0,0) (gray)
- FP not null (dark red)
- Periodic (cyan)
- Quasiperiodic (yellow)
- Chaotic (a1,a2) (orange)
- Chaotic (a1,0) (green)
- Chaotic (0,a2) (dark blue)
- Overpopulation (olive)
- Forbidden barrier (dark red)

Figure A.57: **Orbits diagram** and the corresponding temperature T mean for **DWC** for $C = 3.0$ and $\gamma = 2.9$. **Blue** line corresponds to the value of $T_{opt} = 295.5$ K. Finally, those values of L where **Overpopulation** occurs, are marked by a vertical line with its corresponding color.
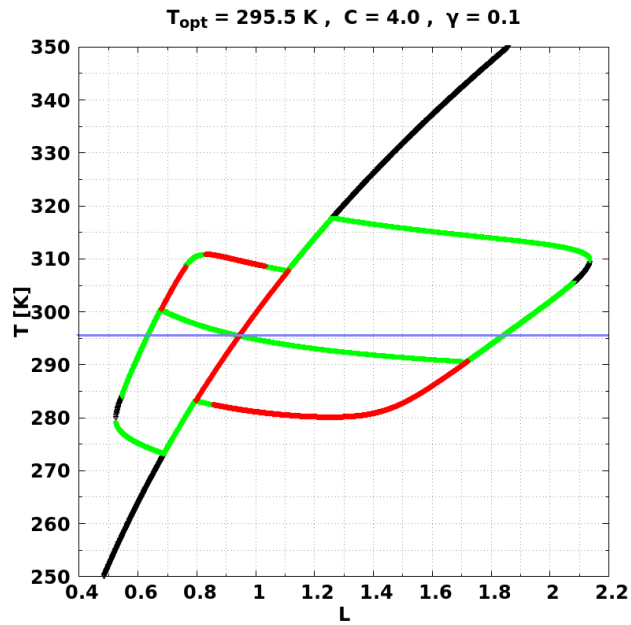
(a) DWC bifurcation for $C = 4.0$ and $\gamma = 0.1$.
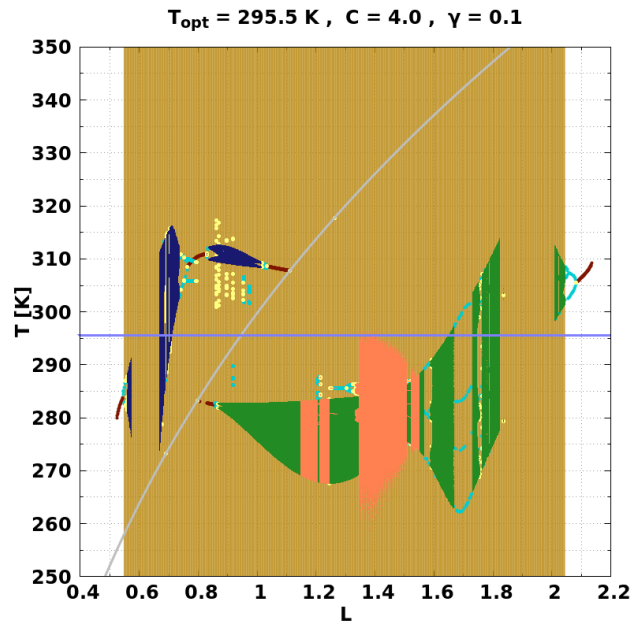
(b) DWC orbits diagram for $C = 4.0$ and $\gamma = 0.1$.
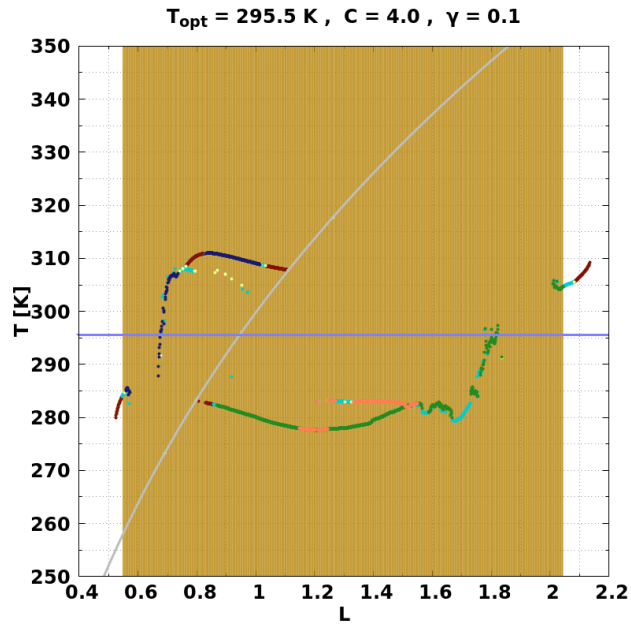
(c) DWC temperature T mean for $C = 4.0$ and $\gamma = 0.1$.

Figure A.58: **Orbits diagram** and the corresponding temperature T mean for **DWC** for $C = 4.0$ and $\gamma = 0.1$. **Blue** line corresponds to the value of $T_{opt} = 295.5$ K. Finally, those values of L where **Overpopulation** occurs, are marked by a vertical line with its corresponding color.
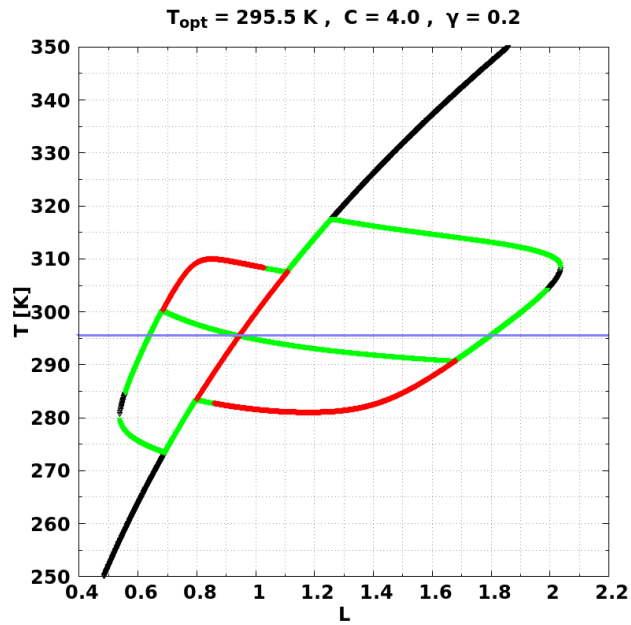
(a) DWC bifurcation for $C = 4.0$ and $\gamma = 0.2$.
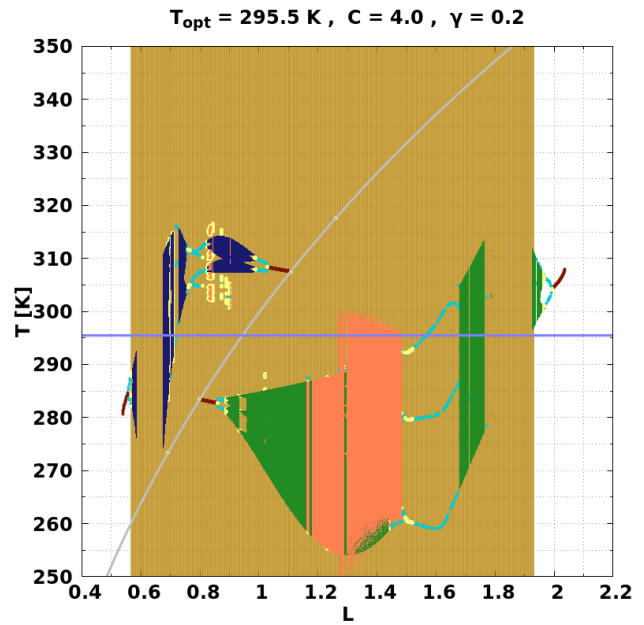
(b) DWC orbits diagram for $C = 4.0$ and $\gamma = 0.2$.
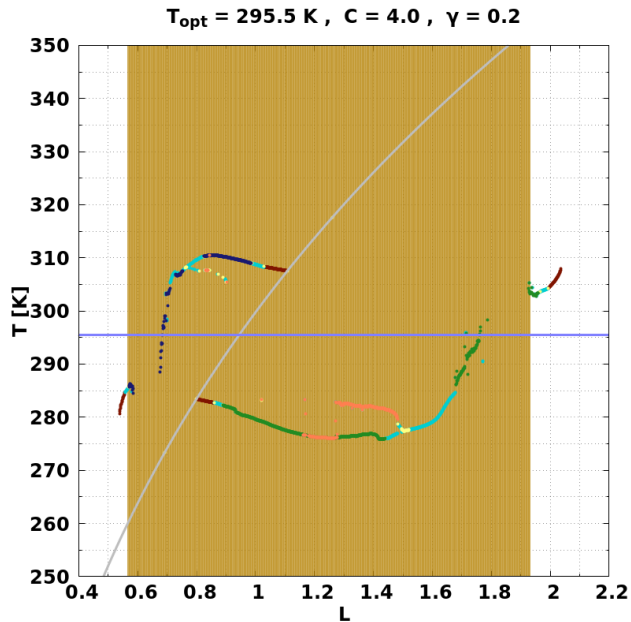
(c) DWC temperature T mean for $C = 4.0$ and $\gamma = 0.2$.

Figure A.59: **Orbits diagram** and the corresponding temperature T mean for **DWC** for $C = 4.0$ and $\gamma = 0.2$. **Blue** line corresponds to the value of $T_{opt} = 295.5$ K. Finally, those values of L where **Overpopulation** occurs, are marked by a vertical line with its corresponding color.
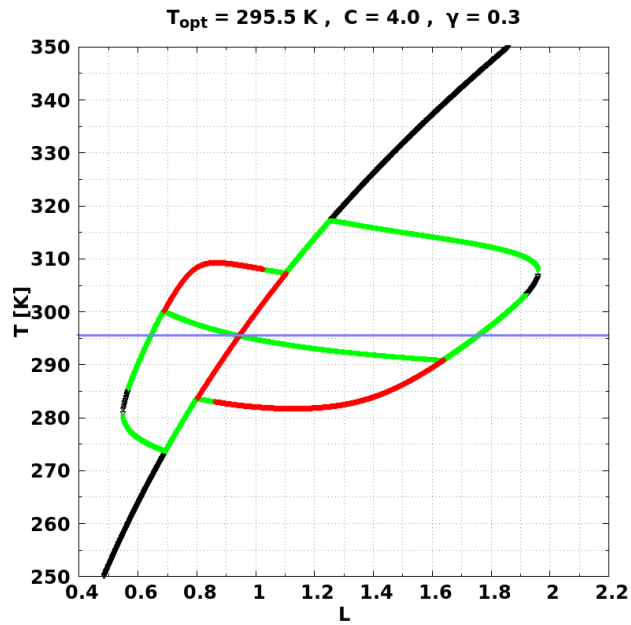
(a) DWC bifurcation for $C = 4.0$ and $\gamma = 0.3$.
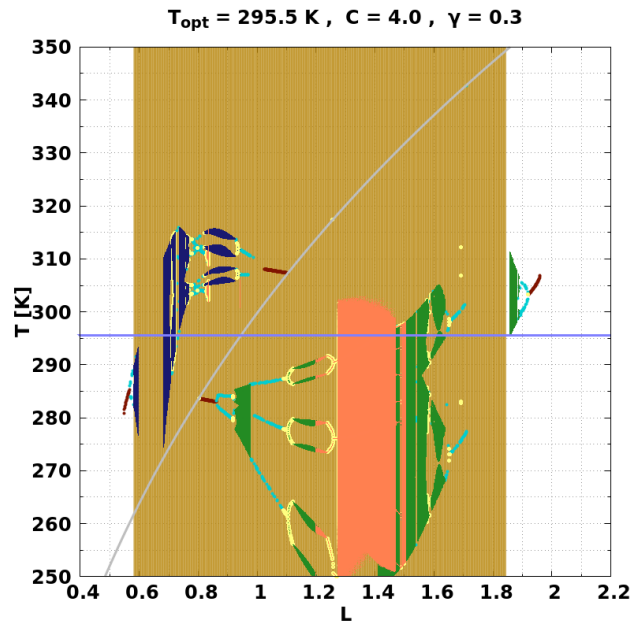
(b) DWC orbits diagram for $C = 4.0$ and $\gamma = 0.3$.
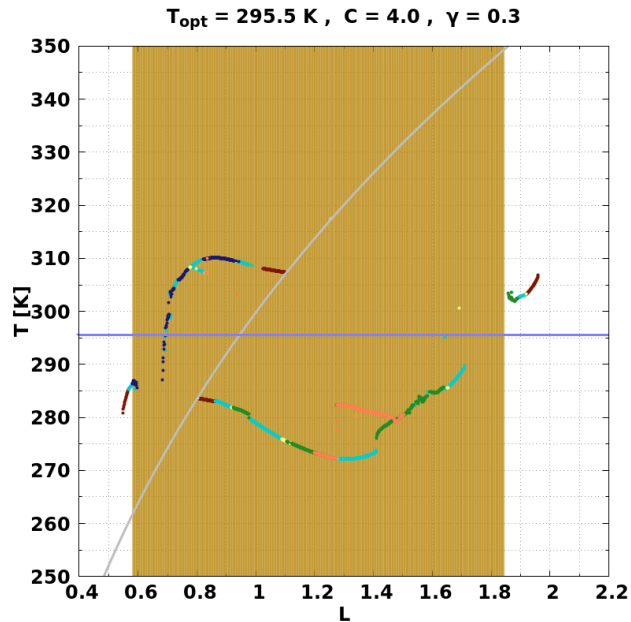
(c) DWC temperature T mean for $C = 4.0$ and $\gamma = 0.3$.

- ● Stable node
- ● Semistable node
- ● Unstable node
- ▣ Null (0,0)
- ▣ FP not null
- ▣ Periodic
- ▣ Quasiperiodic
- ▣ Chaotic (a1,a2)
- ▣ Chaotic (a1,0)
- ▣ Chaotic (0,a2)
- ▣ Overpopulation
- ▬ Forbidden barrier

Figure A.60: **Orbits diagram** and the corresponding temperature T mean for **DWC** for $C = 4.0$ and $\gamma = 0.3$. **Blue** line corresponds to the value of $T_{opt} = 295.5$ K. Finally, those values of L where **Overpopulation** occurs, are marked by a vertical line with its corresponding color.
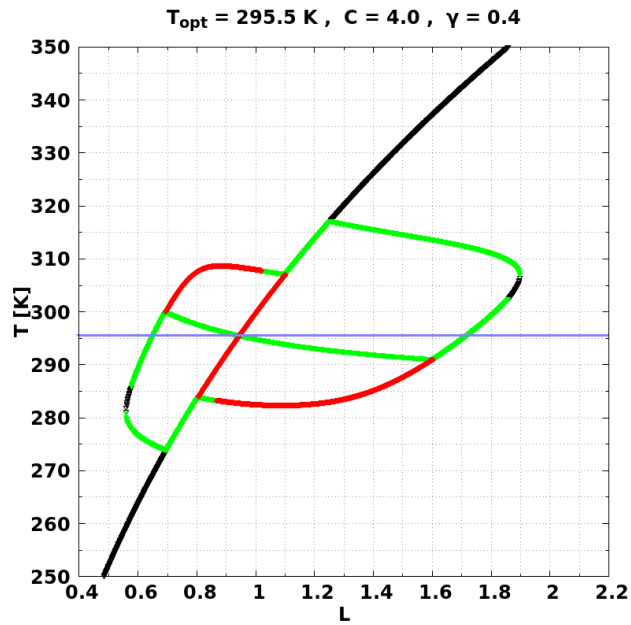
(a) DWC bifurcation for $C = 4.0$ and $\gamma = 0.4$.
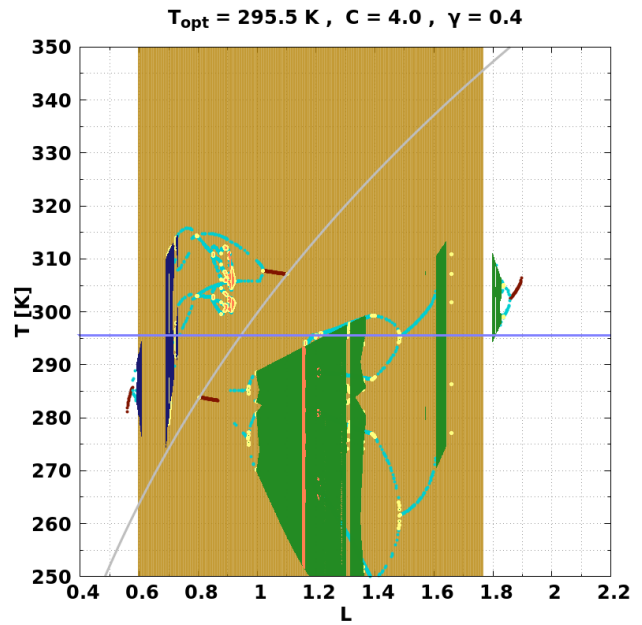
(b) DWC orbits diagram for $C = 4.0$ and $\gamma = 0.4$.
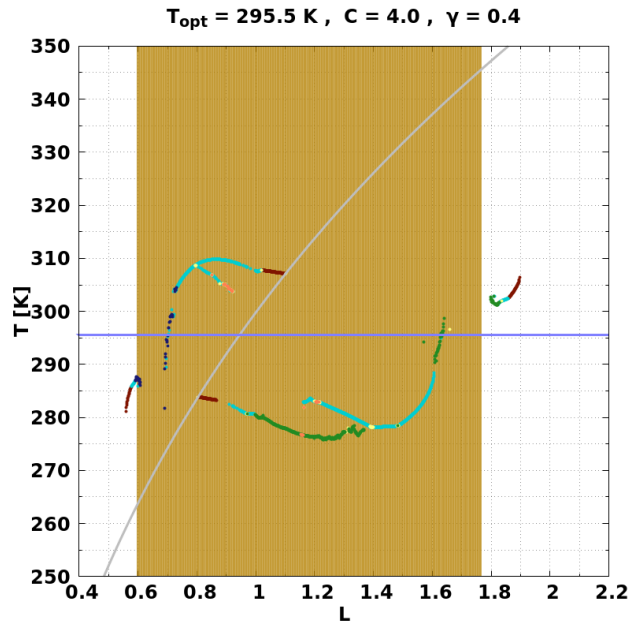
(c) DWC temperature T mean for $C = 4.0$ and $\gamma = 0.4$.

Legend:
- Stable node
- Semistable node
- Unstable node
- Null (0,0)
- FP not null
- Periodic
- Quasiperiodic
- Chaotic (a1,a2)
- Chaotic (a1,0)
- Chaotic (0,a2)
- Overpopulation
- Forbidden barrier

Figure A.61: **Orbits diagram** and the corresponding temperature T mean for **DWC** for $C = 4.0$ and $\gamma = 0.4$. **Blue** line corresponds to the value of $T_{opt} = 295.5$ K. Finally, those values of L where **Overpopulation** occurs, are marked by a vertical line with its corresponding color.
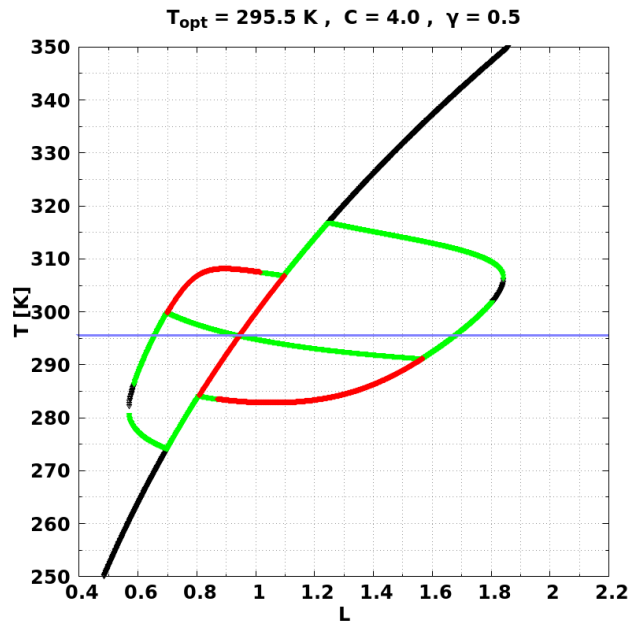
(a) DWC bifurcation for $C = 4.0$ and $\gamma = 0.5$.
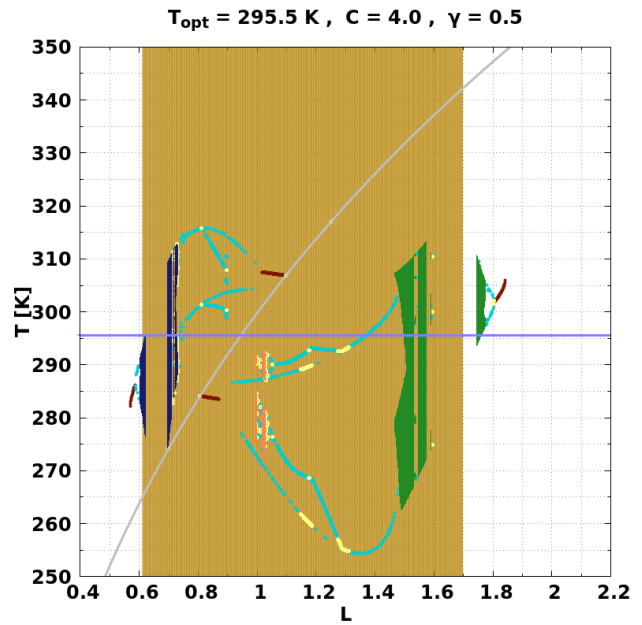
(b) DWC orbits diagram for $C = 4.0$ and $\gamma = 0.5$.
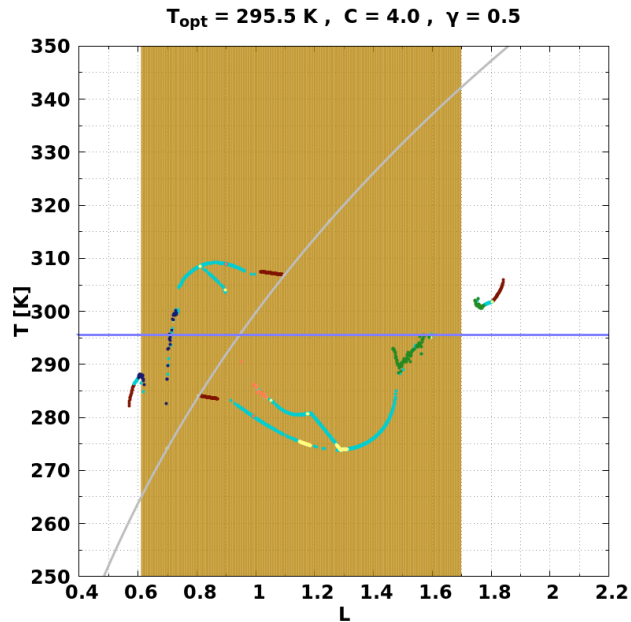
(c) DWC temperature T mean for $C = 4.0$ and $\gamma = 0.5$.

Legend:
- ● Stable node
- ● Semistable node
- ● Unstable node
- ▨ Null (0,0)
- ▨ FP not null
- ▨ Periodic
- ▨ Quasiperiodic
- ▨ Chaotic (a1,a2)
- ▨ Chaotic (a1,0)
- ▨ Chaotic (0,a2)
- ▨ Overpopulation
- ▬ Forbidden barrier

Figure A.62: **Orbits diagram** and the corresponding temperature T mean for **DWC** for $C = 4.0$ and $\gamma = 0.5$. **Blue** line corresponds to the value of $T_{opt} = 295.5$ K. Finally, those values of L where **Overpopulation** occurs, are marked by a vertical line with its corresponding color.
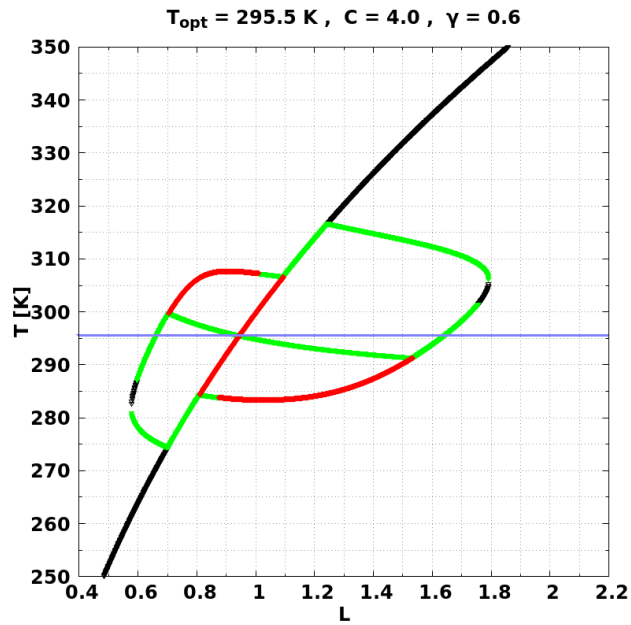
(a) DWC bifurcation for $C = 4.0$ and $\gamma = 0.6$.
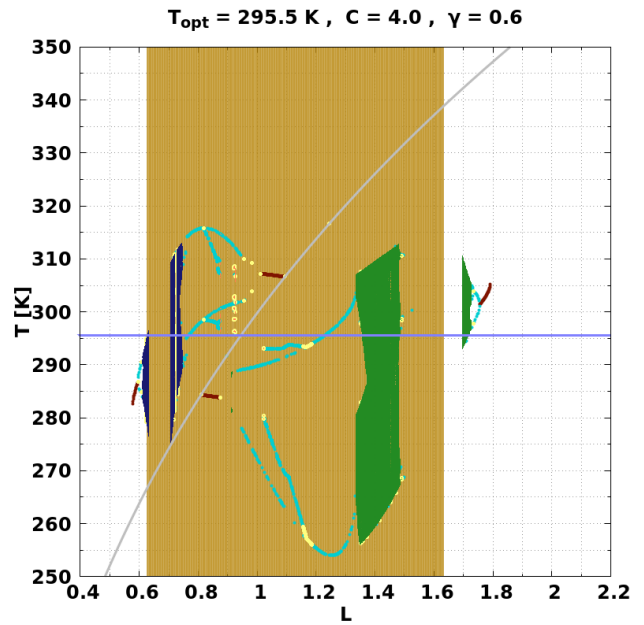
(b) DWC orbits diagram for $C = 4.0$ and $\gamma = 0.6$.
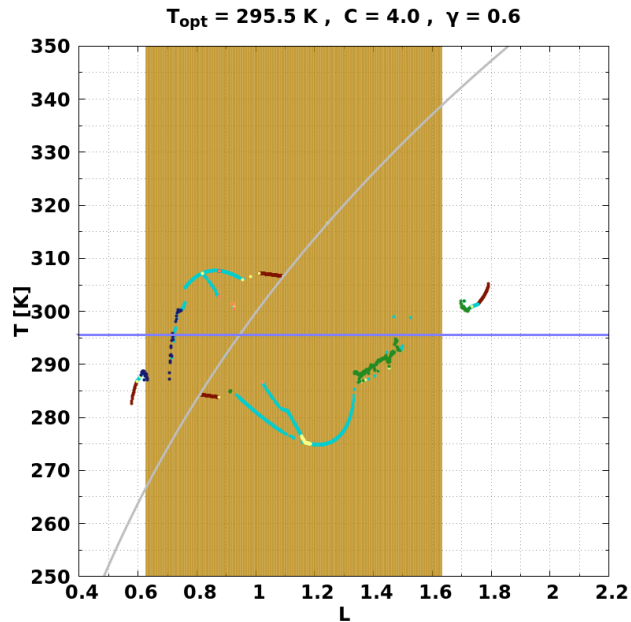
(c) DWC temperature T mean for $C = 4.0$ and $\gamma = 0.6$.

Figure A.63: **Orbits diagram** and the corresponding temperature T mean for **DWC** for $C = 4.0$ and $\gamma = 0.6$. **Blue** line corresponds to the value of $T_{opt} = 295.5$ K. Finally, those values of L where **Overpopulation** occurs, are marked by a vertical line with its corresponding color.
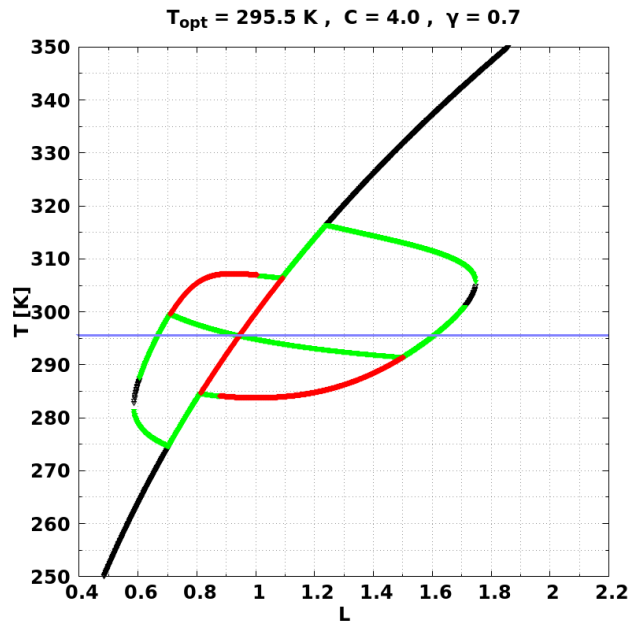
(a) DWC bifurcation for $C = 4.0$ and $\gamma = 0.7$.
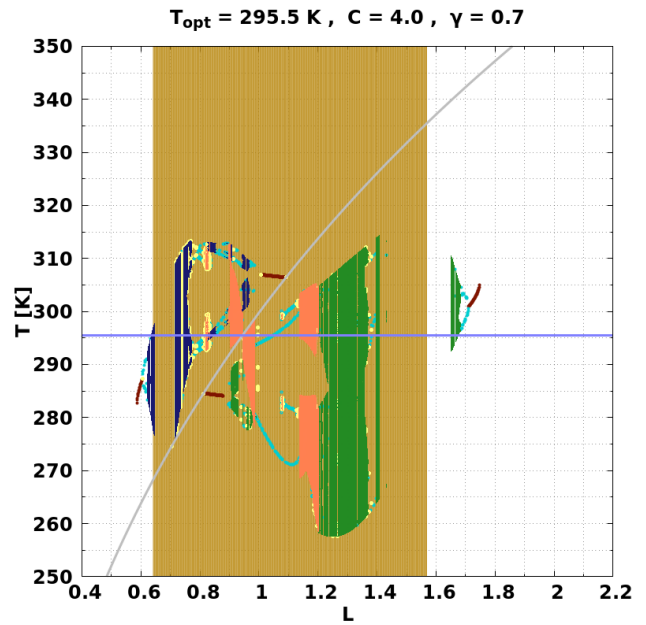
(b) DWC orbits diagram for $C = 4.0$ and $\gamma = 0.7$.
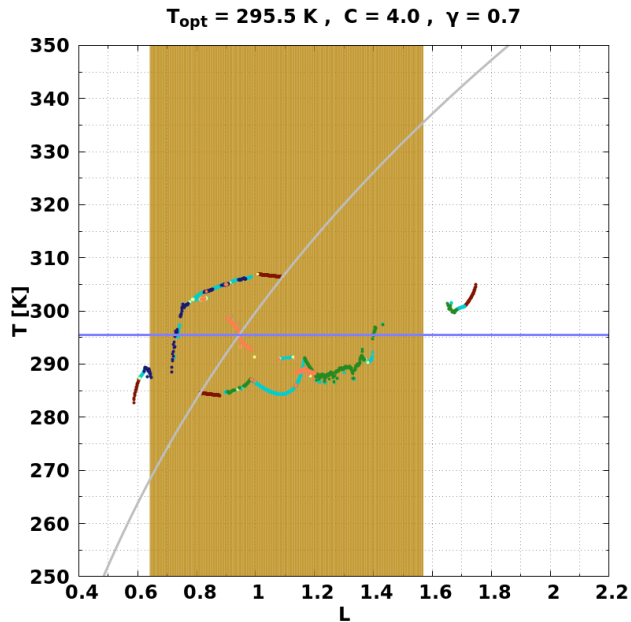
(c) DWC temperature T mean for $C = 4.0$ and $\gamma = 0.7$.

● Stable node
● Semistable node
● Unstable node
▦ Null (0,0)
■ FP not null
■ Periodic
▢ Quasiperiodic
■ Chaotic (a1,a2)
■ Chaotic (a1,0)
■ Chaotic (0,a2)
▦ Overpopulation
━ Forbidden barrier

Figure A.64: **Orbits diagram** and the corresponding temperature T mean for **DWC** for $C = 4.0$ and $\gamma = 0.7$. **Blue** line corresponds to the value of $T_{opt} = 295.5$ K. Finally, those values of L where **Overpopulation** occurs, are marked by a vertical line with its corresponding color.
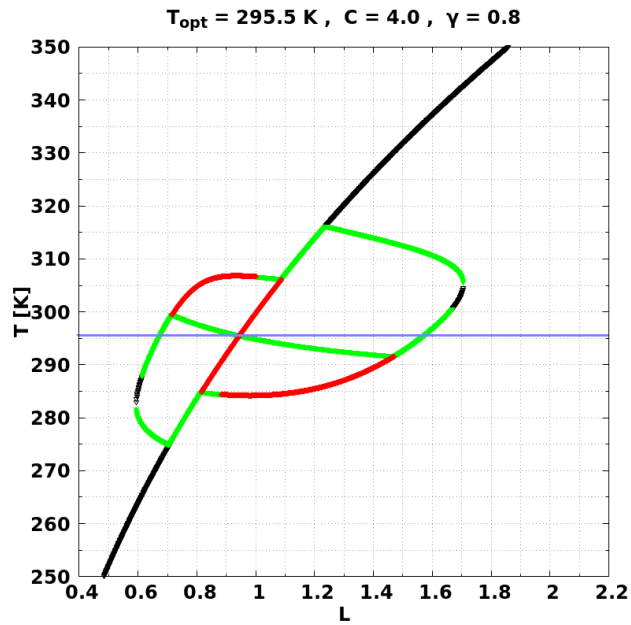
(a) DWC bifurcation for $C = 4.0$ and $\gamma = 0.8$.
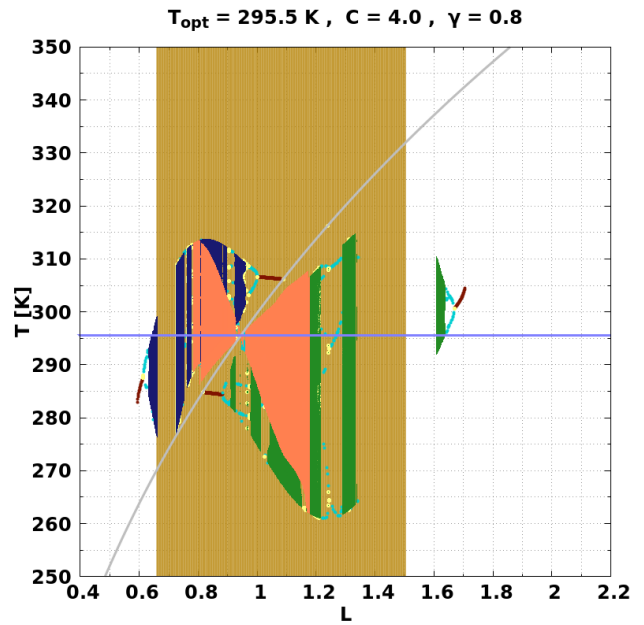
(b) DWC orbits diagram for $C = 4.0$ and $\gamma = 0.8$.
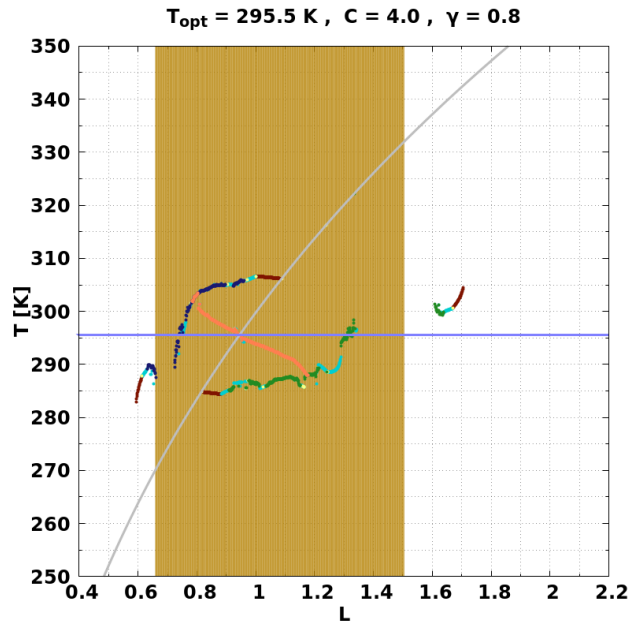
(c) DWC temperature T mean for $C = 4.0$ and $\gamma = 0.8$.

- ● Stable node
- ● Semistable node
- ● Unstable node
- ▨ Null (0,0)
- ▨ FP not null
- ▨ Periodic
- ▨ Quasiperiodic
- ▨ Chaotic (a1,a2)
- ▨ Chaotic (a1,0)
- ▨ Chaotic (0,a2)
- ▨ Overpopulation
- ▬ Forbidden barrier

Figure A.65: **Orbits diagram** and the corresponding temperature T mean for **DWC** for $C = 4.0$ and $\gamma = 0.8$. **Blue** line corresponds to the value of $T_{opt} = 295.5$ K. Finally, those values of L where **Overpopulation** occurs, are marked by a vertical line with its corresponding color.

(a) DWC bifurcation for $C = 4.0$ and $\gamma = 0.9$.

(b) DWC orbits diagram for $C = 4.0$ and $\gamma = 0.9$.

(c) DWC temperature T mean for $C = 4.0$ and $\gamma = 0.9$.

Legend:
- Stable node
- Semistable node
- Unstable node
- Null (0,0)
- FP not null
- Periodic
- Quasiperiodic
- Chaotic (a1,a2)
- Chaotic (a1,0)
- Chaotic (0,a2)
- Overpopulation
- Forbidden barrier
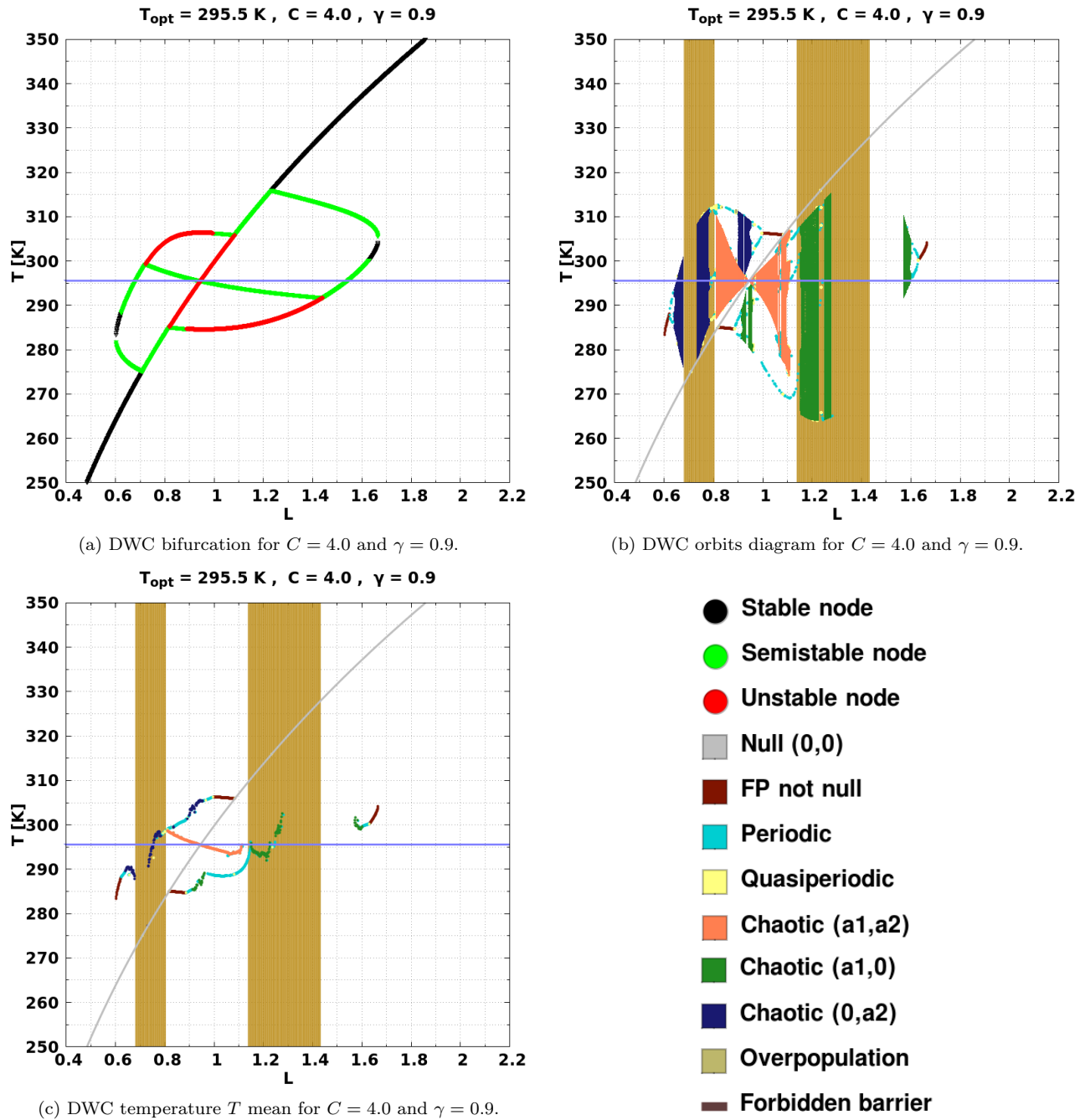
Figure A.66: **Orbits diagram** and the corresponding temperature T mean for **DWC** for $C = 4.0$ and $\gamma = 0.9$. **Blue** line corresponds to the value of $T_{opt} = 295.5$ K. Finally, those values of L where **Overpopulation** occurs, are marked by a vertical line with its corresponding color.
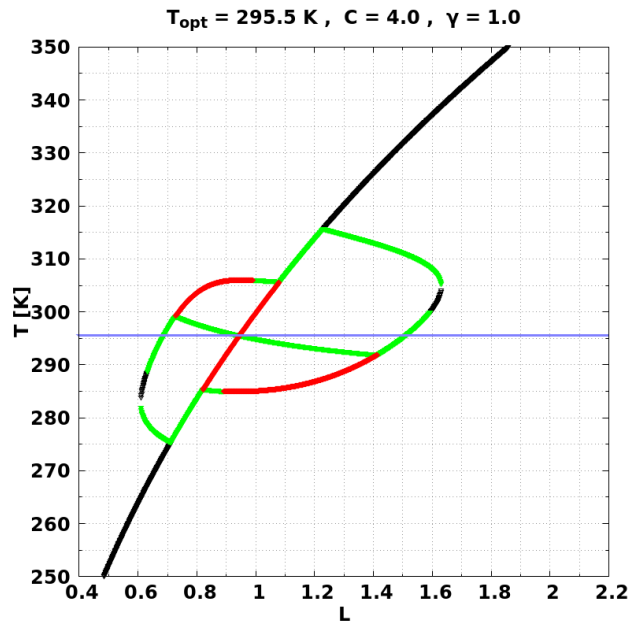
(a) DWC bifurcation for $C = 4.0$ and $\gamma = 1.0$.
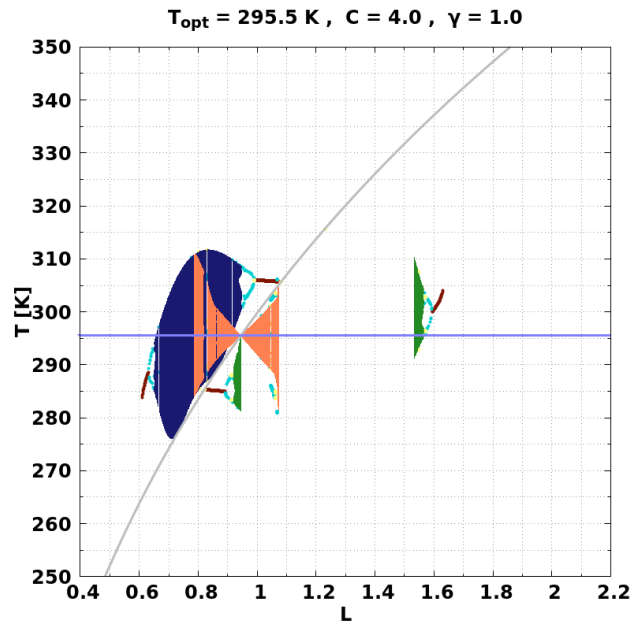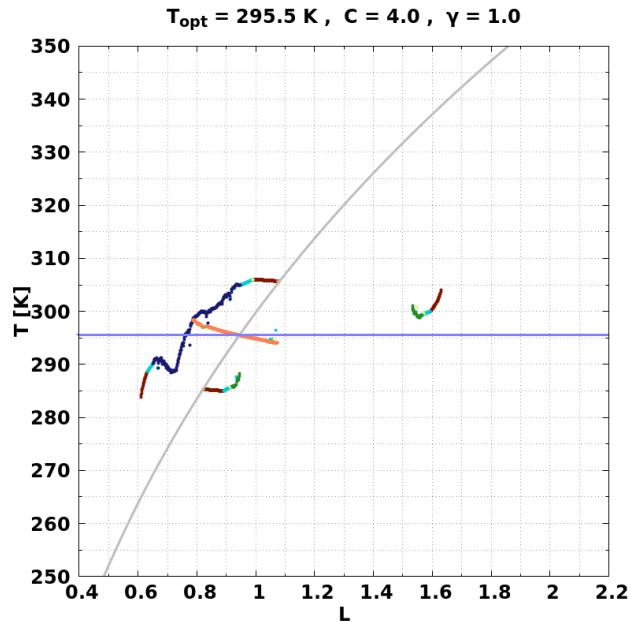
(b) DWC orbits diagram for $C = 4.0$ and $\gamma = 1.0$.

(c) DWC temperature T mean for $C = 4.0$ and $\gamma = 1.0$.

Figure A.67: **Orbits diagram** and the corresponding temperature T mean for **DWC** for $C = 4.0$ and $\gamma = 1.0$. **Blue** line corresponds to the value of $T_{opt} = 295.5$ K. Finally, those values of L where **Overpopulation** occurs, are marked by a vertical line with its corresponding color.
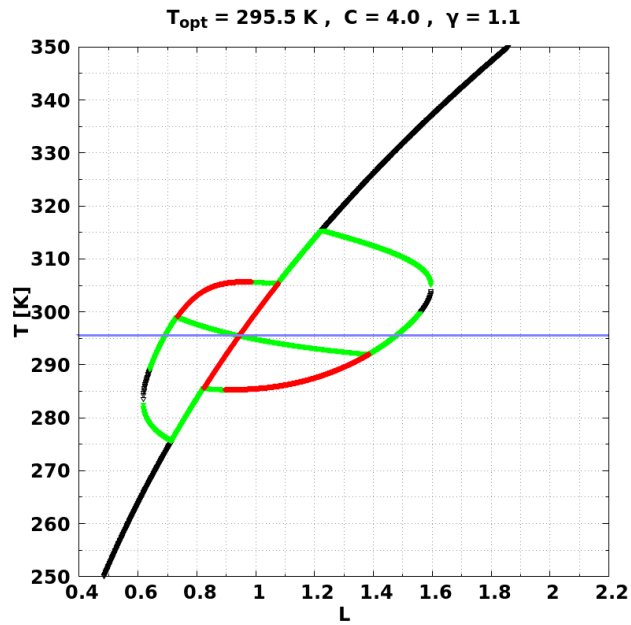
(a) DWC bifurcation for $C = 4.0$ and $\gamma = 1.1$.
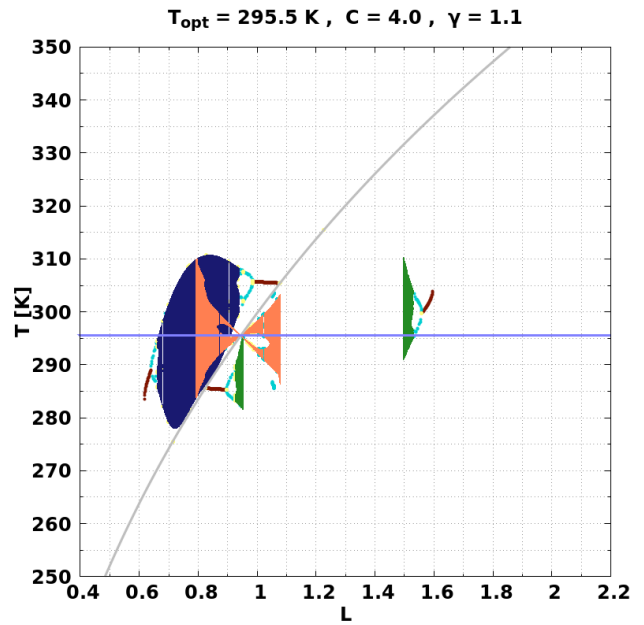
(b) DWC orbits diagram for $C = 4.0$ and $\gamma = 1.1$.
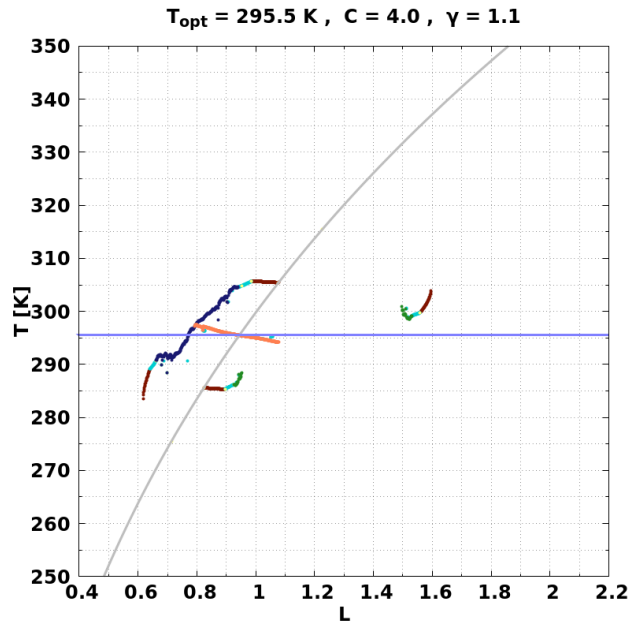
(c) DWC temperature T mean for $C = 4.0$ and $\gamma = 1.1$.

Figure A.68: **Orbits diagram** and the corresponding temperature T mean for **DWC** for $C = 4.0$ and $\gamma = 1.1$. **Blue** line corresponds to the value of $T_{opt} = 295.5$ K. Finally, those values of L where **Overpopulation** occurs, are marked by a vertical line with its corresponding color.
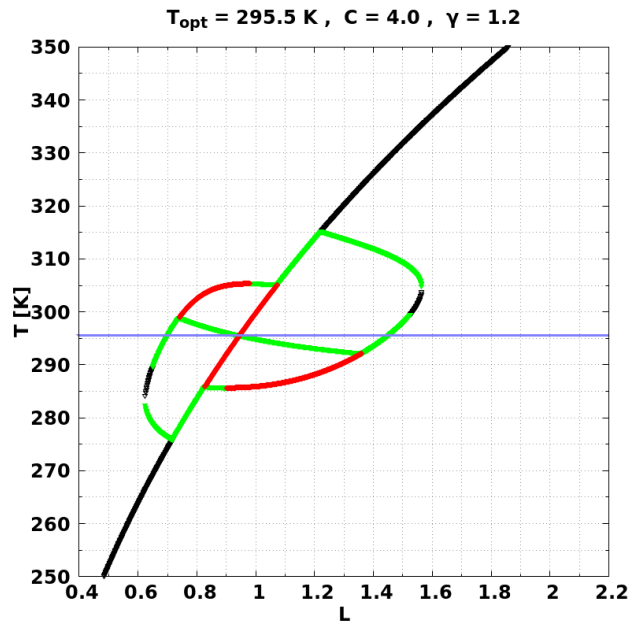
(a) DWC bifurcation for $C = 4.0$ and $\gamma = 1.2$.
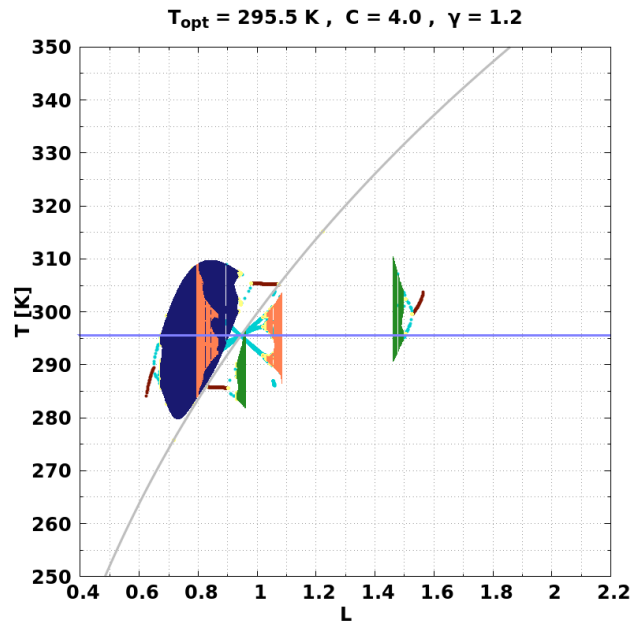
(b) DWC orbits diagram for $C = 4.0$ and $\gamma = 1.2$.
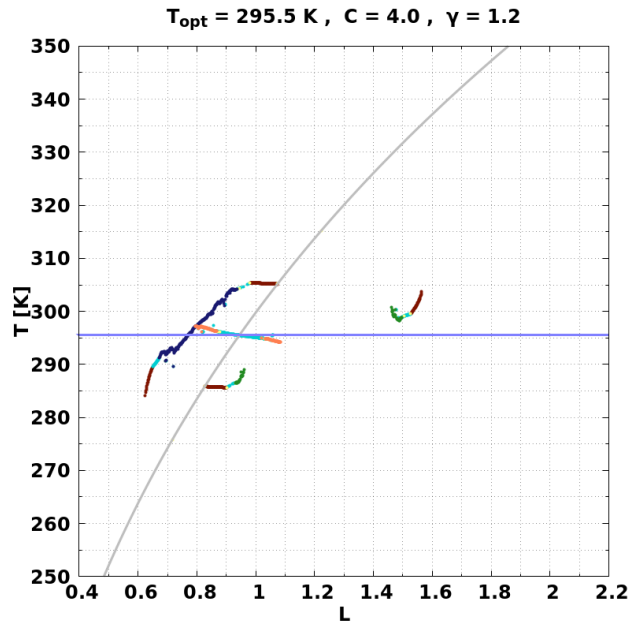
(c) DWC temperature T mean for $C = 4.0$ and $\gamma = 1.2$.

Figure A.69: **Orbits diagram** and the corresponding temperature T mean for **DWC** for $C = 4.0$ and $\gamma = 1.2$. **Blue** line corresponds to the value of $T_{opt} = 295.5$ K. Finally, those values of L where **Overpopulation** occurs, are marked by a vertical line with its corresponding color.
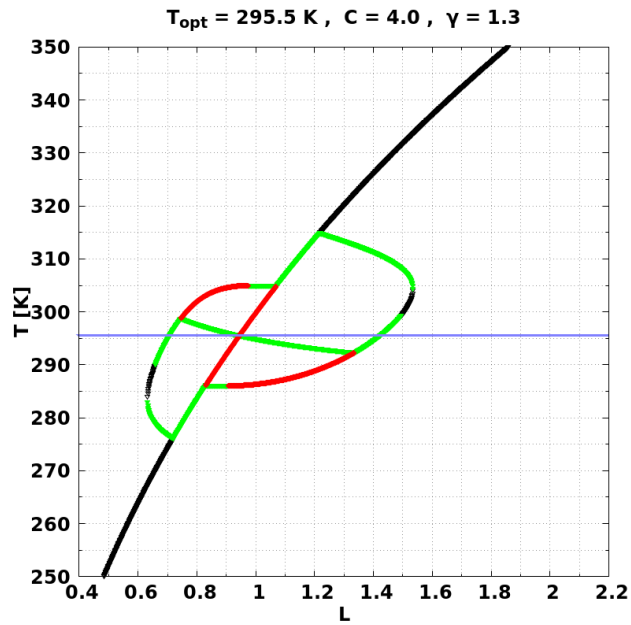
(a) DWC bifurcation for $C = 4.0$ and $\gamma = 1.3$.
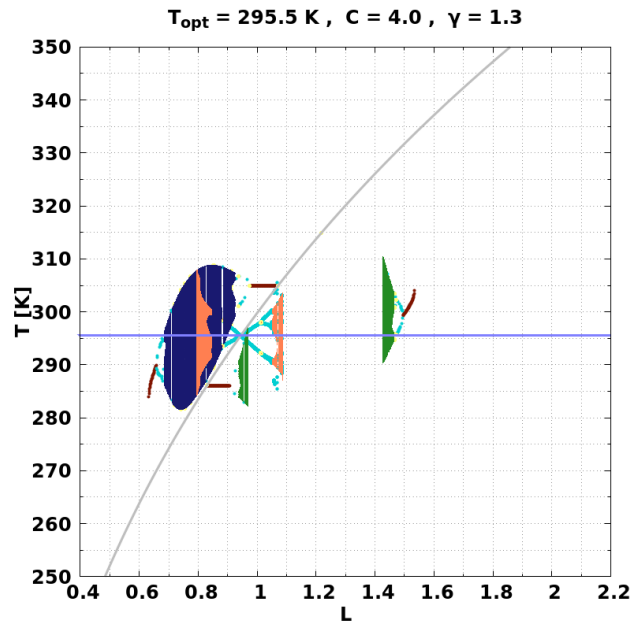
(b) DWC orbits diagram for $C = 4.0$ and $\gamma = 1.3$.
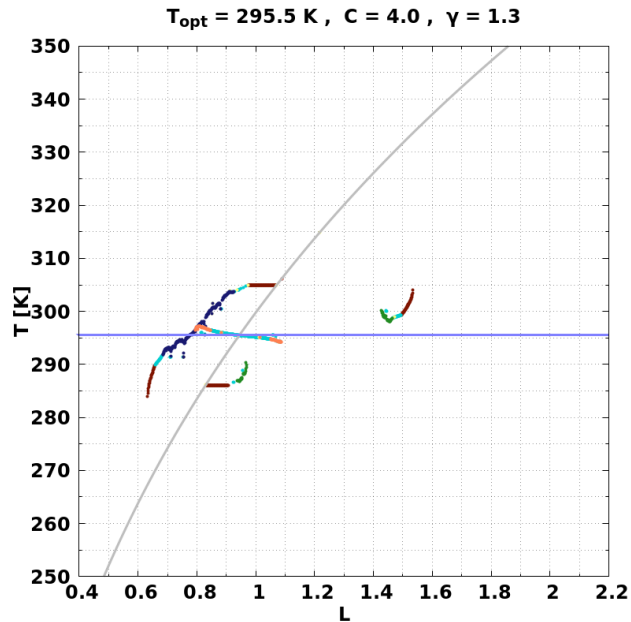
(c) DWC temperature T mean for $C = 4.0$ and $\gamma = 1.3$.

Figure A.70: **Orbits diagram** and the corresponding temperature T mean for **DWC** for $C = 4.0$ and $\gamma = 1.3$. **Blue** line corresponds to the value of $T_{opt} = 295.5$ K. Finally, those values of L where **Overpopulation** occurs, are marked by a vertical line with its corresponding color.
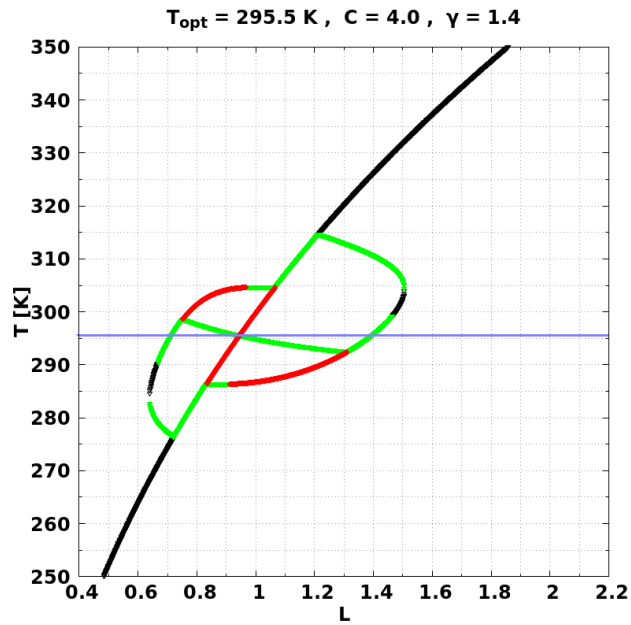
(a) DWC bifurcation for $C = 4.0$ and $\gamma = 1.4$.
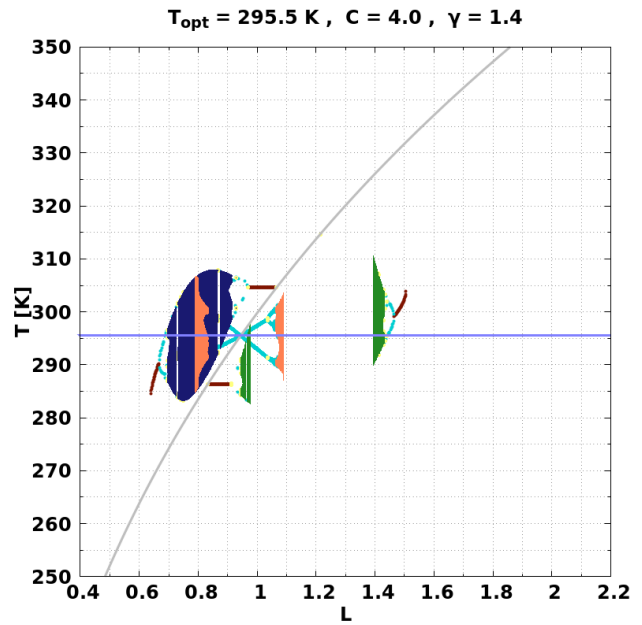
(b) DWC orbits diagram for $C = 4.0$ and $\gamma = 1.4$.
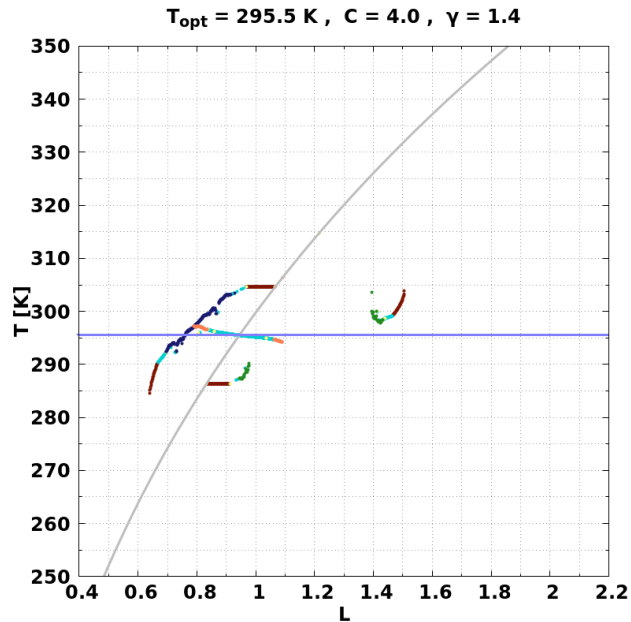
(c) DWC temperature T mean for $C = 4.0$ and $\gamma = 1.4$.

Figure A.71: **Orbits diagram** and the corresponding temperature T mean for **DWC** for $C = 4.0$ and $\gamma = 1.4$. **Blue** line corresponds to the value of $T_{opt} = 295.5$ K. Finally, those values of L where **Overpopulation** occurs, are marked by a vertical line with its corresponding color.
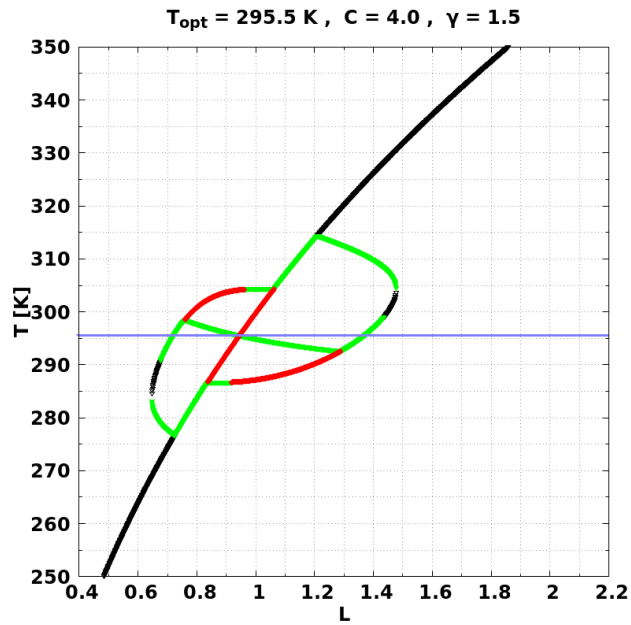
(a) DWC bifurcation for $C = 4.0$ and $\gamma = 1.5$.
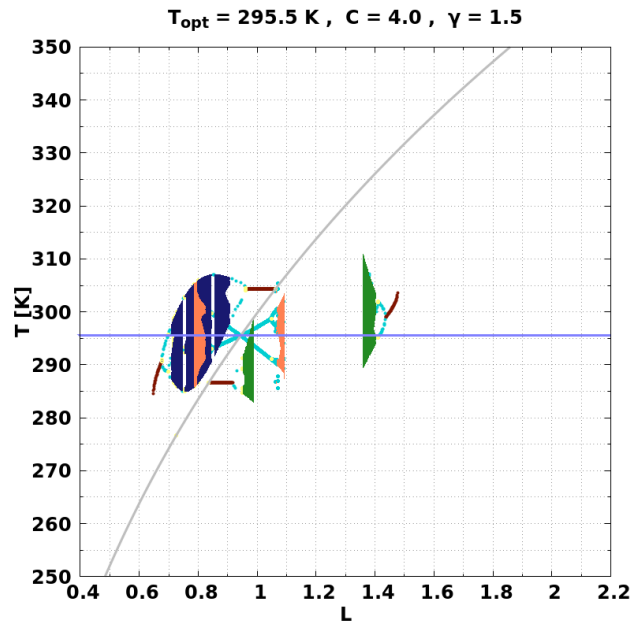
(b) DWC orbits diagram for $C = 4.0$ and $\gamma = 1.5$.
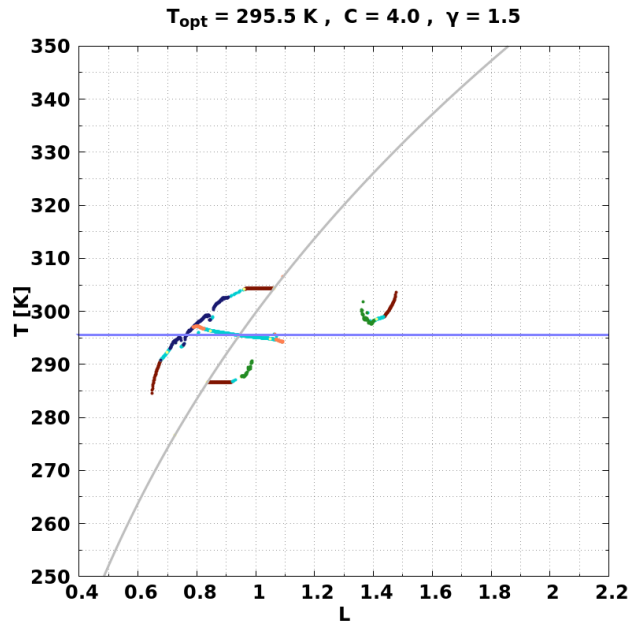
(c) DWC temperature T mean for $C = 4.0$ and $\gamma = 1.5$.

Figure A.72: **Orbits diagram** and the corresponding temperature T mean for **DWC** for $C = 4.0$ and $\gamma = 1.5$. **Blue** line corresponds to the value of $T_{opt} = 295.5$ K. Finally, those values of L where **Overpopulation** occurs, are marked by a vertical line with its corresponding color.
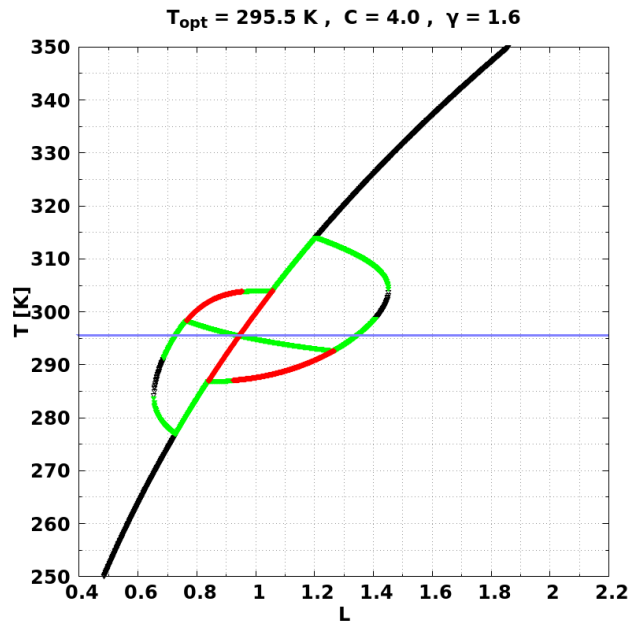
(a) DWC bifurcation for $C = 4.0$ and $\gamma = 1.6$.
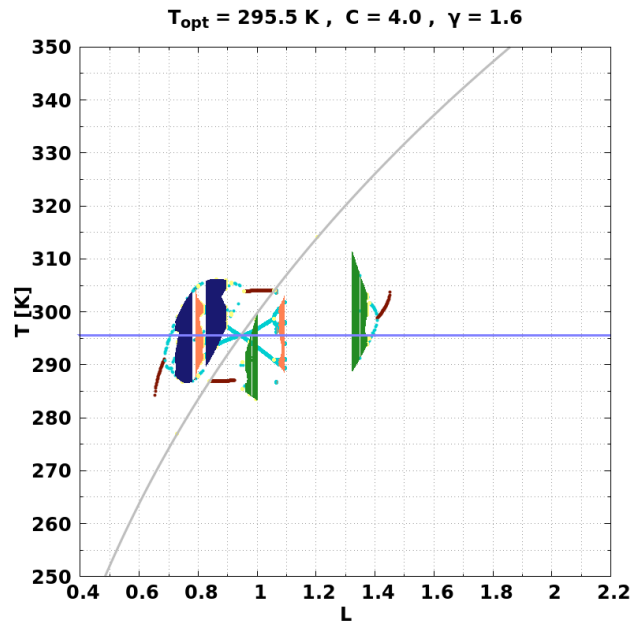
(b) DWC orbits diagram for $C = 4.0$ and $\gamma = 1.6$.
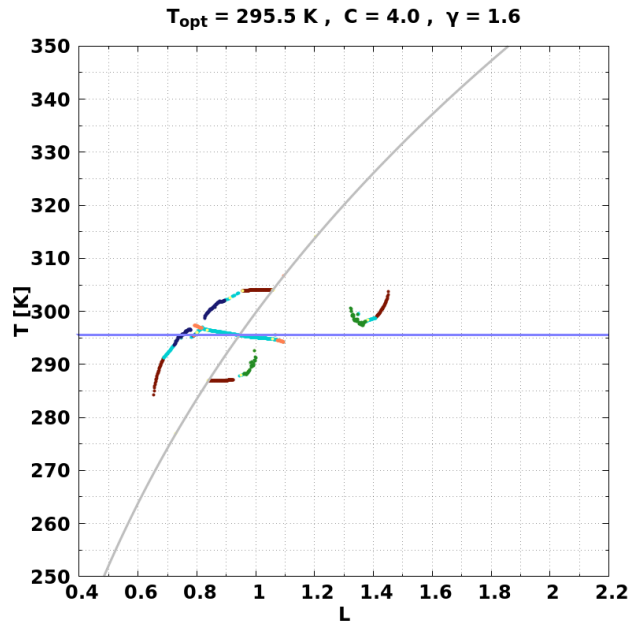
(c) DWC temperature T mean for $C = 4.0$ and $\gamma = 1.6$.

Figure A.73: **Orbits diagram** and the corresponding temperature T mean for **DWC** for $C = 4.0$ and $\gamma = 1.6$. **Blue** line corresponds to the value of $T_{opt} = 295.5$ K. Finally, those values of L where **Overpopulation** occurs, are marked by a vertical line with its corresponding color.
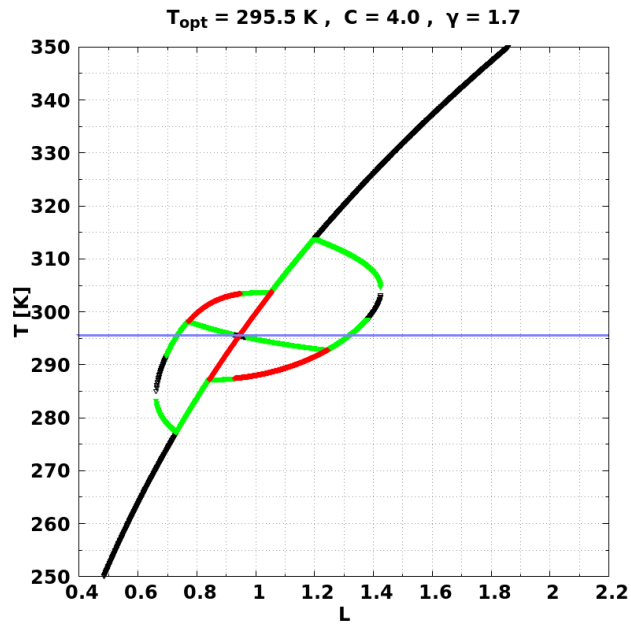
(a) DWC bifurcation for $C = 4.0$ and $\gamma = 1.7$.
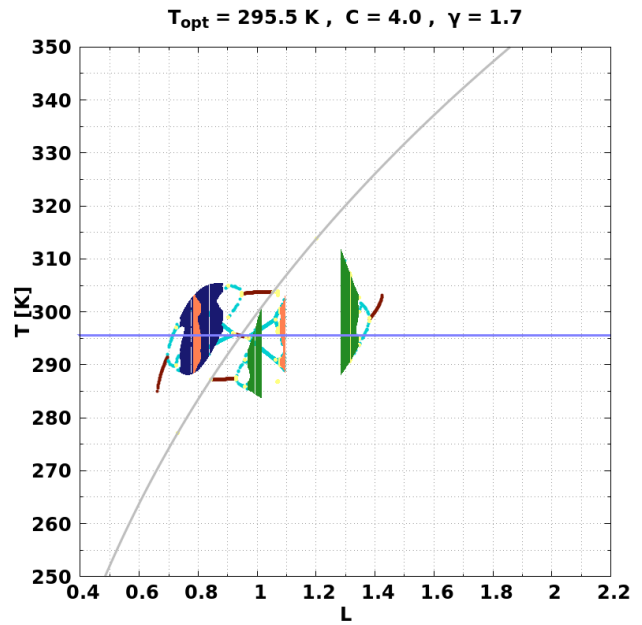
(b) DWC orbits diagram for $C = 4.0$ and $\gamma = 1.7$.
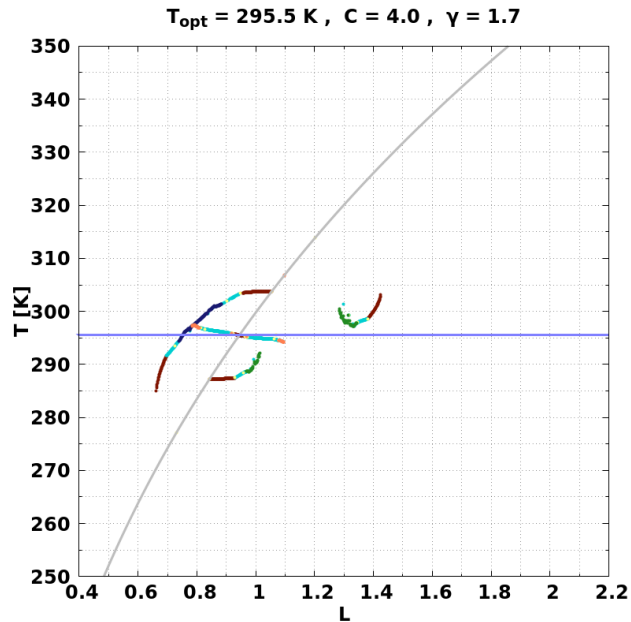
(c) DWC temperature T mean for $C = 4.0$ and $\gamma = 1.7$.

Legend:
- Stable node
- Semistable node
- Unstable node
- Null (0,0)
- FP not null
- Periodic
- Quasiperiodic
- Chaotic (a1,a2)
- Chaotic (a1,0)
- Chaotic (0,a2)
- Overpopulation
- Forbidden barrier

Figure A.74: **Orbits diagram** and the corresponding temperature T mean for **DWC** for $C = 4.0$ and $\gamma = 1.7$. **Blue** line corresponds to the value of $T_{opt} = 295.5$ K. Finally, those values of L where **Overpopulation** occurs, are marked by a vertical line with its corresponding color.
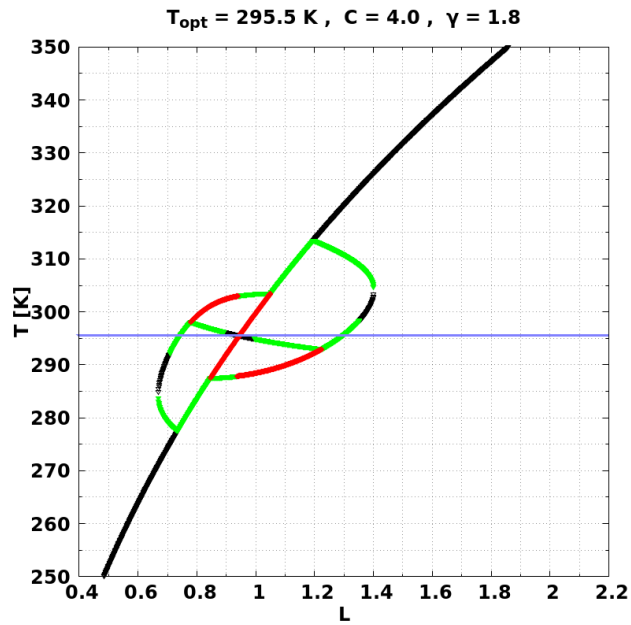
(a) DWC bifurcation for $C = 4.0$ and $\gamma = 1.8$.
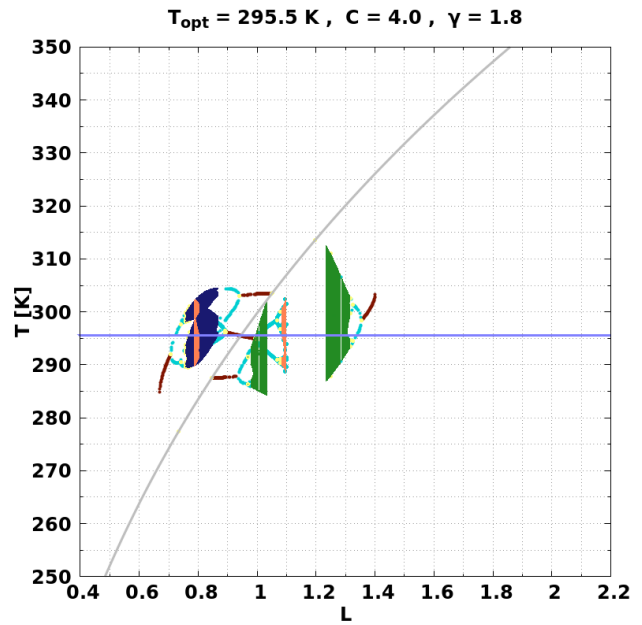
(b) DWC orbits diagram for $C = 4.0$ and $\gamma = 1.8$.
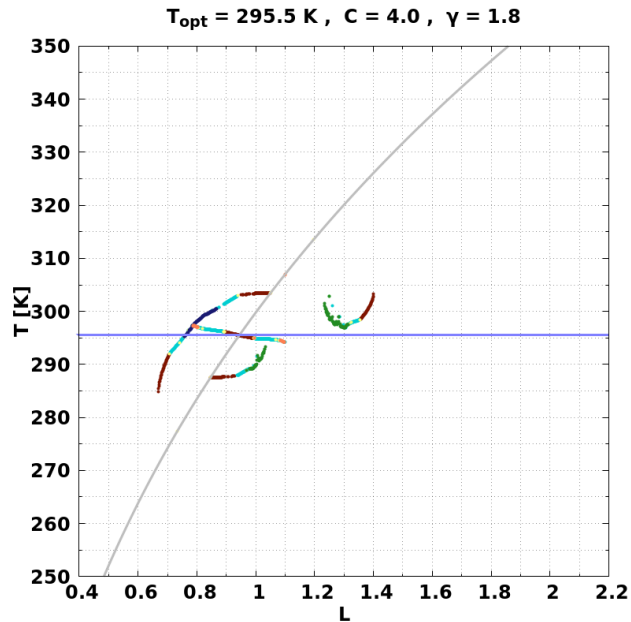
(c) DWC temperature T mean for $C = 4.0$ and $\gamma = 1.8$.

Figure A.75: **Orbits diagram** and the corresponding temperature T mean for **DWC** for $C = 4.0$ and $\gamma = 1.8$. **Blue** line corresponds to the value of $T_{opt} = 295.5$ K. Finally, those values of L where **Overpopulation** occurs, are marked by a vertical line with its corresponding color.
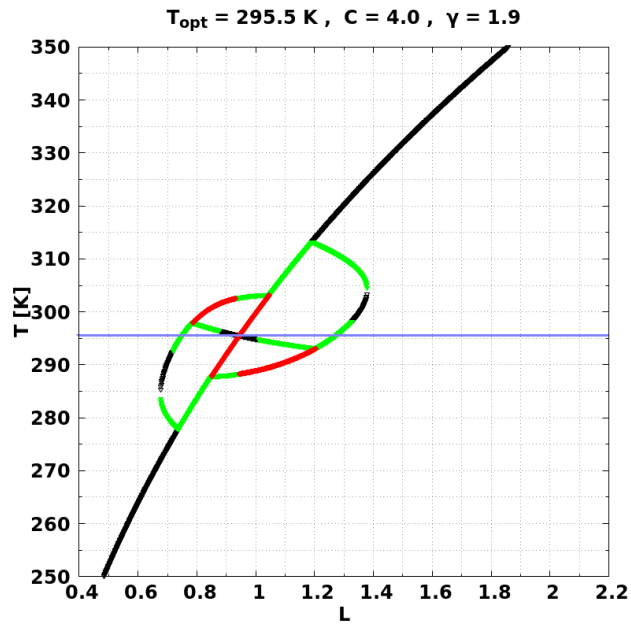
(a) DWC bifurcation for $C = 4.0$ and $\gamma = 1.9$.
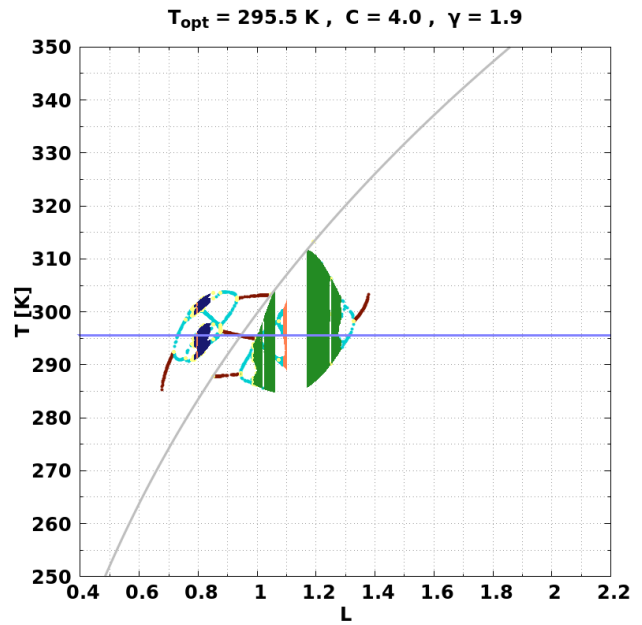
(b) DWC orbits diagram for $C = 4.0$ and $\gamma = 1.9$.
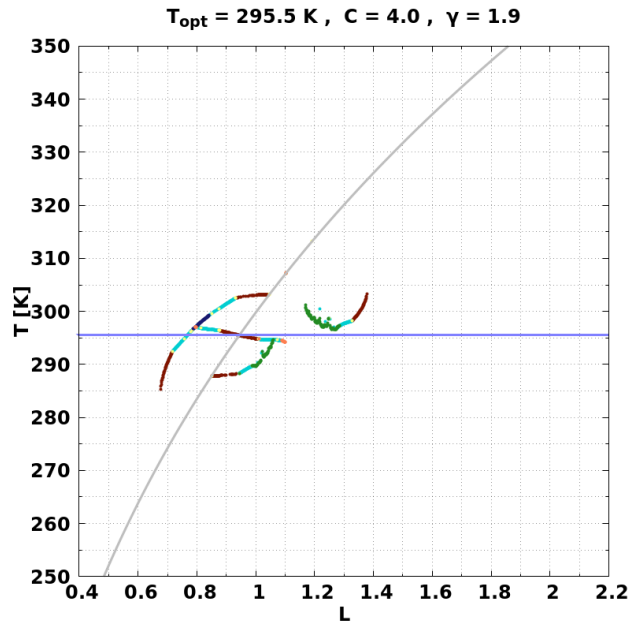
(c) DWC temperature T mean for $C = 4.0$ and $\gamma = 1.9$.

Figure A.76: **Orbits diagram** and the corresponding temperature T mean for **DWC** for $C = 4.0$ and $\gamma = 1.9$. **Blue** line corresponds to the value of $T_{opt} = 295.5$ K. Finally, those values of L where **Overpopulation** occurs, are marked by a vertical line with its corresponding color.
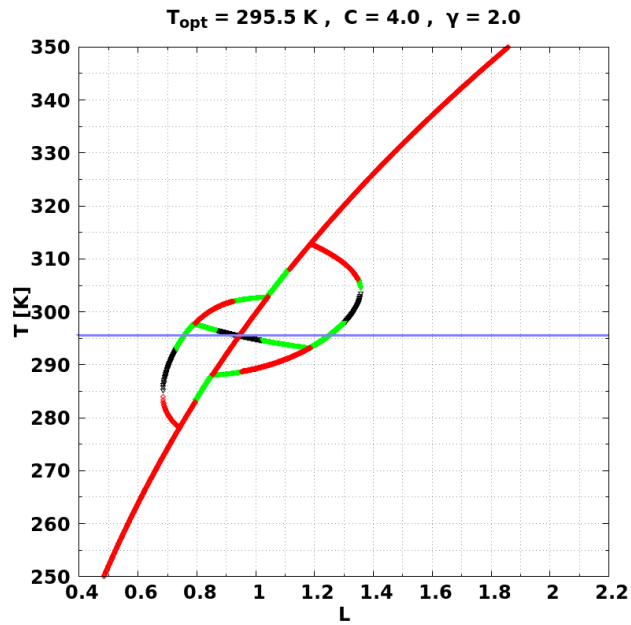
(a) DWC bifurcation for $C = 4.0$ and $\gamma = 2.0$.
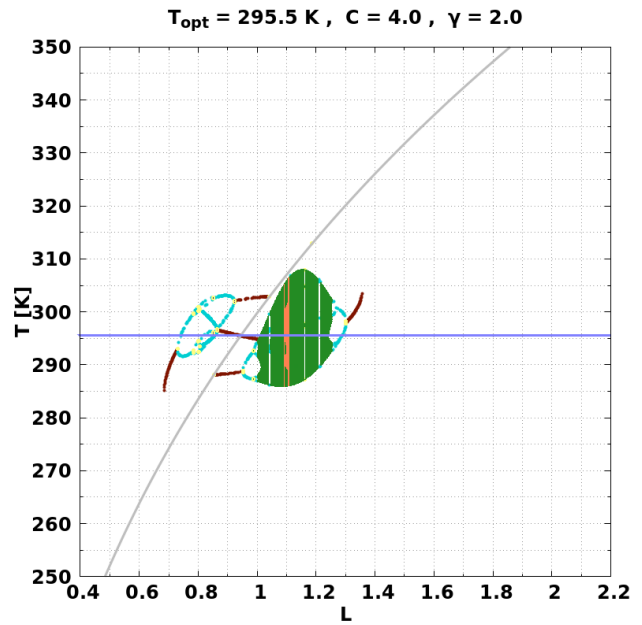
(b) DWC orbits diagram for $C = 4.0$ and $\gamma = 2.0$.
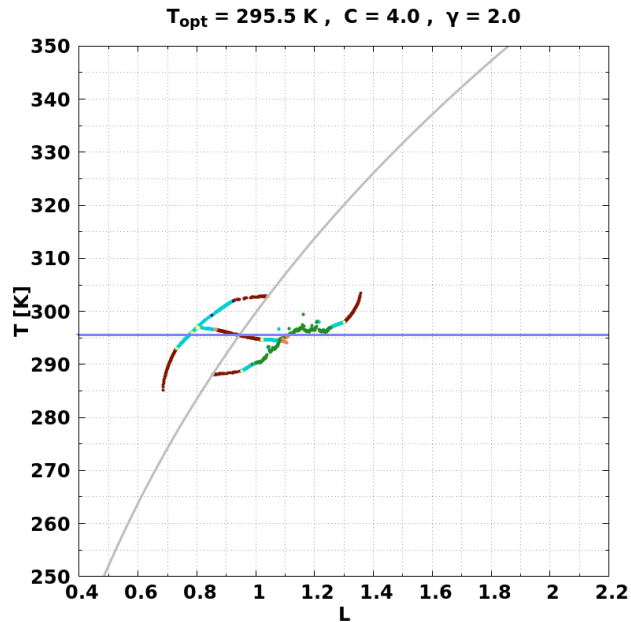
(c) DWC temperature T mean for $C = 4.0$ and $\gamma = 2.0$.

Figure A.77: **Orbits diagram** and the corresponding temperature T mean for **DWC** for $C = 4.0$ and $\gamma = 2.0$. **Blue** line corresponds to the value of $T_{opt} = 295.5$ K. Finally, those values of L where **Overpopulation** occurs, are marked by a vertical line with its corresponding color.
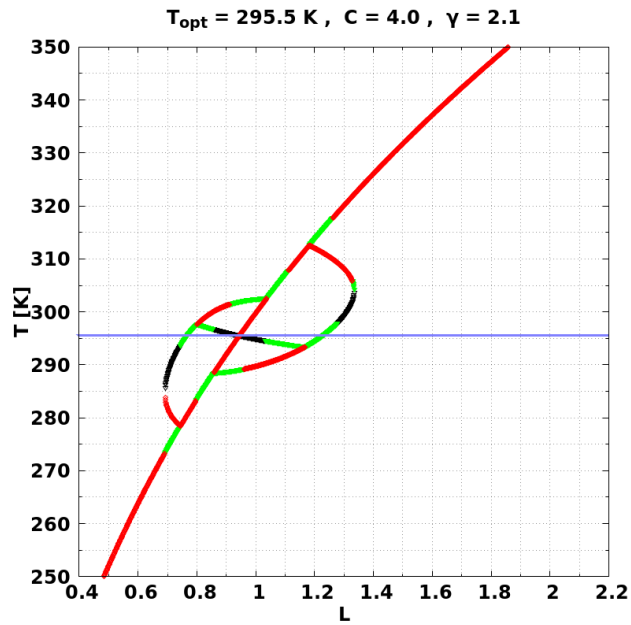
(a) DWC bifurcation for $C = 4.0$ and $\gamma = 2.1$.
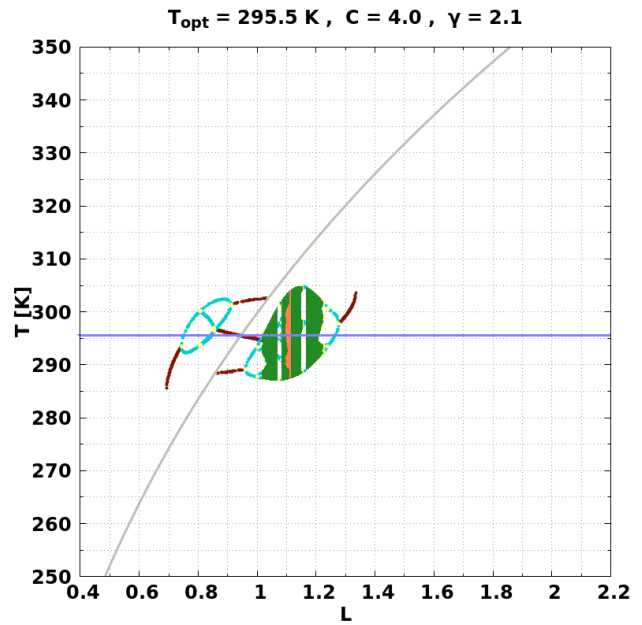
(b) DWC orbits diagram for $C = 4.0$ and $\gamma = 2.1$.
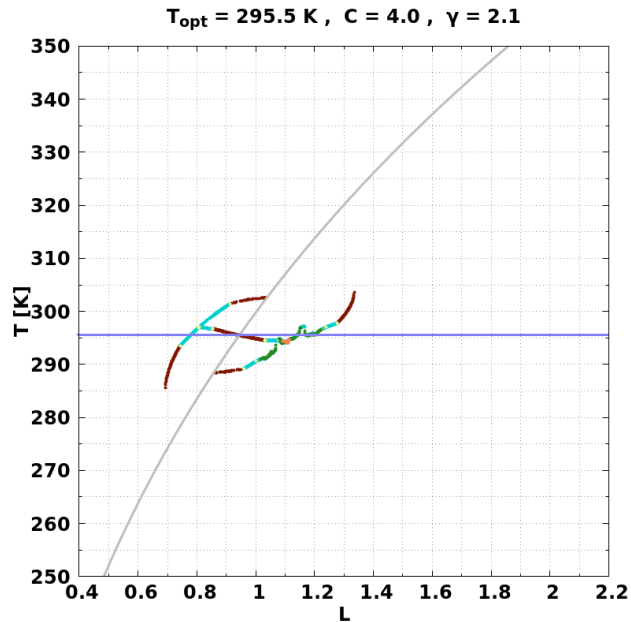
(c) DWC temperature T mean for $C = 4.0$ and $\gamma = 2.1$.

Figure A.78: **Orbits diagram** and the corresponding temperature T mean for **DWC** for $C = 4.0$ and $\gamma = 2.1$. **Blue** line corresponds to the value of $T_{opt} = 295.5$ K. Finally, those values of L where **Overpopulation** occurs, are marked by a vertical line with its corresponding color.
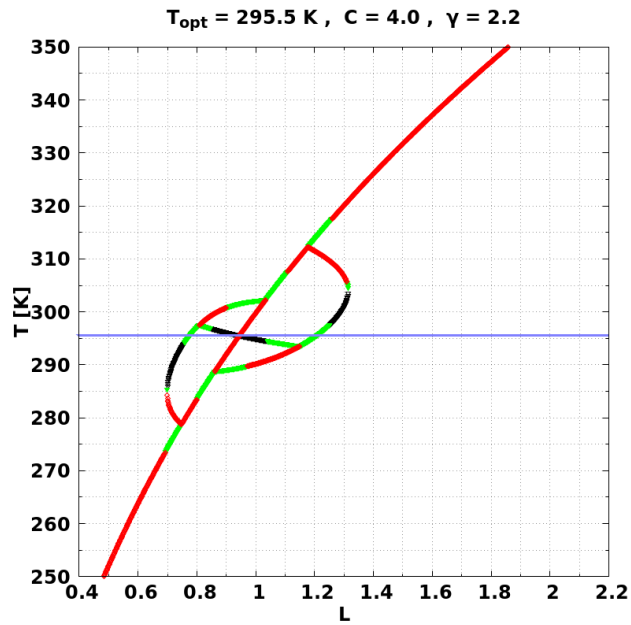
(a) DWC bifurcation for $C = 4.0$ and $\gamma = 2.2$.
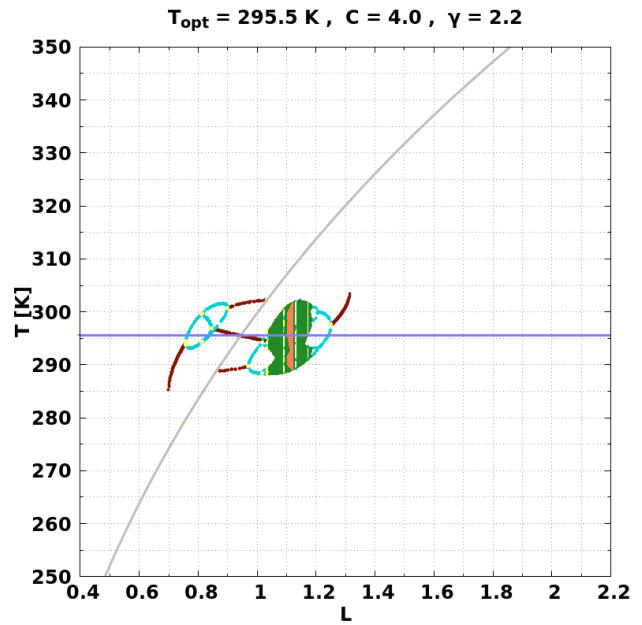
(b) DWC orbits diagram for $C = 4.0$ and $\gamma = 2.2$.
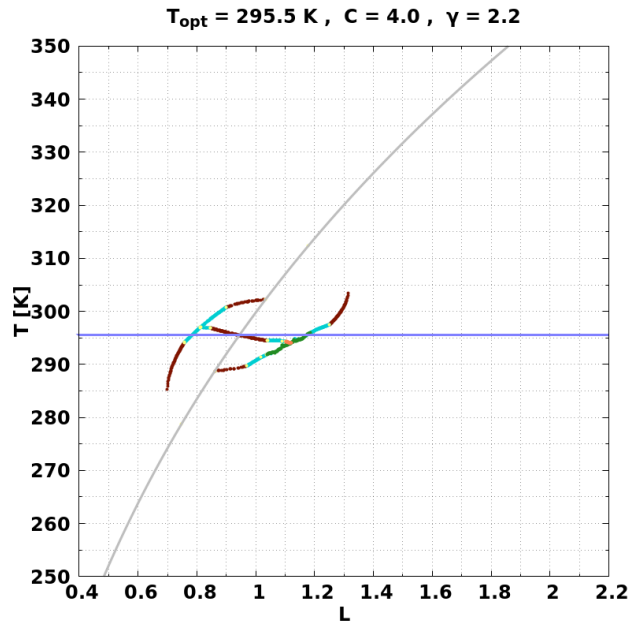
(c) DWC temperature T mean for $C = 4.0$ and $\gamma = 2.2$.

Figure A.79: **Orbits diagram** and the corresponding temperature T mean for **DWC** for $C = 4.0$ and $\gamma = 2.2$. **Blue** line corresponds to the value of $T_{opt} = 295.5$ K. Finally, those values of L where **Overpopulation** occurs, are marked by a vertical line with its corresponding color.
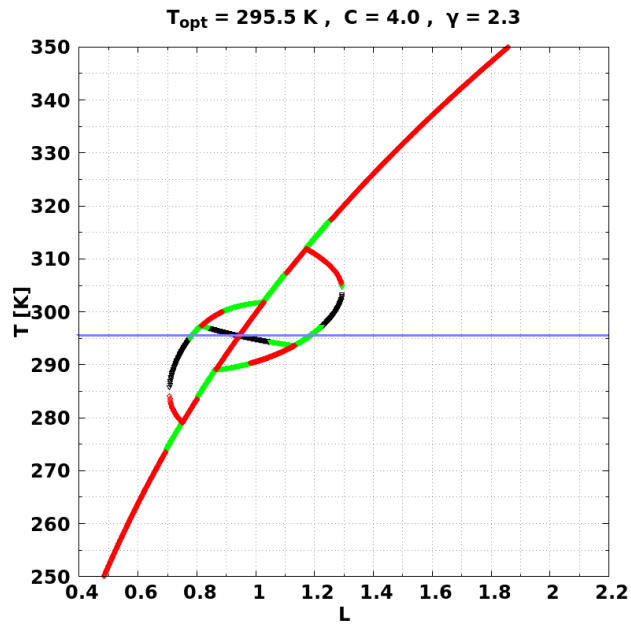
(a) DWC bifurcation for $C = 4.0$ and $\gamma = 2.3$.
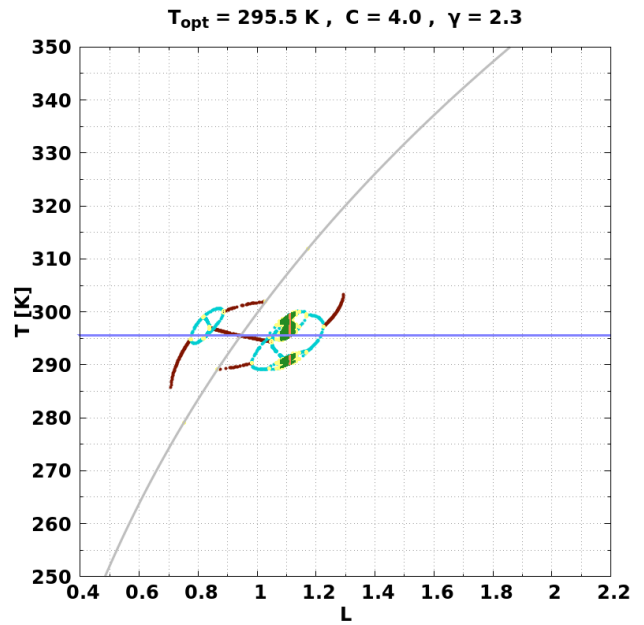
(b) DWC orbits diagram for $C = 4.0$ and $\gamma = 2.3$.
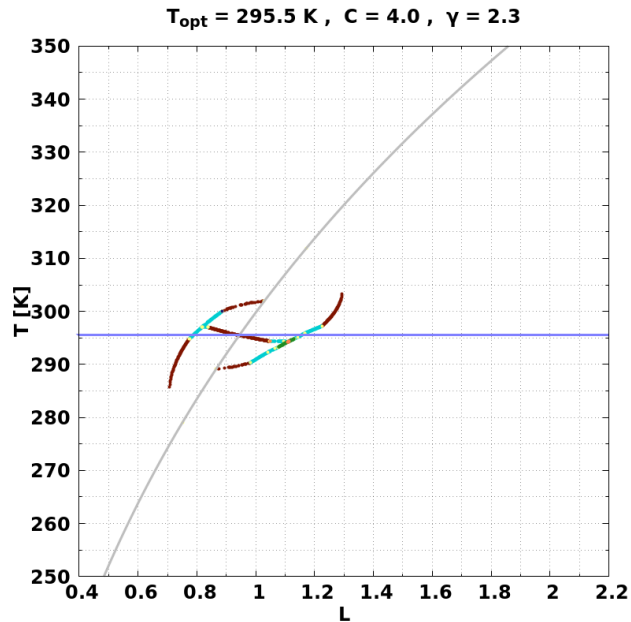
(c) DWC temperature T mean for $C = 4.0$ and $\gamma = 2.3$.

Figure A.80: **Orbits diagram** and the corresponding temperature T mean for **DWC** for $C = 4.0$ and $\gamma = 2.3$. **Blue** line corresponds to the value of $T_{opt} = 295.5$ K. Finally, those values of L where **Overpopulation** occurs, are marked by a vertical line with its corresponding color.
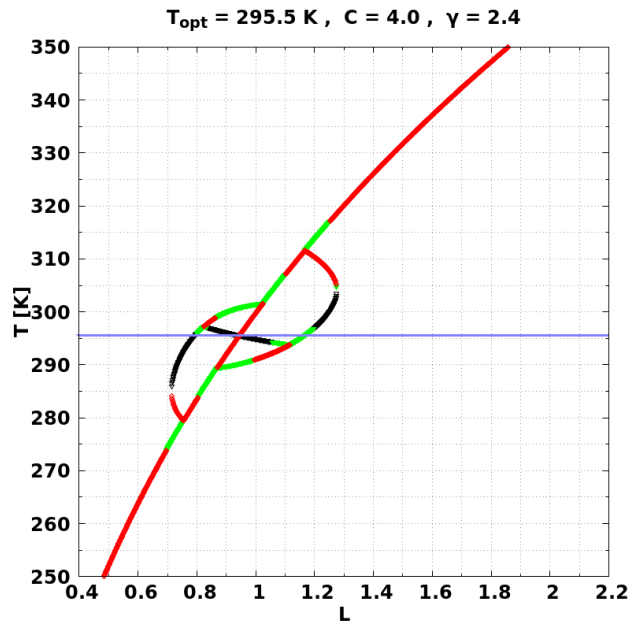
(a) DWC bifurcation for $C = 4.0$ and $\gamma = 2.4$.
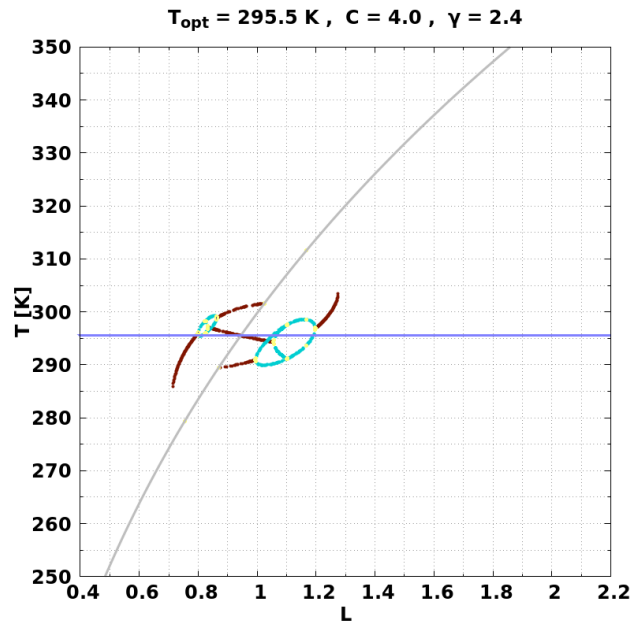
(b) DWC orbits diagram for $C = 4.0$ and $\gamma = 2.4$.
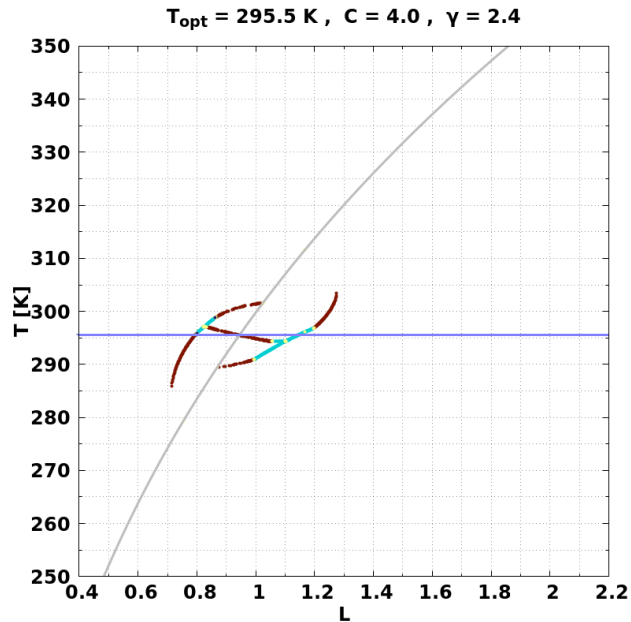
(c) DWC temperature T mean for $C = 4.0$ and $\gamma = 2.4$.

Legend:
- ● Stable node
- ● Semistable node
- ● Unstable node
- ▢ Null (0,0)
- ▢ FP not null
- ▢ Periodic
- ▢ Quasiperiodic
- ▢ Chaotic (a1,a2)
- ▢ Chaotic (a1,0)
- ▢ Chaotic (0,a2)
- ▢ Overpopulation
- ▬ Forbidden barrier

Figure A.81: **Orbits diagram** and the corresponding temperature T mean for **DWC** for $C = 4.0$ and $\gamma = 2.4$. **Blue** line corresponds to the value of $T_{opt} = 295.5$ K. Finally, those values of L where **Overpopulation** occurs, are marked by a vertical line with its corresponding color.
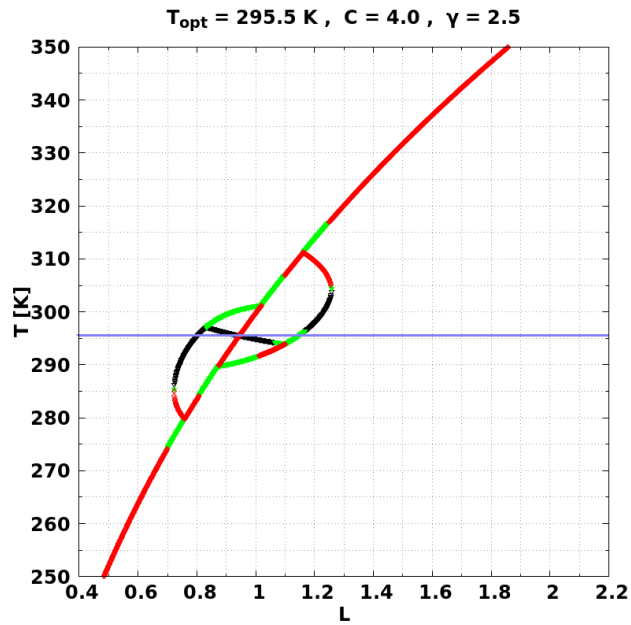
(a) DWC bifurcation for $C = 4.0$ and $\gamma = 2.5$.
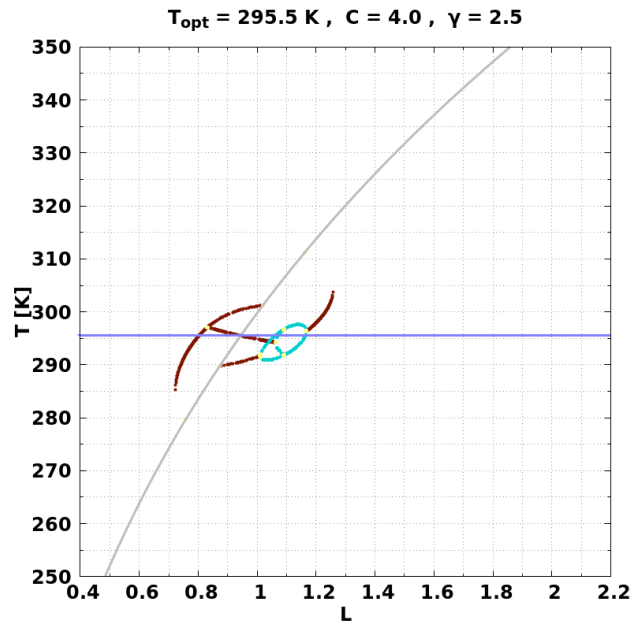
(b) DWC orbits diagram for $C = 4.0$ and $\gamma = 2.5$.
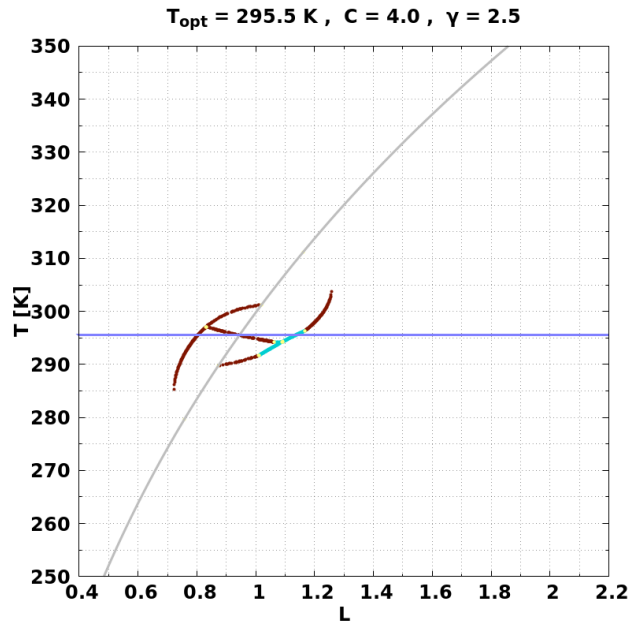
(c) DWC temperature T mean for $C = 4.0$ and $\gamma = 2.5$.

Legend:
- ● Stable node
- ● Semistable node
- ● Unstable node
- ▪ Null (0,0)
- ▪ FP not null
- ▪ Periodic
- ▪ Quasiperiodic
- ▪ Chaotic (a1,a2)
- ▪ Chaotic (a1,0)
- ▪ Chaotic (0,a2)
- ▪ Overpopulation
- ▬ Forbidden barrier

Figure A.82: **Orbits diagram** and the corresponding temperature T mean for **DWC** for $C = 4.0$ and $\gamma = 2.5$. **Blue** line corresponds to the value of $T_{opt} = 295.5$ K. Finally, those values of L where **Overpopulation** occurs, are marked by a vertical line with its corresponding color.
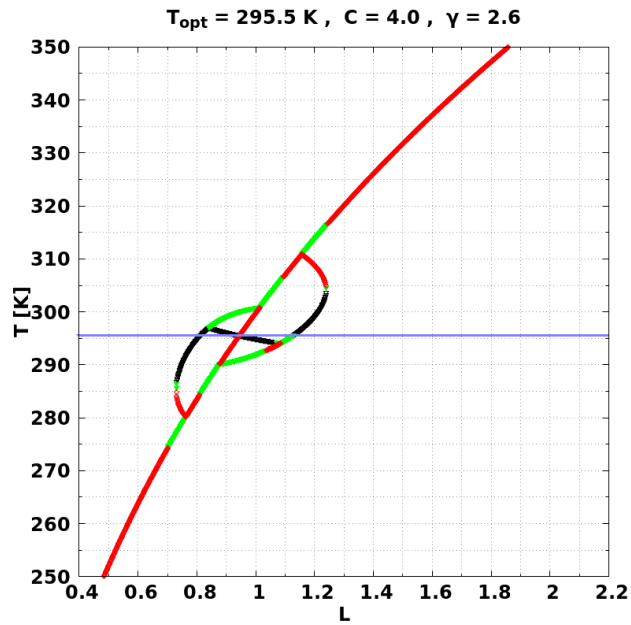
(a) DWC bifurcation for $C = 4.0$ and $\gamma = 2.6$.
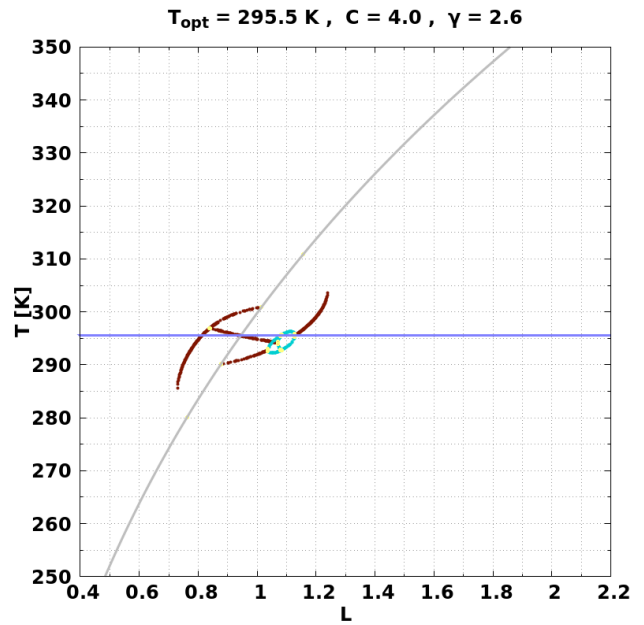
(b) DWC orbits diagram for $C = 4.0$ and $\gamma = 2.6$.
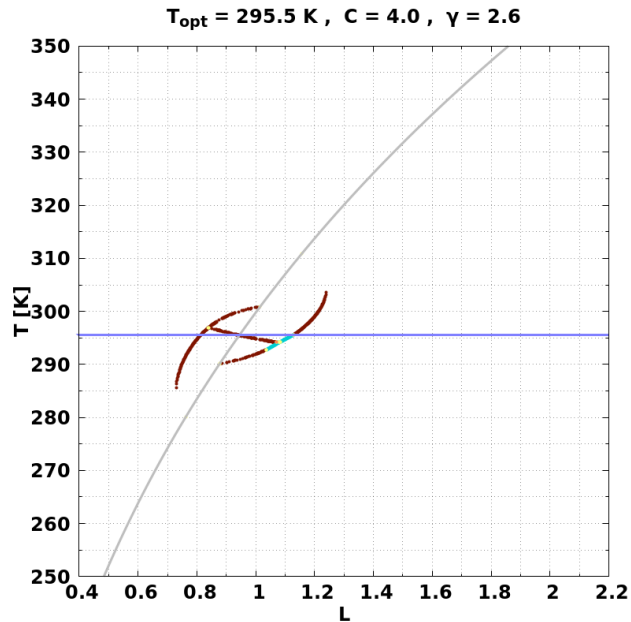
(c) DWC temperature T mean for $C = 4.0$ and $\gamma = 2.6$.

Figure A.83: **Orbits diagram** and the corresponding temperature T mean for **DWC** for $C = 4.0$ and $\gamma = 2.6$. **Blue** line corresponds to the value of $T_{opt} = 295.5$ K. Finally, those values of L where **Overpopulation** occurs, are marked by a vertical line with its corresponding color.
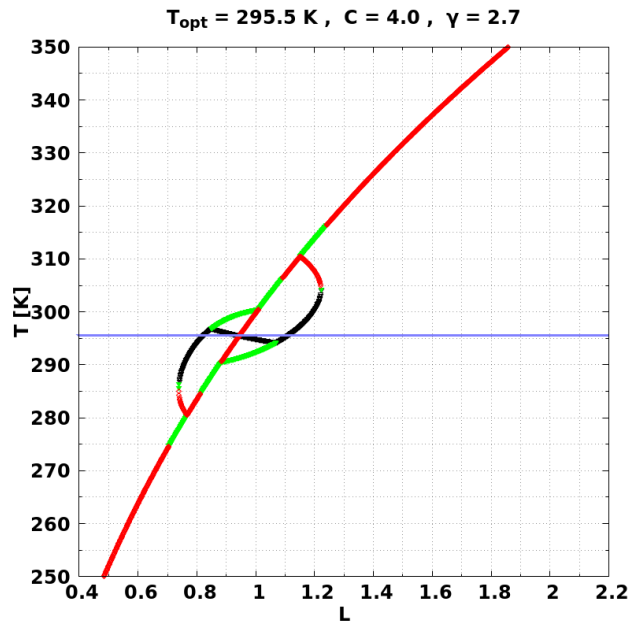
(a) DWC bifurcation for $C = 4.0$ and $\gamma = 2.7$.
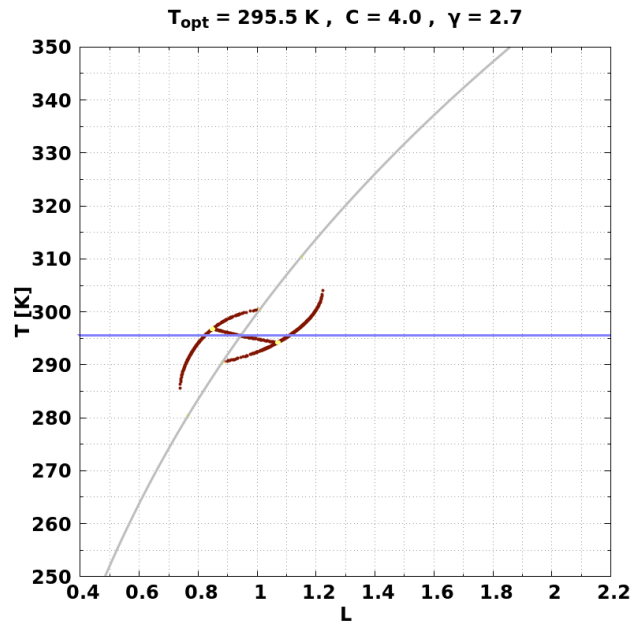
(b) DWC orbits diagram for $C = 4.0$ and $\gamma = 2.7$.
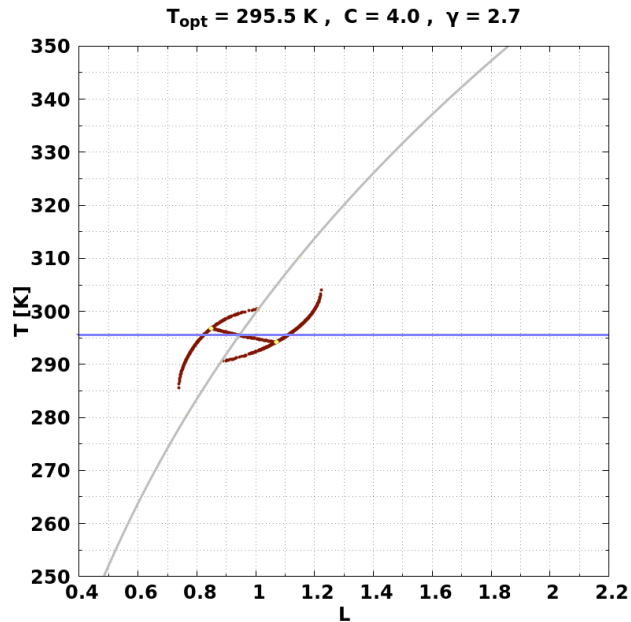
(c) DWC temperature T mean for $C = 4.0$ and $\gamma = 2.7$.

Figure A.84: **Orbits diagram** and the corresponding temperature T mean for **DWC** for $C = 4.0$ and $\gamma = 2.7$. **Blue** line corresponds to the value of $T_{opt} = 295.5$ K. Finally, those values of L where **Overpopulation** occurs, are marked by a vertical line with its corresponding color.
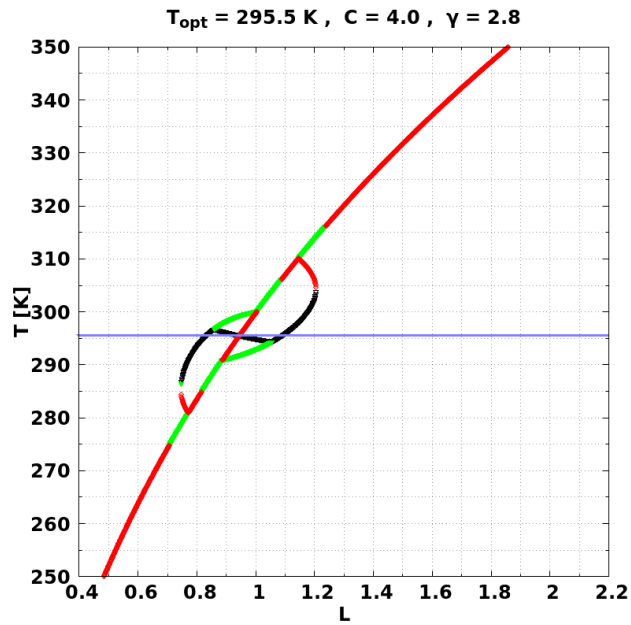
(a) DWC bifurcation for $C = 4.0$ and $\gamma = 2.8$.
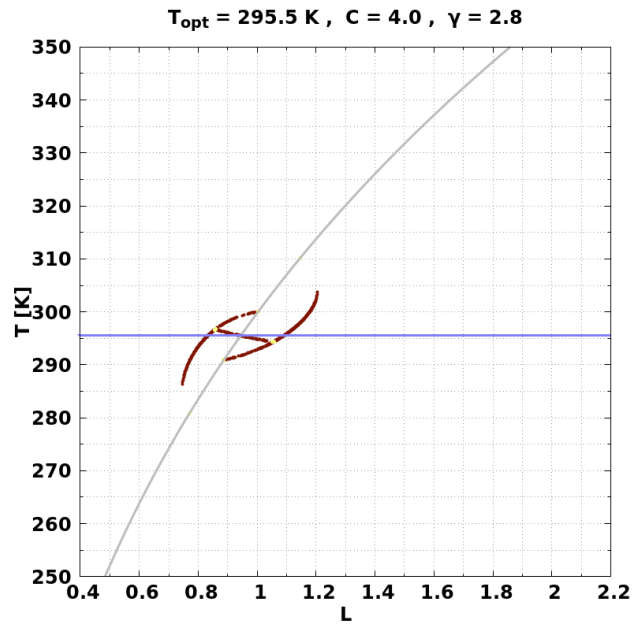
(b) DWC orbits diagram for $C = 4.0$ and $\gamma = 2.8$.
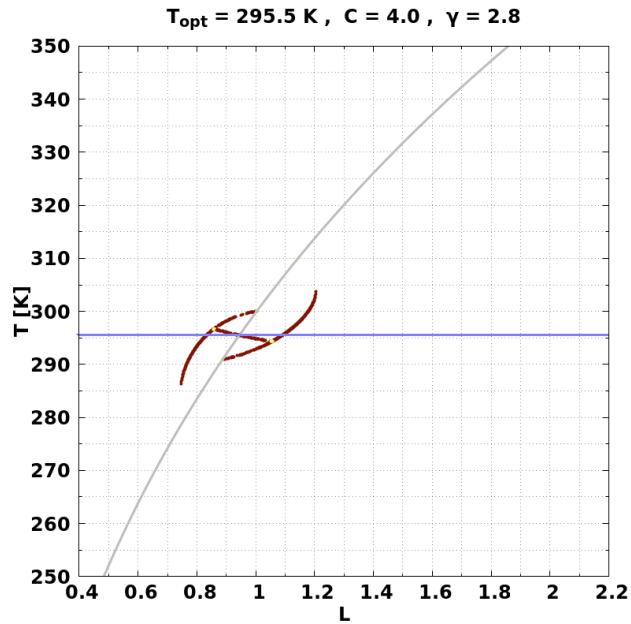
(c) DWC temperature T mean for $C = 4.0$ and $\gamma = 2.8$.

Figure A.85: **Orbits diagram** and the corresponding temperature T mean for **DWC** for $C = 4.0$ and $\gamma = 2.8$. **Blue** line corresponds to the value of $T_{opt} = 295.5$ K. Finally, those values of L where **Overpopulation** occurs, are marked by a vertical line with its corresponding color.
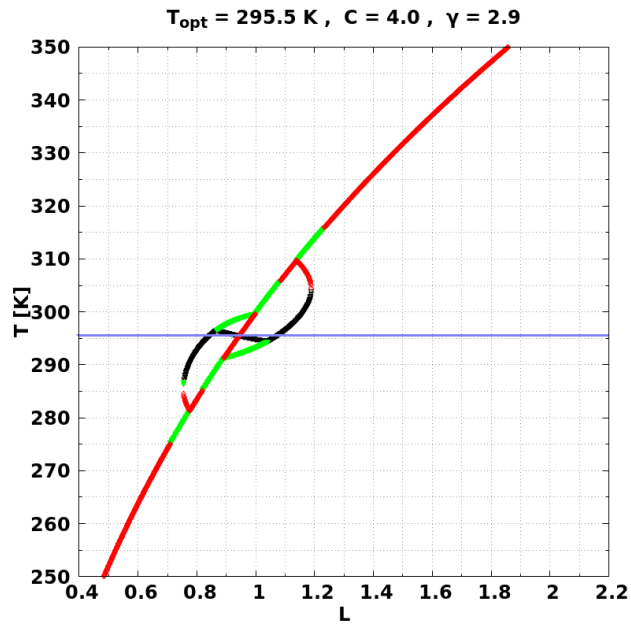
(a) DWC bifurcation for $C = 4.0$ and $\gamma = 2.9$.
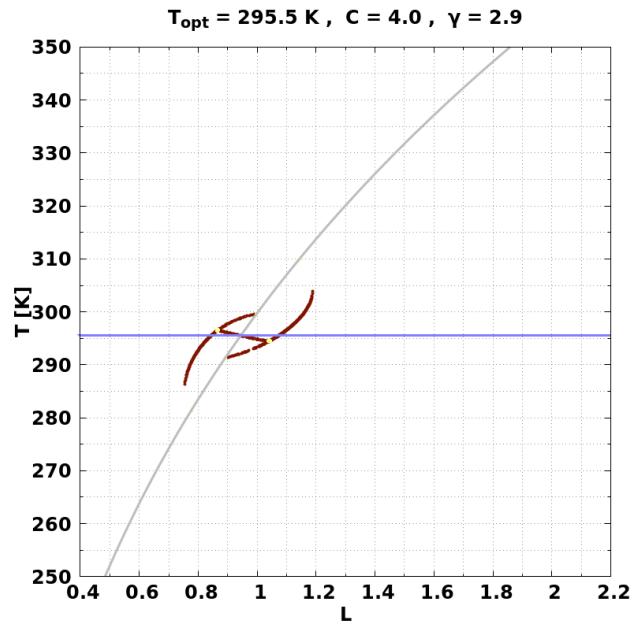
(b) DWC orbits diagram for $C = 4.0$ and $\gamma = 2.9$.
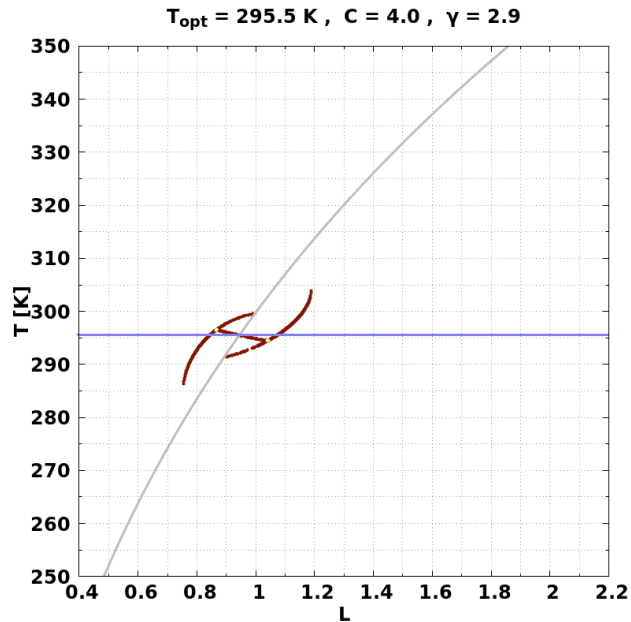
(c) DWC temperature T mean for $C = 4.0$ and $\gamma = 2.9$.

Figure A.86: **Orbits diagram** and the corresponding temperature T mean for **DWC** for $C = 4.0$ and $\gamma = 2.9$. **Blue** line corresponds to the value of $T_{opt} = 295.5$ K. Finally, those values of L where **Overpopulation** occurs, are marked by a vertical line with its corresponding color.
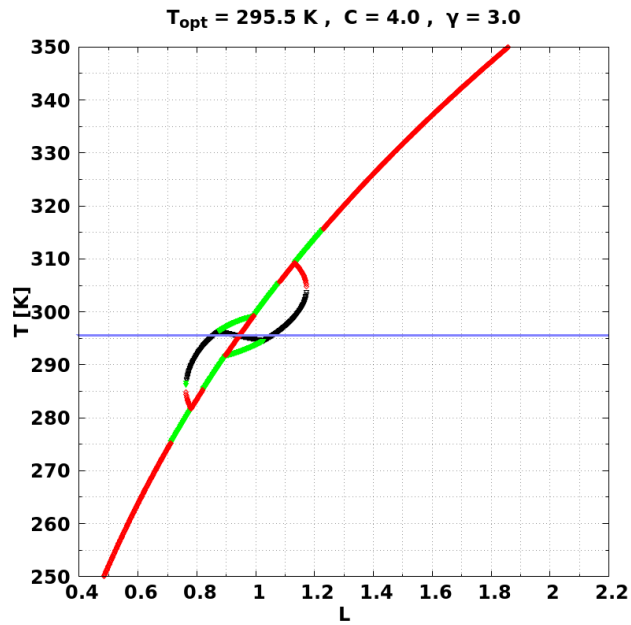
(a) DWC bifurcation for $C = 4.0$ and $\gamma = 3.0$.
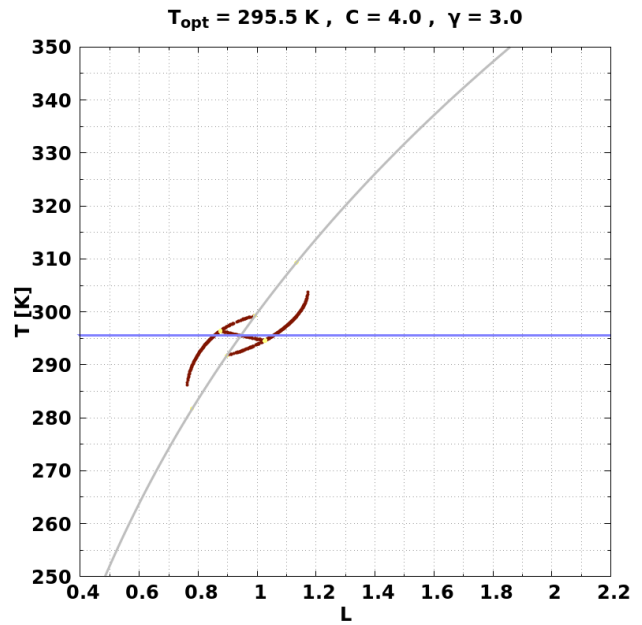
(b) DWC orbits diagram for $C = 4.0$ and $\gamma = 3.0$.
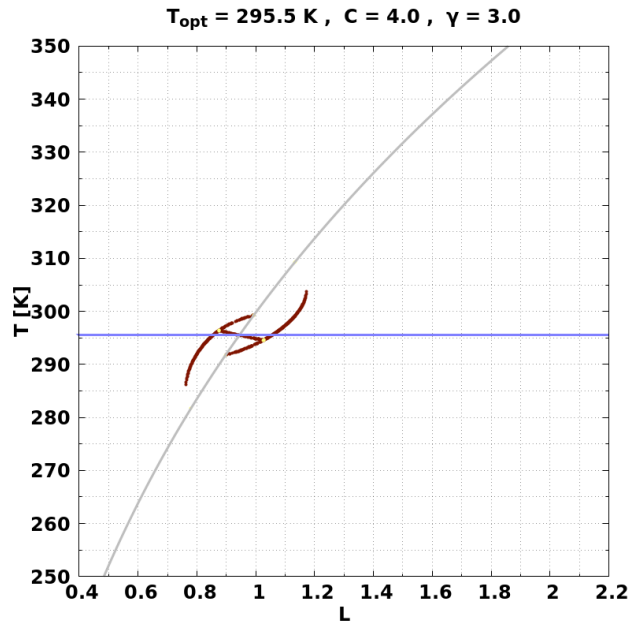
(c) DWC temperature T mean for $C = 4.0$ and $\gamma = 3.0$.

Figure A.87: **Orbits diagram** and the corresponding temperature T mean for **DWC** for $C = 4.0$ and $\gamma = 3.0$. **Blue** line corresponds to the value of $T_{opt} = 295.5$ K. Finally, those values of L where **Overpopulation** occurs, are marked by a vertical line with its corresponding color.
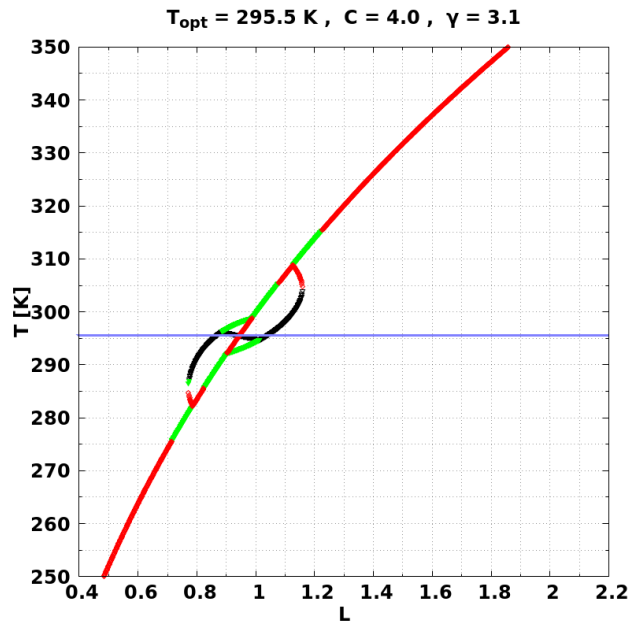
(a) DWC bifurcation for $C = 4.0$ and $\gamma = 3.1$.
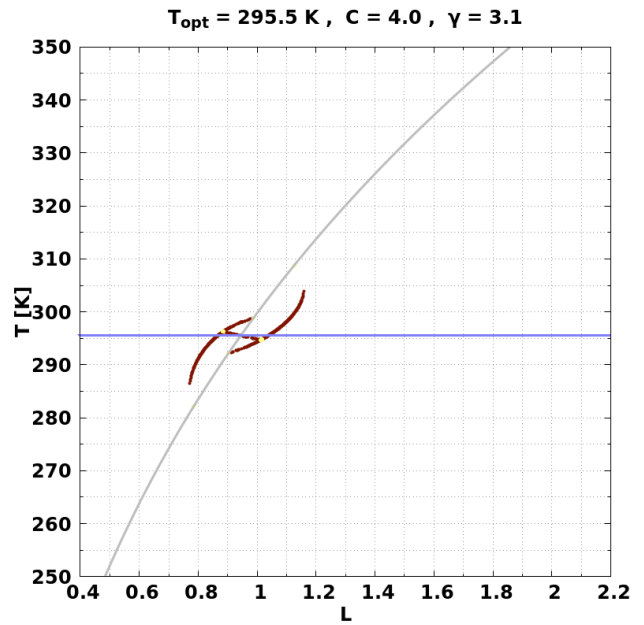
(b) DWC orbits diagram for $C = 4.0$ and $\gamma = 3.1$.
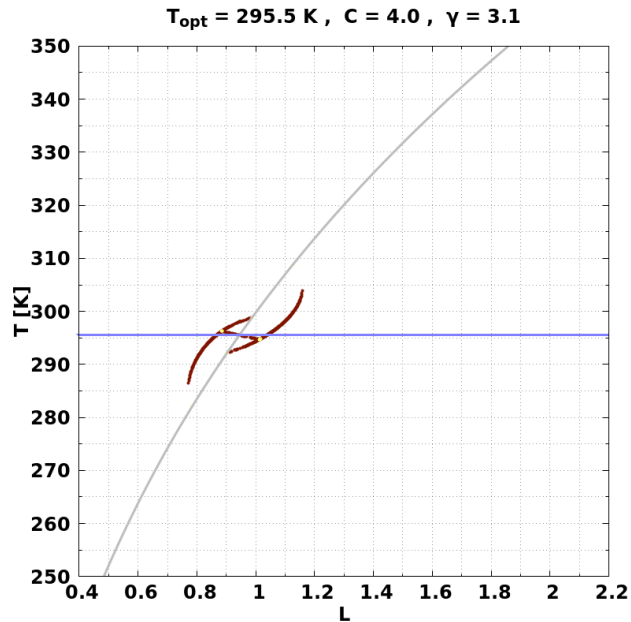
(c) DWC temperature T mean for $C = 4.0$ and $\gamma = 3.1$.

Figure A.88: **Orbits diagram** and the corresponding temperature T mean for **DWC** for $C = 4.0$ and $\gamma = 3.1$. **Blue** line corresponds to the value of $T_{opt} = 295.5$ K. Finally, those values of L where **Overpopulation** occurs, are marked by a vertical line with its corresponding color.
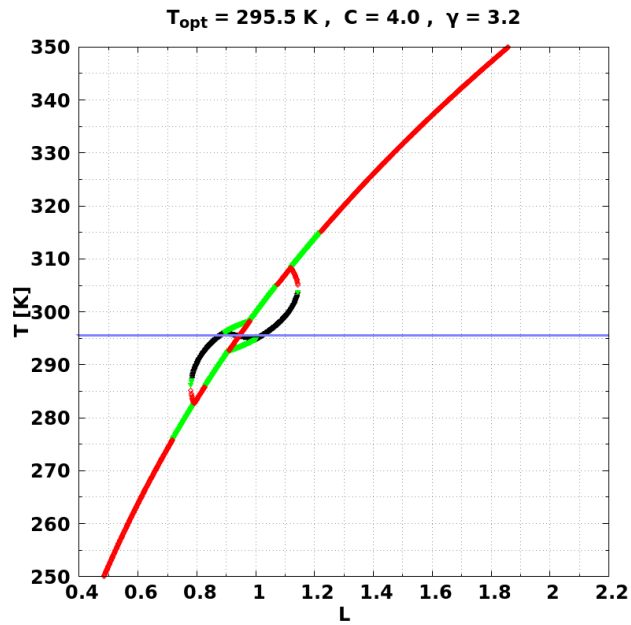
(a) DWC bifurcation for $C = 4.0$ and $\gamma = 3.2$.
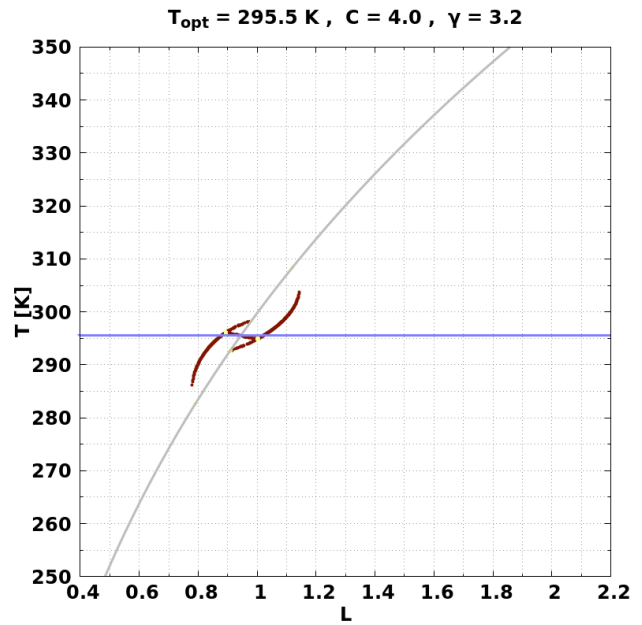
(b) DWC orbits diagram for $C = 4.0$ and $\gamma = 3.2$.
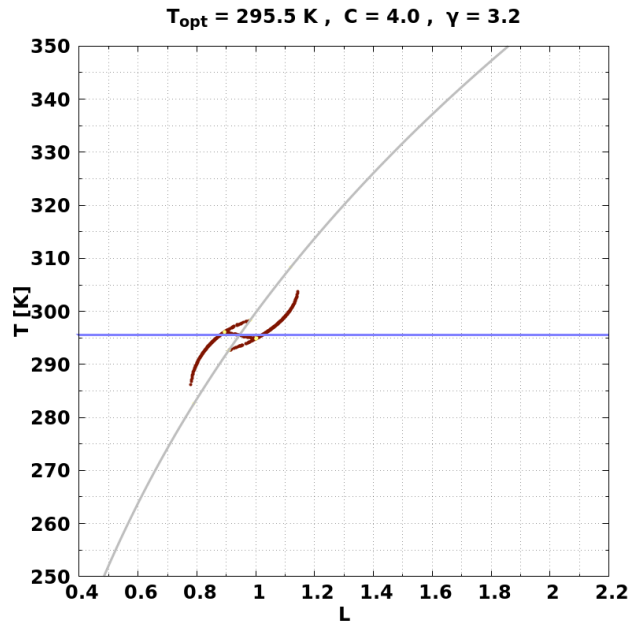
(c) DWC temperature T mean for $C = 4.0$ and $\gamma = 3.2$.

Figure A.89: **Orbits diagram** and the corresponding temperature T mean for **DWC** for $C = 4.0$ and $\gamma = 3.2$. **Blue** line corresponds to the value of $T_{opt} = 295.5$ K. Finally, those values of L where **Overpopulation** occurs, are marked by a vertical line with its corresponding color.
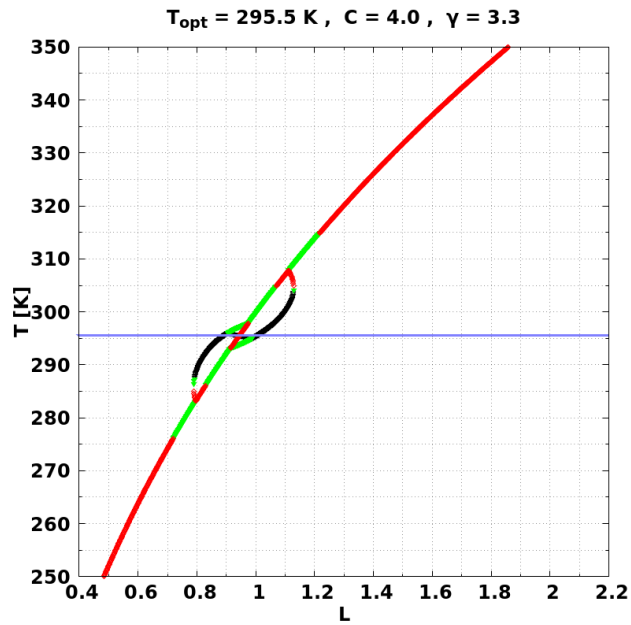
(a) DWC bifurcation for $C = 4.0$ and $\gamma = 3.3$.
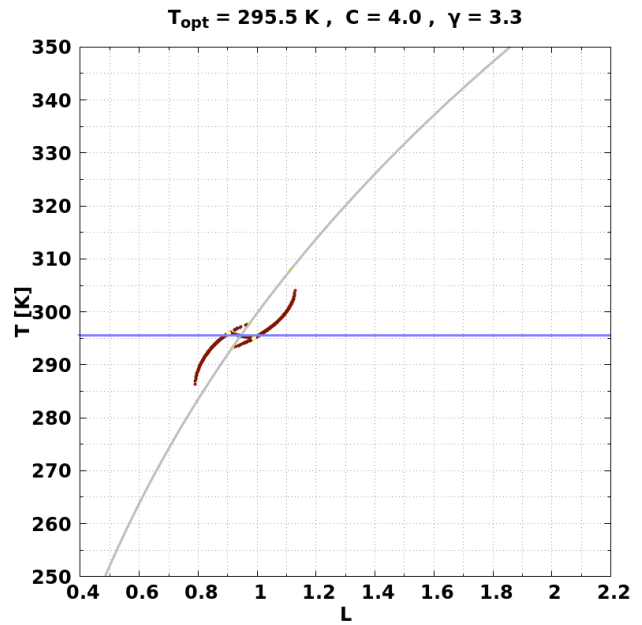
(b) DWC orbits diagram for $C = 4.0$ and $\gamma = 3.3$.
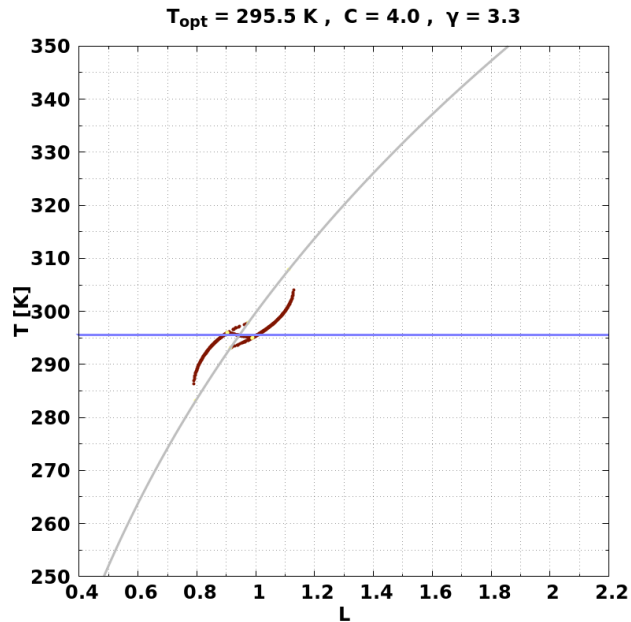
(c) DWC temperature T mean for $C = 4.0$ and $\gamma = 3.3$.

Figure A.90: **Orbits diagram** and the corresponding temperature T mean for **DWC** for $C = 4.0$ and $\gamma = 3.3$. **Blue** line corresponds to the value of $T_{opt} = 295.5$ K. Finally, those values of L where **Overpopulation** occurs, are marked by a vertical line with its corresponding color.
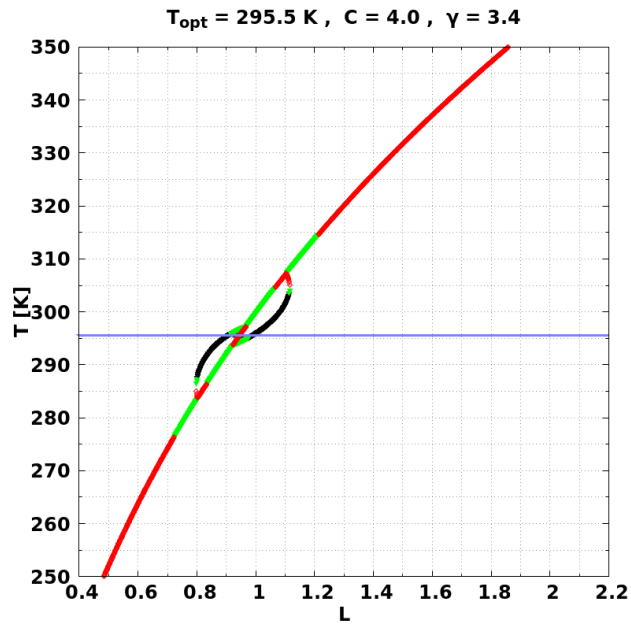
(a) DWC bifurcation for $C = 4.0$ and $\gamma = 3.4$.
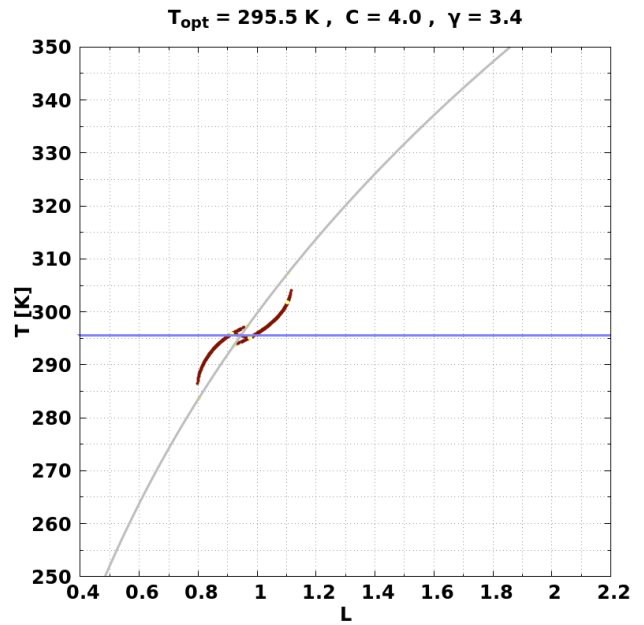
(b) DWC orbits diagram for $C = 4.0$ and $\gamma = 3.4$.
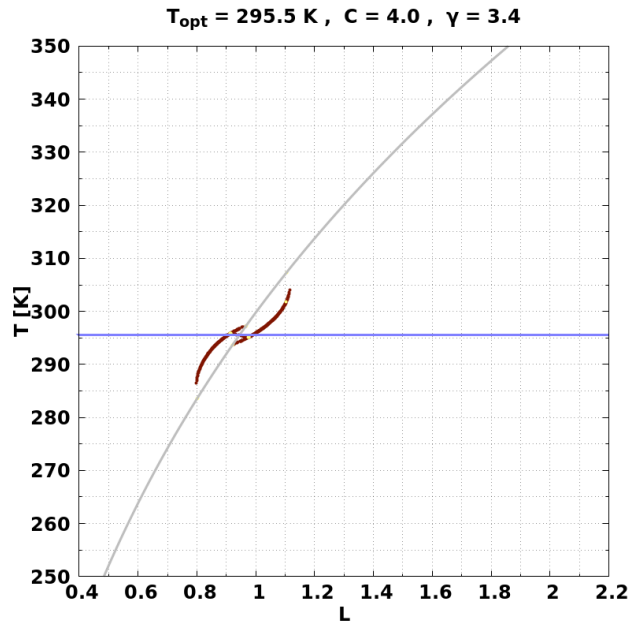
(c) DWC temperature T mean for $C = 4.0$ and $\gamma = 3.4$.

Legend:
- ● Stable node
- ● Semistable node
- ● Unstable node
- ▦ Null (0,0)
- ■ FP not null
- ▦ Periodic
- ▦ Quasiperiodic
- ■ Chaotic (a1,a2)
- ■ Chaotic (a1,0)
- ■ Chaotic (0,a2)
- ▦ Overpopulation
- ▬ Forbidden barrier

Figure A.91: **Orbits diagram** and the corresponding temperature T mean for **DWC** for $C = 4.0$ and $\gamma = 3.4$. **Blue** line corresponds to the value of $T_{opt} = 295.5$ K. Finally, those values of L where **Overpopulation** occurs, are marked by a vertical line with its corresponding color.
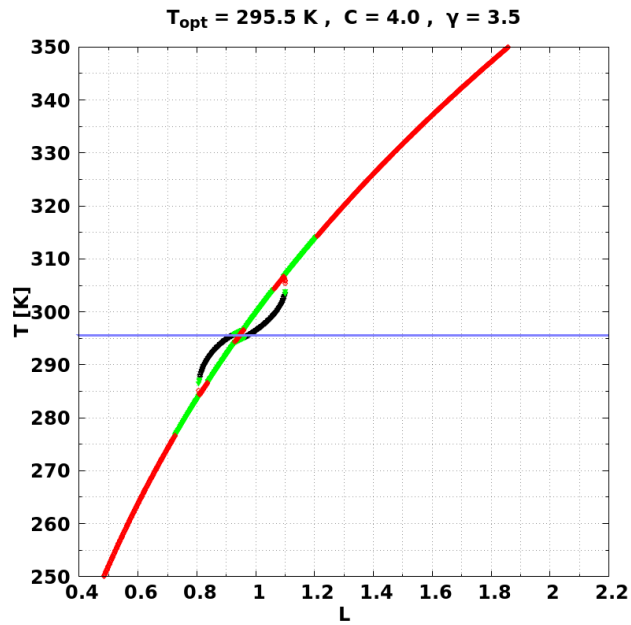
(a) DWC bifurcation for $C = 4.0$ and $\gamma = 3.5$.
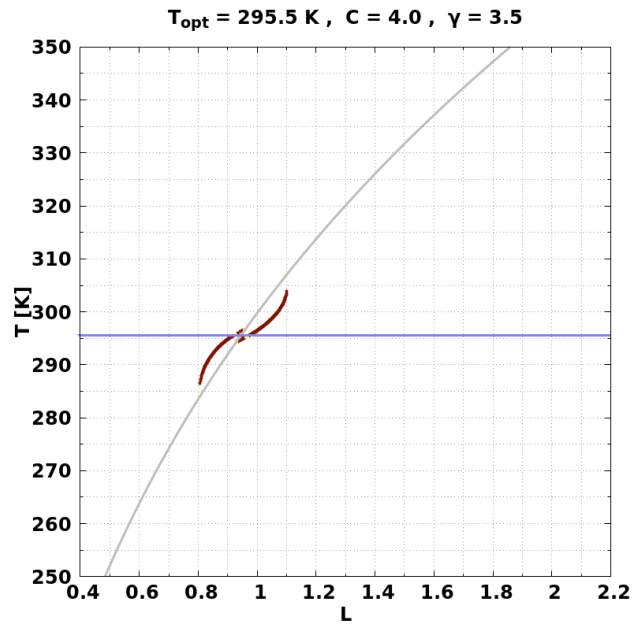
(b) DWC orbits diagram for $C = 4.0$ and $\gamma = 3.5$.
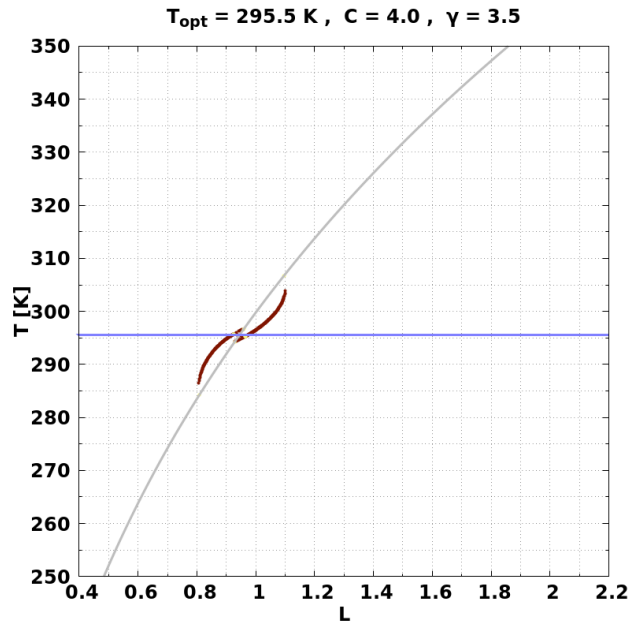
(c) DWC temperature T mean for $C = 4.0$ and $\gamma = 3.5$.

- ● Stable node
- ● Semistable node
- ● Unstable node
- ▨ Null (0,0)
- ▨ FP not null
- ▨ Periodic
- ▨ Quasiperiodic
- ▨ Chaotic (a1,a2)
- ▨ Chaotic (a1,0)
- ▨ Chaotic (0,a2)
- ▨ Overpopulation
- ▬ Forbidden barrier

Figure A.92: **Orbits diagram** and the corresponding temperature T mean for **DWC** for $C = 4.0$ and $\gamma = 3.5$. **Blue** line corresponds to the value of $T_{opt} = 295.5$ K. Finally, those values of L where **Overpopulation** occurs, are marked by a vertical line with its corresponding color.
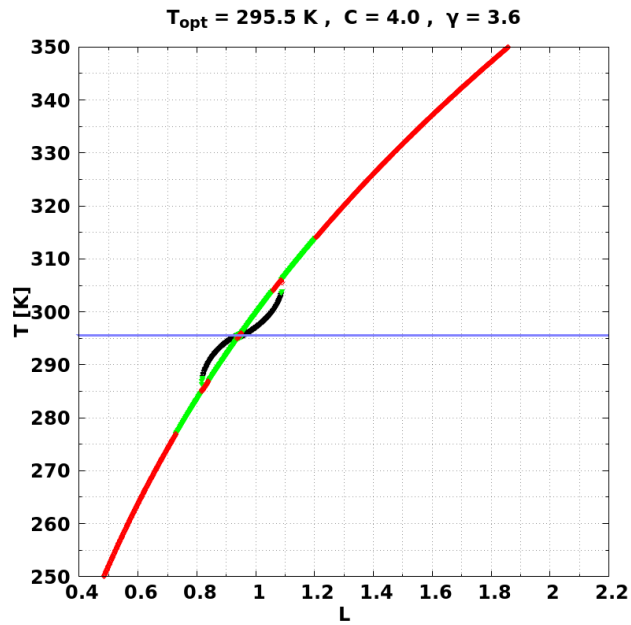
(a) DWC bifurcation for $C = 4.0$ and $\gamma = 3.6$.
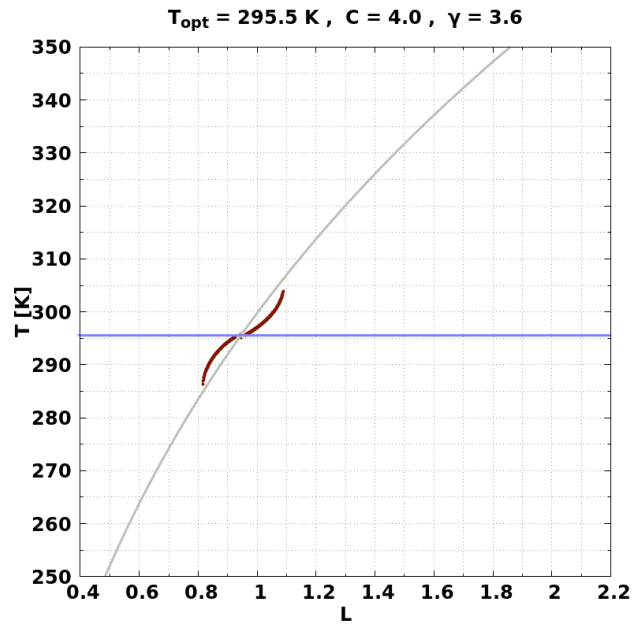
(b) DWC orbits diagram for $C = 4.0$ and $\gamma = 3.6$.
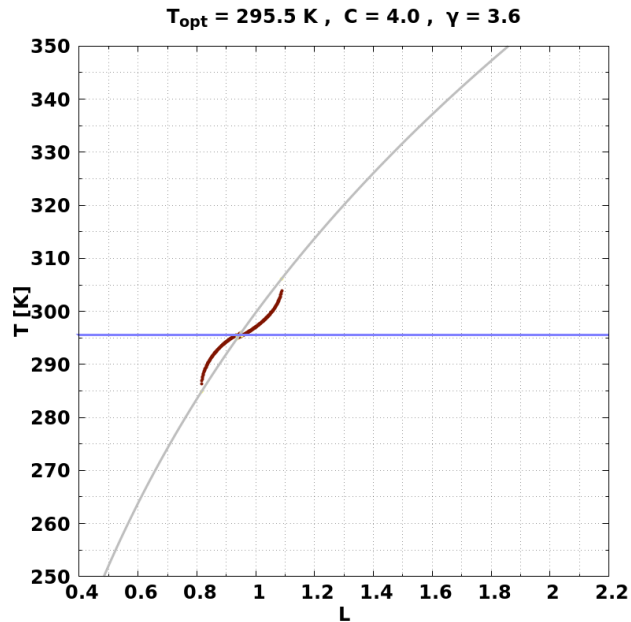
(c) DWC temperature T mean for $C = 4.0$ and $\gamma = 3.6$.

Figure A.93: **Orbits diagram** and the corresponding temperature T mean for **DWC** for $C = 4.0$ and $\gamma = 3.6$. **Blue** line corresponds to the value of $T_{opt} = 295.5$ K. Finally, those values of L where **Overpopulation** occurs, are marked by a vertical line with its corresponding color.
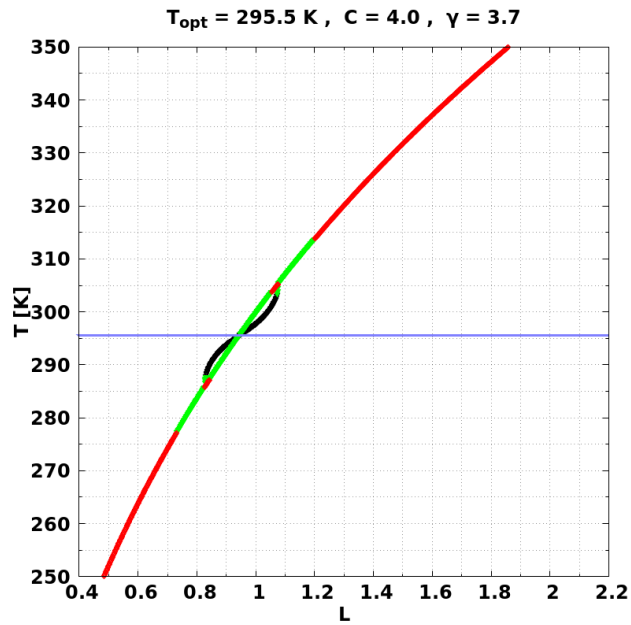
(a) DWC bifurcation for $C = 4.0$ and $\gamma = 3.7$.
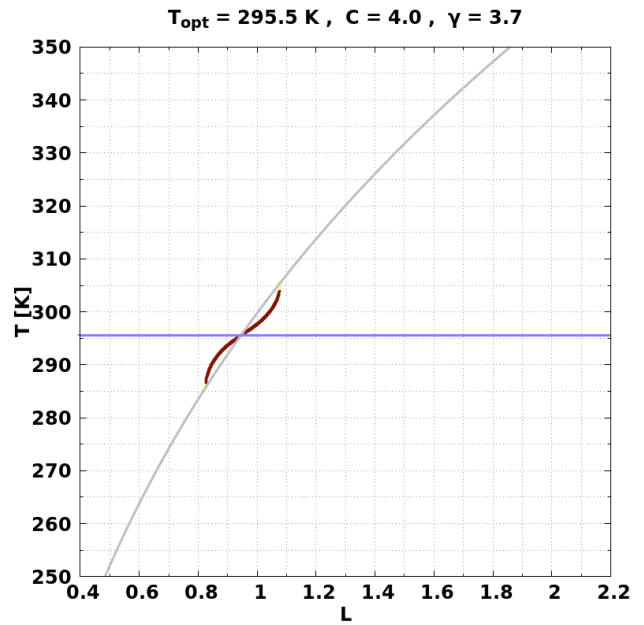
(b) DWC orbits diagram for $C = 4.0$ and $\gamma = 3.7$.
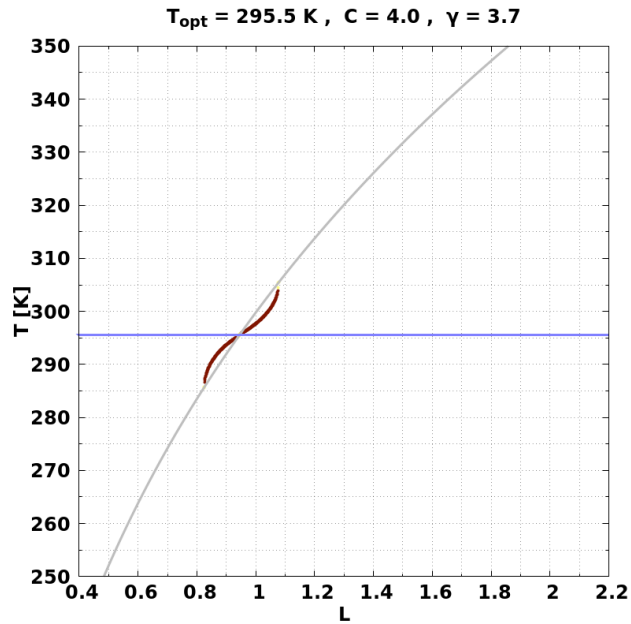
(c) DWC temperature T mean for $C = 4.0$ and $\gamma = 3.7$.

Figure A.94: **Orbits diagram** and the corresponding temperature T mean for **DWC** for $C = 4.0$ and $\gamma = 3.7$. **Blue** line corresponds to the value of $T_{opt} = 295.5$ K. Finally, those values of L where **Overpopulation** occurs, are marked by a vertical line with its corresponding color.

206
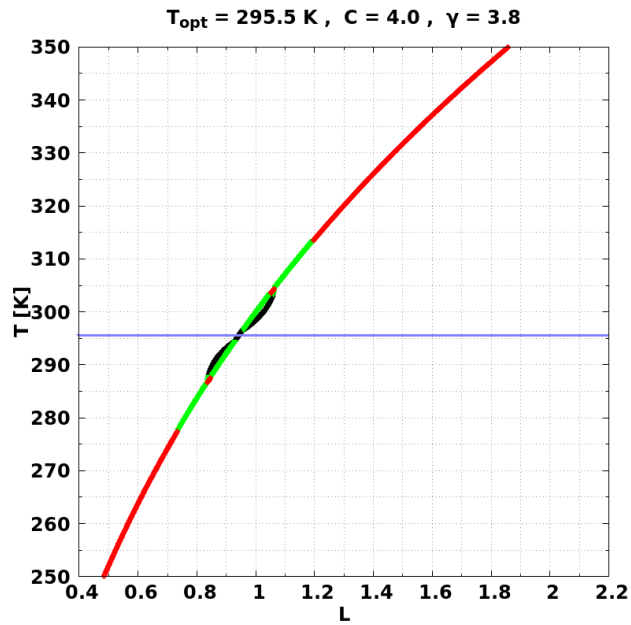
(a) DWC bifurcation for $C = 4.0$ and $\gamma = 3.8$.
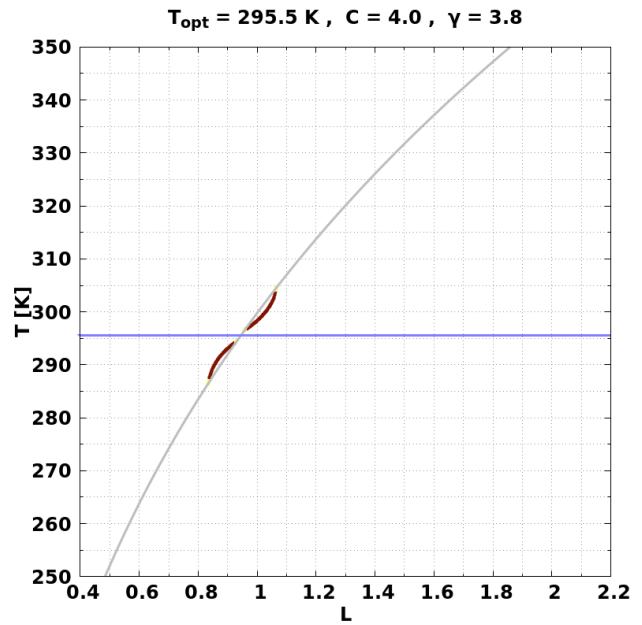
(b) DWC orbits diagram for $C = 4.0$ and $\gamma = 3.8$.
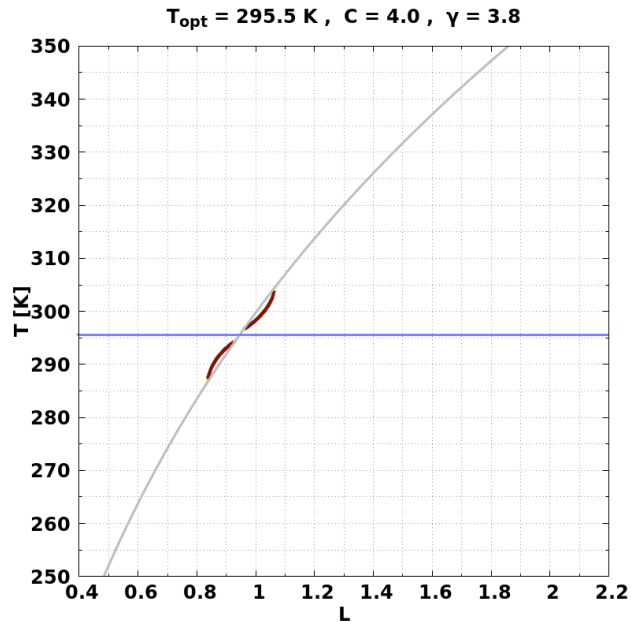
(c) DWC temperature T mean for $C = 4.0$ and $\gamma = 3.8$.

Figure A.95: **Orbits diagram** and the corresponding temperature T mean for **DWC** for $C = 4.0$ and $\gamma = 3.8$. **Blue** line corresponds to the value of $T_{opt} = 295.5$ K. Finally, those values of L where **Overpopulation** occurs, are marked by a vertical line with its corresponding color.
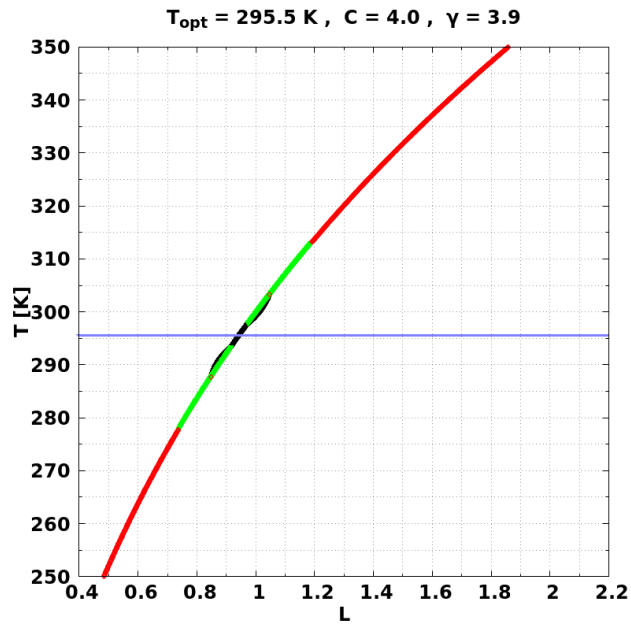
(a) DWC bifurcation for $C = 4.0$ and $\gamma = 3.9$.
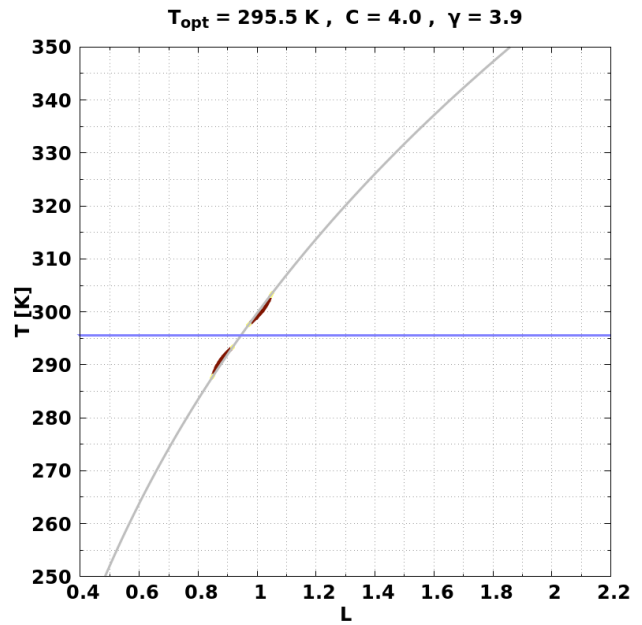
(b) DWC orbits diagram for $C = 4.0$ and $\gamma = 3.9$.
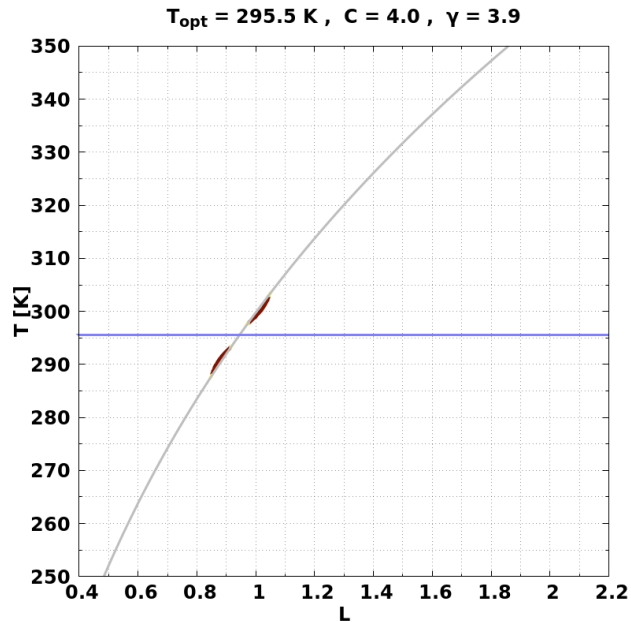
(c) DWC temperature T mean for $C = 4.0$ and $\gamma = 3.9$.

Figure A.96: **Orbits diagram** and the corresponding temperature T mean for **DWC** for $C = 4.0$ and $\gamma = 3.9$. **Blue** line corresponds to the value of $T_{opt} = 295.5$ K. Finally, those values of L where **Overpopulation** occurs, are marked by a vertical line with its corresponding color.

Bibliography

[1] WEAVER, I. S. AND DYKE, J. G., 2012. **"The importance of timescales for the emergence of environmental self-regulation"**, Journal of Theoretical Biology **313**, 172-180.

[2] ZENG, X. ET AL., 1990. **"Chaos in Daisyworld"**, Tellus **42B**, 309-318.

[3] ZENG, X., PIELKE, R. A. AND EYKHOLT, R., 1992. **"Reply to Jascourt and Raymond"**, Tellus **44B**, 247-248.

[4] JASCOURT, S. D. AND RAYMONG, W. H., 1992. **"Comments on "Chaos in Daisyworld" by X. Zeng et al."**, Tellus **44B**, 243-246.

[5] GETTELMAN A. & ROOD R. B. (2016). "Key concepts in Climate Modelling" In *Earth Systems Data and Models, Volume 2, Springer Open*, **Demystifying Climate Models: A Users Guide to Earth System Models (pp. 3-12)**.

[6] MCGUFFIE K. & HENDERSON-SELLERS A. (2005). "A History of and Introduction to Climate Models" In *John Wiley & Sons, Ltd*, **A Climate Modelling Primer, 3rd Edition (pp. 47-78)**.

[7] GETTELMAN A. & ROOD R. B. (2016). " Types of Atmospheric Models" In *Earth Systems Data and Models, Volume 2, Springer Open*, **Demystifying Climate Models: A Users Guide to Earth System Models (pp. 66-69)**.

[8] , POLVANI, L. M. ET AL. (2017, Sept 25). **"When Less Is More: Opening the Door to Simpler Climate Models"**. Retrieved from EOS, 98, https://doi.org/10.1029/2017EO079417.

[9] MCGUFFIE K. & HENDERSON-SELLERS A. (2005). "Climate" In *John Wiley & Sons, Ltd*, **A Climate Modelling Primer, 3rd Edition (pp. 1-45)**.

[10] GAL-CHEN, T. & SCHNEIDER, S. **"Energy-balance climate modeling: Comparison of radiative and dynamic feedback mechanisms"**, Tellus **28**, 108-121 (1976).

[11] NEVISON, C. ET AL. **"Self-sustained temperature oscillations on Daisyworld"**, Tellus **51B**, 806-814 (1999).

[12] HELD, I. **"The gap between simulation and understanding in climate modeling"**, Bull. Am. Meteorol. Soc., **86**, 1609–1614 (2005).

[13] **"Energy balance models"**, UNIVERSITÉ CATHOLIQUE DE LOUVAIN (2008). Retrieved on March 3, 2019, from http://www.climate.be/textbook/chapter3_node6.xml.

[14] McGuffie K. & Henderson-Sellers A. (2005). "Energy Balance Models" In *John Wiley & Sons, Ltd*, **A Climate Modelling Primer, 3rd Edition (pp. 81-115)**.

[15] Peixoto, J. P. & Oort, A. H. (1992). Chapter 6 "Radiation balance" In *AIP-Press*, **Physics of Climate (pp. 44-78)**.

[16] Sanchez-Lavega, A. (2010). Chapter 1 "Introduction to Planets and Planetary Systems" In *CRC Press*, **An Introduction to Planetary Atmospheres (pp. 1-70)**.

[17] Rob, G. (2017, Nov 27). **"Solar Irradiance"**. Retrieved from https://www.nasa.gov/mission_pages/sdo/science/solar-irradiance.html.

[18] Pathria, R. K. and Beale, P. D. (2011). Chapter 7 "Ideal Bose Systems" In *Academic Press*, **Statistical Mechanics, 3rd Edition, (pp. 179 - 229)**.

[19] Sanchez-Lavega, A. (2010). Chapter 2 "Origin and Evolution of Planetary Atmospheres" In *CRC Press*, **An Introduction to Planetary Atmospheres, (pp. 71-114)**.

[20] **"Orbits and Climate - Earth-Sun Orbit (Eccentricity)"**, Department of Agronomy, Iowa State University, 2019. Retrieved on Nomvember 4, 2019, from http://agron-www.agron.iastate.edu/courses/Agron541/classes/541/lesson07b/7b.2.html.

[21] Ross, R. (2019, Feb 20). **"What Are the Milankovitch Cycles?"**. Retrieved on November 4, 2019, from https://www.livescience.com/64813-milankovitch-cycles.html.

[22] Lenton, T. M. **"Gaia and natural selection"**, Nature **394**, 284-289 (1998).

[23] Lovelock, J. E. **"A physical basis for life detection experiments"**, Nature **207**, 568-570 (1965).

[24] Hitchcock, D. R. & Lovelock, J. E. **"Life detection by atmospheric analysis"**, Icarus **7**, 149-159 (1967).

[25] Lovelock, J. E. **"Thermodynamics and the recognition of alien biospheres"**, Proc. R. Soc. Lond. B **189**, 167-181 (1975).

[26] Lovelock, J. E. **"Gaia as seen through the atmosphere"**, Atmos. Environ. **6**, 579-580 (1972).

[27] Newman, M. J. & Rood, R. T. **"Implications of solar evolution for the Earth's early atmosphere"**, Science **198**, 1035-1037 (1977).

[28] Mojzsis, S. J. et al. **"Evidence for life on Earth before 3,800 million years ago"**, Nature **384**, 55-59 (1996).

[29] Walker, J. C. G., Hays, P. B. & Kasting, J. F. **"A negative feedback mechanism for the long-term stabilization of Earth's surface temperature"**, J. Geophys. Res. **86**, 9776-9782 (1981).

[30] Lovelock, J. E. & Margulis, L. **"Atmospheric homeostasis by and for the biosphere: the gaia hypothesis"**, Tellus **26**, 2-10 (1974).

[31] MARGULIS, L. & LOVELOCK, J. E. **"Biological modulation of the Earth's atmosphere"**, Icarus **21**, 471-489 (1974).

[32] LOVELOCK, J. E. & MARGULIS, L. **"Homeostatic tendencies of the Earth's atmosphere"**, Origins Life **5**, 93-103 (1974).

[33] LOVELOCK, J. E. *Gaia: A New Look at Life on Earth, Oxford Univ. Press (1987).*

[34] LOVELOCK, J. E. *The Ages of Gaia, 2nd Ed., Oxford University Press, Oxford (1995).*

[35] LOVELOCK, J. E. AND WATSON, A. J., 1983. **"Biological homeostasis of the global environment: the parable of Daisyworld"**, Tellus **35B**, 284-289.

[36] SALAZAR, J. F., & POVEDA, G., 2009. **"Role of a simplified hydrological cycle and clouds in regulating the climate-biota system of Daisyworld"**. Tellus B: Chemical and Physical Meteorology, **61(2)**, 483-497.

[37] CARTER, R. N. AND PRINCE, S. D., 1981. **"Epidemic models used to explain biogeographical distribution limits"**, Nature **293**, 644-645.

[38] LENTON, T. M., & LOVELOCK, J. E., 2000. **"Daisyworld is Darwinian: constraints on adaptation are important for planetary self-regulation"**, Journal of theoretical Biology **206 (1)**, 109-114.

[39] NIELSEN, P. N. AND DITLEVSEN, P., 2009. **"On the homeostasis and bistability on a Gaian planet"**, Planetary and Space Science **57**, 491-497.

[40] STROGATZ, S. H. (1994). Section 9.3 "Chaos on a strange attractor" In *Perseus Books*, **Nonlinear Dynamics and Chaos: with applications to Physics, Biology, Chemistry and Engineering (pp. 317-325)**.

[41] SPROTT, J. C. (2004). Section 5.6 "Numerical calculation of the largest Lyapunov exponent" In *Oxford University Press*, **Chaos and time series analysis (pp. 116-117)**.

[42] STROGATZ, S. H. (1994). Section 11.4 "Box dimension" In *Perseus Books*, **Nonlinear Dynamics and Chaos: with applications to Physics, Biology, Chemistry and Engineering (pp. 409-411)**.

[43] SPROTT, J. C. (2004). Chapter 12 "Calculation of the fractal dimension" In *Oxford University Press*, **Chaos and time series analysis (pp. 302-328)**.

[44] SPROTT, J. C. (2004). Chapter 13 "Fractal measure and multifractals" In *Oxford University Press*, **Chaos and time series analysis (pp. 329-352)**.

[45] MAY, R. M., 1974. **"Biological Populations with Nonoverlapping Generations: Stable Points, Stable Cycles and Chaos"**, Science **186**, 645-647.

[46] STROGATZ, S. H. (1994). Section 6.3 "Fixed points and linearization" In *Perseus Books*, **Nonlinear Dynamics and Chaos: with applications to Physics, Biology, Chemistry and Engineering (pp. 150-151)**.

[47] ALLIGOOD, K. T, SAUER, T. D. AND YORKE, J. A. (2000). Section 2.5 "Nonlinear Maps and the Jacobian Matrix" In *Springer*, **Chaos: An Introduction to Dynamical Systems, 3rd Edition (pp. 68-77)**.

[48] SPROTT, J. C. (2004). Section 6.5.3 "Routes to chaos" In *Oxford University Press*, **Chaos and time series analysis (pp. 138-141)**.

[49] **"numpy.linalg.lstsq method"**. Retrieved on April 19, 2019, from https://docs.scipy.org/doc/numpy/reference/generated/numpy.linalg.lstsq.html.

[50] STROGATZ, S. H. (1994). Section 10.2 "Logistic Map: Numerics" In *Perseus Books*, **Nonlinear Dynamics and Chaos: with applications to Physics, Biology, Chemistry and Engineering (pp. 353-357)**.

[51] OTT, E. (2002). Section 1.4 "Attractors" In *Cambridge*, **Chaos in Dynamical Systems, 2nd Edition (pp. 10-15)**.

[52] MURRAY, J. D. (2002). Chapter 2 "Discrete Population Models for a Single Species" In *Springer-Verlag New York*, **Mathematical Biology. I. An Introduction, (pp. 44-78)**.

[53] COLE, L. C., 1954. **"The population consequences of life history phenomena"**, The Quarterly review of biology **29 2**, 103-37.

[54] ROBISON, B., SEIBEL, B. AND DRAZEN, J., 2014. **"Deep-Sea Octopus (Graneledone boreopacifica) Conducts the Longest-Known Egg-Brooding Period of Any Animal"**, PLOS ONE **9**, 1-4.

[55] DICKHOFF, W. W. (1989). Chapter 13 "SALMONIDS AND ANNUAL FISHES: DEATH AFTER SEX" In *Academic Press*, **Development, Maturation, and Senescence of Neuroendocrine Systems, (pp. 253 - 266)**.

[56] SIMPSON, M. G. (2010). Chapter 13 "Plant Reproductive Biology" In *Academic Press*, **Plant Systematics, 2nd Edition (pp. 573 - 584)**.

[57] YOUNG, T. P. AND AUGSPURGER, C. K., 1991. **"Ecology and evolution of long-lived semelparous plants"**, Trends in Ecology and Evolution **6 (9)**, 285 - 289.

[58] WITHERS, P. AND COOPER, C. E. (2019). "Dormancy" In *Elsevier*, **Encyclopedia of Ecology, 2nd Edition (pp. 309 - 314)**.

[59] LEE, R. E. (2009). Chapter 79 "Dormancy" In *Academic Press*, **Encyclopedia of Insects, 2nd Edition (pp. 300 - 301)**.

[60] KARSTEN, K. B. ET AL., 2008. **"A unique life history among tetrapods: An annual chameleon living mostly as an egg"**, Proceedings of the National Academy of Sciences **105 (26)**, 8980-8984.